

CRYSTALS
AND
X-RAYS

LONSDALE

676

BELL

**CRYSTALS
AND X-RAYS**

CRYSTALS AND X-RAYS

By

K. LONSDALE, D.Sc., F.R.S.

READER IN CRYSTALLOGRAPHY IN
THE CHEMISTRY DEPARTMENT OF
UNIVERSITY COLLEGE, LONDON



LONDON
G. BELL & SONS LTD

1948

INV.

Printed in Great Britain
by T. and A. CONSTABLE LTD., Hopetoun Street,
Printers to the University of Edinburgh

CONTENTS

CHAP.	PAGE
I. Historical Introduction	I
II. Generation and Properties of X-rays	23
III. The Geometry of Crystals: X-ray Methods of Investigation	50
IV. Geometrical Structure Determination	81
V. Determination of Atomic and Electronic Distribution .	104
VI. Extra-Structural Studies	138
VII. The Importance of the Study of Crystals	165
Textbooks for Reference	191
Index of Subjects	193
Index of Names	198

PLATES

I . . . <i>facing page</i>	16	VIII . . . <i>facing page</i>	144
II . . . „ „	17	IX . . . „ „	145
III . . . „ „	32	X . . . „ „	160
IV . . . „ „	65	XI . . . „ „	161
V . . . „ „	80	XII . . . „ „	176
VI . . . „ „	81	XIII . . . „ „	177
VII . . . „ „	129		

FOREWORD

THIS is not a textbook for advanced students of X-ray crystallography, although I hope that they may learn something from it. It is based on a course of public lectures given at University College, London, in the spring of 1946, and is designed to interest those who do not now use X-ray crystallography, but who might well do so; and to instruct those who do use X-ray crystallographic methods without altogether understanding the tool that has been put into their hands. If I can persuade these two classes of people to pass on from this book to textbooks which are much more thorough, much more precise and much more specialised, I shall have accomplished an even better task than I set out to perform. It will be at once apparent to the informed reader that I myself have been much indebted to the writers of such textbooks. Most of all, however, I am indebted to the late Sir William Bragg, who directed my attention to X-ray crystallography while I was still a student, and under whose inspiring leadership I worked for some sixteen years as one member of a research team all of whom had something to teach each other.

I gratefully acknowledge permission to reproduce figures and plates as follows:

To the Council of the Royal Society of London and to the authors mentioned for Plates II (*f*); V (*f*) (Dr. I. E. Knaggs); VI (*d*) (Dr. M. Perutz); VI (*e*) and (*f*); VIII (*a*)-(*f*); X (*a*)-(*d*); XI (*b*) (*c*) (*e*); figs. 54 (Prof. W. T. Astbury); 59; 69 (Prof. J. D. Bernal); 99, 100, 101 (Prof. J. M. Robertson); 116 (Prof. J. M. Robertson and Miss Ida Woodward); 120 (Prof. A. R. Ubbelohde and Miss Ida Woodward); 134 (Dr. G. A. Jeffrey); 136 (Prof. J. M. Robertson and Prof. A. R. Ubbelohde); 138 (Dr. A. J. Bradley and Dr. A. Taylor).

To the Council of the Physical Society of London for Plates VI (*b*) (and to Prof. G. D. Preston); X (*e*) (*f*); XI (*f*); figs. 61, 63, 64, 65, 66, 67, 113, 114, 115, 117, 118

To the Council of the Chemical Society and to the authors, for figs. 92 (Prof. L. O. Brockway and Prof. J. M. Robertson); 97, 102 (Prof. J. M. Robertson and Miss Ida Woodward); 103, 135 (Prof. J. M. Robertson); 133 (Prof. J. M. Robertson and Mr. J. G. White).

To the Council of the Iron and Steel Institute and to Dr. Bradley, Prof. Sir W. L. Bragg and Dr. C. Sykes for Plate XIII.

To the Editor of the *Journal of Scientific Instruments* for Plate V (c).

To the Director of the British Museum (Natural History) and to the Keeper and Deputy Keeper of Minerals for Table II and fig. 38, and Plate IV (b).

To the Cambridge University Press and Dr. M. H. Pirenne for figs. 9, 10, 79.

To the Clarendon Press and Dr. C. W. Bunn for Plate VII and figs. 30, 33, 34, 42, 78, 98, 107.

To Messrs. Macmillan and Co. for figs. 36, 40, 41, and Plate XI (a).

To Messrs. Longmans, Green and Co. and Prof. F. C. Phillips for fig. 43.

To Prof. S. Tolansky for Plate IV (c).

To Prof. Bijvoet, Prof. Kolkmeijer and Miss C. H. MacGillavry for figs. 55, 95, 104, 128, 131.

To Mr. W. G. Schall for figs. 20, 25, 27, 28, 29.

To the McGraw-Hill Book Co. and Prof. G. L. Clark for fig. 124.

To the Editor of the *Journal of the American Ceramic Society* and to Prof. B. E. Warren for fig. 109.

To Messrs. G. Bell & Sons Ltd. and Prof. Sir W. L. Bragg for figs. 5, 7, 8, 31, 32, 37, 44, 56, 58, 110, 112, and to Prof. Sir W. L. Bragg for 125, 126.

To the Editor of *Chemistry and Industry* and Prof. W. T. Astbury for Plate XII (e) and (f).

To the Council of the Mineralogical Society for Plates III (a) (c) (d) (e), XI (c)-(f).

To the Editor of *Transactions of the Faraday Society* for figs. 74 and 75.

To Prof. W. T. Astbury for Plates VI (a) and XII (a)-(c); Prof. J. M. Robertson for fig. 85; Dr. M. Perutz for Plate IV (d); Dr. D. P. Riley for Plate XII (d); Dr. Dorothy Crowfoot and Mrs. Barbara Rogers-Low for Plate VI (c); Dr. H. P. Rooksby for Plates I (c), V (a); IX (a); Dr. Y. Cauchois for fig. 15, Plate II (b) and (c).

Finally, I must express my gratitude to Mr. H. Smith for assistance in taking many of the remaining photographs here reproduced, and to Mrs. Margaret Stokes, who has helped me in the compilation of the index and in many other ways; to my daughter Jane, who is a much better proof-reader than I am; and to my husband, without whose sympathetic encouragement none of my work would have been possible.

KATHLEEN LONSDALE

University College, London

May 1948

CHAPTER I

HISTORICAL INTRODUCTION

IN giving an account of any modern branch of Science it is necessary to assume some previous knowledge. Every intelligent reader of a newspaper knows more about the atom than Faraday did; even when the newspaper reports a cricket-match, the reader is supposed to know the meaning of technical terms such as boundary, l.b.w., and overthrow. I shall assume that the reader has a general idea of the rudiments of physics and chemistry. Many people who know a great deal about these and other subjects, however, do not fully realise the value of X-ray crystallography as a tool; not merely an industrial tool, but a tool by means of which other sciences may be better understood.

Another such tool, the optical microscope, is used by those whose knowledge of the optics of lens systems is very limited; such people, even if blind, could still have knowledge of the various results obtained by the use of the microscope. X-rays can be used in the investigation of matter on a much finer scale than the microscope, but it is essentially a similar tool.

WHY CANNOT WE SEE THE ATOMS WITH A MICROSCOPE?

Why cannot we magnify an object, say, one hundred times, and then magnify the image one hundred times and so on until finally we have the magnification of $100 \times 100 \times 100 \times 100$ that would make an atom of aluminium look about as big as a moth-ball? Obviously it would be easier to look at atoms, if we could, than to use the elaborate apparatus needed for the generation of X-rays, and the lengthy calculations required before we can understand what X-ray photographs mean in terms of atoms and molecules. There are three requirements that must be satisfied, however, before we can *see* anything. We must have *sufficient* light; the light must be of the right *quality* to affect our eyes in the proper way and send the proper message to the brain; and objects to be seen *separately* must be sufficiently far apart to scatter the light waves differently from each other. Let us consider these points separately: (1) We must have sufficient light. If the daylight is failing (or our eyesight is defective) we can still see large print

although small print, which scatters less light to our eye, may be undecipherable. The light scattered by an individual atom is much too small for the eye to be able to see it as an individual. (2) The light must be of the right quality. Only light of wave-lengths between about 7200 A.U.,* the limit of visible red, and 4000 A.U., the limit of visible violet, can affect the eye in the proper way. When other waves are scattered by objects, their effects must somehow be converted into light waves if we are to see them. (3) Objects to be seen separately must be sufficiently far apart. The eye will only distinguish two such objects if they send different signals, and they will only send different signals to the eye if their distance apart is at least one-third of the wave-length of the light used. The limit of resolution, as this minimum distance is called, is therefore $4000/3 = 1300$ A.U. or thereabouts, for visible light; whereas the distance apart of neighbouring atoms is only about 2 A.U. With an optical microscope we can distinguish (or resolve) things that are upwards of 1300 A.U. apart and they can be magnified up to the size required by the eye, that is, up to 0.1 mm. or larger; but whatever the magnification, the eye could not *distinguish* between particles that were less than 1300 A.U. apart, using visible light only. Smaller particles than this can of course be seen if there is sufficient light. The motes dancing in a sunbeam may be seen, but only as diffraction discs, not as particles of a visible shape.

With the electron microscope, using the much shorter electron waves and using electric and magnetic fields as lenses, a resolution of 10 A.U. can be attained. But as these waves are not of the right quality to affect the eye properly, the electron microscope image must be recorded on a fluorescent screen or on a photographic plate or film before it can be seen.

The X-rays used in studying the arrangement of atoms have a range of wave-lengths from about 0.5 to 2.5 A.U., and are therefore capable of resolving separate atoms, but they cannot be bent sufficiently by any kind of lens to give a direct image of the atomic arrangements. They can only be scattered by the atoms so as to give various kinds of patterns. The patterns can be recorded electrically or they can be made visible by means of a

* 10000,000,0 A.U. (Ångström Units) = 1 centimetre. 1 A.U. = 10^{-8} cm. X-ray wave-lengths were first measured in X units. 1000 X.U. = 1.00202 A.U. = 1 kX unit. All crystal-lengths and wave-lengths used in crystal measurement will in future be expressed in A.U., by a decision of the International Union of Crystallography.

fluorescent screen or by photography. Some photographs of X-ray patterns are shown on Pls. I-III, V-VI and VIII-XIII. Methods of obtaining and of interpreting these will be described in later chapters; meanwhile it is sufficient to say that they can be used to determine the positions and the sizes of the atoms, and the nature of the chemical bonds between the atoms. They can also be used to follow mechanical, physical or chemical processes which involve any change in the atomic arrangement, and therefore X-ray crystallography is a useful and necessary tool in every science and every technical process where atoms and atomic arrangements are concerned. Nowadays that includes almost everything, from the utilisation of atomic energy to problems of meat preservation, from the nature of radiation to the nature of a 'permanent wave,' from the process of lubrication to the waterlogging of soils, from the boiling of an egg to the manufacture of new textile materials, new light alloys or new transformer steels. When we get down to atoms, science is all one. The most vivid way in which to realise what a revolution in scientific thought has been brought about by X-ray crystallography is to take old textbooks on, say, the mechanical properties of solids, or on inorganic chemistry or atomic physics, written before 1912, to see how incomplete and indefinite was the state of knowledge then, and how much more precise it has become as a result of sure information about atomic processes and positions.

THE STATE OF KNOWLEDGE IN 1912

X-rays were discovered by Röntgen in 1895. How much was known about them by 1912? It was known that they would ionise gases or blacken a photographic plate, and these facts were used in their measurement. They could cause fluorescence in certain salts, which in fact was the means by which they were first observed. They could penetrate sheets of metal (usually aluminium), but the transmitted beam would be reduced in intensity; the percentage absorption gave a measure of the quality and homogeneity of the rays, whether they were hard (penetrating) or soft (easily absorbed). They could be scattered, say, by a block of paraffin wax, and the rays scattered in certain directions were polarised; that is to say, a *second* block of paraffin wax could only scatter them in certain directions. This made it seem probable that they were electromagnetic pulses in the ether (then

generally accepted as filling all space), but on the other hand their ionising properties seemed to prove that they were corpuscular in nature. Opinion among scientists was very much divided on this issue. Experiments in Germany on the diffraction of an X-ray beam on passing through a wedge-shaped slit, only a few hundreds of a millimetre broad at its widest part, showed that if the X-rays were electromagnetic waves, their wave-length must be of the order of only 1 A.U. Two other important facts had been demonstrated by Barkla in 1906. He showed that if heavy elements or compounds were irradiated by hard X-rays, then the scattered X-rays would be of two kinds. One kind consisted of X-rays of similar quality, the other kind were softer, much more homogeneous than the primary beam, and characteristic of the scattering material. These characteristic X-rays occurred in two distinct ranges of absorbability, and were called the K and L radiations. This was beautiful work, but the only quantitative part about it was the measurement of relative absorptions.

Natural radioactivity had provided one way of studying the atomic structure of a limited range of heavy atoms; and ionisation, the splitting of the atom into a heavy part carrying a positive charge and a light part (an electron) carrying a negative charge, was known to be attainable in a variety of ways. Practically nothing quantitative was known about nuclear charge, the number of electrons in an atom, or the atomic radii. In the periodic table the atoms had been arranged only in order of their atomic weights and their chemical behaviour. The processes of radiation in terms of changes in the electronic orbits or energy states were not understood, nor was the nature of valency bonds, that is, the way in which atoms link up together. The law of definite proportions and the law of multiple proportions helped chemists to see broadly how molecules were constructed out of atoms, or perhaps one should say, how molecules could be constructed out of atoms. But some of the 'molecules' required by mineral analysis were extraordinarily complex; and metal chemistry could not explain the existence of the free electrons which were emitted when the metal was heated, and which were almost certainly the carriers of heat and electricity in metals and alloys.

What was known about the states of matter before 1912? The comparative uniformity of the behaviour of gases had been one of the first discoveries of experimental philosophy. Pepys tells how Charles II, referring to the meetings of the Gresham College

philosophers (the forerunners of the Royal Society), laughingly described them as having done nothing but 'weigh ayre.' By the end of the nineteenth century the simple laws of gaseous behaviour were well known and had been accurately derived from the kinetic theory of the motion of small particles. Liquids provided a more difficult problem. It was known that if a gas were sufficiently compressed there was a particular (critical) temperature at which it was indistinguishable from its liquid. The earlier approach to the theory of liquid structure, therefore, was inevitably an extension of the theory of gases, but this did not prove very helpful in explaining some of the most characteristic properties of liquids at temperatures far removed from the critical temperature. After all, the main characteristic of an ordinary liquid, apart from fluidity, is *cohesion*; the atoms and molecules in a liquid have lost their independence, they are always in touch with their neighbours, and a mass of liquid therefore has a definite volume, though not a definite shape. But in spite of mutual influences, the atoms or molecules in a liquid are capable of relatively easy interchange of position; the more difficult this is, the more viscous the liquid is said to be. Both liquids and gases are intrinsically homogeneous; their properties are the same in all directions. Anyone who has cycled against the wind or swum against the tide may be inclined to question this, but these inhomogeneities are not inherent properties of the fluid; they vary with time and conditions. That is not so for solids.

The general properties of solids have been extensively studied. This is only natural, for solids play a most important part in every industry and in every part of our daily lives. But facts that are known without being explained are unsatisfactory to a philosopher, and until the advent of X-ray crystallography most attempts at any explanation of the general properties of solids were just vague guesswork. The position at the end of the nineteenth century was admirably epitomised by Professor Perry in a little book on Practical Mechanics, published in 1891. After mentioning many well-known facts about elasticity, fatigue, annealing, breaking strength under steady or fluctuating stresses and the heat-treatment of tools, he continues:

'... I need not give you any more items of a long catalogue of curious properties of materials which we do not yet understand. Workmen know of and depend upon many of these actions, but nobody seems to have any clear idea as to how they take place. It is

not merely that workmen temper steel and find that curious changes occur in the properties of their steel when it is altered a little in its chemical state; the philosopher and the workman are equally aware of these facts, and equally ignorant of their real nature.'*

The chemist, of course, knew a good deal about the behaviour of atoms and molecules and about the part they play in determining some of the properties of various substances. But the chemist's observations are mostly confined to gases, liquids and solutions. He explains processes. He not only requires relatively large numbers of molecules but requires them to be in a condition of change; they may be changing partners or changing their state of combination in any way. One of the greatest moments of chemistry was when Lavoisier explained the act of burning by proving that oxygen was taken from the air and combined with some of the atoms of the burning substance. But since the chemist is concerned with reactions, with atoms that are *doing something*, and since chemical reactions do not, in general, take place in the solid state, the solid state was virtually a closed book to chemists until 1912. Take even the simple case of solid carbon, which can exist as diamond, as graphite or as 'amorphous carbon.' The difference between the three forms was apparent both from a chemical and a physical point of view, but the extent to which these properties depend on the atomic and electronic arrangement was not appreciated and the arrangements themselves were quite beyond the reach of experiment.

Crystallographers did indeed make a study of materials in the solid state, but crystallography was essentially a geometrical science. Crystals grown or allowed to grow without disturbance are bounded by plane faces which may possess a brilliant polish (Pl. IV *b*). Owing to inequalities in their surroundings during growth, these faces may be of different sizes in different specimens, but the angles between the faces do not vary. Usually the number of different kinds of faces is very small, not more than three or four. Quartz crystals (fig. 35) grow as six-sided prisms bounded by six-sided pyramids; the angle between a prism and a pyramid face is always $38^{\circ} 13'$; and occasionally there are very small facets which make angles of $37^{\circ} 57'$ with the prism faces and $28^{\circ} 48'$ with the pyramid faces.

Crystals have directional properties which are related in a

* *Practical Mechanics*, by John Perry, M.E.; Cassell & Co. Ltd., London, 1891. Quotation from p. 67.

precise way to their form, that is, to definite directions in the crystal. They may cleave along certain planes or glide parallel to certain planes and along certain directions in those planes. The hardness of a diamond varies with direction, so that it must be properly orientated if it is to have a good cutting effect in a tool and the optimum wearing properties when in use. Electrical conductivity, thermal conductivity, thermal expansion, refractive index, diamagnetic susceptibility, all vary with direction in non-cubic crystals. If a single crystal of graphite is suspended by a fibre in a uniform magnetic field so that its cleavage face is vertical and it is free to rotate, it will always turn into a position such that the lines of force lie parallel to the cleavage face, and it will do so with considerable momentum.

These characteristic properties have long been known and were believed to indicate that *something* in crystals must be regularly arranged in space. It was not known whether the grouping or unit whose regular repetition led to the geometrical shapes and invariable interfacial angles of crystals and to their directional properties was an atom or a molecule, a part of a molecule or several molecules. In fact, there was nothing definite or quantitative known about the mutual positions of the atoms or the forces between them. Guesses had been made, very acute guesses, notably by Pope and Barlow in 1906-10; these were based on crystal symmetry and on chemical behaviour. But there was no way of confirming these hypotheses and it was equally difficult to criticise them.

As for solids which did not show the smooth regular faces of a crystal, massive metals and alloys, waxes, wood, bone, textile fibres, rubber: these could be examined under the microscope and their general physical properties determined, but of their atomic and molecular framework little or nothing was known.

HISTORICAL OUTLINE OF THE LAUE EXPERIMENT

This was the scientific position prior to 1912, when the famous Laue experiment was made. The historical aspect is worth stressing because, apart from the fact that it represents the birth of X-ray spectroscopy and crystallography, the significance of that experiment as an example of original and fundamental research is not always pointed out as clearly as it should be.

Nowadays, an X-ray tube, high-tension generating equipment

and crystal spectrometer can be bought for a few hundred pounds; a crystal can be set up, either in the form of a chunk of metal or of a powder or of a single specimen weighing less, perhaps, than a hundredth of a milligram; and some photographs can be taken and processed. Then the real work begins; finding out what they mean! The young research student is apt to look back longingly at von Laue's zinc blende and W. L. Bragg's rock-salt and think how easy they must have been. But they were not.

X-ray wave-lengths had not yet been measured and the Bragg law was unknown. It was still not certain that X-rays had any wave-length to be measured. W. H. Bragg firmly believed them to be corpuscular; and with good reason.

M. von Laue was a young man in 1912, an assistant lecturer in Professor Sommerfeld's department at Munich. A student, Paul Ewald, engaged in preparing a Ph.D. thesis, had been assigned a theoretical problem relating to crystal optics and he consulted von Laue about the non-convergency of a series. This drew von Laue's attention to the fact that a crystal was supposed to be a regular arrangement of matter on an atomic scale. The approximate volume V occupied by one atom or one molecule was known. Perrin and Millikan had recently measured Avogadro's number N , the number of molecules (or atoms) whose weight M in grams was numerically equal to the molecular (atomic) weight, and had found $N = 6.2 \cdot 10^{23}$. The volume of a gram-molecule (gram-atom) was therefore $N \cdot V$ and the density $\rho = M/NV$. Hence
$$V = \frac{10}{6.2} \cdot \frac{M}{\rho} \cdot 10^{-24} \text{ c.c.}$$
 For instance, in the case of diamond, composed only of carbon atoms, $M = 12 \text{ gm.}$, $\rho = 3.5 \text{ gm./c.c.}$, therefore $V = 5.5 \cdot 10^{-24} \text{ c.c.}$ The linear separation of the atoms must therefore be of the order of 1 or 2 A.U. But Sommerfeld had already shown that *if* X-rays were electromagnetic waves their wave-length would be about 1 A.U.; and they would thus be just of the right size to be diffracted by a crystal lattice, acting as a three-dimensional diffraction grating. The possibility of such an experiment was discussed between the staff and research students, and two of them, Friedrich and Knipping, who had just taken their doctorates under Professor Röntgen, agreed to try it. What crystal should they use? It appears that they did not at first expect that the primary X-ray beam would be simply diffracted from the crystal acting as an optical grating. They knew that their X-ray beam was heterogeneous and that it might

therefore give very complicated effects. But they also knew that if the irradiated crystal contained heavy atoms, of atomic weight > 50 , it would emit the characteristic, homogeneous X-radiation discovered by Barkla, and this radiation might interact with the crystal producing it, and might give regular diffraction effects. They thought first of copper (atomic weight 63.6), but since it was not easy to get a single crystal of metallic copper, they first used a good crystal of copper sulphate, $\text{CuSO}_4 \cdot 5\text{H}_2\text{O}$. Actually they could hardly have made a worse choice, for copper sulphate (fig. 1) is a crystal of the lowest kind of symmetry and of relatively complicated structure, so that whatever diffraction effects were observed would be most difficult to interpret. However, the object of the first experiment was only to see whether any suggestive results were obtained; and at first they were not. This was because their experimental arrangements were unsuitable.

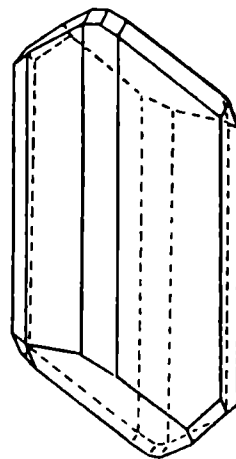


FIG. 1. Triclinic crystal of $\text{CuSO}_4 \cdot 5\text{H}_2\text{O}$.

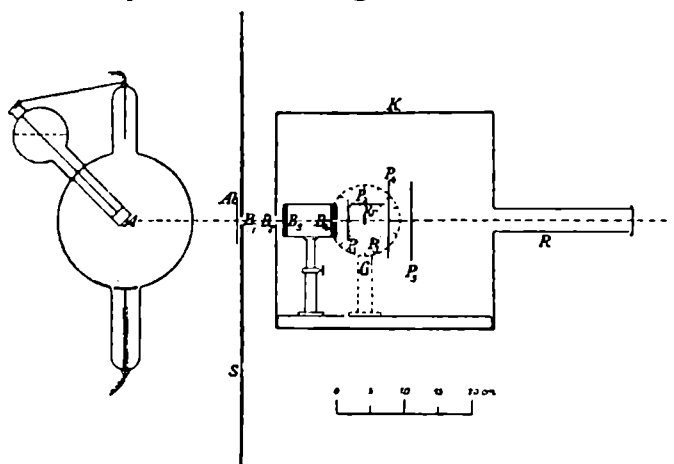


FIG. 2. Laue's original experiment, carried out by Friedrich and Knipping.

Distance, anticathode to crystal	. . .	35 cm.
„ crystal to plates P_1, P_2 or P_3	. . .	2.5 cm.
„ „ „ plate P_4	. . .	3.5 cm.
„ „ „ „ P_5	. . .	7.0 cm.

Fig. 2 shows the arrangement adopted, which was similar to that formerly used for investigating the scattering of X-rays by blocks of carbon or paraffin. The photographic plate was at first

placed either *between the crystal and the X-ray source* (P_1), or *parallel to the X-ray beam* (P_2 , P_3). This was reasonable enough, since in the case of scattering experiments that was just where *scattered* X-rays were found. But it was not where *diffracted* X-rays would be found, and it was not until Friedrich and Knipping, trying every possibility, however unlikely, placed the plate *behind* the crystal (P_4), that a pattern was observed. The pattern, seen on Pl. I *a*, was a very asymmetric one, but it proved that something was happening. A second plate was placed behind the first, and the enlarged pattern then obtained showed that the diffracted X-rays *must be travelling in straight lines*. The apparatus was refined and better pictures obtained; the crystal was powdered roughly and the pattern broke up into flecks; then it was powdered finely and the pattern disappeared, leaving only a general fogging of the plate. A single crystal was moved parallel to itself at a constant distance from the plate; the pattern did not change. But it did change when the crystal orientation was varied.

Then it was decided that a more symmetrical crystal should be examined and zinc blende, ZnS , was chosen because of the heavy Zn atom (atomic weight 65.4) that it contained. A crystal plate of ZnS , measuring $10 \times 10 \times 0.5$ mm., was borrowed and it was found that when the X-ray beam, 1 mm. diameter, was incident along the cube axis, a square pattern was obtained; with the beam along the cube diagonal the pattern was trigonal; with the beam along a face diagonal the pattern showed 2-fold symmetry only. Other cubic crystals were tried; single crystals of Cu, NaCl, FeS_2 , CaF_2 , Cu_2O ; they all gave spots on the photographic plate in the *same pattern*, but with *different intensities*; some spots being absent altogether in some cases. Neither Na (atomic weight 23) nor Cl (atomic weight 35.5), however, were heavy enough to give characteristic secondary radiation; and it was then found that even a slip of diamond, composed only of light carbon atoms, also gave a good pattern; and not merely a transmission pattern, but also a pattern on the side (Pl. I *b*) and back plates (cf. Pl. I *c*). One hypothesis put forward by Laue to account for the high intensity of the back reflections from diamond was that in this hard substance the thermal vibrations might be smaller, a suggestion that is in fact quite correct.

The experiments with rock-salt and diamond crystals showed that it was not characteristic X-rays *from the crystals themselves* that were responsible for the patterns obtained; but it still

remained to be proved that they were due to X-rays at all. They might have been caused by secondary electrons, or by some new kind of radiation. If they were due to X-rays, were the X-ray beams giving the spots on the pattern of the same quality, the same penetrating power, as was the primary beam? The experiments needed considerable extension before they could be regarded as conclusive. One of the original hypotheses, that heavy atoms were necessary, had turned out to be wrong; but that did not matter; careful investigation always leads away from a wrong hypothesis and in a right direction. The experimenters measured the penetrating power of the primary and the various diffracted beams by interposing Al sheet, and found that the various spots on the photographs were given by X-rays of differing quality, but that the range of X-rays responsible for the diamond pattern was roughly the same as that which gave the ZnS pattern. The shapes of the spots were also studied; and it was noted that although the X-ray tube became much harder through continuous running and had to be regenerated several times during the course of the experiments, the positions of the spots on the pattern were independent of the quality of the incident beam.

So far the experiments had been carried out successfully and with great care. But in the attempt to interpret the pattern of ZnS, von Laue's treatment took the wrong turning. It began well: he first considered the diffraction effects to be expected from a row of diffracting centres, regularly spaced at distance a apart. The incident beam makes an angle ϕ_0 , and a diffracted beam makes an angle ϕ , with the row of centres. Reinforcement of diffracted beams from successive centres occurs when the path difference of the beams is a whole number of wave-lengths, that is, when $a(\cos \phi_0 - \cos \phi) = h\lambda$, where $h = 0, \pm 1, \pm 2, \pm 3 \dots$ (fig. 3). Diffraction by a cubic arrangement of centres, the incident beam being parallel to a cube axis, may be regarded as the superposition of diffraction by three mutually perpendicular rows of centres, one parallel and

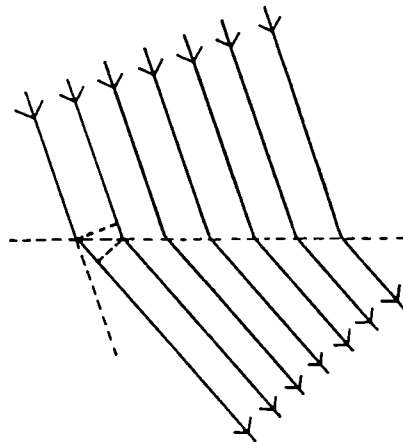


FIG. 3. Diffraction by a row of scattering centres.

two perpendicular to the incident beam, according to the three Laue conditions

$$\begin{aligned} a \cos \phi_1 &= h_1 \lambda \\ a \cos \phi_2 &= h_2 \lambda \\ a(1 - \cos \phi_3) &= h_3 \lambda, \end{aligned}$$

$\cos \phi_1$, $\cos \phi_2$, $\cos \phi_3$ being the direction cosines of the diffracted beam relative to the three cube directions x , y , z (fig. 4).

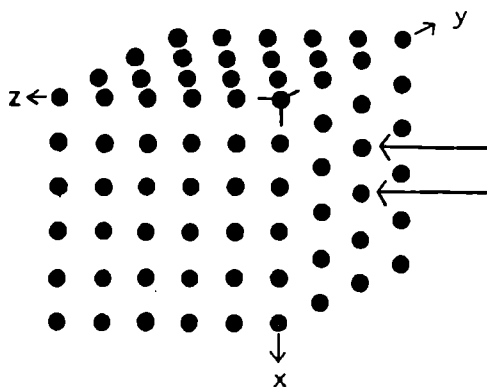


FIG. 4. Diffraction by a cubic arrangement of scattering centres; X-rays parallel to cube edge.

The directions in which the three Laue conditions are simultaneously fulfilled (h_1 , h_2 , h_3 having integral values) are the directions in which spots will be found on a photographic plate. But in general such a simultaneous fulfilment of the three conditions can only take place for special values of λ/a . In order to make an estimate of the value of a , von Laue wrongly assumed that the

ZnS structure was built up on a *simple* cubic framework, and then he found that if he supposed that the three conditions given above need only be *approximately* fulfilled together, he could explain all the observed spots by a relatively few values of the wave-length λ . He did not, however, try enough patterns, or he would have found that the range of values of λ would have to become bigger and bigger, and he would have noted the absence of some spots that ought to have been there. He thought that the diffraction centres in the crystal were not the atoms themselves but the points of the space-lattice, the framework; and this was not unreasonable, for the structure suggested by Pope and Barlow for ZnS had been a very complicated one containing 32 atoms in the repeating group, while on the other hand the pattern obtained for *any* cubic crystal was a characteristically simple one, invariant except for intensity relationships. From this point of view, however, the patterns could not be expected to give very much information about the atoms in the crystal, although they provided powerful new evidence of the electromagnetic wave nature of the X-rays.

EARLY EXPERIMENTS IN ENGLAND

But not conclusive evidence; and at this point the research was taken up in England, by W. L. Bragg at Cambridge, by W. H. Bragg at Leeds, and by Moseley and Darwin in Manchester. W. H. Bragg first checked the fact that the diffracted beams did really consist of X-rays, that they could ionise gases, and that they were absorbed like X-rays. He used ionisation methods to detect the directions of maximum diffraction; Moseley and Darwin worked with photographic methods and found that although the primary and diffracted beams were not equally penetrating, their penetrating power in Al sheet was of the same order.

W. L. Bragg, still believing that the X-rays might be corpuscular, investigated the possibility that the spots on the pattern might have been caused by the deviation of corpuscles down avenues between the atoms in the crystal. This explanation did not work, but he noticed a curious fact about his photographs. This fact was that the diffracted beam responsible for any spot was slightly *converging* (fig. 5), and it could be quite simply explained if the slightly *divergent* primary beam was being *reflected* from some kind of planes in the crystal. An easy test could be applied: if the crystal were turned slowly, the spot, if due to some kind of reflection, should move slowly and synchronously, like an optical reflection from a rotating mirror. The test succeeded. Now, what could be the 'mirrors' in the crystal? If they were planes in which there was a high atomic density, then it might be expected that a crystal such as mica, having an excellent cleavage surface, would prove an excellent X-ray reflector. This was also successfully shown to be the case. W. L. Bragg then turned his attention to *Laue* patterns, obtained with a heterogeneous incident

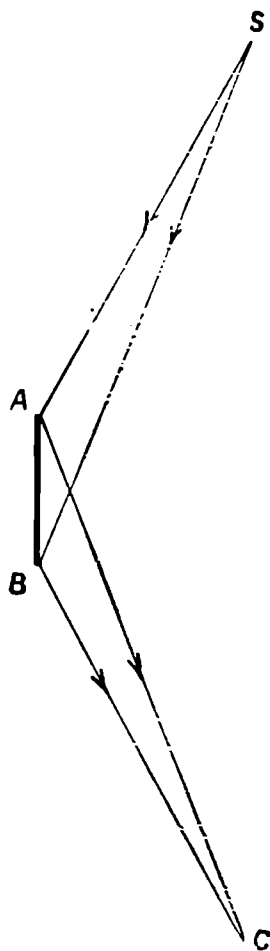


FIG. 5. A divergent incident beam gives a convergent diffracted beam. (Laue method.)

(W. H. & W. L. Bragg, *X-rays and Crystal Structure*: Bell.)

beam and a stationary crystal. Instead of at first investigating ZnS, which although cubic has not the full symmetry of the cubic system, and to which Pope and Barlow had assigned a rather

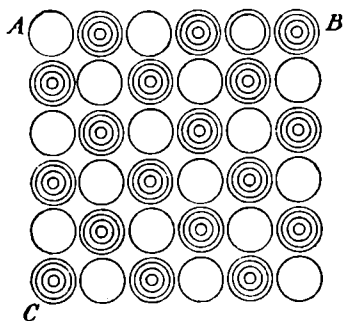


FIG. 6. Chessboard pattern of KCl, etc.

complicated structure, he tackled the more symmetrical alkali halides, KCl, NaCl, KBr, KI; and he assumed, as a working hypothesis, the three-dimensional chess-board structure (fig. 6) which had been suggested by crystallographers many years before. (A model of this kind for NaCl is to be seen in Edinburgh University, dating back nearly to 1880.) He found that such structures did indeed explain all the spots found on the Laue

patterns and they also explained the variations in intensity of the spots when heavy atoms were substituted for light ones, provided that *three* assumptions were correct: First, that the various planes of atoms in the crystal could act as 'X-ray mirrors.' Second, that the X-ray beam was quite heterogeneous, consisting not of a few wave-lengths, but of a continuous range of wave-lengths. Third, that the scattering power of the atom was dependent upon its atomic weight. Using a corrected value of Avogadro's number, $N = 6.06 \cdot 10^{23}$, he calculated d , the distance apart of the Na and Cl atoms, as being 2.81_4 A.U. (really kX), from $\rho = M/NV = M/2Nd^3$, where $\rho = 2.163$ gm./c.c., $M = (23.0 + 35.6)$ and $V = 2d^3$ (since Na + Cl, volume V , contains 2 atoms).

W. L. Bragg also showed that, given X-ray diffraction by regularly spaced atomic centres in a set of planes of spacing d , and using *homogeneous* radiation of wave-length λ , reinforcement would take place only at those angles which fulfilled the simple condition $n\lambda = 2d \sin \theta$, n being an

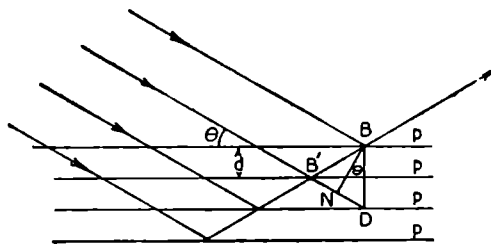


FIG. 7. Historical proof of the formula $n\lambda = 2d \sin \theta$.

(W. H. & W. L. Bragg, *X-rays and Crystal Structure*: Bell.)

integer and θ the glancing angle of incidence of the primary beam, or of reflection of the diffracted beam, relative to the atomic planes (fig. 7), within the crystalline medium. This

equation is really only another way of expressing the simultaneous fulfilment of the three Laue conditions. For a cubic lattice, and the incident X-rays along a cube axis, this is easily proved. The Laue conditions are:

$$\begin{aligned}a \cos \phi_1 &= h_1 \lambda \\a \cos \phi_2 &= h_2 \lambda \\a(1 - \cos \phi_3) &= h_3 \lambda,\end{aligned}$$

and since $\cos \phi_1$ etc. are direction cosines, we have

$$\cos^2 \phi_1 + \cos^2 \phi_2 + \cos^2 \phi_3 = 1, \text{ and } \cos \phi_3 = \cos 2\theta;$$

hence $\lambda = \frac{2a \sin \theta}{\sqrt{h_1^2 + h_2^2 + h_3^2}}$, which is identical with $n\lambda = 2d \sin \theta$

if $\frac{d}{n} = \frac{a}{\sqrt{h_1^2 + h_2^2 + h_3^2}}$.

The integers $h_1 h_2 h_3$ are the Miller *indices* of the reflecting plane, and will be met again in Chapter III.

While W. L. Bragg was investigating the structures of simple crystals by this method, W. H. Bragg constructed an apparatus, the ionisation spectrometer, with which the position and intensity of X-rays reflected from crystal planes could be accurately measured. The ionisation or Bragg spectrometer is like an optical spectrometer, in which X-rays take the place of light, a crystal replaces the usual prism or diffraction grating, and an ionisation chamber and electroscope or recording device is substituted for the telescope or photographic plate (fig. 8). Using first mica and then other crystals, W. H. Bragg showed that the beam from an X-ray tube having a Pt target consisted of continuous radiation analogous to white light plus several types of monochromatic radiation of different wave-lengths probably characteristic of the Pt emitter. Knowing the spacing d of the reflecting planes of NaCl, it was possible to use the Bragg law $n\lambda = 2d \sin \theta$ to measure λ very accurately, for these monochromatic rays. Knowing λ , it was then possible to measure d very accurately, for crystals other than those simple substances already investigated by the Laue method. Hence it would also be possible to obtain, by this new method, the values of M (molecular weight), ρ (true crystal density) and atomic sizes, in cases where these were not already known. W. H. Bragg also measured the critical wave-lengths corresponding to absorption edges, wave-lengths at which

a sharp step in the absorption of X-rays by an element takes place.

Two main lines of investigation, therefore, developed from the early use of the Bragg spectrometer: (1) The determination of crystal structure, using X-rays of known wave-length; *X-ray crystallography*. (2) The determination of X-ray wave-lengths,

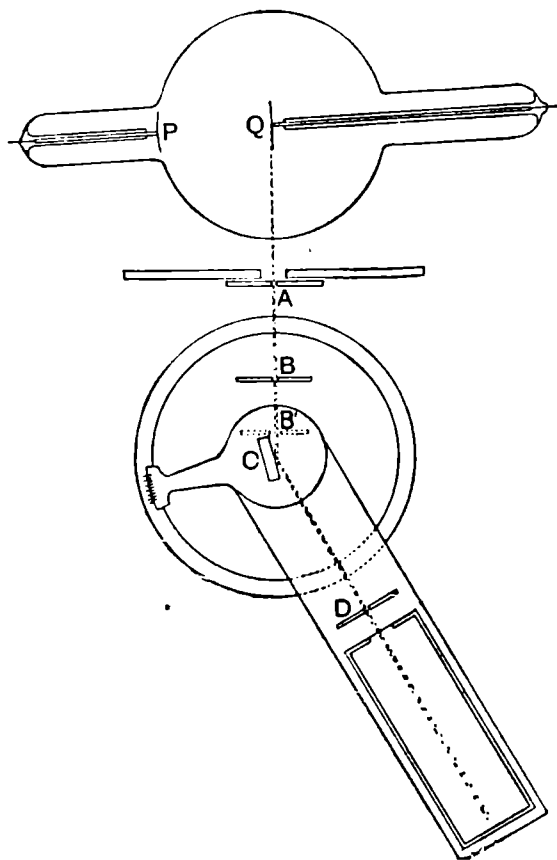
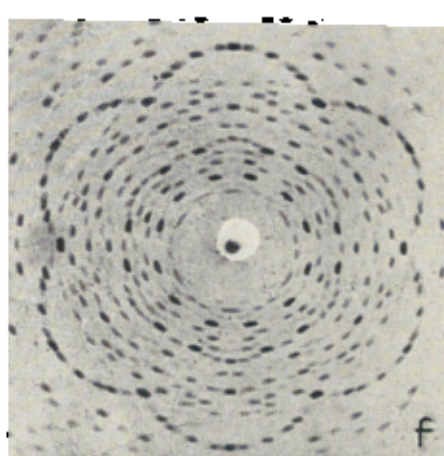
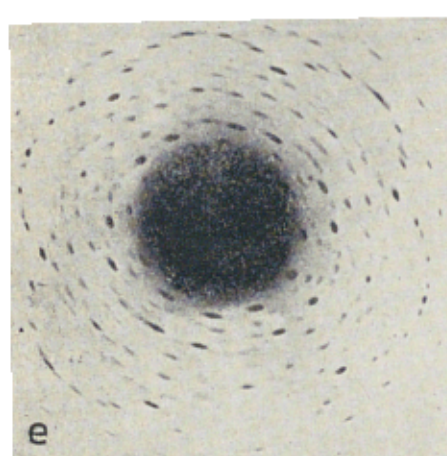
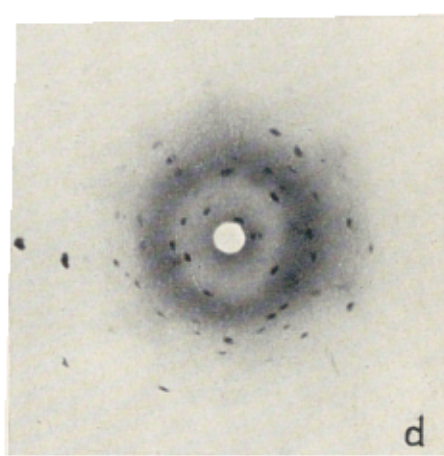
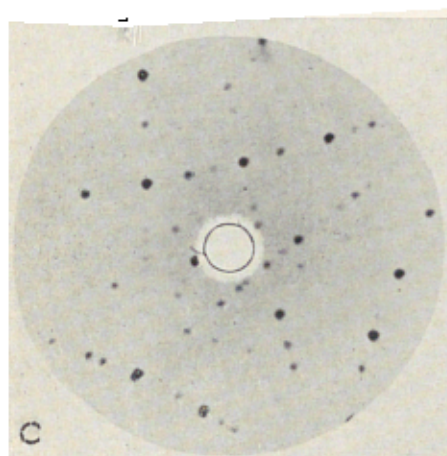
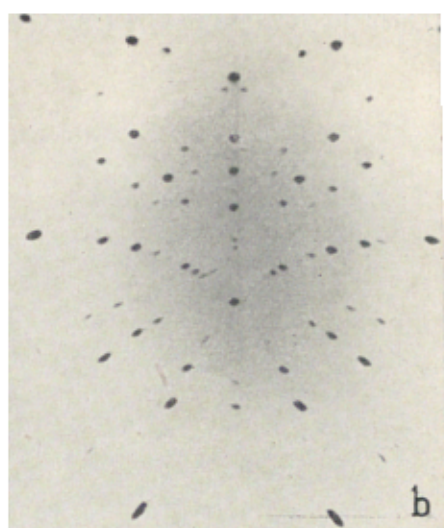
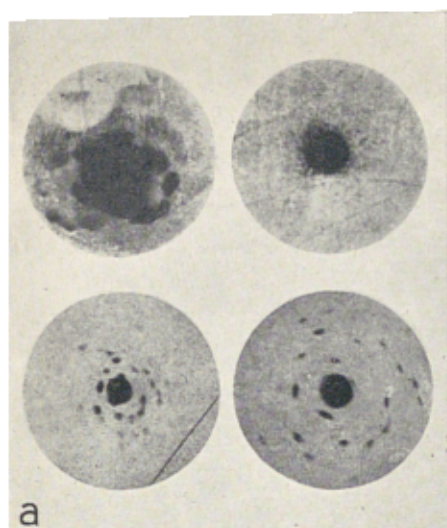


FIG. 8. Bragg ionisation spectrometer.

(W. H. & W. L. Bragg, *X-rays and Crystal Structure*: Bell.)

emission or absorption, using crystals of known structure; *X-ray spectroscopy*.

Less directly, it also exercised a profound influence on the development of the theories of radiation and of atomic structure. W. H. Bragg was able to show that when the quantum law suggested by Max Planck in 1906, $E = h\nu = 1.965 \cdot 10^{-6}/\lambda$, was used to calculate the *quantum energies* of the K and L radiations that he had observed, these calculated energies corresponded to the energy



(a) Original Laue photographs of $\text{CuSO}_4 \cdot 5\text{H}_2\text{O}$. *Top*—single crystal with large X-ray beam; roughly powdered crystal. *Bottom*—single crystal with narrow X-ray beam, photographic plates at different distances.

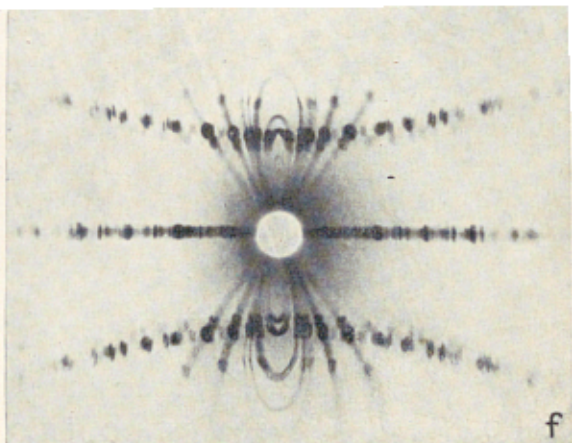
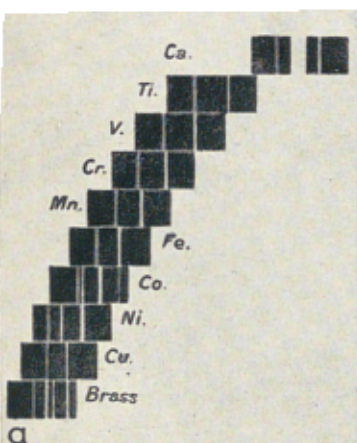
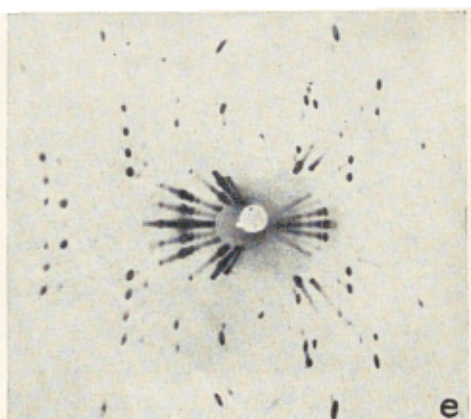
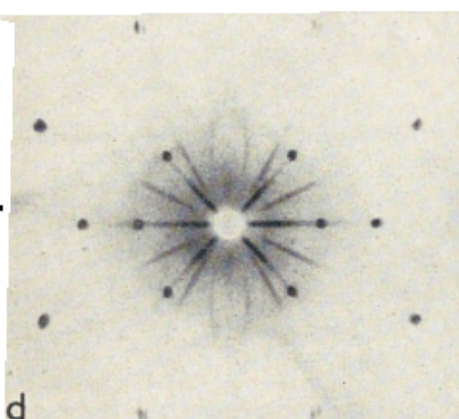
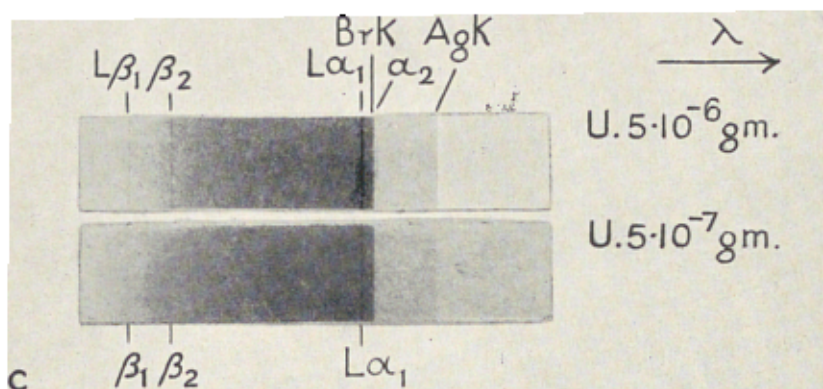
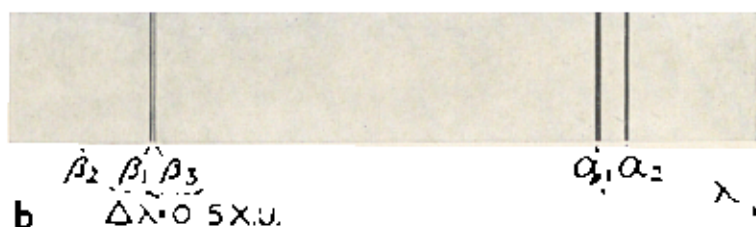
(b) Laue photograph of diamond; photographic film *parallel* to X-ray beam. Radiation from Fe target.

(c) Black reflection Laue pattern of sapphire crystal, oblique orientation. Radiation from Cu target (Rooksby).

(d) Laue photograph of ice, melting during exposure, showing diffuse ring due to water superimposed on sharp spots from ice.

(e) Laue photograph of an hexagonal crystal without central stop.

(f) Same as (e) but with central stop.



(a) (at foot) Moseley's spectra, showing progressive displacement with changing atomic number.

(b) K spectrum of rhodium, showing α_1 , α_2 , β_1 , β_2 and γ lines (Cauchoux).

(c) Identification of small quantities of uranium by the L spectrum. The BrK and AgK absorption edges may also be seen (Cauchoux).

(d) Rotation photograph of sodium single crystal, showing white radiation streaks with short wave-length limit and intensity maximum.

(e) Oscillation photograph of triphenylbenzene.

(f) Rotation photograph of sorbic acid, showing extra reflections due to contamination of CuK radiation by WL.

of the cathode rays used to excite the radiations. This was support for the corpuscular theory of X-rays, but clearly the experiments as a whole showed that although in X-ray phenomena energy was transferred in quanta, in other respects X-rays behave like electromagnetic waves. Moseley and Darwin stated the problem succinctly in a letter to *Nature* dated January 30, 1913. 'Since the rays are reflected, they must be some kind of pulse with an extended wave-front, yet after reflection they retain their corpuscular character. Thus the energy of the X-rays appears to show the contrary properties of extension over a wave-front and concentration in a point.' W. H. Bragg, in an earlier letter, dated November 28, 1912, put the matter very simply: 'The problem then becomes, it seems to me, not to decide between the two theories of X-rays, but to find . . . one theory which possesses the capacities of both.'

Thus the early experiments in X-ray crystallography underlined the necessity for the development of the quantum theory of radiation, of which Bohr's theory of atomic structure, outlined in 1913, was the next manifestation.

Moseley and Darwin, working in Manchester under Rutherford, had continued to investigate the rays reflected from crystal planes, by photographic methods, and they were able to confirm the presence of characteristic lines as well as of a continuous spectrum. The characteristic lines were reflected at special angles only, the continuous spectrum at all angles. Moseley continued this investigation alone, making a systematic photographic record of the line spectra of all known elements from Al to Au that could be obtained either pure or in combination with other elements. He found that they formed a continuous series (Pl. II *a*); that when each element was assigned a *number* beginning with Al = 13, those numbers plotted against the square root of the frequency for a given line of the spectrum in each case gave a straight-line graph. These *atomic numbers* represented the order of the elements in the periodic table, arranged in respect of their atomic weights. Moseley's conclusions, which were given in half a page at the end of a brief paper of only 10 pages (*Phil. Mag.* (1914), 27, 713) have made scientific history. They were as follows:

1. Every element from aluminium to gold is characterised by an integer N which determines its X-ray spectrum (Pl. II *a, b*). Every detail in the spectrum of an element can be predicted from the spectra of its neighbours.

2. This integer N , the atomic number of the element, is identified with the number of positive units of electricity contained in the atomic nucleus.

3. The atomic numbers for all elements from Al to Au have been tabulated on the assumption that N for Al is 13.

4. The order of the atomic numbers is the same as that of the atomic weights, except where the latter disagrees with the order of the chemical properties.

5. Known elements correspond with all the numbers between 13 and 79 except three. There are here three possible elements still undiscovered.

6. The frequency of any line in the X-ray spectrum is approximately proportional to $A(N - b)^2$ where A and b are constants.

This work by Moseley (1) helped to form the basis of the modern theory of atomic structure and radiation; (2) provided a better method of classification of the elements; (3) gave a powerful new way of discovering new elements; (4) allowed elements in minerals and in chemical compounds to be identified without the destruction of the material. Using modern apparatus such as the Cauchois spectrograph, even 10^{-9} or 10^{-10} grs. of an element can be identified (Pl. II *c*).

DIFFRACTION FROM NON-CRYSTALLINE OR IMPERFECTLY CRYSTALLINE MEDIA

So far we have discussed only the diffraction of X-rays by a regular array of atoms. The development of X-ray crystallography proper will be dealt with systematically in the succeeding chapters. But X-ray analysis has also helped us to understand the structure and arrangement of atoms and molecules in the gaseous and liquid states. All scattering of X-rays takes place by means of the forced vibrations of the electrons, and the X-rays scattered from different electrons even of the same atom will in general have different phases and will interfere with each other. The intensity of scattering (I) will be a maximum in the forward direction, for which $\theta = 0$, and it will fall off (fig. 9) as θ increases, though less rapidly for long wave-lengths. The form of the 'atomic scattering factor' curve, I v. $\frac{\sin \theta}{\lambda}$, can be calculated for various assumed electronic distributions in the atom, and a comparison with experiment will then give useful information

about this electronic distribution. The simplest kind of experiment is a determination of the scattering of X-rays, for different values of $\frac{\sin \theta}{\lambda}$, for gases such as neon in which all the atoms behave quite independently. Such gases give a scattering curve which is identical with the atomic scattering factor (p. 105). The form of these curves proves conclusively that the Bohr atomic model is not satisfactory, and that the Sommerfeld model, in

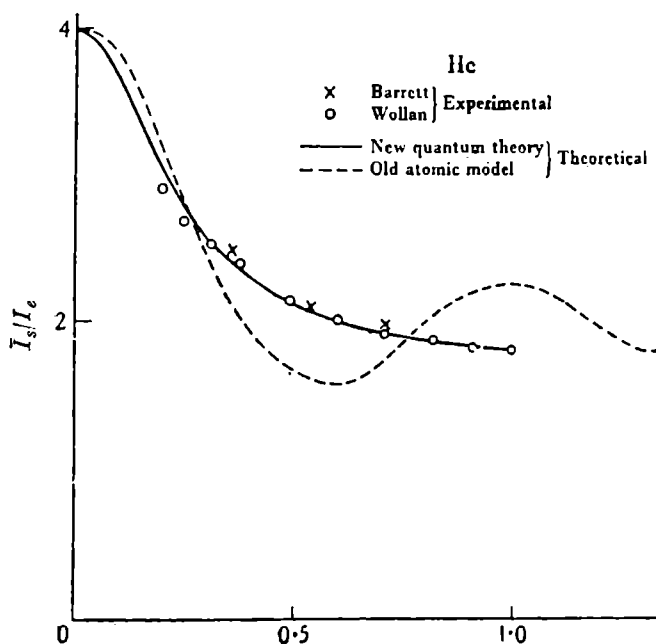


FIG. 9. Atomic scattering curve for He.

(Pirenné, *The Diffraction of X-rays and Electrons by Free Molecules*: C.U.P.)

which the electrons are not located in definite orbits, is much nearer to the truth. But the atomic scattering factor is fundamental to scattering by atoms in any state of combination and can be deduced, or alternatively must be allowed for, whatever the medium on which measurements are being made. Scattering of X-rays by gases in which the molecules contain heavy atoms can, however, tell us more. In carbon tetrachloride, CCl_4 , for instance, scattered rays from Cl atoms in the same molecule will reinforce or interfere with each other at definite angles, giving a curve (fig. 10) from which the mutual distances and arrangement of the Cl atoms can be deduced. The Cl to Cl distance in a single molecule of this substance is 2.99 A.U., but in chloroform,

CHCl_3 , the distance increases to 3.11, and in CH_2Cl_2 it is 3.21 A.U., owing to the mutual repulsion of the like atoms. It is found also, for example, that although in $\text{ClH}_2\text{C} \cdot \text{CH}_2\text{Cl}$ (1.2 dichloroethane) there is, theoretically, free rotation about the C to C bond, yet in fact the Cl atoms spend most of their time in the 'trans'-position, at a maximum distance from each other of 4.4 A.U.

The study of liquids and solutions is even more fascinating, but the X-ray scattering curves are by no means easy to interpret

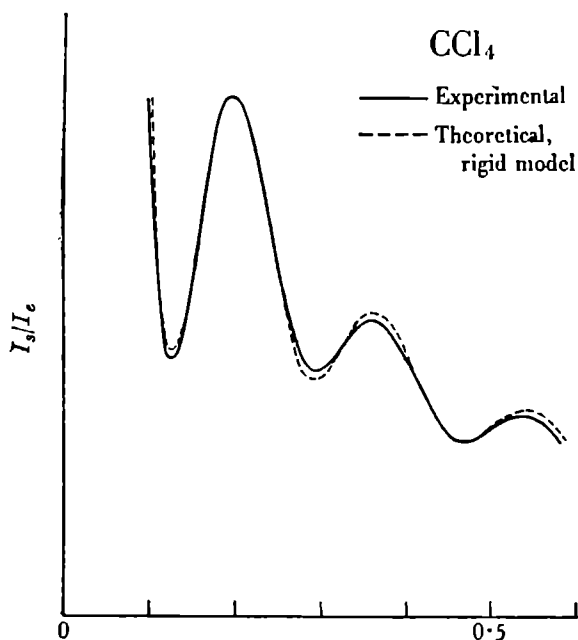


FIG. 10. Molecular scattering curve for CCl_4 .

(Pirenne, *The Diffraction of X-rays and Electrons by Free Molecules*: C.U.P.)

(Pl. VI *e*). It is clear that the atoms in a liquid cannot approach closer than a certain minimum distance to each other, and that one atom cannot have more than a certain maximum number of neighbours. There is a tendency to the formation of temporary groupings which simulate crystallographic regularity, but which are persistently broken up by thermal vibration. Even the configuration of these groupings is not constant; it is a function of temperature and pressure. Nevertheless, especially where molecules are flat or elongated, or maintain a definite shape of space occupied, even when thermal movements are allowed for, there will be in the liquid certain preferred distances between atoms or molecules, and these will give diffraction rings of varied sharpness.

In solutions the hydration of ions can also be detected from X-ray photographs. Thus the present tendency is for a liquid to be regarded more like a solid possessing fluidity, rather than as a gas showing cohesion.

X-ray photographs also show that the break between the solid and the liquid state is in general just as sharp as the sharpness of the melting-point would lead us to expect. If a crystal melts during an X-ray exposure, the photograph will show sharp spots or lines plus a diffuse liquid ring or rings (Pl. I *d*).

Some special substances, however, form intermediate states (sometimes called 'liquid crystals') in which there is partial arrangement, without entire loss of fluidity. In the 'nematic' state the long molecules are arranged with their lengths parallel to each other, but without any periodicity; like a large number of parachutists in the air. In the 'smectic' state there is orientation in equi-spaced planes, but no side-ways periodicity, like people moving freely on the various floors of a skyscraper. These states have received detailed study on account of their peculiar optical and magnetic properties, properties which show discontinuities at definite temperatures.

It is interesting that X-ray analysis has revealed that textile and other fibrous substances, including minerals such as asbestos, also have a partial arrangement of their constituent atoms, though without the accompanying fluidity of liquid crystals. Other apparent solids, such as glass, have no regularity of structure and no fluidity under ordinary conditions, but they also have no definite melting-point, and they give X-ray diffraction rings similar to those of liquids. The structure of glass is almost certainly one (fig. 11) in which Si and O atoms are linked together so that each Si atom is surrounded by four O atoms and each O joined to two Si atoms, but without further regularity of arrangement. Perhaps the difference between a glass, a liquid and a crystal may be illustrated by the suggestion that an amorphous solid, such as glass, is like a crowd waiting to see a procession, regularly arranged in time but not in space, or

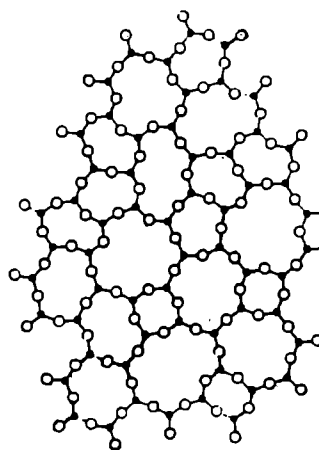


FIG. 11. Suggested 2-dimensional structure of glass (after Zachariasen). The fourth Si—O bond would be in the third dimension.

at least subject only to very slow rearrangement; a liquid is like a shopping crowd, regularly arranged neither in time nor space, though occasionally groups may form which are stable for a short time; while a crystal is like a class of children arranged for drill, but standing at ease, so that while the class as a whole has regularity both in time and space, each individual child is a little fidgety! Perhaps one of the most interesting discoveries made in the comparatively early history of X-ray analysis was the fact that silk and even paper are more crystalline than glass.

CHAPTER II

GENERATION AND PROPERTIES OF X-RAYS

X-RAYS are generated when high-speed electrons strike the atoms of any element. The production of X-rays therefore depends on, firstly, producing electrons, and secondly, on giving them a sufficiently high speed in the direction of a target, generally a metal target. This high speed is attained by having a high vacuum in the X-ray tube, and applying a high accelerating force (difference of potential) in the right direction across it. Let us begin by considering what kinds of X-rays we get under different conditions and what we can do with them; then we shall know what to ask for in our X-ray equipment.

NATURE AND PROPERTIES OF X-RAYS

An X-ray spectrum can be either a continuous or a line spectrum.

The *continuous spectrum* (also called white or general radiation) is always produced if X-rays are produced at all; it is due to the sudden reduction of energy of the bombarding electrons. The

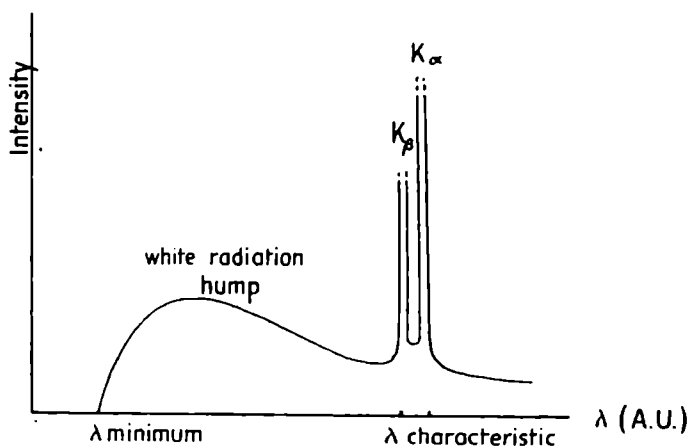


FIG. 12. Continuous X-ray spectrum with characteristic line spectrum superimposed.

spectrum appears to begin abruptly at a short wave-length limit and theoretically extends to infinity in the long wave-length direction (fig. 12). There is an intensity maximum, at a wave-

length related to target thickness, which becomes more pronounced and shifts to shorter wave-lengths as the voltage V across the X-ray tube is increased. The energy in the continuous spectrum is proportional to $Z \cdot V^2$ (Z being the atomic number of the target element) and is therefore greater for the heavy elements. The short wave-length limit, λ_{\min} , corresponds to the case where the bombarding electrons give up *all* their kinetic energy in the production of X-rays. λ_{\min} is related to the maximum voltage, V_{\max} , across the X-ray tube by means of the quantum formula previously quoted

$$E = V \cdot e = h\nu = \frac{hc}{\lambda}; \quad \text{from which, } \lambda_{\min} \cdot V_{\max} = 1.234 \cdot 10^{-4}$$

(cm. volts); a relationship which is easy to remember and which can be used as a means of measuring V_{\max} . Alternatively, a measure of both λ_{\min} and V_{\max} will give an estimate of the fundamental Planck constant h .

Important practical consequences of the emission of the continuous spectrum are:

(1) That X-ray patterns can be obtained from a stationary crystal. For such a crystal, d and θ in the Bragg relation $n\lambda = 2d \sin \theta$ are both invariable. It is therefore necessary to be able to vary λ , that is, to use the original Laue method. Laue photographs (using white radiation only) may be used to study crystal symmetry, crystal orientation, distortion and texture. In particular, the use of 'back' photography of massive specimens (with the photographic film *between* the specimen and the X-ray source) (Pls. I c, V a) has many industrial applications. Pl. I e shows a Laue photograph of a hexagonal crystal having full six-fold symmetry. But it is spoilt by halation due to the intense photographic effect of the main, undeviated X-ray beam. In order to prevent this a small lead stop is often put just in front of the photographic film, where the beam would strike it (Pl. I f).

This has also been done in the case of Pl. III e, a Laue photograph of the mineral bröggerite; in this photograph the spreading of the spots radially indicates a small disorientation of the crystal grains which together compose an approximately single crystal.

(2) This photograph also, however, illustrates the fact that white radiation may be scattered by the air in the X-ray camera, to give an unwanted and often intense halo just around the main beam. This can be prevented by using a vacuum or a hydrogen-filled

camera, or more simply (fig. 13) by putting a very small Pb stop just behind the crystal instead of just in front of the film. Of course, if a circular camera or a back-reflection camera is used, care must be taken to avoid scattering from the Pb stop itself. In that case a deep but narrow X-ray trap is brought close up to the crystal, to 'collect' the central beam.

(3) On photographs taken with a rotating or an oscillating crystal (Pl. II *d, e, f*) the white radiation gives radially directed streaks. Each reflecting plane gives, in

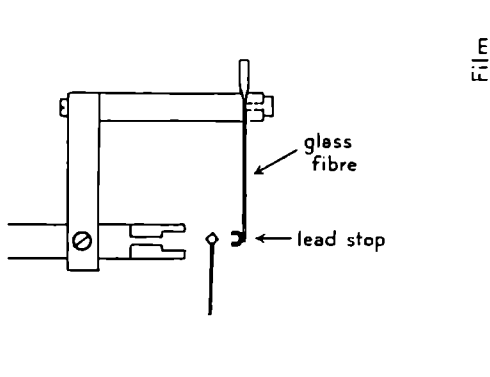


FIG. 13. Small lead stop for central X-ray beam, to prevent air-scattering and halation on photographic film.

fact, a complete (or in the case of the oscillating crystal a partial) spectrum of the wave-lengths emitted from the X-ray tube. If the specimen is powdered, white radiation in the incident beam contributes, unevenly in a radial direction, to the general background of the powder photograph.

A *line spectrum*, characteristic of the target material, is emitted when the energy of the bombarding electrons is sufficient to ionise the atoms of the target by the removal of electrons from the innermost orbits. In X-ray crystallography we almost exclusively use the K spectrum, the X-rays which are emitted when the energy of the innermost electrons changes from that of a higher energy state into that of the normal or ground state of the atom. The elements Cr to Ag are those most frequently employed, the K lines of Cu being much the most useful for general purposes. The main lines of the K spectrum are α_2 , α_1 , β_1 , which in the case of Cu are emitted with relative intensities of approximately 5:10:2 at the target surface. These lines (Pl. II *b*) are all emitted together when the voltage applied to the X-ray tube exceeds a certain minimum critical value, the excitation voltage, and their intensity ratio is independent of the applied voltage. Thus the β radiation cannot be weakened or eliminated by alteration of voltage. There are other line spectra corresponding to different energy levels in the atom, but of these only the L spectrum need concern us, and for this reason. It sometimes

happens that a Cu target becomes contaminated with a layer of W, some of whose L lines occur in the CuK wave-length region. This can be particularly troublesome in powder photography, where it is most desirable to have pure radiation; and even in rotation photographs (Pl. II *f*) spots due to WL radiation may very well cause confusion. It is necessary, for the same reason, to avoid impurities in the target metal.

As the applied voltage rises above the critical excitation voltage, the output of K radiation increases, but so also does that of the white radiation, and in practice there is an optimum voltage for *contrast* between line spectrum and background. For a Cu target this optimum corresponds to a *steady* potential difference of about 30 kV, but if the potential difference is intermittent or varying, the value of the optimum maximum voltage may have to be found empirically.

It was mentioned in Chapter I that X-rays could be excited not only by high-speed electrons but by primary X-rays of sufficient energy. This is seldom done deliberately in X-ray crystallographic technique, but it is often done involuntarily.

Let us consider what happens to high-energy X-rays, forming part either of the characteristic or of the continuous spectrum, when they are incident on a thin sheet, thickness t , of absorbing material:

(1) Some will get through, unchanged in direction but reduced in intensity from I_0 to I . $I = I_0 e^{-\mu t}$, where μ is the *linear absorption coefficient*.

(2) Some of the absorbed energy is used in heating up the material. In the neighbourhood of the melting-point it is possible to drill a neat hole in a sheet of ice by means of an X-ray beam. This heating effect provides one method, though not an easy one, of measuring I_0 .

(3) The incident X-rays may ionise some of the atoms and produce photo-electrons.

(4) When X-ray photons collide with free electrons there is a redistribution of energy and momentum, and the X-rays are transformed into X-rays of lower energy and longer wave-length. This is the *Compton effect*. The change of wave-length depends, to a first approximation, only on the scattering angle; but the *intensity* of Compton scattering depends on the scattering angle, the original wave-length and the nature of the scattering material. From our point of view it is necessary to remember that Compton

scattering tends to blacken photographic films at high angles, and that it is relatively more important for light elements and at low temperatures (fig. 14); relative, that is, to scattered X-rays of unmodified wave-length.

(5) The unmodified scattered X-rays are due to the production, by the incident X-ray beam, of forced oscillations in either free or bound electrons of the material. These forced oscillations are of the same frequency (about 10^{18} /second) as that of the incident X-rays, and the electron therefore radiates, in all directions, X-rays of the same frequency as that of the incident beam. If the electron is moving or has a natural vibration of its own, the

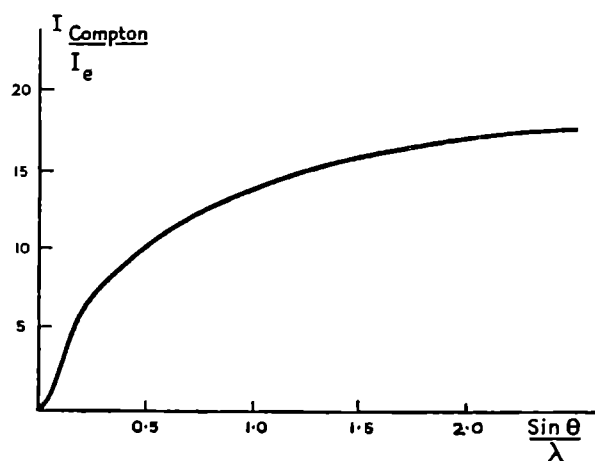


FIG. 14. Compton scattering curve for argon.

wave-length of the scattered rays will be slightly modified, but to a quite unmeasurable degree. This scattered radiation is polarised and may include Bragg reflections if the absorbing screen is crystalline.

(6) But, as Barkla found in 1906, the incident X-rays may also produce, apart from heat, photo-electrons, Compton scattering and ordinary coherent or incoherent scattering, other X-rays of longer wave-length which are *characteristic of the element of the scatterer*—that is, *fluorescent X-rays*. In other words, X-rays characteristic of a particular element may be produced either by bombardment with high-speed electrons or by penetration of high-energy X-rays. In either case the mechanism is that of ionisation by removal of one of the inner electrons and the falling-in of another electron from a state of higher energy to take its place. We found that in order to produce the K series of copper by high-speed

electrons, those electrons had to have a minimum energy Ve , which, applying the relationship $h\nu = Ve$, or $\lambda \cdot V_{\text{critical}} = 1.234 \cdot 10^{-4}$, corresponds to an X-ray wave-length of 1.378 A.U., just less than the smallest wave-length of the CuK series. In order to excite the K radiation of copper by an incident X-ray beam, that beam must contain wave-lengths of 1.378 A.U. or less. This wave-length is called the *K absorption limit* because if we send a beam of heterogeneous white radiation through a sheet of copper, then rays of wave-length less than 1.378 A.U. are heavily absorbed and those of longer wave-length are readily transmitted (fig. 15).

The practical importance of the K absorption limit arises from the fact that since the wave-lengths of the K series are longer

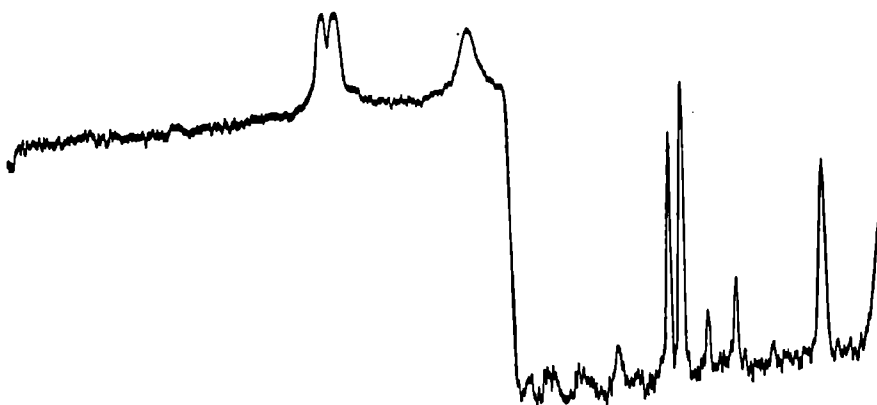


FIG. 15. Photometered record of K absorption edge of Ni.
Wave-length decreasing left to right (Cauchois).

than the wave-length at the K absorption edge, any element is very transparent to all the lines of its own K series, but strongly absorbs those from elements whose atomic number is 2 or 3 higher than its own. The K absorption limit of Fe is 1.740 A.U., just less than the shortest of the FeK lines, but longer than any of the CuK lines. If therefore we were so ill-advised as to try to photograph a crystal containing Fe by means of CuK radiation, there would be two undesirable consequences: (1) the Cu rays would be heavily absorbed; (2) fluorescent FeK radiation would be copiously excited; with the result that the photograph would show weak Cu diffraction lines or spots on a heavily blackened background. In examining any crystal (or liquid) by means of X-rays, therefore, one should avoid using a primary beam containing a wave-length near to, but less than, the K absorption edge of any atom in the specimen; that is, a radiation should *not*

be used for elements of atomic number 2 or 3 less than that of the target giving the radiation. This particularly applies when the crystal contains heavy atoms, because the fluorescence yield (ratio of the number of atoms emitting the characteristic fluorescent radiation to the number of atoms that have been ionised) is highest for heavy elements. In this connection it is as well to remember that the heavy atom in the crystal may be an impurity and that the short wave-length in the primary beam may be an intense component of the white radiation or a harmonic of a monochromatised radiation (see p. 49). The result will still be an unpleasant and unwanted background on the photograph. In fact, fluorescent X-rays are nearly always a nuisance in X-ray crystallography, although otherwise they have their uses.

The absorption of X-rays in a screen of thickness t , that is, the reduction of primary beam intensity from I_0 to $I = I_0 e^{-\mu t}$, is due then to all the processes outlined in (2)—(6), as well as to some others that need not be considered here. The linear absorption coefficient μ of the screen varies both with the state of the scattering material and with the wave-length of the X-rays. The mass absorption coefficient $\mu_m = \mu/\rho$ (ρ = density) is independent of the physical or chemical state of the atoms of the scatterer; in the equation $I = I_0 e^{-\mu_m \cdot \rho t}$, ρt is the mass per square centimetre of the absorbing screen. The atomic absorption coefficient is μ_m multiplied by the absolute mass of the atom (A/N , where A is the atomic weight, N Avogadro's number); and the linear absorption coefficient of a crystal, μ , may be determined from a table giving μ_m for the different elements, by means of the formula $\mu = \frac{n}{V} \sum \mu_m \cdot \frac{A}{N}$, where there are n molecules in a unit cell of volume V c.c.

The importance of absorption in X-ray crystallography where relatively long radiations are used may be judged from the data given in Table I on page 30 (data from *Taschenbuch für Chemiker und Physiker*, Berlin, 1943; and from Guinier's *Radiocristallographie*, Paris, 1945).

X-rays must leave an X-ray tube by way of a window; yet Al foil 0.01 mm. thick absorbs 12 per cent. $\text{CuK}\alpha$ and 33 per cent. $\text{CrK}\alpha$ radiation; Lindemann glass only 0.12 mm. thick would absorb 20 per cent. $\text{CuK}\alpha$ and 50 per cent. $\text{CrK}\alpha$ radiation; Be windows are useful if they can be obtained, but it is not easy to make them sufficiently thin. At the Davy Faraday Laboratory, London, Li windows are used, since the absorption even of 1 mm.

thickness is only 9 per cent. for CrK and less for shorter radiations. Li windows are made by squeezing a small piece of Li to the required thickness between greased glass plates, cutting to size with a cork-borer, and sealing on to the tube, with wax and a small flame if necessary, after removing the grease from the inner surface. Such windows will last for months if the tube vacuum is held up and the outside of the window is kept lightly greased.

Since no one has yet succeeded in making a photographic emulsion which is sensitive to X-rays but not to light, it is necessary, in all but light-tight cameras, to cover the X-ray film or

TABLE I

	t (cm.)	I/I_0			
		CrK α	CuK α	CuK β	MoK α
Hydrogen } normal	10 cm.	1	1	1	1
Oxygen } p, T	10 "	0.60	0.85	0.89	0.97
Aluminium	0.002 "	0.45	0.77	0.82	0.97
Nickel	0.002 "	0.08	0.42	0.0075	0.42
Lindemann glass	0.025 "	0.22	0.60	0.67	0.94
Beryllium	0.05 "	0.63	0.86	0.89	0.97
Lithium	0.1 "	0.91	0.94	0.96	0.99
Black paper	0.01 "	0.80	0.93	0.94	0.99

Wave-lengths of radiation in A.U.
(1000 X.U. = 1.00202 A.U.)

CrK α_2	2.294	CrK α_1	2.290
CuK α_2	1.544	CuK α_1	1.540
CuK β	1.392		
MoK α_2	0.714	MoK α_1	0.709

plate with black paper or some other light-tight cover. Yet even 0.1 mm. of black paper absorbs 7 per cent. Cu and 20 per cent. Cr radiation! While of course the absorption of the crystal itself is a serious factor to be allowed for in the interpretation of the intensities of diffracted beams. The relative intensities of the K α and the K β radiation will also be changed by the various processes of absorption in window, air, crystal and film cover, since, in general, the K β radiation, being shorter, will be less absorbed.

The existence of absorption edges makes it possible, by selective absorption, to filter out the β rays (fig. 16) from the K spectrum and to leave the α rays. In the case of Cu radiation, Ni is the most suitable filter and may indeed be used as the window of the X-ray tube. But it must be remembered that Ni foil of, say,

0.021 mm. thickness, which will reduce the intensity of the $\text{CuK}\beta$ line to one six-hundredth of that of the $\text{CuK}\alpha$, will also cut out 60 per cent. of the $\text{CuK}\alpha$ intensity. Filtering is often essential, but it is always expensive in terms of intensity. Lists of suitable filters may be found in the *Journal of Scientific Instruments* (1941), 18, 132, and in some textbooks. It is an interesting point that some specimens are self-screening; a crystal containing Ni atoms will give only $\text{CuK}\alpha$ and not $\text{CuK}\beta$ reflections.

If a crystal does give fluorescent radiation, it is sometimes possible to remove most of it by selective absorption in a screen

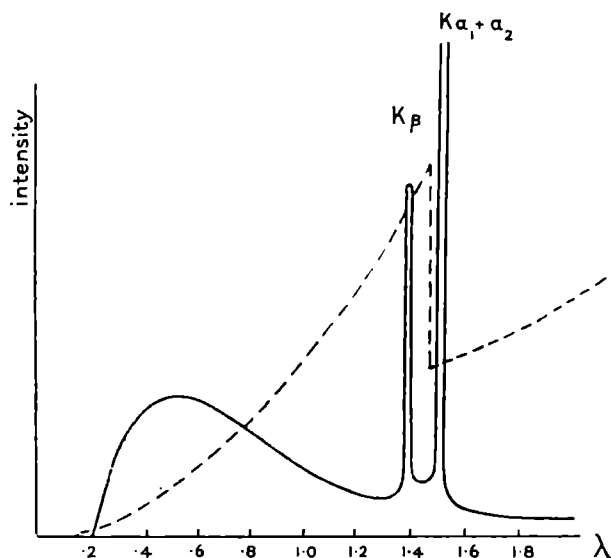


FIG. 16. Filtration of $\text{CuK}\beta$ radiation by Ni.

(placed between the crystal and the film) which lets through only the shorter, primary radiation. One other point of interest with regard to absorption is that the Ag and the Br of the photographic emulsion also show selective absorption (Pl. II c).

X-rays may also be *refracted*. Although early work on X-rays did not reveal the fact, they do suffer a slight change of direction, corresponding to a refractive index u of just less than 1, on entering a crystal from air or a vacuum. If $u = 1 - \delta$, then $\delta = 1.35\rho \cdot \lambda_0^2 \cdot 10^{10}$ (ρ density in gm./c.c., λ_0 wave-length in air, in cm.), except for wave-lengths in the neighbourhood of an absorption edge. Two important results follow from this refraction of X-rays, small though it is. (1) The Bragg law, which holds *inside the crystal*, does not hold exactly if λ_0 and θ are

measured outside the crystal (as in fact they are). For precision work, especially with specimens of high density and relatively long X-rays, a modified equation, $n\lambda_0 = 2d\left(1 - \frac{\delta}{\sin^2 \theta}\right) \sin \theta$, must be used. This particularly applies to low-order planes, for which $\sin \theta$ is small. (2) At small glancing angles, total reflection is possible from very smooth surfaces. The critical glancing angle for total reflection is $\theta_c = \sqrt{2\delta} = \sqrt{2 \cdot 7\rho} \cdot \lambda_0 \cdot 10^5$ where θ_c is expressed in radians. For lead glass and $\text{CuK}\alpha$ radiation, the critical angle is $18'$. This has been applied in the use of totally reflecting collimating systems (fig. 17) which have a theoretical

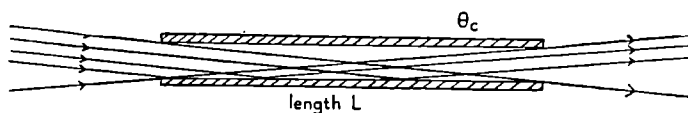


FIG. 17. Totally reflecting collimating system.

optimum length L , for diameter d , where $\frac{d}{L} = \tan \theta_c$. For a $\frac{1}{4}$ mm. diameter cylindrical slit system made out of lead glass capillary tubing for use with $\text{CuK}\alpha$ radiation, $L = 10$ cm.; but it is necessary to choose a good piece of tubing, and to remember that the resulting X-ray beam will not be parallel, but will diverge by $18'$ all ways.

A most important application of these facts to pure physics is to be found in the *measurement of X-ray wave-lengths* by diffraction from ruled gratings, within the region of total reflection (fig. 18).

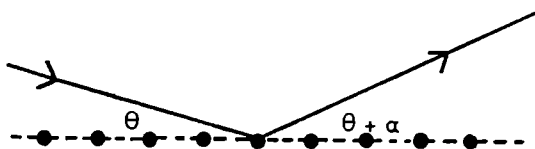
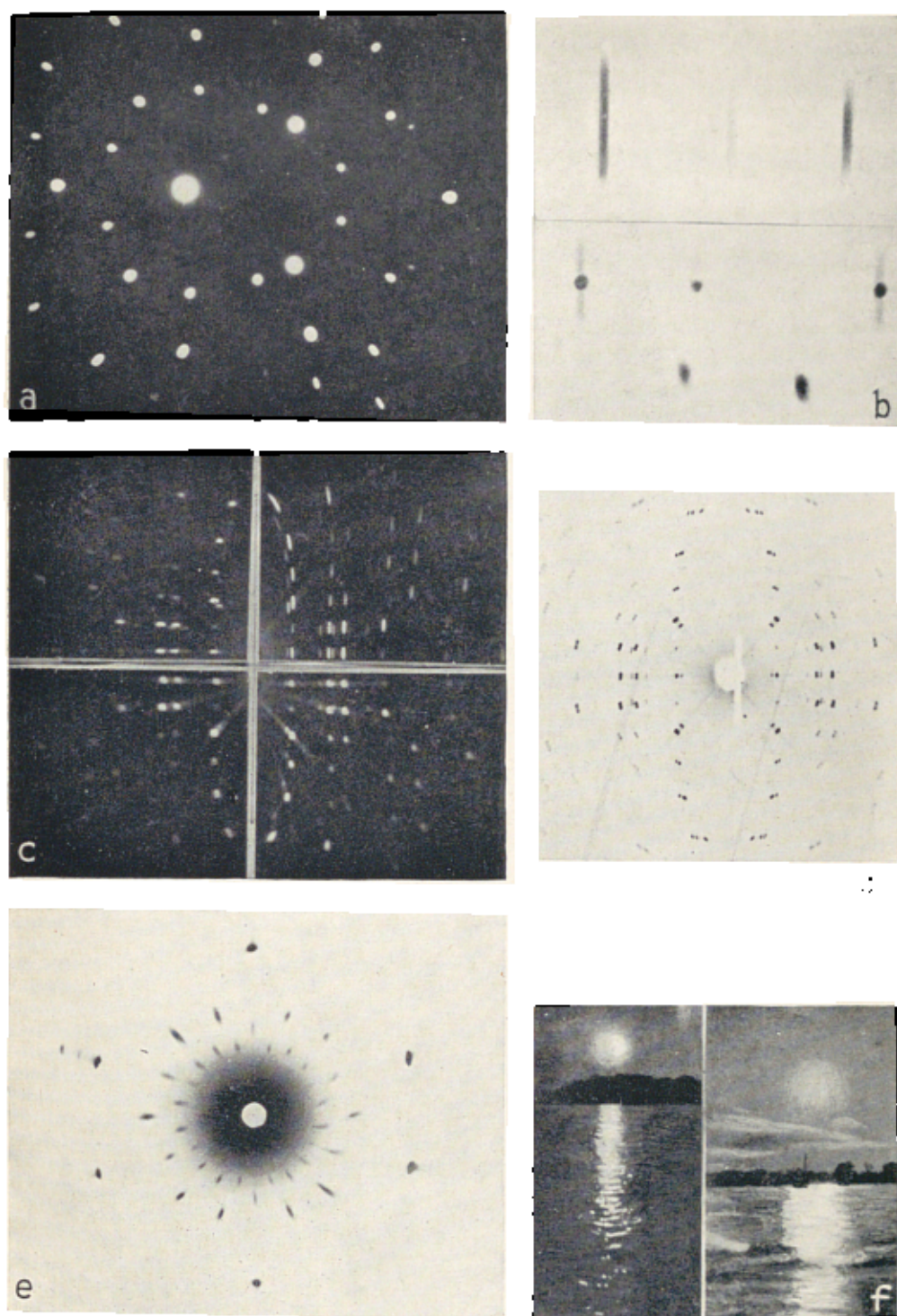


FIG. 18. Diffraction by ruled grating within region of total reflection.

From the formula $n\lambda = a[\cos \theta - \cos (\theta + \alpha)] = a(a\theta + \frac{1}{2}\alpha^2)$, λ could be obtained to six significant figures. For a long time scientists were aware of a serious discrepancy, of 0.2 per cent., between the values of λ given by this ruled-grating method and those obtained from the most accurate crystal measurements. There seemed to be no possibility of any such error in the ruled-grating method; θ and α , though both very small, could be most



(a) Interferential fringe photograph (positive print) of a beam of light, $\lambda = 632.8 \text{ m}\mu$, showing distinctive shape of reflections.

(b) Pinhole photographs of focus by different X-ray tubes.

(c) Composite photograph (positive print) of beam, taken by four different X-ray tubes under otherwise similar conditions for comparison of focus.

(d) Slightly mis-set rotation photograph of beam, taken under similar conditions but with a sharp focus X-ray tube showing excellent resolution of reflection.

(e) Lamp photograph of broggerite, showing crystal distortion and air scattering in low angle region.

(f) Reflection of sun's rays from rippling water.

accurately measured; a could be found by counting the number of lines per mm. with a microscope, or by calibrating the grating with visible light of known wave-length. Critical examination of the accuracy of the crystal method in respect of each measurement involved showed that the only possible entry of an error of this size was through an error in Avogadro's number N . The value of N , in turn, depended on the accuracy of measurement of the *charge e on the electron*. Now, e had been measured by a method (Millikan's oil-drop method) which involved a knowledge of the viscosity of air, and this could not be determined with anything like the accuracy of all the other measurements. A redetermination of e by the oil-drop method has given a value which does, in fact, remove the previous discrepancy, but it is recognised that the value of e deduced from the two sets of X-ray measurements, ruled grating and crystal spacing, is far more accurate than the direct method of measurement can claim to be. X-ray crystallography, therefore, has provided the most accurate measurement of two of the most important fundamental constants of atomic physics. The latest values are:

By X-ray methods $e = (4.8025 \pm 0.0010) \cdot 10^{-10}$ abs. e.s.u.

By oil-drop method $e = (4.802 \pm 0.01) \cdot 10^{-10}$ abs. e.s.u.

By X-ray methods $N = (6.0228 \pm 0.0011) \cdot 10^{23}$.

Among other properties of X-rays that are useful in X-ray crystallography we may mention their power of causing visible *fluorescence in certain salts* such as CaWO_4 and activated ZnS . This gives a method of observing the path and shape of beams of X-rays, which can be used for the adjustment of apparatus, for obtaining a rough assessment of intensity and so on. It will be remembered that it was by the glowing of a screen of barium platino-cyanide that Röntgen first detected the existence of X-rays at all. Made-up fluorescent screens are fairly expensive and should be protected from getting dirty by means of a cellophane cover, but it is quite simple to buy fluorescent ZnS in powdered form and sprinkle it with a pepper-pot on to a sticky postcard. ZnS screens are sometimes disliked, however, because of the phosphorescence they continue to show after removal of the exciting source (or after exposure to ordinary light), but in certain circumstances phosphorescence is an advantage. It enables a screen to be inserted into a space where it cannot be seen and then viewed after removal! Fluorescent screens can also be used for purposes of

intensification if placed in close contact with a photographic plate or film. A back screen, which of course absorbs none of the radiation that would otherwise affect the film, is often more useful than a front one. Care should be taken, however, *not* to use an intensifying screen if correct relative intensities of spots are required, or if the exact shapes of the spots are of consequence (see Pl. III a).

The *ionising properties* of X-rays are made use of in the ionisation-chamber method and the Geiger-counter method of measuring intensity. These, though somewhat tedious in performance if large numbers of measurements are required, are the most accurate means we have of obtaining absolute intensity measurements provided that care is taken in calibration of

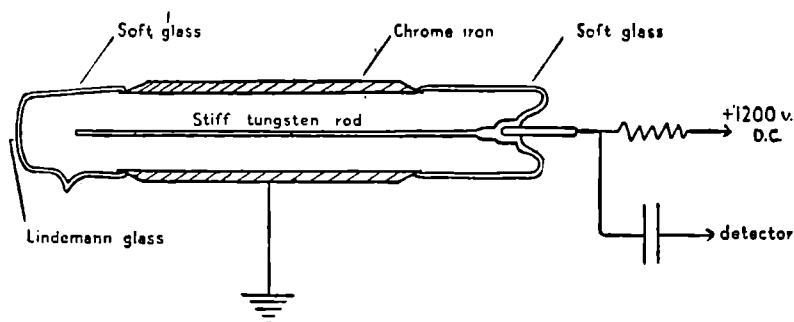


FIG. 19. Geiger-counter tube and basic electrical connections (after Friedman).

measuring instruments. Such measurements are of greater value if made with really monochromatic X-rays. Moreover, the ionisation is much more effective if the gas ionised contains heavy atoms. Methyl bromide or iodide may be used, but argon for Cu radiation and krypton for Mo radiation are much better. An excellent though somewhat idealised account of Geiger-counter methods was given by H. Friedman in *Electronics*, April 1945. Fig. 19 shows the simplest form of counter tube, a coaxial wire and metal cylinder enclosed in a glass envelope containing the ionisable gas mixture at a pressure less than atmospheric. The passage even of a single quantum of radiation can be detected by a modern counter tube with suitable amplification, whereas some 10,000 to 100,000 quanta are needed to give a visible photographic reflection on a film. The Geiger-counter methods have therefore a big future, especially for the measurement of weak scattering effects.

But for most purposes the *photographic action* of X-rays provides the most generally useful method of recording and of measuring the relative intensity of diffraction effects. The relationship between the intensity of an X-ray beam and its blackening effect on a photographic emulsion is a complicated function of many variables. But there is, fortunately, one very simple relationship: the same photographic density (as measured with a photometer) is produced by an intensity A acting for a time B, or by an intensity B acting for a time A. This is known as the Reciprocity Law and it holds for X-rays, but not for ordinary light. It provides a convenient means of intensity calibration. The pattern on a photographic emulsion is given in a definite time by X-ray beams of varying intensity. In order to calibrate the pattern we use an X-ray beam of constant intensity acting for different, known, periods of time. Our time (intensity) scale may be represented by a 'wedge' of uniformly varying or of 'stepped' blackening, or by a row of crystal reflection spots. The latter method is best for single crystal X-ray analysis, because the reflection used to give the calibration scale (corresponding to known exposure times) can be a suitable reflection from the crystal actually under examination, so that it gives spots similar in shape to those on the photograph to be measured. The comparison between the calibration spots and the spots on the photograph is only really satisfactory if both are made on the same plate or film and processed together, and if the beams whose intensities are to be compared are incident on the film at similar angles. No intensifying screens should be used when measurements of intensity are required.

An ideal photographic emulsion for X-ray work would combine speed and contrast with high resolution. Unfortunately these are mutually incompatible. If the X-ray intensity is so high that speed is undesirable, as for example when taking pinhole photographs of the focus of an X-ray tube, then the slow emulsion on a lantern slide is very suitable. If high resolution is essential, speed must to a large extent be sacrificed; process film can then be used. But, in general, double-coated, coarse-grained, blue-base film, giving speed and contrast, but not high resolution, is best for most purposes.

One last word of warning is necessary before proceeding to the consideration of X-ray equipment. X-rays are not dangerous unless the worker exposes himself quite unnecessarily to them;

but while the dangers of exposure should not be overestimated, they should not be neglected; many research and technical workers have routine blood tests made twice a year or oftener.

X-RAY EQUIPMENT

It is now possible to buy X-ray equipment for crystallographic work; but in order to get value for money it is necessary to know what is wanted and what it is wanted for. An X-ray tube suitable for studying distortion in single crystals of metal will not be most suitable for the taking of powder photographs, nor for the determination of the structure of virus crystals. An 'all-purposes' tube is one that is not particularly well suited for any particular job.

X-ray tubes themselves can be classified in either of two ways. These are:

(1) Gas tubes (cold-cathode or ion tubes), in which electrons are obtained by the bombardment of a cold, light-atom cathode by positive ions.

(2) Filament tubes (hot-cathode or electron tubes), in which electrons are obtained by thermionic effect from a hot wire.

Either of these may be (a) sealed-off and therefore permanently evacuated, or (b) demountable and continuously evacuated by pumps.

Most early *gas tubes*, such as those used by Röntgen, were sealed-off, but as they tended to become harder in running owing to the adsorption of gas-atoms by walls and metal parts, they had to be 'regenerated' by introducing more gas. This could be done by heating a suitable chemical provided in an auxiliary tube. If the tube became too soft, owing to over-heating of the target, it could be hardened by passing a very weak current at intervals. We must distinguish between the terms *hard* and *soft* as applied to an X-ray tube and as applied to the X-rays coming from the tube. An X-ray tube becomes 'too hard' when the vacuum is too high or the emission of electrons too small for the discharge to pass at all. It becomes 'too soft' when the pressure is too high and electron emission too large for the applied voltage to be able to direct the electrons with sufficient energy towards the target. A soft X-ray tube will pass a large current in one direction, but the current will not be effective in generating X-rays. That is the principle of the rectifying valve, of which more will be said

later. In general, the harder the tube the more penetrating or 'harder' the *white* radiation it emits, but that does not apply to characteristic radiation. The *quality* of the characteristic radiation is independent of the hardness or softness of the tube, although the *quantity* or *intensity* of characteristic emission is most dependent upon the vacuum, electron emission and applied voltage.

The earliest arrangement of X-ray equipment (fig. 20) consisted of an induction coil, some form of current interrupter, a condenser to reduce the breaking spark and a variable primary resistance for current control. In the secondary circuit a milliammeter gave some indication of the mean secondary current through the X-ray tube and a spark-gap some indication of the potential across the tube. The spark-gap also served as an alternative path for the secondary discharge if the tube should become too hard for the current to pass.

Modern gas tubes for X-ray crystallographic work are all demountable, but the vacuum equipment required to exhaust them is simple, for the pressure in a gas tube is about 0.01 mm. Hg and a modern two-stage oil rotary pump will

attain this quite easily. The reason why the gas tube can be run at such a relatively high pressure is that it needs a supply of gas to provide the ions with which the cathode is to be bombarded. The exact mechanism of the discharge is not altogether clear, but it seems that as the potential across the tube is increased those ions which are always present in any specimen of air are attracted towards the cathode with some force and release a few electrons from the low-atomic-weight metal of which it is made (usually Al). These electrons move towards the anticathode with a greater speed, ionise the air by collision, and more positive ions are then flung at the cathode, to release still more electrons, which are, of course, replaced by the electric current flowing in from outside. A certain

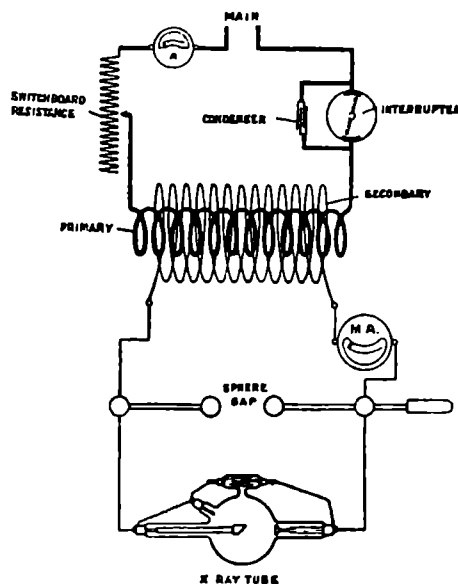


FIG. 20. Early arrangement of X-ray equipment.

(Schall, *X-rays*: John Wright & Sons, Ltd.)

minimum voltage across the tube (the ionisation potential) is necessary before the released electrons can have sufficient energy to ionise the residual gas, and this ionisation potential is higher the less gas there is present to ionise. If the voltage is raised above the ionisation potential for a certain degree of vacuum, the tube current will increase, because the passage of electrons with higher speeds will mean more ionisation and more electrons. Thus the gas pressure in the tube determines the minimum voltage at which the tube will function, and both the pressure and voltage together determine the current. The current through a gas tube is often pulsating in character, the frequency being higher than that of the pulses in the secondary circuit. This may be due to the formation and dispersal of space-charges in the tube, and can be controlled, partly at least, by the design of the anticathode end of the tube. Gas tubes as designed by G. Shearer in 1921, and since modified by A. Müller, have been in constant use for 25 years at the Davy Faraday Laboratory, London. The metal parts, except for the actual cathode and anticathode, are of steel, and a miner's lamp-glass, free from flaws, is used to insulate the high-potential cathode end from the earthed anticathode end of the tube. One source of the efficiency of this design is that the windows can be placed within $1\frac{1}{4}$ cm. from the target centre. The X-rays generated in the target emerge in all directions, but whereas anticathodes used to be arranged with their surface at 45° to the electron stream, now they are normal or nearly normal to it, and the X-rays emerging at nearly grazing incidence are used, being let out of the tube through one or more windows made (as previously mentioned) of Li; though Be, Lindemann glass, Al, Ni and mica windows are used in other types of tube. In order to maintain a constant supply of gas molecules in the gas tube in spite of the pumping, it is necessary to have a controlled leak of air into the tube. This can be arranged by means of a needle working into a conical socket, by a capillary tube of variable length, by two pieces of metal pressed closely together, or even by specially designed screw-clips on pressure tubing, and there may be an electrical control which adjusts the leak to the pressure so that the X-ray tube runs continuously without attention (as in equipment designed by W. A. Wooster at Cambridge). The leak may connect to the outside atmosphere or to an intermediate vacuum. Gas tubes fortunately seem to run better with air as the residual gas than with argon or other gases.

Most X-ray tubes on the market to-day are *filament tubes*, which may be either sealed-off or demountable. In these tubes the source of high-speed electrons is a tungsten (or sometimes tantalum) wire heated by an auxiliary current. This filament may be in the form of a V, a spiral or a helix, but its design and that of the shield surrounding it are most important in the efficient running of the tube. The vacuum in a filament tube has to be about 10^{-4} mm. Hg, and this, in the case of demountable tubes, involves an efficient pumping system: rotary oil pumps on the fore-vacuum or backing side, oil vapour or Hg diffusion or molecular pumps on the high vacuum side. An important point to be watched is the speed of the system (the volume of gas extracted per second at any given pressure). It must not take too long re-exhausting a demountable tube that has been opened up for servicing. A good general article on pumps is to be found in the *Journal of Scientific Instruments* for November 1945. Since the supply of electrons in a filament tube depends on the temperature of the filament and not on the gas pressure, the tube current, and therefore the *intensity* of X-rays produced, can be controlled by altering the filament current. For any given cathode temperature, however, an increase of the voltage across the tube can only increase the tube current up to a certain value, the 'saturation current,' when all the electrons emitted by the filament are being flung at the target. After that, an increase in voltage does not increase the tube current, but it does increase the speed of the electrons and thus controls the *quality* of the X-rays produced. The fact that filament temperature controls intensity and voltage controls quality, independently, is an important feature of hot cathode tubes.

There are many factors in X-ray tube design which are of equal importance in either gas or filament tubes. For instance, since less than 1 per cent. of the electron energy is used in producing X-rays and more than 99 per cent. goes to heat up the target, it is very important that this *heat generated in the target* should be dissipated or minimised. This can be done in a number of ways:

(1) By using as a target a metal with a high melting-point, such as tungsten (3370°C.), molybdenum (2620°C.) or rhodium (1955°C.).

(2) By using high-conductivity metals, such as copper or silver; or by using thin sheets of other metals soldered (with a high-conductivity solder) or plated on to a copper or silver base.

(3) By air-cooling with fins or fans.

(4) By the circulation of oil or cold water; it is important to remember that steam is relatively non-conducting and that a steam layer must not be allowed to form between the metal of the target and the cooling water. Turbulence and pressure are of more importance in beating off any steam layer formed than the actual volume of water passed. It must also be remembered that *hard* water will in time deposit a non-conducting layer on the back of the target.

(5) The use of a helix-shaped filament to give a line focus

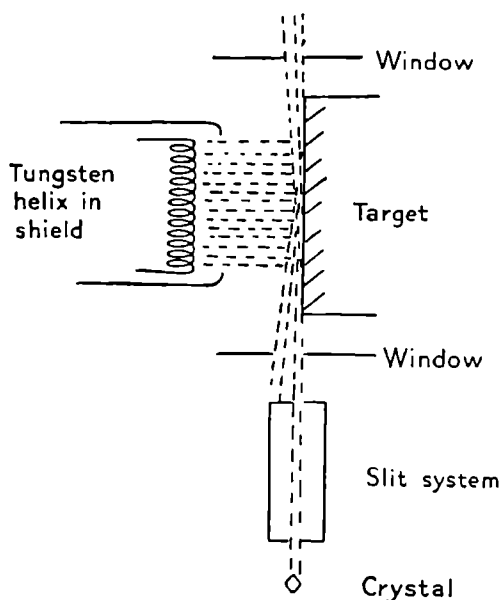


FIG. 21. Production of narrow X-ray beam by projection of line focus.

spreads out the energy over the surface of the target so that the loading, in watts per mm^2 , is decreased without increasing the *projected* focal area (fig. 21).

(6) For very high energy inputs a moving target is necessary. This does not cause dispersion or enlargement of the focal area, it simply introduces a fresh cold surface to the bombardment of the stream of electrons in successive instants. The target may be rotating or it may oscillate to and fro. Rotating-anode tubes vary very widely in

their construction and performance: in the 50 kW X-ray tube at the Royal Institution, London, the target (copper or steel) is 20 inches in diameter and runs at 2000 r.p.m., with a tube current of up to 2000 mA at 30 kV; the shaft is horizontal and the high vacuum is maintained by the use of stuffing-boxes evacuated by a battery of three high-vacuum oil-diffusion pumps in parallel, backed by a smaller oil-diffusion pump, backed in turn by a two-stage rotary oil pump.

In the department of Textile Physics in Leeds University the rotating-anode tube consumes only 2.1 kW, and has a target $7\frac{3}{4}$ inches in diameter, with a vertical shaft running at 620 r.p.m.

In use the vacuum is permanent, being maintained by a liquid Hg seal, covered with a layer of apiezon oil to prevent access of Hg vapour to the tube. The tube current is 70 mA at 30 kV. An oscillating-anode tube is also running satisfactorily, with a stroke of 4 cm. at 3 complete oscillations per second, care being taken to avoid repeated stationary points at the ends of the simple harmonic motion. This tube can take 44 mA at 28 kV, and the vacuum is maintained by two lengths of metal bellows sealed on to the X-ray tube at their inner ends and on to the anode at their outer ends.

The relative efficiencies of such tubes do not depend merely on the ratio of tube currents, but rather on the actual focal area and loading of the targets, bearing in mind the particular purpose for which the tube is to be used.

(7) One most important and most often neglected method of cooling is *not* to use a larger focus than is actually required for a particular job. With an extended focus (fig. 22) it is more difficult for the heat to be conducted away from the

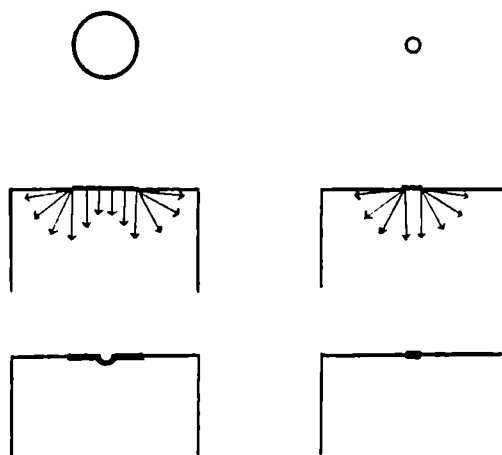


FIG. 22. For the same loading in watts per mm.², a large focus is more likely to pit than a small focus, owing to inefficient cooling.

centre than from the periphery, and therefore the centre of the focus is liable to melt and form a crater with projecting edges, entirely spoiling the effect of the tangential emission of X-rays. Indeed, any *roughening of the target surface* is detrimental to high output of X-rays. Moreover, for a given load in watts per mm.² the total energy input is larger for a large focus than for a small one and there is therefore a bigger strain on the cooling devices, which have to remove more total heat from a large focus than from a small one.

A large focus, therefore, not only wastes wattage, since it may consume ten or twenty times the input of a small one, but it also involves an unnecessary strain on the cooling. In any case, it is obvious that if a slit system of a certain size is to be used, then any

X-rays that do not go through the slit are pure waste. Some waste is inevitable, but the most economical arrangement is one in which the focal spot is of the same shape as, and no larger than, the cross-section of the collimator; and that means that it should vary to fit the job for which it is to be used. For use with a secondary focussing device such as a curved crystal monochromator, a large focus may be suitable. In the case of a powdered specimen mounted on a hair or a wire, or in a non-absorbing capillary tube, an X-ray beam 2 mm. long by $\frac{1}{4}$ mm. wide may be the best. For a single crystal specimen in which, owing to small unit cell size, the diffracted beams are well separated, a cylindrical beam of 1 mm. diameter circular section is often quite suitable. But for crystals containing large molecules,

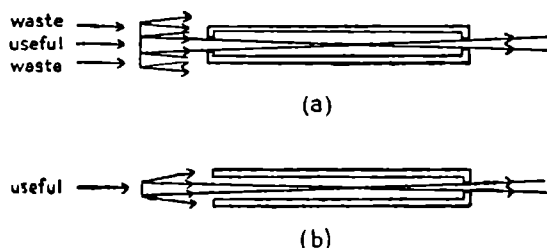


FIG. 23. (a) Large focus; collimation required; input to periphery of focus wasted. (b) Small focus; no collimation required; pin-hole utilises all usable input to focus (after Guinier).

such as protein structures, the spots will not be resolved at all unless the beam is only 0.1 or 0.2 mm. diameter circular section. If the projected focal spot is equal in size and shape to the section of the beam required, then it is not necessary to use a collimator at all; a simple pinhole will do (fig. 23). If reliance is placed, for focussing, on the design of the cathode shield, then the focal spot can be made quite small, but there may be appreciable scattering of electrons, giving a weak, and unwanted, penumbra. It is perhaps better to control the focussing of the electrons by means of a differential potential between the tungsten helix and its shield, in which case it is also possible to vary the size of focus if required (fig. 24). Magnetic focussing may also be employed if the applied voltage can be stabilised so that the electron stream is of constant velocity. Pl. III c shows how the size and shape of the focus can affect the shape and intensity of the reflections on a single crystal photograph, all other conditions being kept invariable. The tubes

used in order to obtain this photograph, two of them gas tubes and two filament tubes, all had a focal spot much too large for good single-crystal work. By way of contrast, Pl. III *d* shows the same crystal photographed with a sharp-focus X-ray tube, the crystal being slightly mis-set in order to show the high resolution obtainable.

Another way of determining the size and shape of the focal spot is to take direct photographs of the X-ray beam, through a fine pinhole in a lead sheet, using lantern slides or process plates. Pl. III *b* shows three such images; in the first the focus is far too large, in the second the focal spot is small, but some electrons are straying from the main beam to give a penumbra of X-rays, and in the third the filament has sagged and the focus is effectively doubled.

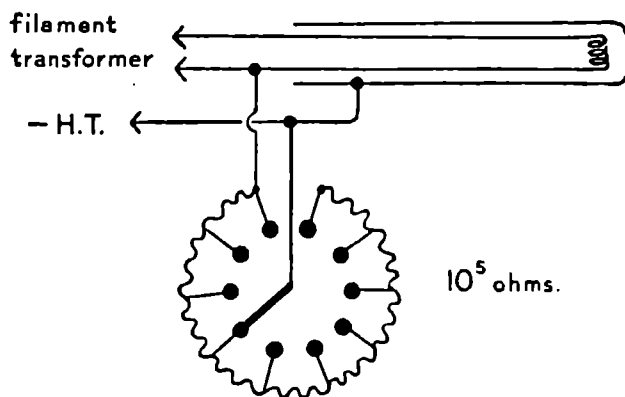


FIG. 24. Electrostatic control of focal size by differential potential between filament and filament shield (after Guinier).

One of the difficulties encountered in filament tubes is that tungsten from the cathode evaporates and settles on the target and on the inside of the window. This has two bad effects. Firstly, it absorbs the X-radiation strongly and reduces intensity; secondly, it causes tungsten L lines to be emitted and the radiation is contaminated, as was shown in Pl. II *f*. In demountable tubes the target and window can be cleaned or a new window inserted, but in sealed-off tubes the deposition of tungsten, which happens only too frequently, is a fatal defect. A further disadvantage of sealed-off tubes where expense must be considered is that, in general, a different tube is required for each target material needed to give varying radiations, whereas in a demountable tube different targets can be inserted as required.

Gas tubes require frequent servicing, not because of tungsten deposition (gas tubes usually give very pure radiation) but because positive ions tend to knock whole atoms out of the Al cathode, which becomes pitted and needs repolishing quite frequently, say every six hours' working time, for maximum output; and also because the target tends to roughen.

GENERATION OF HIGH VOLTAGES

All X-ray tubes can be run either on a steady high potential (applied of course in the right direction!) or on an intermittent and varying high potential, as obtained from a direct current induction coil and interrupter, or from an alternating current transformer, preferably rectified. Some X-ray tubes are themselves self-rectifying and will only pass current in the right direction as long as the target temperature is kept low.

The Shearer-type gas tube can be run very efficiently with a direct current induction coil and electrolytic interrupter at a very small cost. The induction coil has an open iron core and although the mains supply may be direct and relatively constant, there will be an alternating potential difference in the secondary unless the 'make' is much more gradual than the 'break.' The Newman electrolytic interrupter, which consists of a platinum wire sealed into a Pyrex tube as anode, and an aluminium bottle as cathode, with saturated ammonium phosphate solution as the electrolyte, produces a very abrupt 'break' with a frequency of upwards of 300 per second, depending on the length of Pt point. Oscillograph records indicate that with such an arrangement very high peak potentials, of the order of 150 kV, and high maximum secondary currents, of the order of 100 mA, are reached with an input of less than 2 kW, but these maxima would not be recorded by any instrument in the circuit. Unfortunately it is difficult to avoid low potential oscillations, which are useless for the production of characteristic radiation, and there is also a considerable loss of primary circuit energy through heating of the electrolyte and of the induction coil itself. The actual amount of energy reaching the target, measured by the rise in temperature per unit quantity of cooling water, is found to be only about 40 per cent. of the actual kilowatt consumption.

Alternating current transformers differ from induction coils in having closed iron cores to prevent magnetic leakage; there is

no sudden break of the primary current, but a steady rise and fall at a much lower frequency of some fifty cycles per second. Electron tubes are now almost always run with transformer equipment. The primary voltage fed to the transformer may be controlled by a resistance (which can only reduce the mains voltage) or by a small transformer (which has the advantage of

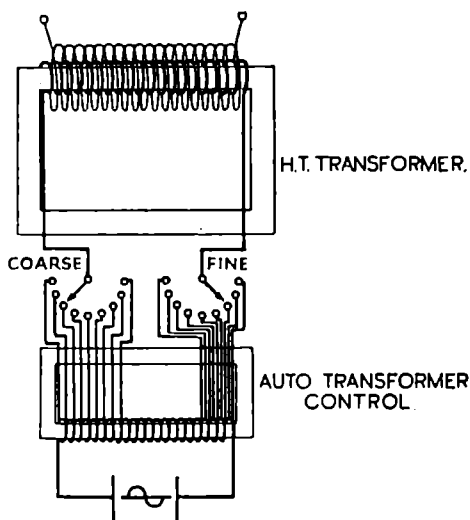


FIG. 25. Transformer fed by auto-transformer, showing coarse and fine control.

Schall, *X-rays*: John Wright & Sons, Ltd.)

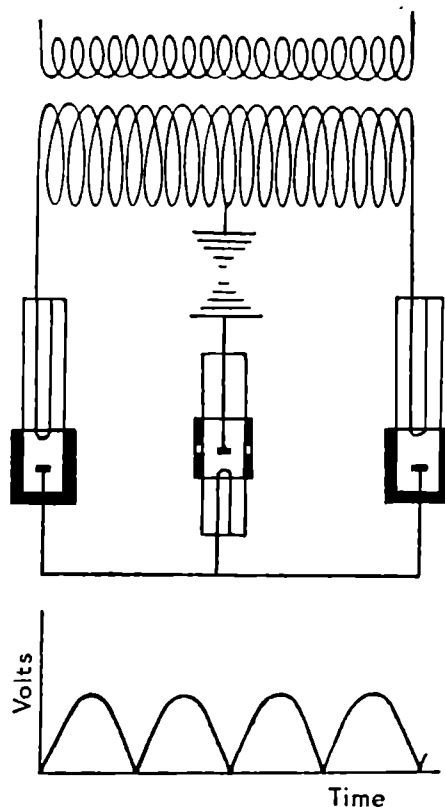


FIG. 26. Full-wave rectification with centre-tapped transformer and two valves.

being able to step up as well as step down). Usually an auto-transformer is used, which has only one winding instead of two on the iron core, the mains current flowing through a fixed number of turns, while the transformer primary is supplied with voltage as required, by tapping off a variable number (fig. 25).

The secondary current may be rectified either mechanically or by means of hot-cathode valves, gas valves or metal rectifiers. Mechanical rectifiers are not now used in most laboratories. The hot-cathode valve differs from the hot-cathode X-ray tube in

that its filament is run at a higher temperature, the cathode rays are not focussed, and the anticathode is a large sheet of a light metal. The vacuum in the valve is lower than in an X-ray tube and the copious supply of electrons move comparatively slowly,

too slowly to produce X-rays.

The valve resistance is small and the tube current large, but the filament current indicated on the valve must be adhered to; if less is used, the resistance rises, higher voltages must be applied to run the valve, the electrons move faster, X-rays are produced (which are dangerous to the operator) and the anticathode heats up, spoiling the unidirectional action of the valve. Gas or dull-emitter valves are less critical in operation, but do not always work easily in cold weather. There seems to be a considerable future for metal rectifiers, although, since they have rather high internal resistance, a number of them must be used in parallel if high currents are to be passed, and this means a considerable capital expenditure.

Rectifiers are often used merely to suppress one-half of the alternating secondary current (half-wave rectification), but by using two auxiliary valves (fig. 26 on page 45) with a centre-tapped transformer it is possible to double the input

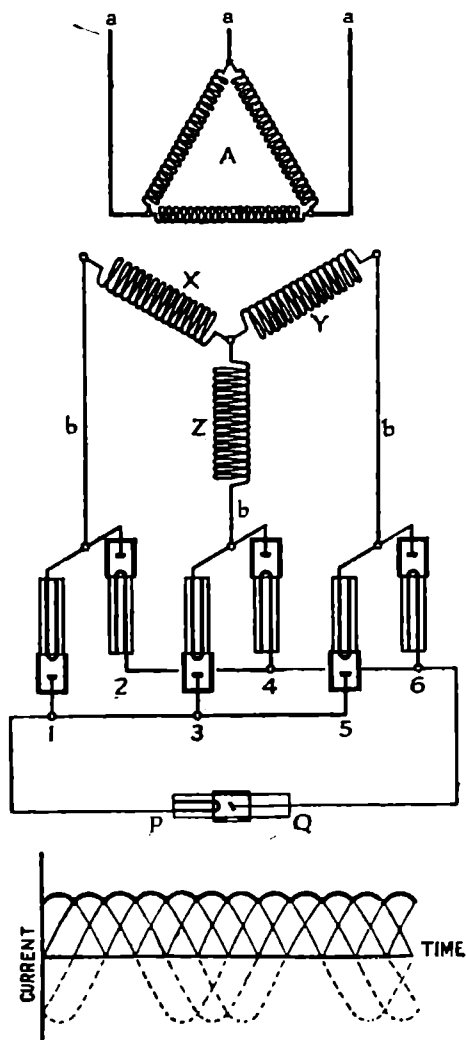


FIG. 27. Hexaphase rectification; circuit and wave form.

(Schall, *X-rays*: John Wright & Sons, Ltd.)

by using the full rectified wave. Even so, however, the voltage applied to the tube drops below the critical, useful, value 100 times a second. A smoothing-off of the voltage curve may be achieved in either of two ways. A three-phase transformer unit,

rectified by six valves, can be used (fig. 27); or a condenser is used with a single-phase transformer and rectifier. The first method is preferable if large currents are being taken from the mains, as for example in the case of the 50-kW tube at the Royal Institution, which takes 70 amps. off each phase. For smaller units, a condenser system gives an almost uniform voltage, the condenser being charged up quickly and then slowly discharging over the period of the cycle (fig. 28). The

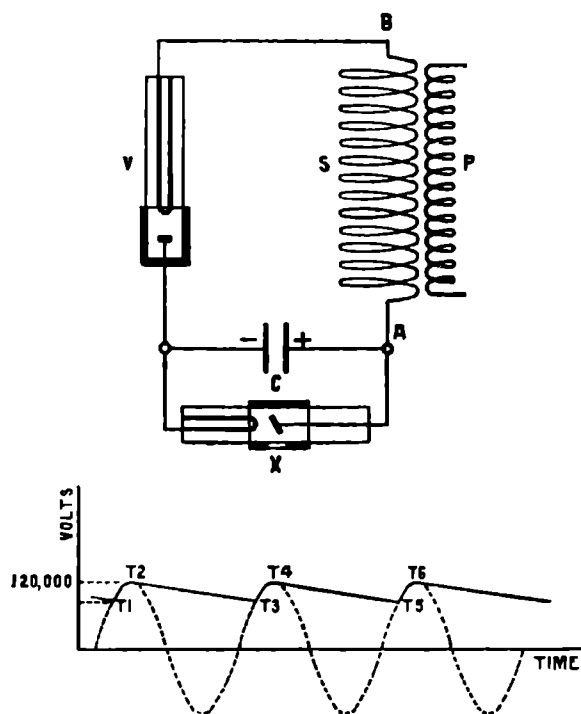


FIG. 28. Single condenser unit and wave form. $T_1T_2T_3 \dots$ is the actual voltage through the X-ray tube X.

(Schall, *X-rays*: John Wright & Sons, Ltd.)

Greinacher circuit, employing two valves and two condensers, will not only smooth off the potential but doubles the applied voltage (fig. 29). Useful practical information on this subject will be found in Schall's *X-rays*. (John Wright & Sons, Ltd., Bristol, 1944.)

When using an X-ray tube it is always as well to remember that one end of it is at a dangerously high potential. Commercial tubes are usually well shielded, but this does not always apply to laboratory-made equipment. H.T. equipment should be sur-

rounded by earthed shields and any possible opening of the shield should operate an earthing system for the H.T. generator. Other safety devices, such as relays which stop the tube current when the water supply fails or when the anticathode stops rotating,

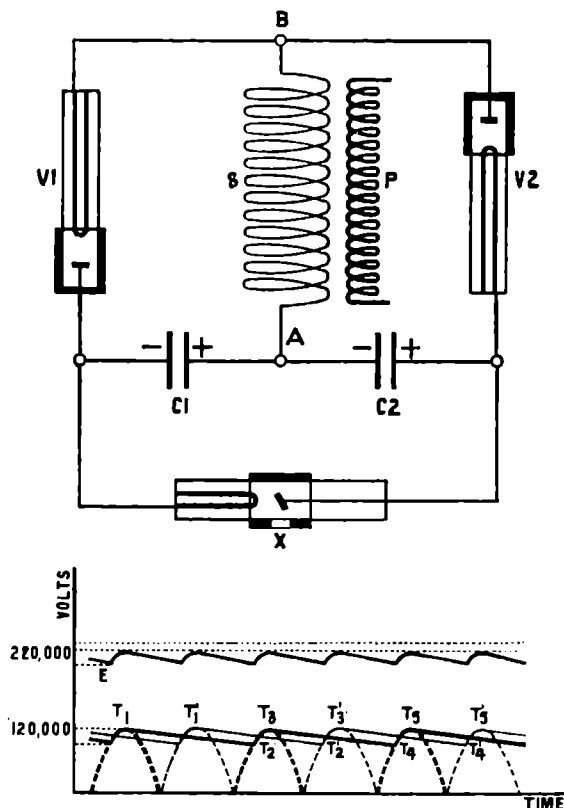


FIG. 29. Greinacher circuit and wave-form, for continuous current generation at twice the applied voltage.

(Schall, *X-rays*: John Wright & Sons, Ltd.)

and so on, are useful; but they can be multiplied to a point where they are a nuisance to the research worker, however essential to the technician.

MONOCHROMATISATION OF X-RAY BEAM

Much modern research work requires, or would be facilitated by the use of, strictly monochromatic radiation. Filters only cut out *most* of the β radiation and *part* of the continuous radiation. If one single wave-length only is required, it must be obtained by Bragg reflection from a suitable crystal. An excellent article

on the choice of monochromator crystals is to be found in the *Journal of Scientific Instruments*, October 1945. Straight crystal monochromators can be used inside a demountable X-ray tube or outside, but close to the window. Curved quartz crystals, using wide-angle X-rays, have been employed to give an intense focussed monochromatic beam, but should be used with a suitable camera to take advantage of the focussing; such crystals cannot be brought near to the X-ray tube.

One point to be remembered when using a beam monochromatised by crystal reflection is that it will be polarised; the intensity formulae to be applied in crystallographic analysis must be modified to take account of that fact.

If the crystal reflection used for monochromatisation has higher orders, then harmonics of wave-length $\lambda/2$, $\lambda/3$ etc. will be present in the monochromatised beam. It may in some cases be advisable to use for monochromatisation a crystal reflection, such as that from diamond (111), where the second order at least (and therefore the $\lambda/2$ harmonic) is absent. Harmonics due to higher orders can be eliminated by downward adjustment of the X-ray tube potential.

CHAPTER III

THE GEOMETRY OF CRYSTALS: X-RAY METHODS OF INVESTIGATION

NEARLY all solids are crystalline. Between the crystalline solid state of any substance and its liquid or gaseous state there is a definite point of fusion (Pl. I *d*) or sublimation which occurs at a definite temperature dependent upon pressure and purity. Glasses, which have only a softening and not a definite melting-point, are found not to be crystalline; their structure is not regular (fig. 11).

DEFINITION OF A CRYSTALLINE SUBSTANCE

A crystalline substance is one in which the internal atomic or molecular arrangement is regular and periodic in three dimensions over intervals which are large compared with the unit of periodicity. (Those which are regular and periodic in only two or one dimension are sometimes called semi- or partially crystalline.) Crystalline solids need not be single crystals; they may be, and most common solids are, composed of an aggregate of crystals which can be distinguished as separate individuals under the microscope (as in the case of the sample of embrittled steel shown in Pl. IV *a*) or of crystallites, that is, of crystals in which the pattern repeats only a few (10, or 100, or 10,000) times in each direction, and which cannot therefore be resolved by ordinary microscopic examination, although they can sometimes be 'seen' by means of the electron microscope. The crystallite size is extremely variable and not easy to measure, but sometimes the crystallites are so nearly parallel to each other that the solid as a whole can be called a single crystal. Perfectly monolithic crystals are rare; even the beautiful crystals seen in Pl. IV *b* do not necessarily possess a perfectly regular internal arrangement throughout their whole volume. But in general, though not always, single crystals which are perfectly regular, or which are composed of nearly parallel crystallites, grow large faces and assume definite geometrical shapes. The faces may sometimes show a magnificent natural polish or they may be roughened, pebbled or stepped. Actually even the best faces show a stepped structure on an atomic scale,

as Tolansky has proved by a beautiful method described in the *Journal of Scientific Instruments*, September 1945 (Pl. IV *c*). Single crystals themselves vary in size from the finest powder to specimens several feet across or perhaps, as in the case of natural ice, even much more (Pl. IV *d*). Fine large specimens of perfect shape rarely occur in Nature; natural diamonds, for instance, usually look like little glassy pebbles (Pl. IV *e*). Pl. IV *f* shows crystals of fluorspar, calcite, galena and quartz growing together, as obtained from a lead mine at Rotherhope Fell.

GEOMETRICAL RELATIONSHIPS IN CRYSTALS

The faces on a crystal grow in zones, a *zone* being a set of planes (not necessarily occurring as crystal faces) having one common direction in space, the *zone axis*. The *interfacial angles*

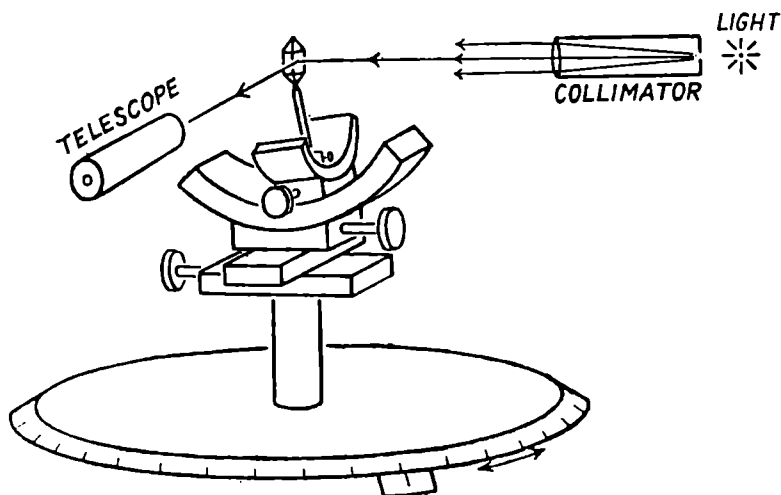


FIG. 30. Principle of the reflecting goniometer.

(Bunn, *Chemical Crystallography*: Clar. Press.)

are invariable, however well or badly developed the faces may be. These interfacial angles can be measured by means of an optical goniometer (fig. 30), and the optical reflections from the faces are useful as a means of setting a zone axis vertical, ready for X-ray measurements. The early Bragg spectrometer was simply an optical goniometer or spectrometer in which the light was replaced by X-rays, the collimator by a slit system and the telescope by an ionisation chamber. But the Bragg X-ray spectrometer

could measure not only angles between faces, but angles between planes that were not faces, and it was used, in fact, to determine the actual size and shape of the fundamental repeat pattern in the crystal.

We know now that the reason why the crystal faces occur at definite angles to each other is that they bear a definite, simple relationship to the internal periodic structure of the crystal. The planes that occur as crystal faces, or that can be obtained by cleavage, are in fact planes that contain relatively large numbers

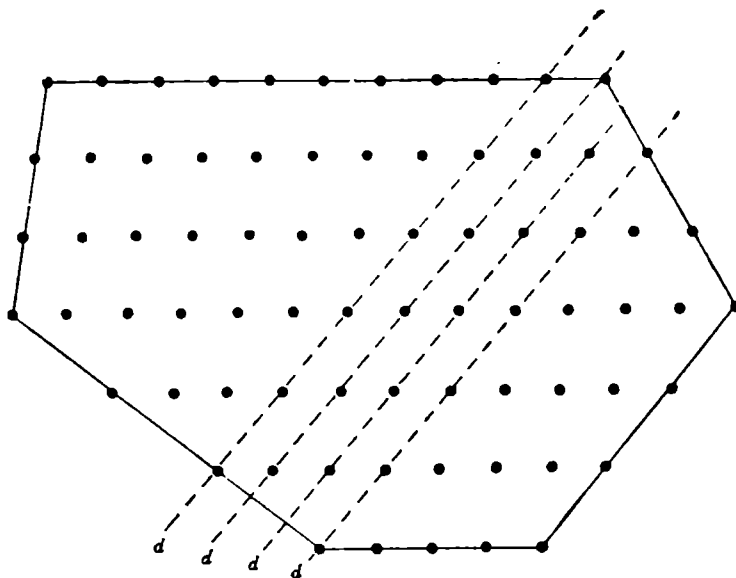


FIG. 31. Parallelism of external faces of crystal to prominent internal planes.

(W. H. & W. L. Bragg, *X-rays and Crystal Structure*: Bell.)

of atoms or molecules, and the faces are parallel to many such planes inside the crystal (fig. 31). It is possible to identify crystal faces, or internal planes, by reference to imaginary axes of coordinates along each of which the unit of distance has a value equal to the repeat distance in that particular direction in the crystal. These axes of coordinates define a framework, or *lattice*, that is fundamental to the description of the crystal structure (fig. 32), and it is the first thing we have to determine in any crystal structure analysis. It is the scaffolding, as it were, upon which the structure is built. It gives us the repeat unit, the *unit cell*, but without defining just what arrangement of matter is contained in that unit cell. That does not matter at the first stage. The steel

scaffolding must come before any consideration of the internal decoration or furniture.

There are different ways in which the *primitive triplet*, that is, the three fundamental vectors which define the unit cell, can be chosen, but they lead to the same periodic lattice-work in space, and, in general, we try to choose the one nearest to a rectangular parallelopiped. Once the primitive triplet, $\vec{a}, \vec{b}, \vec{c}$,* is chosen, the planes can be named in terms of the intercepts they make on the axes $\vec{a}, \vec{b}, \vec{c}$. If those intercepts are $\frac{\vec{a}}{h}, \frac{\vec{b}}{k}, \frac{\vec{c}}{l}$, then the plane is called (hkl) where h, k, l can be positive or negative.

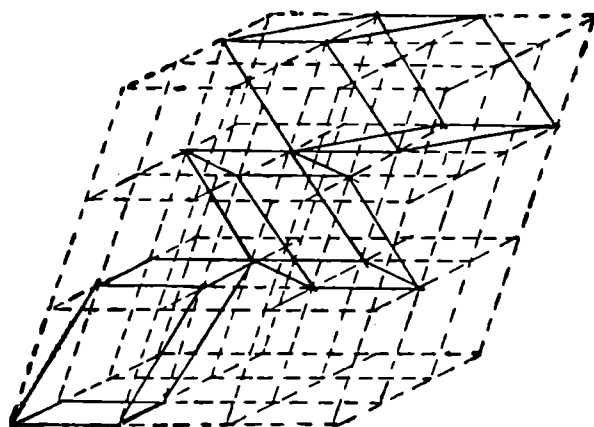


FIG. 32. The space-lattice showing alternative ways of choosing the unit cell.

(W. L. Bragg, *The Crystalline State*, Vol. I : Bell.)

The '*law of rational indices*' expresses the fact, commonly observed, that the indices (hkl) of the faces on a crystal are usually quite low integers, seldom greater than 3. Planes parallel to one of the vectors $\vec{a}, \vec{b}, \vec{c}$ will have one index 0, those parallel to two of the primitive vectors will have two indices 0 (fig. 33 on page 55). The symbol (hkl) really represents, of course, not one plane but a whole set of parallel planes (fig. 34 on page 55) whose uniform distance d apart (the *spacing*) in a direction perpendicular to the planes can be expressed in terms of a, b, c, h, k, l and the angles α, β, γ between the axes $\vec{a}, \vec{b}, \vec{c}$ (where α is the angle between \vec{b} and \vec{c} , etc.).

* The arrow above a, b, c indicates that *direction* as well as length is taken into account. It is omitted if only length matters.

The most mathematically compact formula for d , in the most general case, is:

$$\frac{1}{d^2} = \frac{\frac{h}{a} \begin{vmatrix} \frac{h}{a} \cos \gamma \cos \beta \\ \frac{k}{b} & 1 & \cos \alpha \\ \frac{l}{c} \cos \alpha & & 1 \end{vmatrix} + \frac{k}{b} \begin{vmatrix} 1 & \frac{h}{a} \cos \beta \\ \cos \gamma & \frac{k}{b} \cos \alpha \\ \cos \beta & \frac{l}{c} & 1 \end{vmatrix} + \frac{l}{c} \begin{vmatrix} 1 & \cos \gamma & \frac{h}{a} \\ \cos \gamma & 1 & \frac{k}{b} \\ \cos \beta \cos \alpha & \frac{l}{c} & \end{vmatrix}}{\begin{vmatrix} 1 & \cos \gamma \cos \beta \\ \cos \gamma & 1 & \cos \alpha \\ \cos \beta \cos \alpha & & 1 \end{vmatrix}}$$

which is easy to remember, because of its symmetry. In order to use this expression it must be expanded, according to the convention that

$$A \begin{vmatrix} a_1 & b_1 & c_1 \\ a_2 & b_2 & c_2 \\ a_3 & b_3 & c_3 \end{vmatrix} = A [(a_1 b_2 c_3 + b_1 c_2 a_3 + c_1 a_2 b_3) - (a_1 c_2 b_3 + b_1 a_2 c_3 + c_1 b_2 a_3)].$$

For example, if α, β, γ are all 90° , so that $\cos \alpha = \cos \beta = \cos \gamma = 0$, expansion and simplification give

$$\frac{1}{d^2} = \frac{h^2}{a^2} + \frac{k^2}{b^2} + \frac{l^2}{c^2}.$$

Or if $a = b \neq c$ and $\alpha = \beta = 90^\circ$, $\gamma = 120^\circ$, then

$$\frac{1}{d^2} = \frac{4}{3a^2}(h^2 + hk + k^2) + \frac{l^2}{c^2}.$$

Any point on the crystal lattice can be given indices pqr corresponding to its actual coordinates \vec{pa} , \vec{qb} , \vec{rc} . If we take a row of points ooo ; u, v, w ; $2u, 2v, 2w$; etc., they define a *direction* $[uvw]$. The plane whose indices are (hkl) contains the direction $[uvw]$ if $hu + kv + lw = 0$. Two planes $(h_1 k_1 l_1)$ and $(h_2 k_2 l_2)$ both contain $[uvw]$ if $h_1 u + k_1 v + l_1 w = h_2 u + k_2 v + l_2 w = 0$, that is if $u = k_1 l_2 - l_1 k_2$, $v = l_1 h_2 - h_1 l_2$, $w = h_1 k_2 - k_1 h_2$. (Or in matrix shorthand $u = \begin{vmatrix} k_1 l_1 \\ k_2 l_2 \end{vmatrix}$ etc.) $[uvw]$ is then the zone axis of the two planes. For example, the planes (111) and (123) intersect

in the line $u = 1, v = -2, w = 1$, i.e. $[1\bar{2}1]$. Any other plane in the zone of (111) and (123) must satisfy the condition that $h - 2k + l = 0$. These relationships may seem tiresome, but it

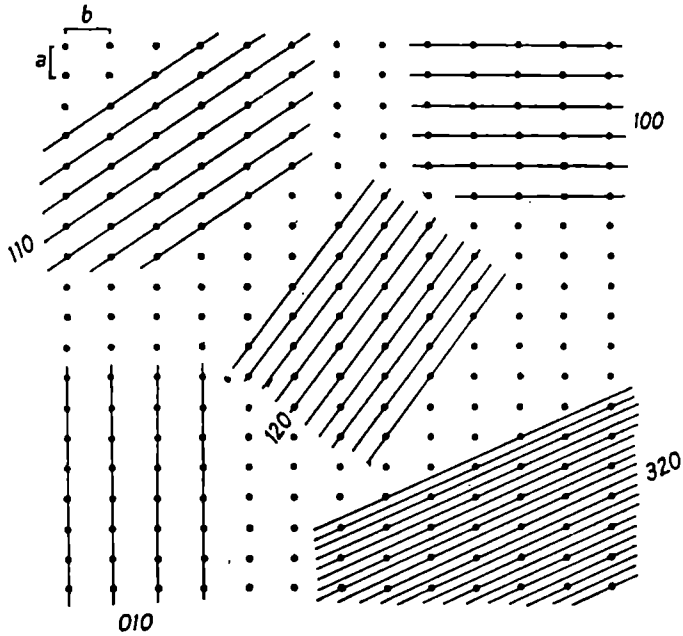


FIG. 33. Various sets of planes in a crystal.
(Bunn, *Chemical Crystallography*: Clar. Press.)

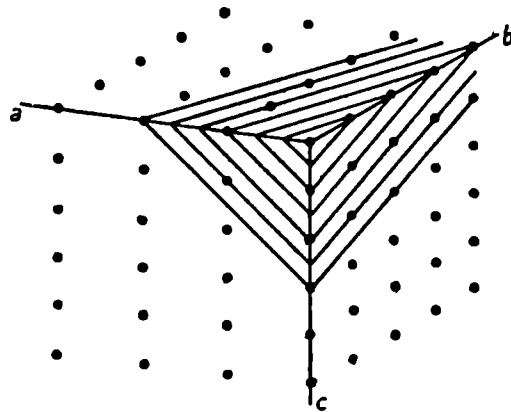


FIG. 34. Set of planes with indices (312) .
(Bunn, *Chemical Crystallography*: Clar. Press.)

is really necessary to know them in order to be able to interpret, say, a rotation X-ray photograph taken about any zone axis as axis of rotation.

Now we have defined the indices of a point, a direction and a crystal plane, and have discussed the relationship between the indices of a zone axis and of the planes that meet in it. The next question to be answered is: What kinds of lattice-work are possible? Well, at one end of the scale the values of a , b , c and of the angles α , β , γ can be all unequal, giving a triclinic unit cell; or at the other end we may have $a = b = c$ and $\alpha = \beta = \gamma = 90^\circ$, in the cubic unit cell. There are, in all, seven fundamental systems: *triclinic*, *monoclinic*, *orthorhombic*, *tetragonal*, *trigonal (rhombohedral)*, *hexagonal*, *cubic*. But before these can be considered further the idea of *symmetry* must be introduced. Single crystals, as illustrated in Pl. IV *b*, not only have faces, which can be given

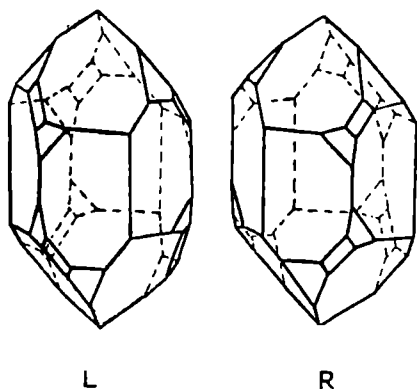


FIG. 35. Left- and right-handed forms of quartz, showing vicinal faces.

indices based on the fundamental primitive triplet, but they show the existence of certain *symmetry elements*; that is to say, if certain operations are performed on them they can be brought to self-coincidence. This symmetry is often, though not always, apparent from the development of faces on the crystal (see, for instance, quartz, fig. 35); and it can be confirmed or often determined by measurements of physical properties such as optical or

magnetic anisotropy (though these can be misleading if the crystal happens to be in a state of strain); or by etching, which is the treatment of crystal faces with an extremely small quantity of solvent to produce small solution pits of geometrical shapes (fig. 36); or by natural striations on the crystal faces (iron pyrites, fig. 37). The different fundamental symmetry elements are quite few in number. There are 1, 2, 3, 4 and 6-fold rotation axes, symbolised by the numbers 1, 2, 3, 4, 6. And there are inversion axes, symbolised by $\bar{1}$, $\bar{2}$, $\bar{3}$, $\bar{4}$, $\bar{6}$, which involve the combined operation (rotation and inversion). The $\bar{2}$ axis is equivalent to a symmetry plane normal to the axis, symbol m (mirror). Some of these symmetry elements are clearly illustrated in the Laue photographs shown in Pls. I, III *e*, X, XI, together with some possible combinations of them. A crystal (or a photograph) showing a plane of symmetry could be reflected in

a mirror parallel to that plane, and it would look just the same as before. A crystal or photograph with a 2-fold (dyad) axis could be rotated through 180° about that axis without apparent change. Two planes of symmetry at 90° to each other

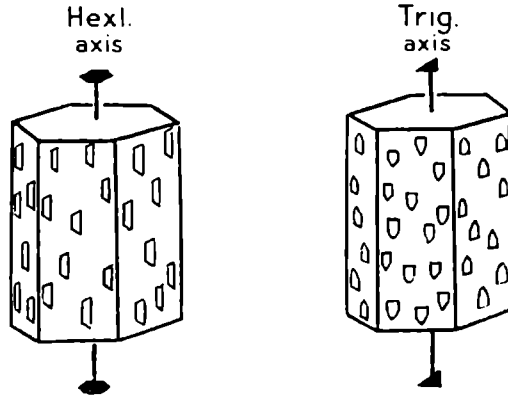


FIG. 36. Etch figures on a hexagonal crystal (apatite) and on a trigonal crystal (calcite) (after Tutton).

necessarily involve a 2-fold axis in their direction of intersection. But why cannot there be 5-fold, 7-fold or higher symmetry axes? The reason is that the unit of pattern possessing the given sym-

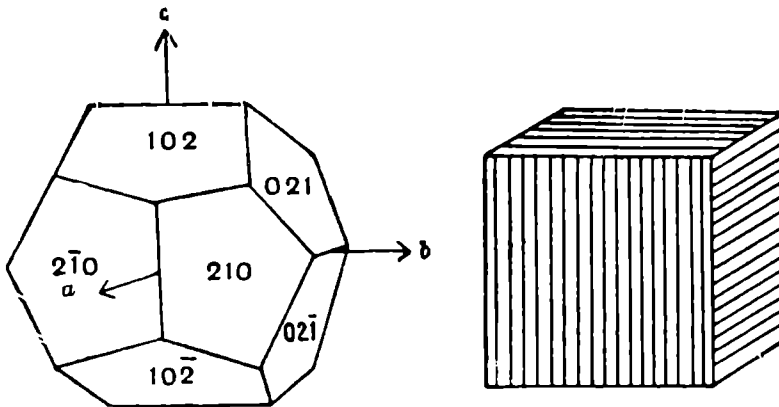


FIG. 37. Striations occurring on cubes of iron pyrites.
(W. H. & W. L. Bragg, *X-rays and Crystal Structure*: Bell.)

metry must be capable of repetition in space, *without leaving gaps*. It is true that if a milk-bottle is emptied quickly, the bottle is left nearly full of 5-sided bubbles, but there are frequent misfits in the mass of bubbles. Hexagons can repeat to fill space, as

in the honeycomb; but octagons cannot, they leave square gaps (fig. 38).

Symmetry is really much more important than shape in differentiating the seven systems, typical unit cells of which are shown

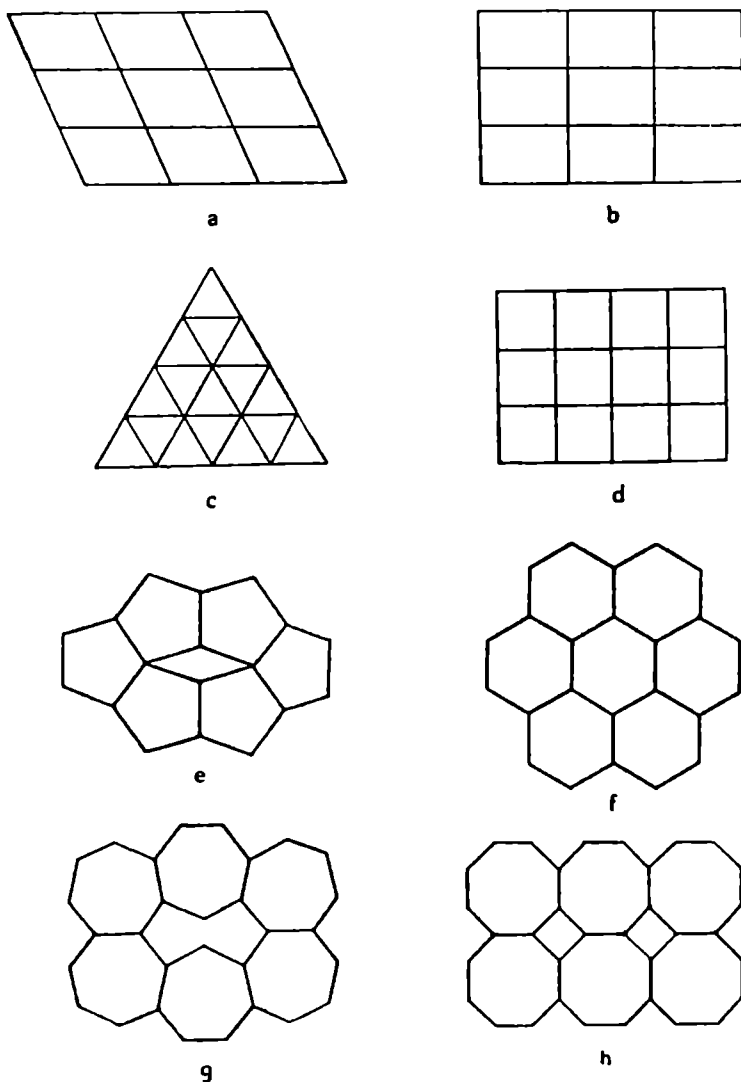


FIG. 38. Limitations to the symmetry of crystals. Only a, b, c, d, f will fill space without leaving gaps.

(*Crystal Symmetry*: British Museum [Nat. Hist.])

in fig. 39. The *triclinic* unit cell has only 1-fold symmetry, it must be rotated about 360° before it will coincide with itself. The sides of the triclinic unit cell need not be equal, nor need any of the angles be equal to each other or to 90° . If in fact they are,

then the lattice may belong to a higher system, although the contents have only triclinic symmetry. This is unusual but not impossible. Such a structure would probably show *pseudo-symmetry* of a higher kind. The *monoclinic* unit cell has 2-fold

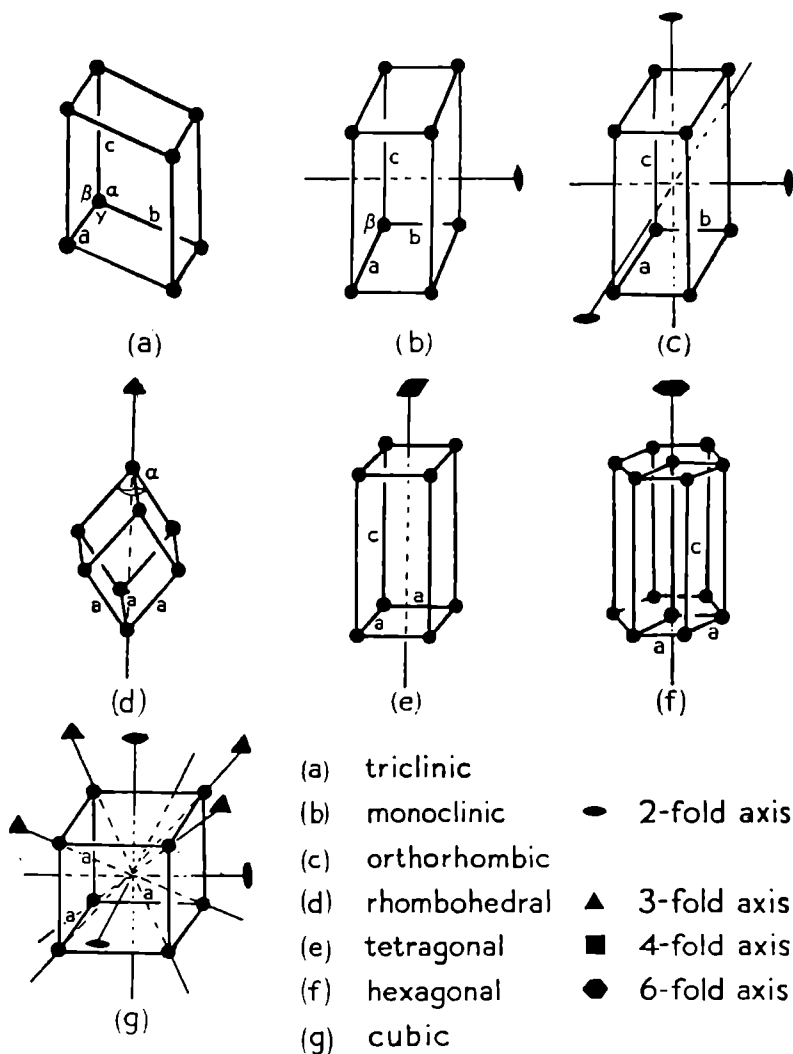


FIG. 39. Unit cells of the seven systems.

symmetry, a rotation of 180° will bring it to self-coincidence. The 2-fold axis is taken as the \vec{b} crystal axis and it is at right angles to \vec{a} and \vec{c} , which need not be equal or normal to each other.

The *orthorhombic* unit cell has three 2-fold axes mutually perpendicular, and these are parallel to the three axes \vec{a} , \vec{b} , \vec{c} , which, however, need not be equal to each other in length. The *rhombo-*

hedral cell has one 3-fold (trigonal) axis; a rotation about that axis (which is equally inclined to \vec{a} , \vec{b} and \vec{c}) of 120° brings the unit cell to self-coincidence. a , b and c must now be equal in length, but the angles between pairs of them, though also equal, need not be 90° , but must of course be less than 120° .* The *tetragonal* (or quadratic) cell has one 4-fold axis; a rotation of 90° about that axis brings the structure to self-coincidence. This axis is taken parallel to \vec{c} , which need not therefore be equal in length to \vec{a} or \vec{b} , although it must be normal to them; \vec{a} and \vec{b} must be equal in length and normal to each other. The *hexagonal* unit cell has a 6-fold symmetry axis parallel to its \vec{c} axis, which is therefore normal, but need not be equal in length, to \vec{a} and \vec{b} ; the \vec{a} and \vec{b} axes are equal in length and at 120° to each other. The *cubic* unit cell, which has \vec{a} , \vec{b} , \vec{c} all equal in length and normal to each other, has at least four 3-fold axes (parallel to the cell diagonals) and six 2-fold axes (parallel to the cube face diagonals).

There are, however, as we saw before, other elements of symmetry besides rotation axes. The *triclinic* cell cannot possess a plane of symmetry; no reflection in any plane can bring it to coincidence with itself; although in all other systems one or more planes of symmetry are possible. Yet crystals in the triclinic system can possess a *centre of symmetry*, a 1-fold inversion axis, $\bar{1}$. To each face on a centro-symmetrical crystal there will be one parallel on the opposite side. X-ray methods cannot in general distinguish the presence or absence of a centre of symmetry because, in general, the two sides of the same plane behave identically to X-rays. That is *Friedel's law*. This law does break down in the neighbourhood of an absorption edge, and in the case of certain kinds of non-Laue scattering due to thermal and other effects, but its otherwise general application imposes a limitation on the X-ray determination of true crystal symmetry.

The combination of symmetry axes, inversion axes and planes of symmetry gives 32 different *symmetry classes*, distributed among the 7 systems. These are shown in Table II,† with their appro-

* The trigonal or rhombohedral cell can also be described in terms of a \vec{c} axis parallel to the trigonal axis, and \vec{a} and \vec{b} axes at 120° to each other, both normal to the \vec{c} axis. For this reason the trigonal (rhombohedral) system is sometimes described as a sub-group of the hexagonal system.

† Taken by kind permission from *Crystal Symmetry*, published by British Museum (Natural History), London.

TABLE II

System of Symmetry	Special Directions	Symmetry Class Symbols	Example
Cubic	Four-fold, four-fold inversion or two-fold axis (cube-edge); three-fold axis (cube diagonal); two-fold or one-fold axis (face-diagonal)	m 3 m $\bar{4}$ 3 m m 3 4 3 2 3	fluorite blende pyrite no example known sodium uranyl acetate
Tetragonal	Four-fold or four-fold inversion axis (prism axis); two-fold, two-fold inversion or one-fold axis (edge of the square base); two-fold, two-fold inversion or one-fold axis (diagonal of the square base)	4/m m m $\bar{4}$ 2 m 4 m m 4/m 4 2 4 $\bar{4}$	idocrase chalcopyrite strontium hydroxide scheelite nickel sulphate iodosuccinimide pentaerythritol
Hexagonal	Six-fold or six-fold inversion axis (prism axis); two-fold, two-fold inversion or one-fold axis (edge of the hexagonal base); two-fold, two-fold inversion or one-fold axis (perpendicular to edge of the hexagonal base)	6/m m m 6 m m $\bar{6}$ m 2 6/m 6 2 6 $\bar{6}$	beryl pyrrhotine benitoite apatite lithium iodate iodoform no example known
Rhombohedral	Three-fold or three-fold inversion axis (prism axis); two-fold, two-fold inversion or one-fold axis (edge of the triangular base, i.e. the line joining mid-points of median edges of the rhombohedron)	3 m $\bar{3}$ m 3 2 3 $\bar{3}$	tourmaline calcite quartz sodium periodate phenakite
Orthorhombic	The directions of the three mutually perpendicular two-fold or two-fold and two-fold inversion axes	m m m m m 2 2 2	barytes struvite sodium potassium tartrate
Monoclinic	Two-fold or two-fold inversion axis	2/m m 2	euclase scolecite sucrose
Triclinic	No special directions	1 1	copper sulphate strontium tartrate

appropriate symbols and examples of each class. The symmetry shown is fundamental; other symmetry is often necessarily implied, without being explicitly stated in the symbol. For instance, the most symmetrical class of the monoclinic system has a 2-fold

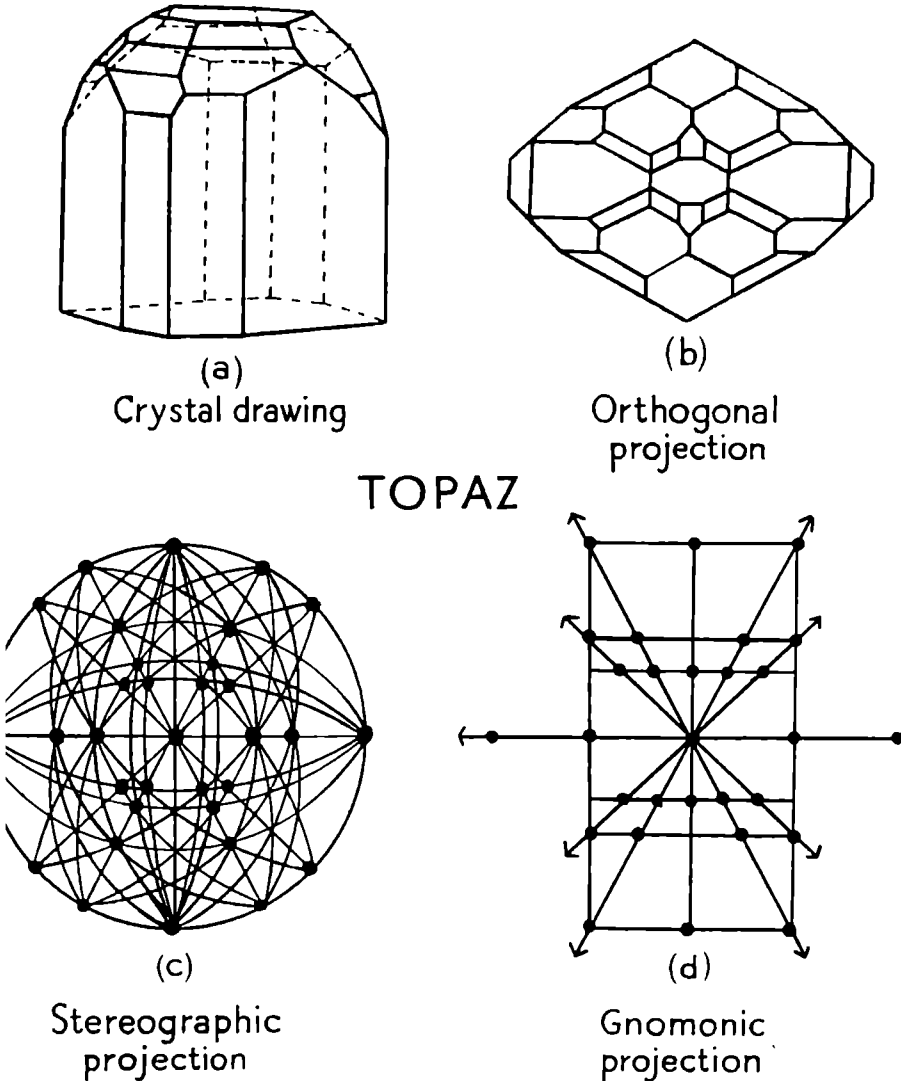


FIG. 40. Different methods of crystal projection (after Tutton).

axis perpendicular to a plane of symmetry, shown by the symbol $2/m$. But this class must also have a $\bar{1}$ axis and could equally well be recognised by the symbol $\bar{1}/m$; nevertheless such a symbol would not show the fundamental monoclinic symmetry of the class. Calcite has a $\bar{3}$ axis together with a plane of symmetry *parallel*

to that axis, which of course must be multiplied by the axis to three such planes. Its symmetry symbol is $\bar{3}m$. In beryl (cf. Pl. I e, f) there is a 6-fold axis perpendicular to a plane of symmetry, with two more symmetry planes parallel to the 6-axis and at 30° to each other. These fundamental symmetry elements involve quite a number of others, but the symmetry of beryl is sufficiently indicated by $6/mmm$.

CRYSTAL DRAWING AND PROJECTION

Drawings of crystals, or of unit cells, are always (fig. 35) made in *parallel perspective*, with lines which are really parallel in space shown as parallel on the drawing, not coming closer together in the distance. Such drawings are also made as if the eye were looking down from a little above and slightly to the right (fig. 40 a), like a benevolent Conservative government. Occasionally crystals, and very often crystal structures, are shown in *orthogonal projection*, that is, as seen directly from above or from the front (fig. 40 b). Sometimes *spherical projection* is used. Imagine a point within the crystal and a sphere drawn round the point as a centre (fig. 41). Normals to crystal planes form radii of the

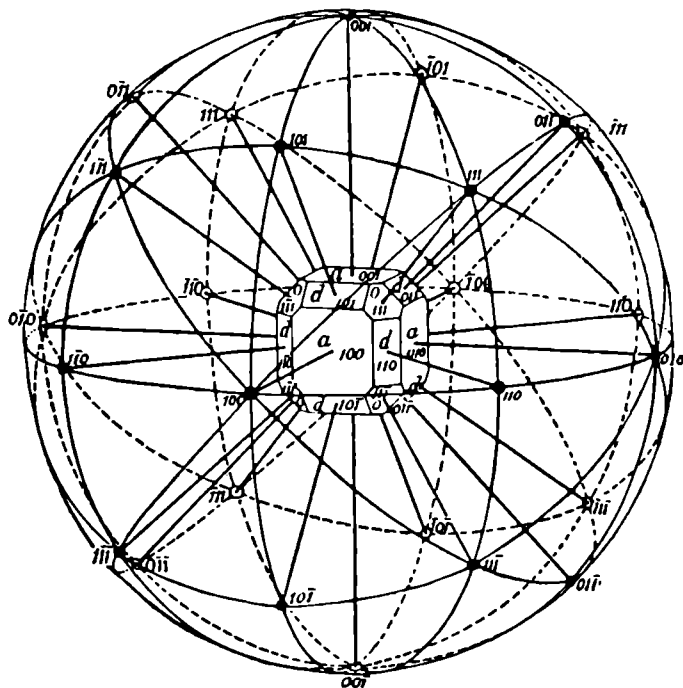


FIG. 41. Spherical projection.

(Tutton, *Crystallography and Practical Crystal Measurement*, Vol. I: Macmillan.)

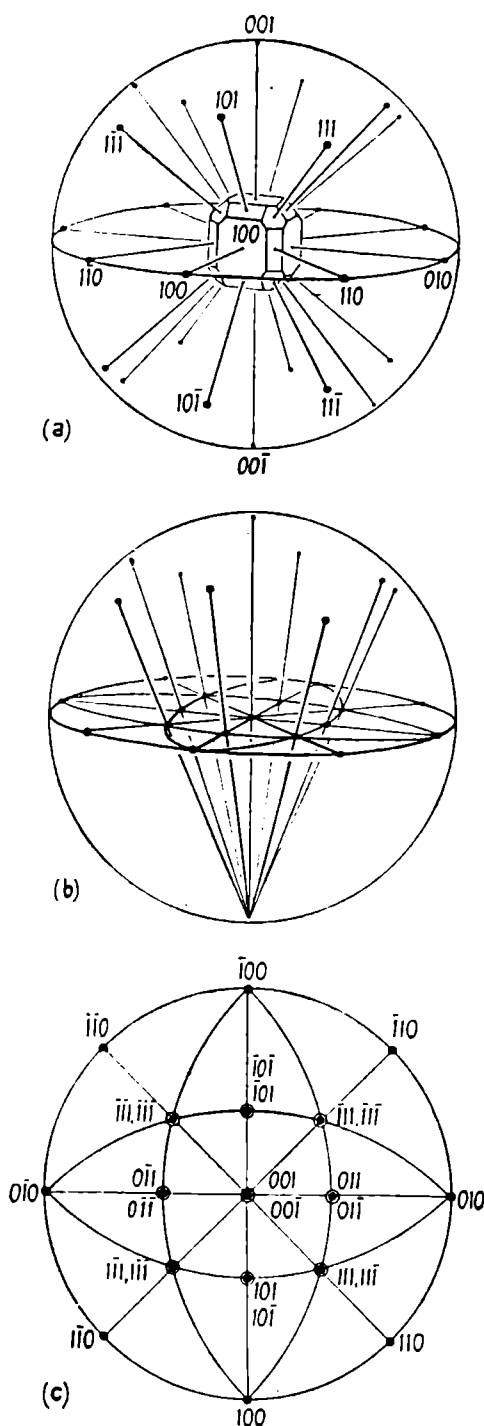
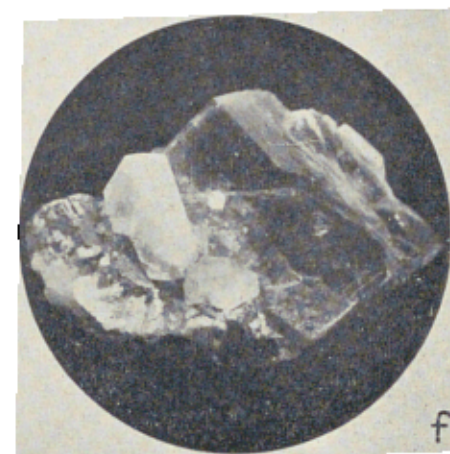
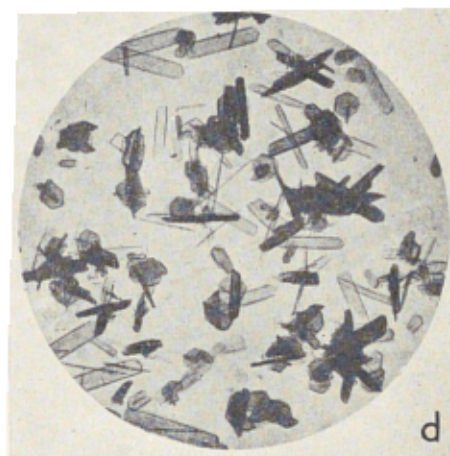
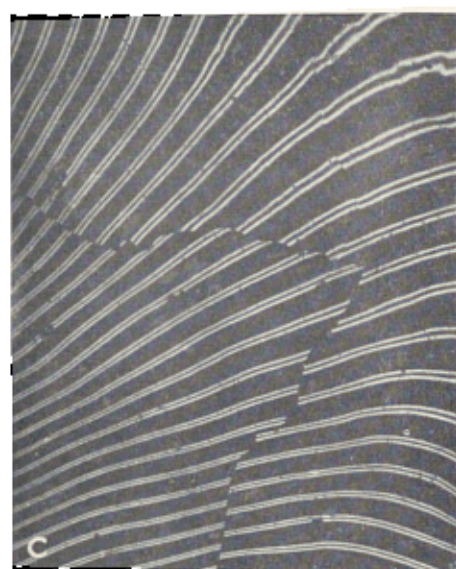
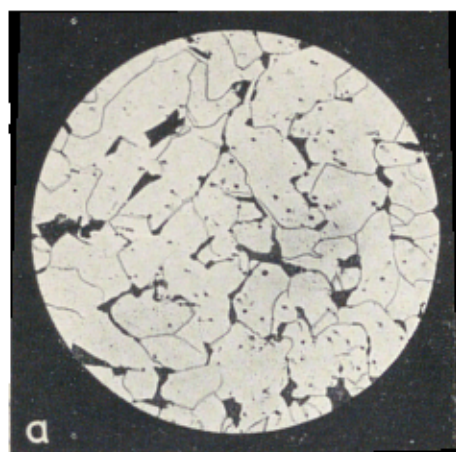


FIG. 42. Principle of stereographic projection.

(Bunn, *Chemical Crystallography*: Clar. Press.)

sphere, and intersections of these normals with the surface form the spherical projection. Points corresponding to planes in any one zone lie on a great circle of the sphere. This kind of projection is, however, difficult to reproduce on paper, so we use instead the *stereographic projection*, in which the pole of projection is at one end of a diameter and the plane of projection is the diametral plane normal to the diameter (figs. 40 c, 42). The points on the surface of the sphere are projected on the diametral plane and so patterns are obtained from which the crystal symmetry can be seen and the crystal orientation determined. Stereographic projection of the essential planes provides a neat way of representing the 32 crystal classes (fig. 43).

In the early days of X-ray crystallography Laue photographs were interpreted by drawing the stereographic projections not of the normals to the planes themselves, but of the observed reflections from planes. This had the advantage of converting spots on ellipses into spots on small circles, each circle



(a) Unannealed steel, showing large irregular crystallites.
 (b) Museum specimens of single crystals of barites, from Felsobanya (British Museum, Natural History).
 (c) Interference fringes of yellow light from the surface of muscovite mica, showing cleavages (Polonsky).
 (d) Single crystals of haemoglobin (Perutz, *Diogenes*).
 (e) Collection of rough diamonds.
 (f) Fluorite, calcite, galena and quartz crystallising together; specimen from Itzherhope, Tull lead mine.

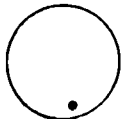
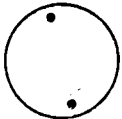
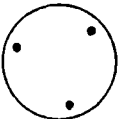
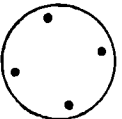
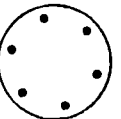
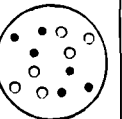
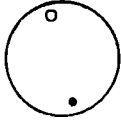
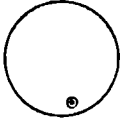
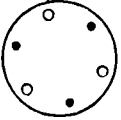
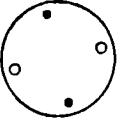
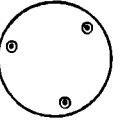
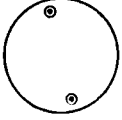
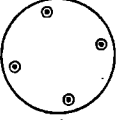
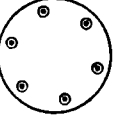
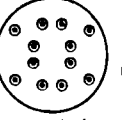
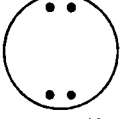
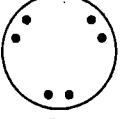
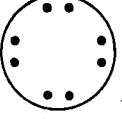
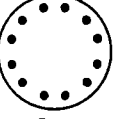
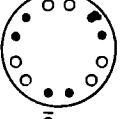
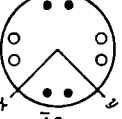
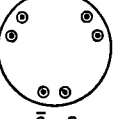
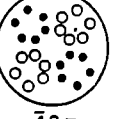
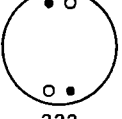
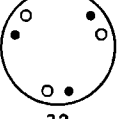
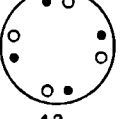
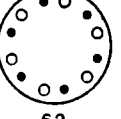
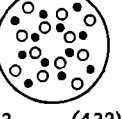
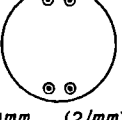
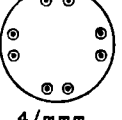
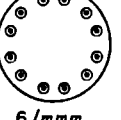
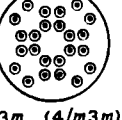
TRICLINIC	MONOCLINIC AND ORTHORHOMBIC	TRIGONAL	TETRAGONAL	HEXAGONAL	CUBIC
 1	 2	 3	 4	 6	 23
 $\bar{1}$	 m	 $\bar{3}$	 4	 $\bar{6}$	$\bar{2}3 = 2/m\bar{3}$
$1/m = \bar{2}$	 $2/m$	$3/m = \bar{6}$	 $4/m$	 $6/m$	 $m3$ ($2/m\bar{3}$)
$1m = \bar{2}$	 mm ($2m$)	 $3m$	 $4mm$	 $6mm$	$2m\bar{3} = 2/m\bar{3}$
$1m = 2/m$	$\bar{2}m = 2m$	 $\bar{3}m$	 $\bar{4}2m$	 $\bar{6}m2$	 $\bar{4}3m$
$12 = 2$	 222	 32	 42	 62	 43 (432)
$1/m\bar{m} = 2m$	 mmm ($2/m\bar{m}$)	$3/m\bar{m} = \bar{6}m$	 $4/mmm$	 $6/mmm$	 $m3m$ ($4/m\bar{3}m$)

FIG. 43. Stereogram of the 32 classes with nomenclature.

(Phillips, *An Introduction to Crystallography*: Longmans, Green & Co.)

FIG. 45. Gnomonic projection. R is the trace of the Laue spot, when $\angle OCR = 2\theta$. G is its gnomonic projection, when CG is normal to the reflecting plane.

corresponding to a zone. The indices of the reflecting planes could then be read off (fig. 44).

In *gnomonic projection* the pole of projection is the centre of the circle and the plane of projection is a tangential plane. This

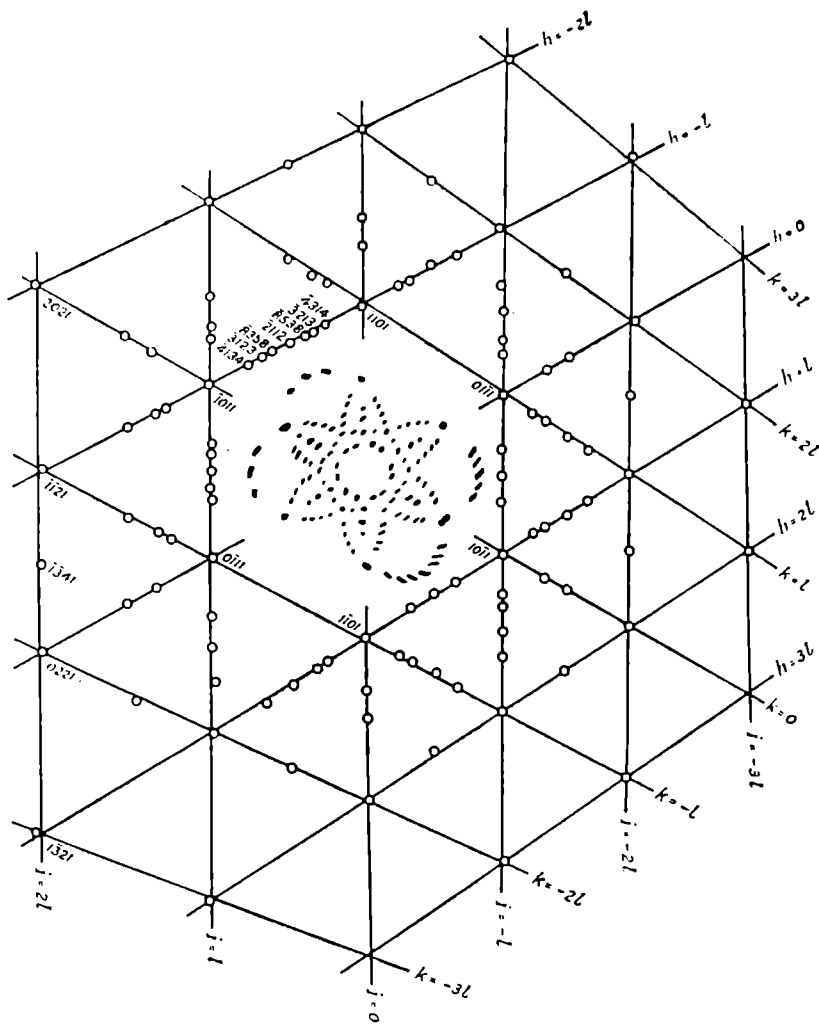


FIG. 46. Gnomonic projection of Laue photograph of zinc; X-rays nearly along $[0001]$; crystal to film 3.0 cm. Presence of 8358 spot gives λ_{\min} . approx. 0.2 A.U. Hence $V_{\max.} > 61,000$ volts.

brings all points corresponding to a zone of planes on to a straight line (figs. 40 *d*, 45). Gnomonic projection is useful for Laue photographs, but by the gnomonic projection of a Laue photograph (fig. 46) is meant the gnomonic projection of the planes corresponding to the reflections and *not* of the reflections themselves. The method, which is described in Wyckoff's *The Structure of*

Crystals, is a useful way of determining orientation, symmetry and axial ratios, but it does not give absolute axial lengths. Modern stereographic projection of Laue photographs also refers to planes and not to reflections from planes (fig. 42).

SPACE-GROUPS

A given external symmetry can be built up from various kinds of internal structure, even using the same fundamental unit. This is illustrated in the simple case of a symmetry plane by figs. 47-50. Fig. 47 shows a mirror-image plane, figs. 48, 49, 50

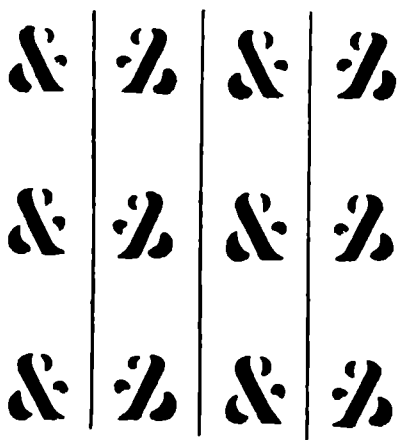


FIG. 47. Mirror plane (010).

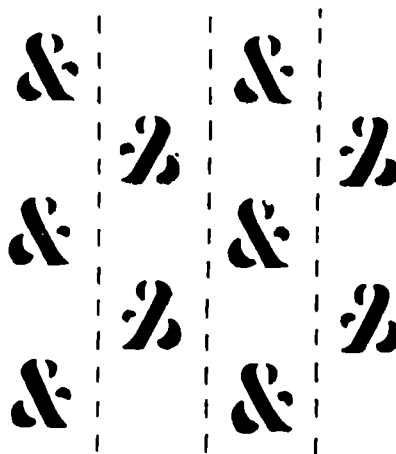


FIG. 48. Glide plane (010), with translation $\vec{a}/2$.

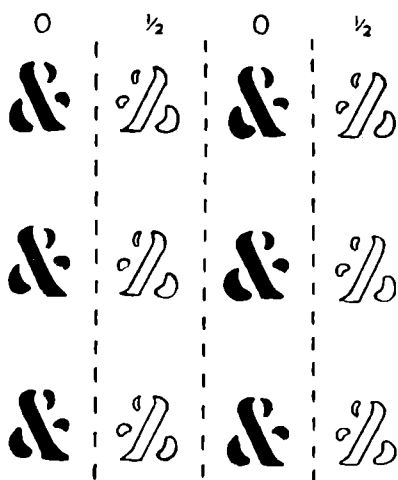


FIG. 49. Glide plane (010), with translation $\vec{c}/2$.

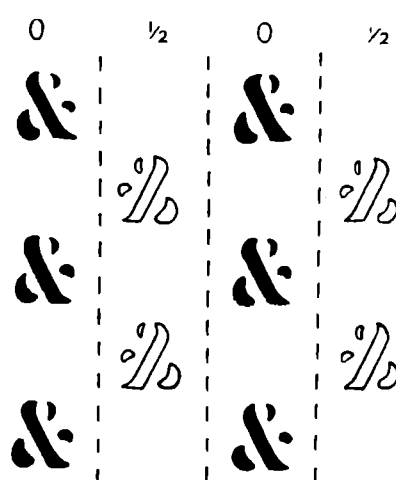


FIG. 50. Glide plane (010), with translation $(\vec{a} + \vec{c})/2$.

show *glide planes* involving a reflection plus a translation parallel to the plane of reflection, the translation being equal to one-half the repeat distance in various directions. When the fundamental units are atoms or molecules the translation corresponding to a glide plane is so small, relative to the size of the crystal as a whole, that the two sides of the crystal are, in fact, reflections of each other. Similarly, we can have screw axes as well as simple rotation axes (figs. 51, 52, 53).

The introduction of combinations of planes, axes and inversion axes to the 7 systems increased them to 32 classes. The addition of translations (giving glide planes and screw axes) increases the number of possible frameworks to 230 *space-groups*. Fig. 54 shows diagrams of a few of them and it must be remembered that the space-group is still only the framework; it is the *pattern* into which ions, atoms or molecules can be introduced in an infinite variety of ways. In these figures the half-arrow represents an asymmetric group which is multiplied by the various symmetry operations of the space-group. Each space-group can be de-

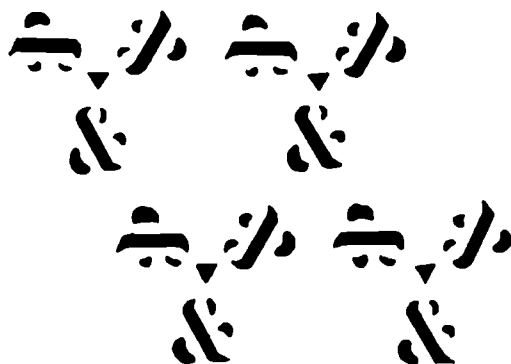


FIG. 51. Three-fold rotation axis.

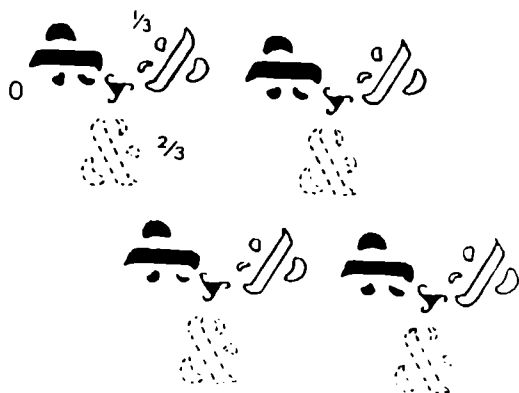


FIG. 52. Three-fold screw-axis.

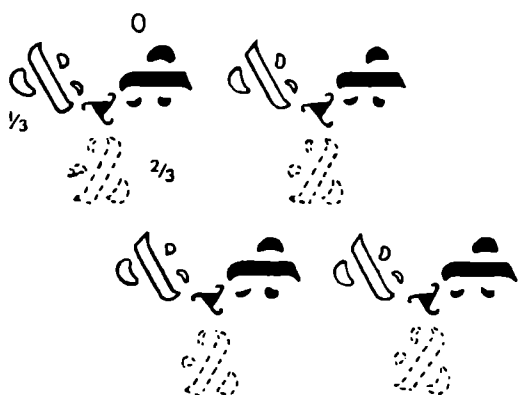
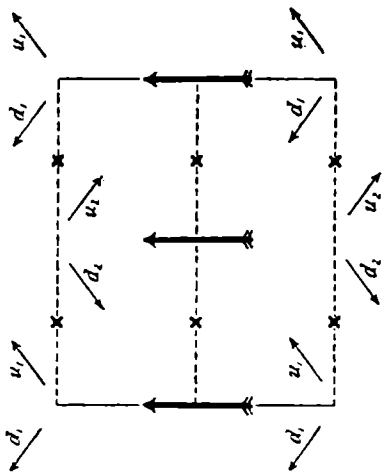
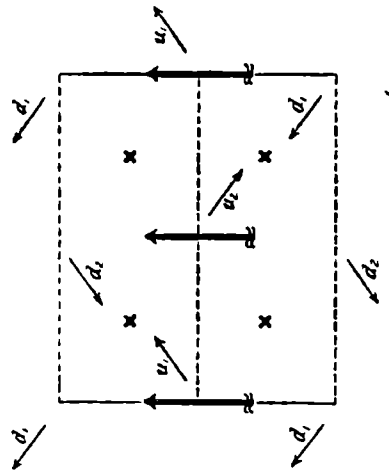


FIG. 53. Three-fold screw-axis enantiomorphous to that shown in fig. 52.

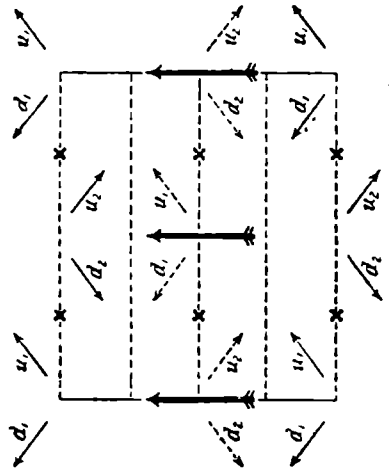
Each space-group can be de-



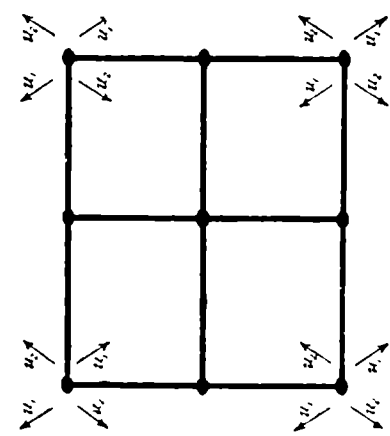
13 $P2/c$



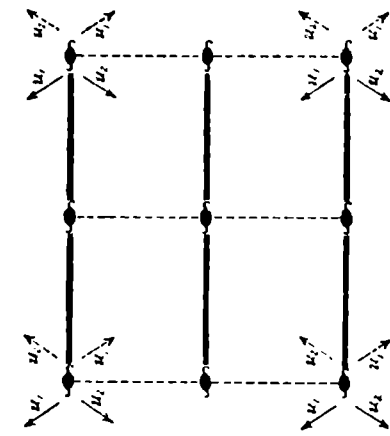
14 $P2_1/c$



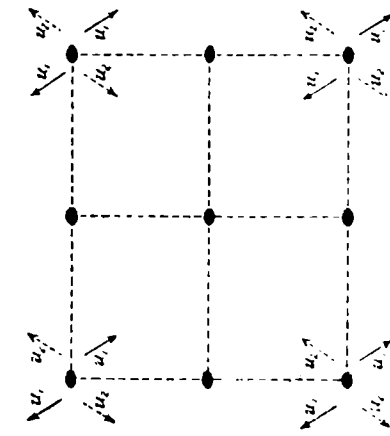
15 $C2/c$



16 Pmm



17 Pcm



18 Pcc

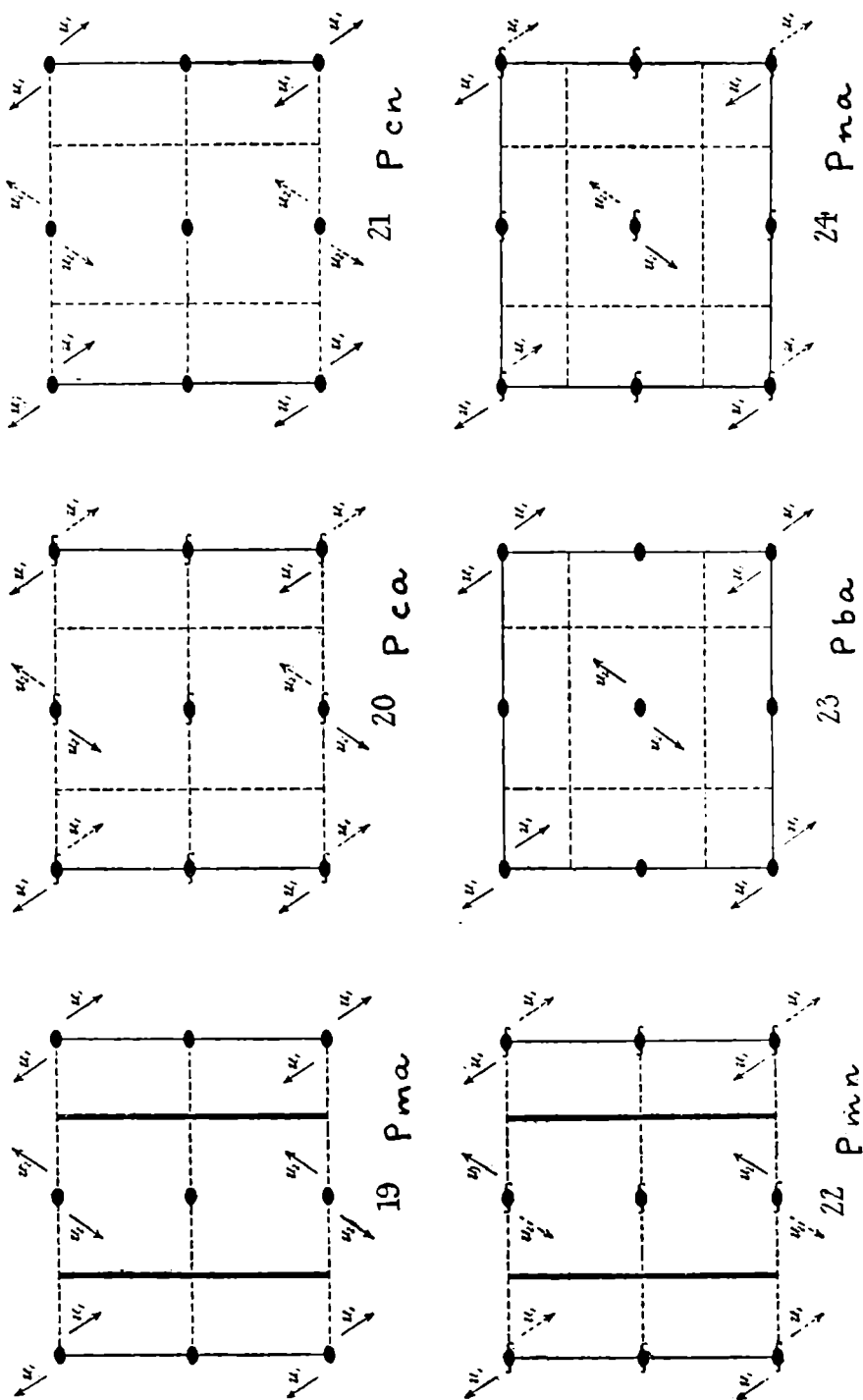


FIG. 54. Some space-groups in the orthorhombic system as shown diagrammatically in the Astbury-Yardley Tables.
(Astbury and Yardley, *Phil. Trans.*, Pl. 6, A. 224, 1924.)

scribed in a way that indicates the minimum essential symmetry belonging to that space-group. It has been mentioned before that m is the symbol of a plane of symmetry. For glide planes we use

the symbols a , b , c or n , if the translation is $\frac{\vec{a}}{2}$, $\frac{\vec{b}}{2}$, $\frac{\vec{c}}{2}$ or $\frac{1}{2}$ the face diagonal $\left(\frac{\vec{a} + \vec{b}}{2}, \frac{\vec{b} + \vec{c}}{2} \text{ or } \frac{\vec{c} + \vec{a}}{2}\right)$. The symbols for rota-

tion axes are 1, 2, 3, 4, 6. Those of screw axes are 2_1 , 3_1 , 3_2 etc., the subscript indicating that the screw translation is $\frac{1}{2}$, $\frac{1}{3}$, $\frac{2}{3}$ etc. Combinations of symmetry are shown, for example, by $2_1/c$, which indicates a 2-fold screw axis perpendicular to a glide plane

whose translation is $\frac{\vec{c}}{2}$. Since this is monoclinic symmetry, the

axis must be parallel to $[010]$ and the plane to (010) . In the space-group symbol, however, a capital letter, usually P, C, F, I, R, precedes the symbols for axes and planes. The letter refers to the *Bravais lattice*. Instead of using a plain (P) framework, it is sometimes more convenient to use a body-centred (I) lattice, a face-centred (F) lattice or a lattice with a pair of faces centred (C if they are (001) faces). There are 14 Bravais lattices distributed among the 7 systems (fig. 55), and in all cases it would be possible to use a simple P lattice, perhaps with a smaller unit cell, as in fig. 56, which shows the three cubic lattices, but it is much more convenient to use a unit cell having the full symmetry of the system and to label it accordingly. Pna then means the space-group having a plain Bravais lattice, a glide plane parallel

to (100) , of translation $\frac{\vec{b} + \vec{c}}{2}$, and a plane parallel to (010) , of translation $\frac{\vec{a}}{2}$. This is necessarily an orthorhombic space-group,

and it will have a screw axis parallel to $[001]$, but this need not be stated explicitly in the symbol, for it is implicit in it; the combination na cannot fail to involve such a screw axis also. A complete list of the space-group symbols is given in W. L. Bragg's *The Crystalline State*, and diagrams corresponding to each space-group will be found in the *International Tables for the Determination of Crystal Structure*, vol. I.

For structures based on a rhombohedral lattice it is always possible to use a simple rhombohedral lattice, or a hexagonal

THE GEOMETRY OF CRYSTALS

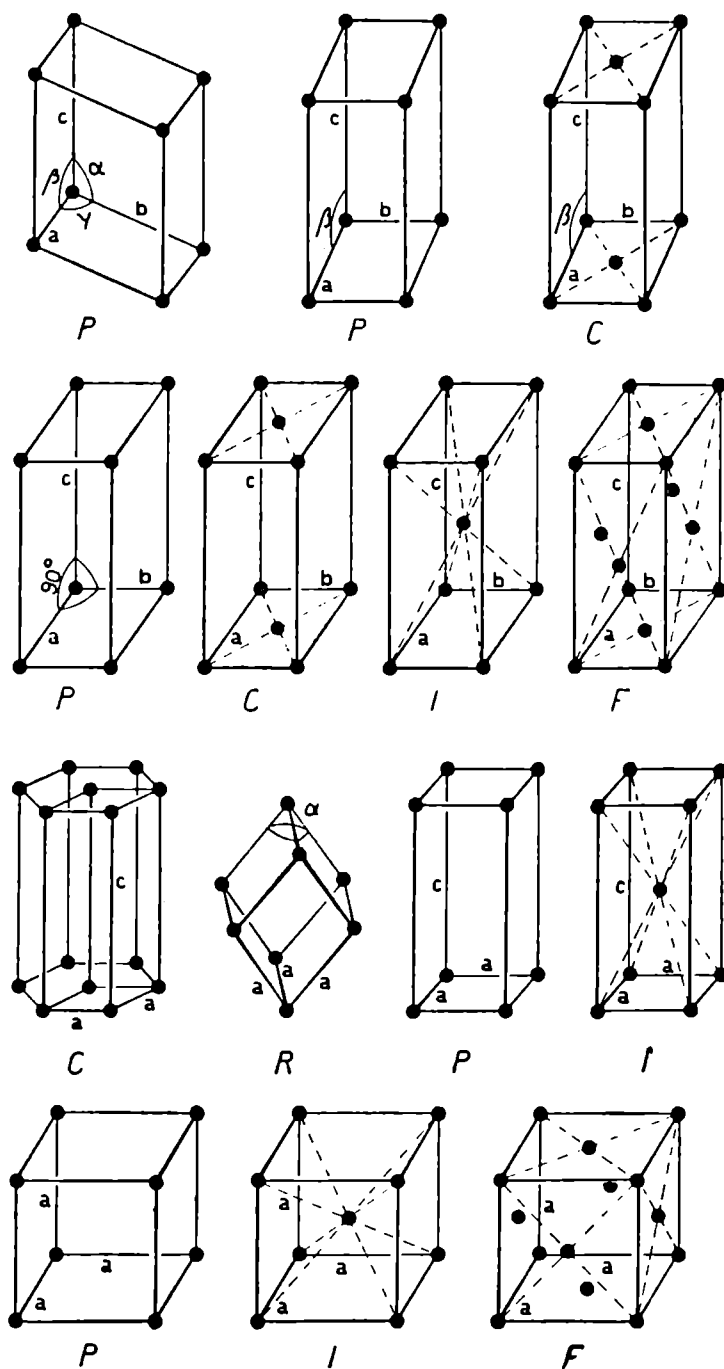


FIG. 55. The 14 Bravais Lattices with their symbols.

(Bijvoet, Kolkmeijer & MacGillavry, *Röntgenanalyse von Krystallen*: Springer.)

lattice with a unit cell of three times the volume of the simple rhombohedral unit cell. The relationships between these two cells are set out very clearly in Guinier's *Radiocristallographie*, p. 69.

X-RAY DETERMINATION OF CRYSTAL GEOMETRY

The system, the class, the Bravais lattice and the space-group can, in general, all be determined by means of X-rays even when no information whatever is available from the external shape, or the chemical or physical properties of the crystalline substance. The framework on which to build must be known before we can

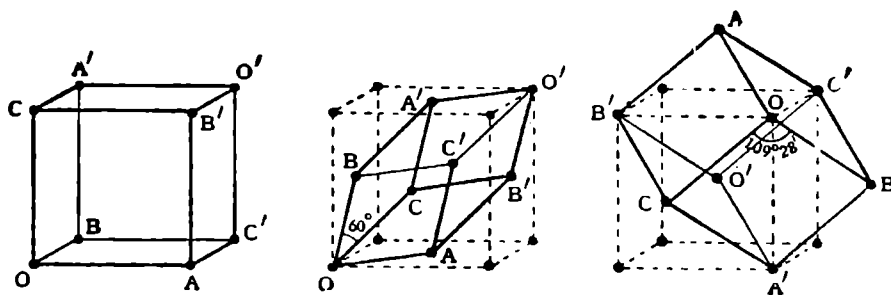


FIG. 56. Simple Lattices alternative to cubic Bravais Lattices.

(W. L. Bragg, *The Crystalline State*, Vol. I: Bell.)

go on to the arrangement of atoms and the determination of electron density distribution.

Of course, when the early workers dealt with simple structures like that of rock-salt (fig. 6) or with relatively simple ones, like calcite, they did not consciously determine the space-group first. Knowing the system and class from the external symmetry, they simply looked for an arrangement of atoms that would give X-ray reflections in the observed positions, with observed intensities. That can be done to-day, if the structure is simple enough. We can calculate the sort of X-ray patterns that various possible simple structures would give, and identify the right one by inspection. But for more complex structures, and especially for molecular structures of relatively low symmetry, a space-group determination must precede all structural analysis. In order to follow the procedure it is necessary to consider briefly what different X-ray methods can be used and what information each gives. Each method will be discussed in relation to the Bragg 'reflection' formula $n\lambda = 2d \sin \theta$, where n can have integral

values only (various orders of reflection) and the values of d , the crystal spacing, are fixed.

In the *Laue method*, already mentioned, the crystal is stationary and therefore the values of θ , the glancing angles between the incident X-ray beam (a fine pencil) and the various crystal planes, are also fixed. But the incident X-radiation is 'white,' containing a continuous range of values of the wave-length λ and therefore the condition $n\lambda = 2d \sin \theta$ can be satisfied so long as $2 \frac{d}{n} \sin \theta$ comes within that range. If the crystal is at distance D from a plane photographic film or plate, placed perpendicular to the incident beam (fig. 57), the photograph will show a number of

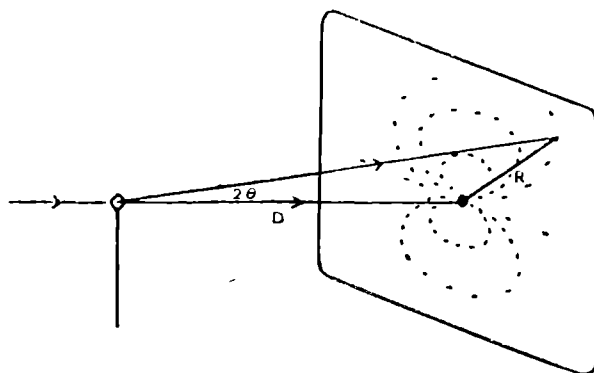


FIG. 57. Laue method; stationary single crystal, continuous X-ray spectrum.

reflection spots at various distances R from the primary beam origin, where $R = D \tan 2\theta$. Each such spot will be due to all the orders of reflection $n = 1, 2, 3$ etc. superimposed, from a single plane, given by wave-lengths $\lambda (= 2d \sin \theta)$, $\lambda/2$, $\lambda/3$ etc. down to the minimum wave-length emitted from the target.

Assume that we know nothing about the crystal to begin with; it looks, shall we say, like a little pebble (Pl. IV *e*); we know no spacings or interplanar angles and we have, of course, no easy method of measuring λ for any particular spot. All the Laue photograph gives us is a series of values of θ for different crystal planes, together with the orientation of each \vec{R} relative to horizontal and vertical directions on the photograph. It gives us, in fact, just what an optical goniometer gives, but in rather more detail, for it gives the orientations of planes that are *not* external faces. Using an optical goniometer alone, it is possible to deter-

mine the system (that is, the symmetry), the axial ratios a/b , c/b and the axial angles α , β , γ , provided that the crystal possesses four faces, one of which intersects the other three. Just the same information can be obtained from Laue photographs even when there are no external faces and the initial crystal orientation is unknown. A Laue photograph of a crystalline pebble, lump or rod, set in *any* orientation on goniometer arcs, can be taken, a stereographic or gnomonic projection made, and by calculation it can then be found how much the specimen must be turned on the arcs in order to get the incident X-ray beam along or perpendicular to a zone axis. When the optical goniometer alone is used, and the number of crystal faces is limited, a mistake can easily be made in the choice of the *simplest* unit cell; but by means of Laue photographs showing the orientations of several planes in two or three main crystal zones, it is not difficult to choose the most suitable coordinate axes consistent with the symmetry, that is, the axes which will give the simplest indices to the main planes. But Laue photographs, like the optical goniometer, will not give the *size* of the unit cell, only its shape, because it gives a measure of angles only, not of spacings. If a crystal shows even one face or one edge, the work of determining orientation is so much the easier. A Laue photograph with the incident X-rays normal to the face or parallel to the edge will usually indicate the position of some of the main axial directions. As shown in Pls. I, III *e*, etc., the crystal class is also indicated by the symmetry of Laue photographs taken along the main axial directions, although the inevitable addition of a centre of symmetry must be remembered. Since Laue photographs give the orientation of planes, they can also be used to measure *distortion*, as will be mentioned later, in Chapter VI.

For *powder photography* monochromatic radiation is used (λ constant), but the specimen is a mass of tiny crystals orientated in all directions (θ variable). Reflections occur only at values of $\sin \theta$ equal to $n\lambda/2d$, that is, the powder reflections form cones about the incident X-ray beam (fig. 58 *a*). There will be, on a plane photographic plate placed normal to the incident beam, one circle for each order of reflection from each set of crystal planes having a given spacing (Pl. V *a*). If a strip is used instead of a wide plate, the photograph consists of a series of slightly curved lines, and if the incident beam cross-section is a very narrow vertical rectangle and the specimen is a narrow vertical

rod, the lines are effectively straight (Pls. IX *a*, XIII). For each line on a plane plate or film we have, as before, $R = D \tan 2\theta$; on a cylindrical strip $R = D \cdot 2\theta$; but since λ is now known, the values of θ give direct measures of the spacings d (or rather d/n).

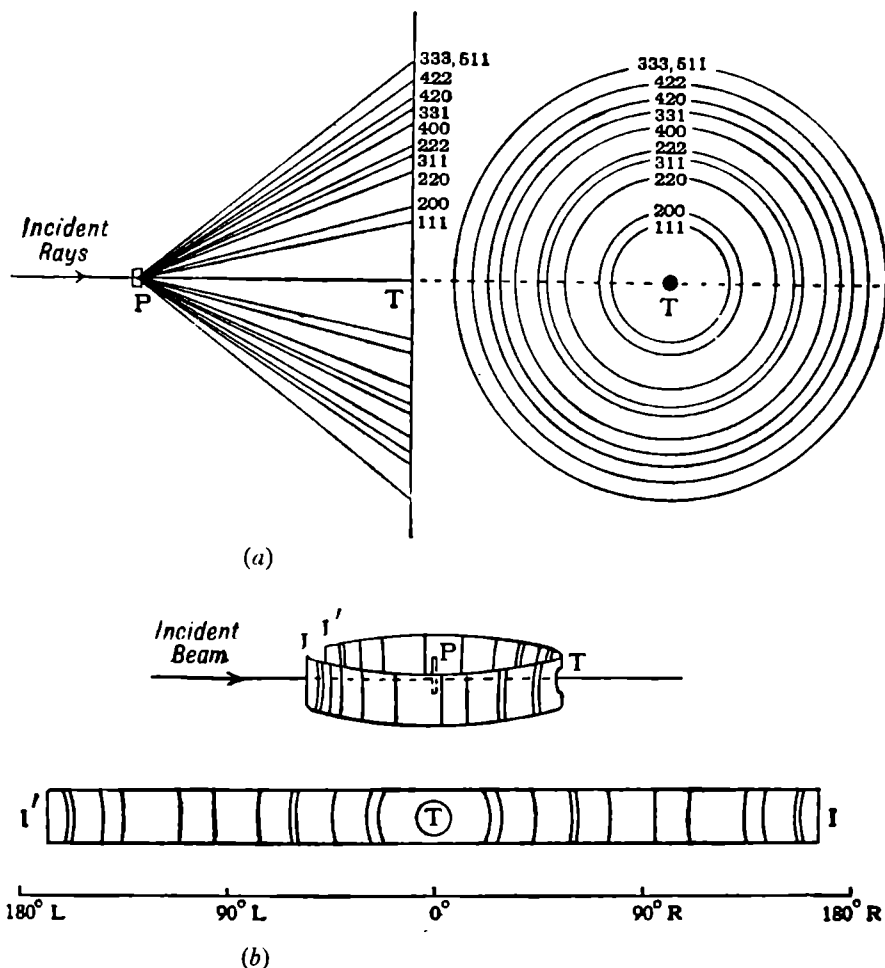


FIG. 58. Powder method. (a) Flat plate perpendicular X-ray beam (rings shown for face-centred cubic lattice). (b) Cylindrical film (schematic).

(W. L. Bragg, *The Crystalline State*, Vol. I: Bell.)

There is now, however, no way of measuring interplanar angles. In the high-symmetry classes a number of planes will contribute to each powder line. For instance, the twelve diagonal planes of a cube, (011) $(0\bar{1}1)$ $(01\bar{1})$ $(0\bar{1}\bar{1})$ (101) $(10\bar{1})$ $(\bar{1}01)$ $(\bar{1}0\bar{1})$ (110) $(\bar{1}\bar{1}0)$ $(1\bar{1}0)$ $(\bar{1}\bar{1}0)$, which are all included in the symbol $\{011\}$, will give one powder line, which will therefore be twelve times as intense as if it were due to the reflection from only one diagonal

plane. Also, since planes in the cubic system have spacings $a/\sqrt{h^2 + k^2 + l^2}$, planes such as $\{522\}$ and $\{441\}$ (for both of which $h^2 + k^2 + l^2 = 33$) will contribute to the same powder line. However, it is easy to tabulate the lines that would be given by cubic structures, simple, face-centred, body-centred, diamond-type and so on, and to identify them by inspection. With tetragonal or hexagonal structures it is also possible to use powder photography, because charts showing the logarithm of spacings plotted against varying axial ratio c/a have been made, against which the data from powder photographs can be matched, and in that way the unit cell can be determined, in size as well as in shape. An unequivocal determination of space-group is rarely possible, owing to the overlapping of reflections in the systems of higher symmetry, but the structure can nevertheless sometimes be wholly or partly determined. Powder photographs of unknown structures of low symmetry or great complexity are, however, almost useless by themselves for purposes of X-ray analysis, with rare exceptions in special cases. They have proved exceedingly useful in investigations of metals and alloys (Pl. XIII), in series of long-chain compounds, and in measurements of lattice distortion and particle size (Pl. IX *a*). In Bunn's *Chemical Crystallography* there is an excellent description of the use of the powder method for purposes of what has come to be known as 'finger-print' identification, where the powder diagram of the unknown substance is compared with that of a known substance, or mixture of substances, which it is suspected to be; or where the unknown pattern is identified from a file of patterns from known substances, arranged in respect of spacings and intensities of the three or four lines of highest spacing.

For the *rotating crystal* method, a monochromatic beam, or a beam containing a strong monochromatic component, is used, together with a single crystal. The rotation enables the Bragg law to be satisfied for a considerable number of planes, when the angle made by each plane with the incident beam becomes $\theta = \sin^{-1} \frac{n\lambda}{2d}$; this happens only momentarily, it is true, but long enough for a reflection to take place. Not every plane can reflect; for example, a plane which always contained the incident beam during the whole rotation could never reflect; nor could one whose spacing was so small that $\lambda/2d > 1$. But if the axis of rotation is a fairly prominent zone axis, then the reflections will be found

drawn out along curves known as 'layer lines' and 'row lines.' On a cylindrical film whose axis is the rotation axis of the crystal, the layer lines will be straight parallel lines when the film is laid out straight; but if the rotation photograph is taken on a plane plate or film parallel to the rotation axis, then the layer lines are hyperbolae (Pl. V *b, e*). On a film perpendicular to the rotation axis and parallel to the beam, they are circles (Pl. V *c*). The row lines are more complicated curves (Pl. V *d*). As in the case of powder photographs, the spacing corresponding to any reflection on a plane plate can be obtained from the relationships $R = D \tan 2\theta$; $d = n\lambda/2 \sin \theta$. But even in rotation photographs it is not easy to determine the indices of reflecting planes unequivocally, nor the angles between them, as reflections from planes in different orientations may coincide or overlap on the film; so several modifications of the method have been devised. The two most frequently employed are the *oscillation* and the *Weissenberg* methods. In the former, the number of planes which can reflect during an exposure are restricted by oscillating the crystal through a small angle only, the whole range being covered in a series of photographs by a succession of overlapping oscillations (Pl. II *e*). In the latter method the crystal rotates through the whole or part of a complete revolution, but the (cylindrical) film is translated parallel to the axis of rotation at the same time, the to and fro movement of the film being synchronised with the crystal rotation; screens are also arranged so that only one layer line is recorded at a time. In this way photographs are obtained from which both spacings and angles between planes are directly obtainable, each plane giving an individual reflection. Weissenberg photographs (so called after the theoretical physicist who first thought of the method) can be used, therefore, for determining crystal symmetry. Pl. V *f* shows a Weissenberg photograph of the zero layer line of a crystal of cyanuric triazide, rotating about the hexagonal axis. The planes $(2\bar{1}30)$, $(12\bar{3}0)$ etc. have the same spacings but different $(30 : 14)$ intensities; there is, therefore, no plane of symmetry parallel to the principal axis.

On such photographs (Pl. VI *c*), also, all the different orders of reflection from one plane are drawn out along straight lines whose slope is dependent upon the rate of translation of the film and of rotation of the crystal. It is then easy to see whether all the orders are present, or whether some are of zero intensity. It is the absence of certain sets of reflections that enables us to determine

the Bravais lattice and to locate screw axes or glide planes, and thus to find the space-group. This can usually be done from oscillation or (more easily) from Weissenberg photographs, but the actual identification of the indices of reflecting planes needs more consideration. In the next chapter, therefore, the principle of the rotating crystal methods, and the interpretation of photographs, will be considered in rather more detail.

By using a point source of *divergent X-rays* close to a stationary

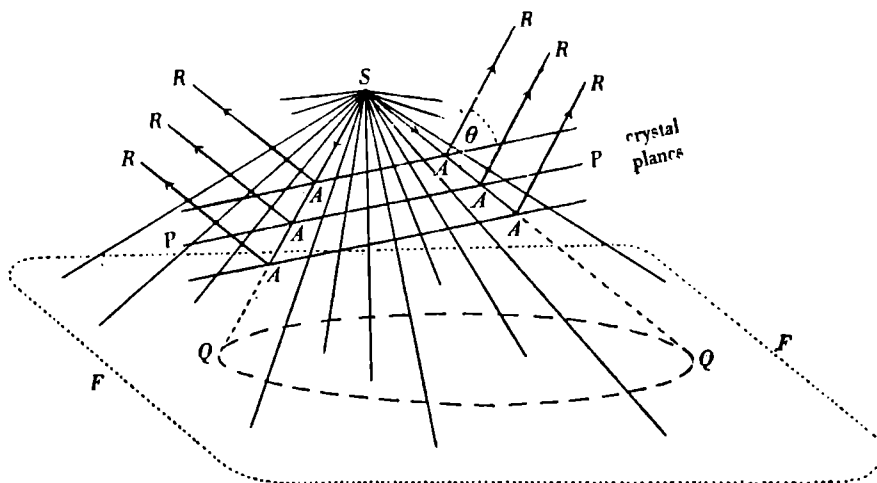
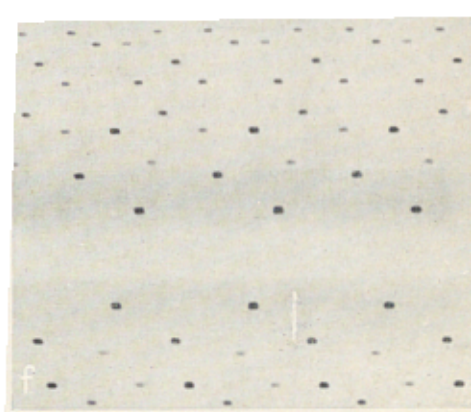
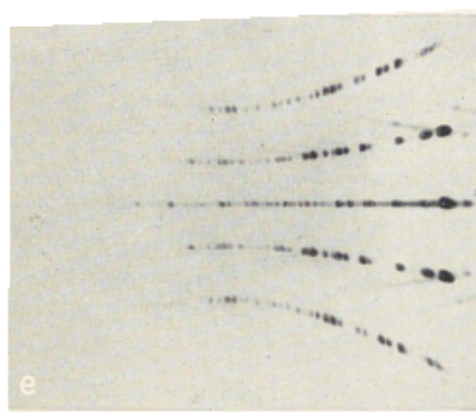
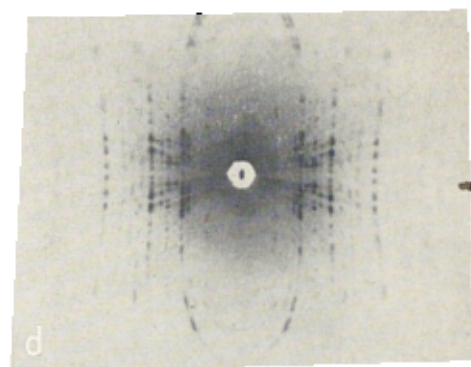
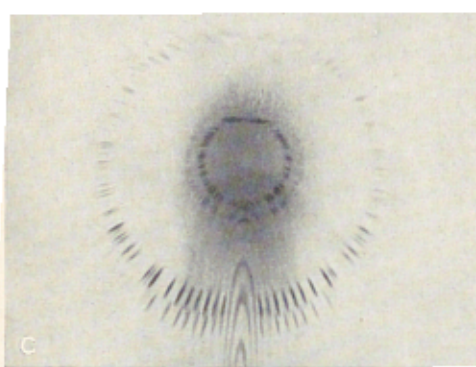
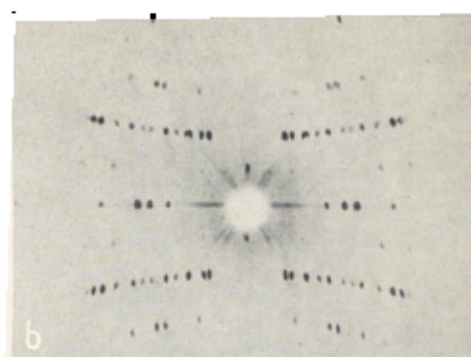
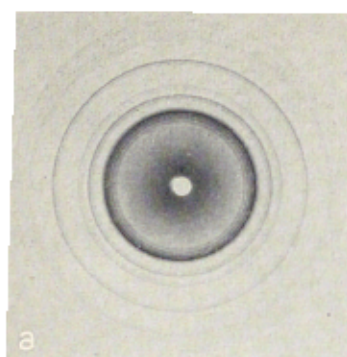


FIG. 59. Principle of divergent beam method. SA, incident rays; AR, reflected rays; QQ, trace on film F.

(Lonsdale, *Phil. Trans. Roy. Soc., A*, **240**, 222, 1947.)

crystal, very beautiful patterns (Pl. VIII) can sometimes be obtained which are quite unlike those given by other X-ray methods. They consist of white lines on a grey background, the lines themselves being sections of conics. Fig. 59 shows the principle of the divergent-beam method, which records in effect the increased *absorption* of X-rays in directions corresponding to Bragg reflection. The curvature of the absorption lines gives the Bragg angle and hence the spacing, while the *symmetry* of the crystal, and its orientation, are seen almost by inspection. This method will be referred to again in Chapter VI, where crystal texture is discussed.



(a) Black reflection powder photograph of α -alumina (Rooksby).

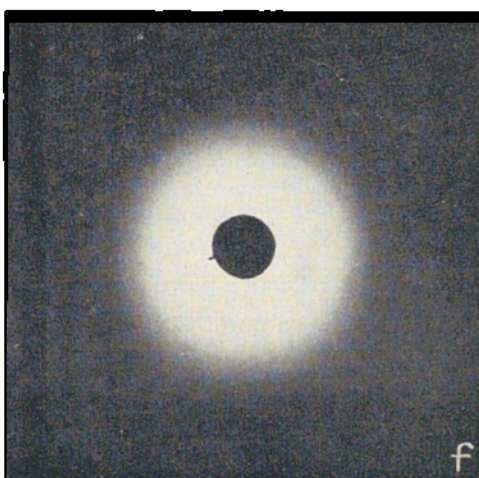
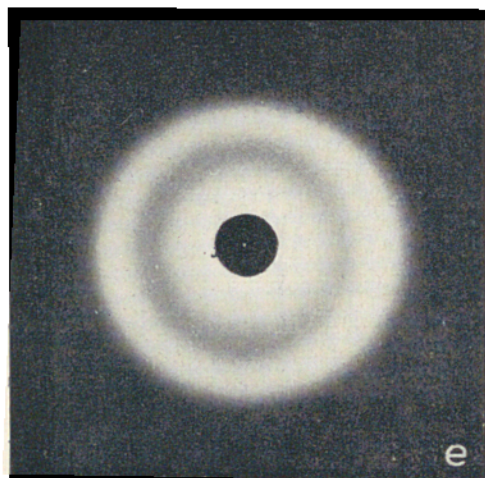
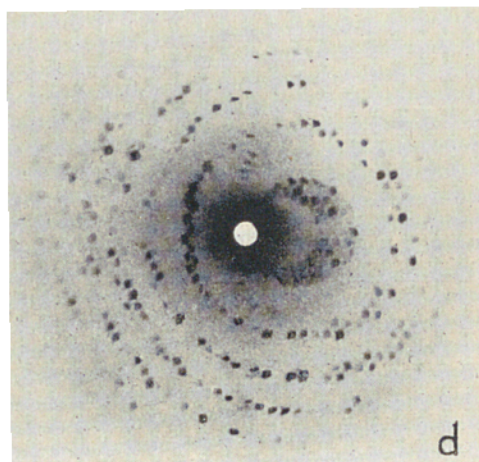
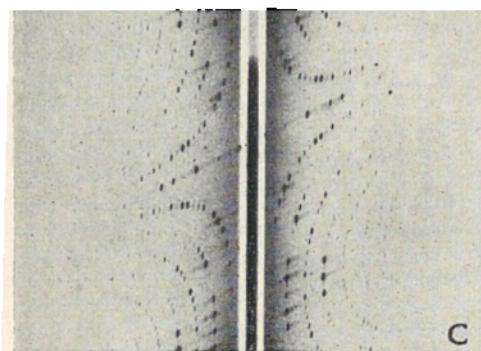
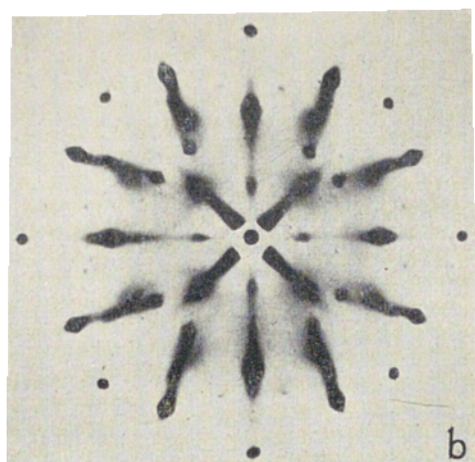
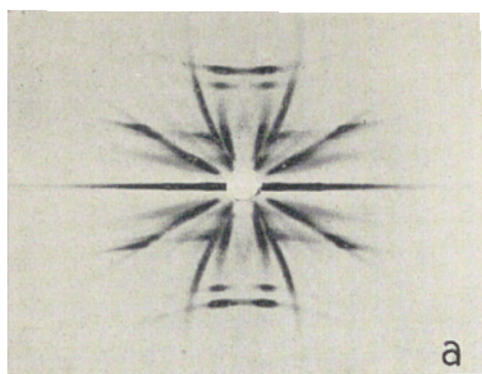
(b) Rotation photograph of urea nitrate, CuK radiation, showing well-marked 0, 1 etc. layer lines, and very weak 2, 3 etc. layer lines.

(c) Rotation photograph of ammonium oxalate monohydrate, CuK radiation, film normal to rotation axis.

(d) Rotation photograph of diphenyl butadiene, CuK radiation, showing well-marked row lines. The identity period along the rotation axis is about 32 Å.U.

(e) Rotation photograph of diphenyldiacetylene with film parallel to the rotation axis, but making an angle of only 10° with the X-ray beam.

(f) Weissenberg photograph of cyanuric triazide; note the *horizontal* rows of spots having intensities alternately strong and weak, and thus proving the absence of planes of symmetry parallel to the principal axis (Knaggs).



(a) Fibre photograph of asbestos (chrysotile), showing partial streaking along layer lines, due to breakdown of sideways periodicity (Astbury).

(b) Laue photograph showing formation of lamellae in age-hardened alloy (Preston, *Proc. Phys. Soc.*).

(c) Weissenberg photograph of single crystal of potassium penicillin II (Crowfoot and Rogers-Low).

(d) Oscillation photograph of horse methaemoglobin showing sections of reciprocal lattice nets by sphere of reflection (Perutz, *Proc. Roy. Soc.*).

(e) Scattering of CuK radiation by liquid oxygen streaming over a narrow cellulose acetate tube (positive print).

(f) Scattering by cellulose acetate tube only (positive print).

CHAPTER IV

GEOMETRICAL STRUCTURE DETERMINATION

IN order to be able to identify the reflections on an X-ray rotation photograph we must first of all consider what happens when an X-ray beam is scattered by a row of points perpendicular to it. The Laue condition mentioned in Chapter I is satisfied when $I \cos \phi = n\lambda$, I being the identity period, ϕ the complement of the angle of diffraction. The X-ray beam is, say, 1 mm. diameter, and I , the identity period, is only about one ten-millionth of a millimetre, and therefore the exact placing of the row of diffracting points does not matter as long as it is perpendicular to the X-ray beam. Diffraction by rows of points, having a common identity period I and a common direction, would give the same set of diffraction cones, even if the rows had no sideways periodicity at all. A photograph of disconnected rows of points would show *continuous* layer lines corresponding to $n = 0, 1, 2, 3 \dots$. If the least distance of the n th layer line from the origin (trace of undeviated X-ray beam) is y_n (fig. 60), and D the distance from crystal to film (the film being parallel to the row of points), then $D/y_n = \tan \phi$. Hence I can be obtained in terms of n, λ, D, y_n .

Almost continuous layer lines are found on X-ray monochromatic photographs of asbestos (Pl. VI *a*), the mineral chrysotile ($3\text{MgO} \cdot 2\text{SiO}_2 \cdot 2\text{H}_2\text{O}$). Such a photograph is obtained even when the crystal is stationary, not rotating, as long as the fibre axis is perpendicular to the X-ray beam. The streaks are not quite continuous because there is *some* periodicity perpendicular to the fibres, but there is also a good deal of randomness. Incidentally there is a very easy *cleavage* parallel to the fibre length, in fact more than one, as we should expect, since the forces perpendicular to the fibre length must be very weak. But there are also some spots on the layer lines. What do these mean? If the monochromatic X-ray beam is diffracted, not by a row of points but by a network of points kept stationary relative to the beam, there would be two intersecting sets of diffraction cones, giving spots at the points of intersection. If the network rotates about a row of points in it, or if there are networks whose direction is variable, but in which there is one common row of

points perpendicular to the X-ray beam, then there will be layer-line streaks of limited length, strong towards one end; these will correspond to the Laue condition $a(\cos \epsilon - \cos \phi) = n\lambda$, ϵ varying from $0 \rightarrow 2\pi$.

Another case in which there are two-dimensional networks formed is during the age-hardening of certain alloys, when a second phase is beginning to separate out in little sheets which

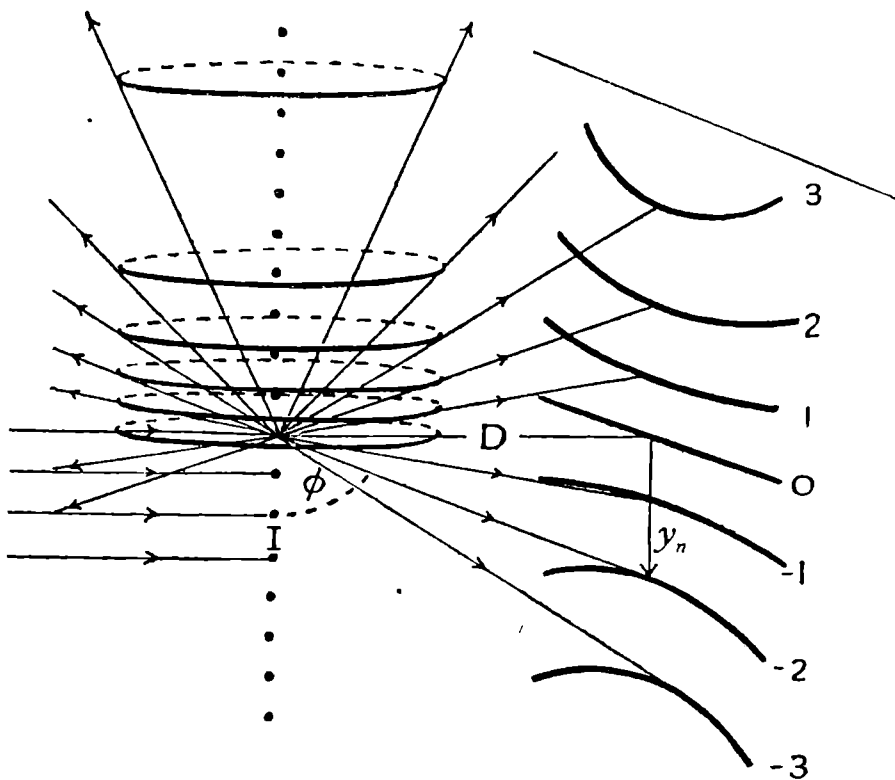


FIG. 60. Diffraction by a row of points giving layer lines from which the identity period I is determined.

are arranged at random in three orthogonal directions. This means that a Laue photograph taken with X-rays having a range of wave-lengths but with one strong monochromatic component would show an ordinary Laue photograph of the main phase and in addition it would show three superimposed two-dimensional spot-patterns given by the monochromatic rays diffracted from networks in the three orthogonal positions. They are seen in Pl. VI *b*.

But substances having periodicity in only one or two directions are very special cases. The vast majority of substances we know

have either no periodicity or have periodicity in three directions. In the latter case there are three sets of cones, resulting from the three Laue conditions. But three sets of cones do not in general intersect simultaneously in any random setting, for monochromatic radiation. They can only be made to do so by keeping one set constant in position and rotating the other two about it. The result is a series of spots arranged along layer lines, corresponding to the points where the three Laue conditions or, what is the same thing, the Bragg relation, is satisfied. The same conditions as in the one-dimensional case: $I \cos \phi = n\lambda$, $D = y_n \tan \phi$, give the identity period $I = \vec{ua} + \vec{vb} + \vec{wc}$ along the rotation axis $[uvw]$. Hence $I = \frac{n\lambda}{y_n} \sqrt{y_n^2 + D^2}$ if the film is parallel to the rotation axis. If it is not, (Pl. V c), then a slightly different formula holds. The indices of the planes giving reflections along layer lines must obey certain rules. If $[uvw]$ is the rotation axis, then planes in the zone $[uvw]$ will give reflections along the central or zero layer line. For all reflections in the zero layer line $hu + kv + lw = 0$. For the next layer lines $n = \pm 1$ in the Laue condition; that is, $hu + kv + lw = \pm 1$ for the first layer lines. For the second layer lines $n = \pm 2$, for the third $n = \pm 3$, and so on. If the crystal is rotating, for example, about the $[100]$ direction, then for the zero layer line $h = 0$; for the first, $h = \pm 1$; for the second, $h = \pm 2$, and so on. If the first layer lines are very weak, as in Pl. V b, that means that all (hkl) $(\bar{h}kl)$ planes give weak reflections, and that there must be some scattering unit half-way along the $[100]$ axis, not exactly like the one at the corner, but sufficiently like to weaken the first layer-line reflections.

By taking the crystallographic axes $[100]$, $[010]$, $[001]$ as rotation axes, the repeat distance \vec{a} , \vec{b} , \vec{c} can be determined. Other rotations will give the Bravais lattice very directly; for instance, if the identity period along $[111]$ is found to be not $\vec{a} + \vec{b} + \vec{c}$ (added vectorially), but $\frac{\vec{a} + \vec{b} + \vec{c}}{2}$, then the lattice must be a body-centred one; if the repeat distance along $[110]$ is $\frac{\vec{a} + \vec{b}}{2}$, then the (001) faces are centred by atoms, molecules or groups *identical* with those at the corners of the unit cell. For a

face-centred cube the identity distance along a cube edge is a , along any face diagonal it is $a/\sqrt{2}$ and along a cube diagonal it is $\sqrt{3}a$; and so on. Instead of taking several rotation photographs, however, it may be possible to get the same information (and some not otherwise obtainable) from a single rotation photograph and two or more Weissenberg photographs. The Weissenberg photograph corresponding to the zero layer line of a $[uvw]$ rotation contains only reflections from planes (hkl) for which $hu + kv + lw = 0$, that is, it contains only reflections from a single zone. Distances parallel to the translatory movement of the film correspond to angles about the rotation axis of the crystal, while distances perpendicular to that direction correspond to crystal spacings. The reflections are drawn out along well-defined curves (Pl. VI c) and indices can usually be assigned by inspection. In general, however, the actual identification of reflections, whether on a rotation or on an oscillation or a Weissenberg photograph, is greatly facilitated by consideration of what is known as the *reciprocal lattice* of the crystal. Later, when we consider deviations from strict periodicity in the crystal, the reciprocal lattice idea is almost indispensable.

WHAT IS THE RECIPROCAL LATTICE?

If one were asked for the description of a person, the reply given would depend on what the description was needed for. For a passport, the description would give height, colour of hair, colour of eyes, distinguishing marks and so on. For an insurance company, the description required would be a medical report, state of heart, lungs, etc. For an employment reference, the description would have to be one of character and behaviour: honest, industrious, sober, punctual! Each description has its place, none is complete in itself and they are not interchangeable for their particular purpose. It is the same with the description of a crystal. A purely crystallographic description would give symmetry, size and shape of the unit cell, and space-group. For the study of crystal physics or crystal chemistry, the arrangement of ions, atoms or molecules is required, and the nature of the forces between them. A description of the crystal in terms of its behaviour towards X-rays is given by an account of its reciprocal lattice, its *periodic distribution of reflecting power*. All of those descriptions are equally real—or perhaps we should say unreal.

After all, the space-lattice is quite imaginary; there is no actual framework. The atomic model is quite imaginary; the crystal is much more like a quivering jelly full of vibrating pips. The space-lattice and the atomic models are convenient for certain purposes; the reciprocal lattice is convenient for the purpose of the interpretation of photographs, or the study of reflecting power generally.

The Bragg relation, $n\lambda = 2d \sin \theta$, introduces the idea of reciprocity. If λ is constant, then a large d corresponds to a small θ ; the bigger the spacings the closer are the reflections to the incident beam direction. Then again we find that, theoretically, only crystals of infinite size in all directions give *point* reflections. The smaller the crystal the broader the reflections become; in fact, as we shall see presently, the size of colloidal crystallites can be calculated from the breadth of the reflections they give. Even the *habit* of crystals shows a reciprocal relationship with the shape of their unit cells. If the unit cell is long and thin, as in the case of long chain compounds, the crystal is sure to be of flaky or tabular growth, with the chain lengths nearly normal to the flake face. Crystals having a needle-like habit, among which are the penicillin salts, nearly always have the shortest axis parallel to the length of the needle. The reciprocal of a cube is an octahedron, since in either shape the distance from the centre to the surface in any particular direction is the inverse or reciprocal of that in the other. Many cubic crystals grow naturally as octahedra.

How do we represent the behaviour of crystals towards X-rays in *reciprocal space*? We begin by representing any infinite set of planes in ordinary space by an infinite set of points along a direction parallel to that of the normal to the planes (fig. 61). The distances of these points from an arbitrary origin are $\frac{k}{d}, \frac{2k}{d}, \frac{3k}{d} \dots$ where k is a constant controlling the size of the pattern, which for convenience' sake we shall take as 1. The first point of this set, at distance $1/d$ from the origin, has co-ordinates hkl , the indices of the set of planes (hkl) to which it corresponds. The other points will be $2h, 2k, 2l; 3h, 3k, 3l$; and so on. Corresponding to a zone of planes in the ordinary lattice there will be a *network* of points in the reciprocal lattice; the zone axis direction will be perpendicular to the plane of this network. Corresponding to the space-lattice of intersecting planes in ordinary space, there is a three-dimensional lattice of

points in reciprocal space; the reciprocal lattice: *Any* plane network of points in the reciprocal lattice corresponds to a zone

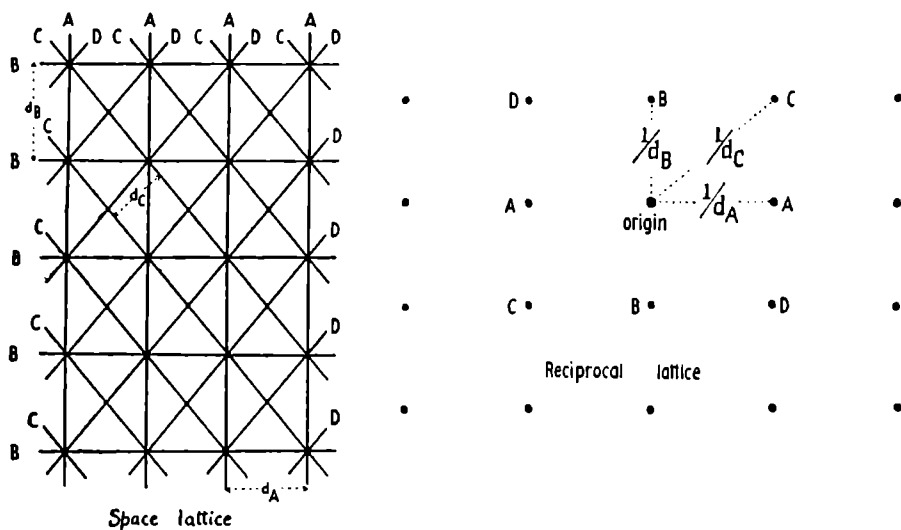


FIG. 61. Points reciprocal to the sets of planes in a zone.

(Lonsdale *Proc. Phys. Soc.*, 54, 314, 1942.)

of planes in the crystal. If the crystal is rotated about a zone axis, that is equivalent to rotating the reciprocal lattice about the perpendicular to a network of points. Now suppose the infinite

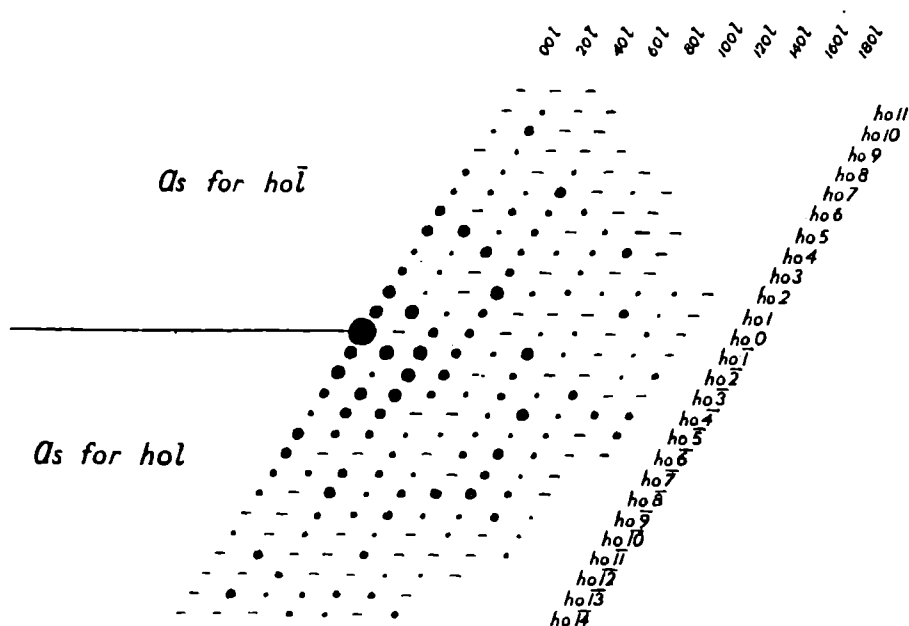


FIG. 62. Reciprocal Lattice, network [010] for metal-free phthalocyanine with points weighted to represent possible X-ray spectra.

set of planes, of spacing d , gives a set of n X-ray spectra, corresponding to $n\lambda = 2d \sin \theta$. These spectra will have certain intensities (some of which may be zero). Let us weight each of our nh, nk, nl points in reciprocal space with the scattering power of the n th order reflection from the appropriate set of (hkl) planes (fig. 62). Then the points in reciprocal space may be taken to represent the *potential* X-ray spectra from all the planes in the crystal. If the crystal is infinite in extent and perfectly periodic, the scattering power (potential scattering power, that is) of the crystal will be confined exactly to the points, the nodes, of the reciprocal lattice. Any limiting or irregularity of the crystal will result in a spreading of the scattering power in reciprocal space. We shall come to that when we consider small particle size, thermal vibrations, order and disorder in alloys and other kinds of departure from the perfect lattice; but let us now suppose the crystal to be infinite and perfect, and let us consider what is the geometrical condition that X-ray reflection shall actually take place; what is the significance of the Bragg law in reciprocal space?

Suppose the X-ray beam is incident in any given direction with reference to the crystal lattice (fig. 63). Let us say that it is normal to a zone axis and makes an angle of about 72° to the normal to a set of planes (hkl) . We can draw that direction in reciprocal space, passing through the origin O and coming from a point C such that $CO = \frac{k}{\lambda}$ (but we are taking $k = 1$). If with C as centre we then draw a sphere of radius $\frac{k}{\lambda}$ ($k = 1$), the surface

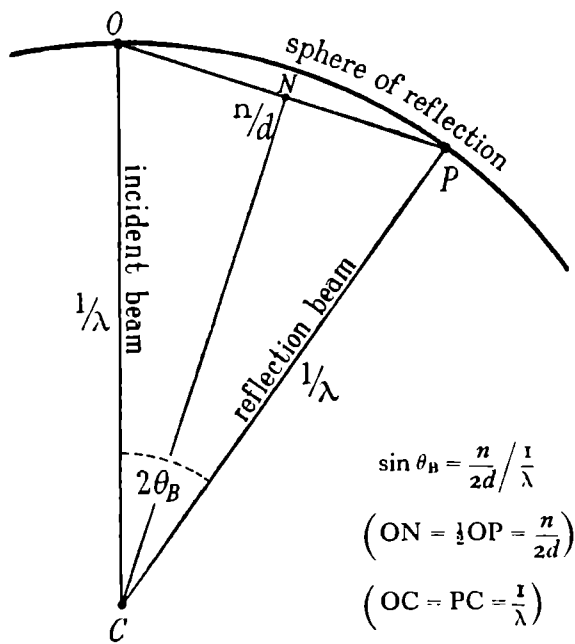


FIG. 63. Geometrical representation of Bragg reflection in reciprocal space.

(Lonsdale, *Proc. Phys. Soc.*, 54, 314, 1942.)

of this sphere will pass through the origin O and may perhaps pass through some other reciprocal lattice point P, at distance $\frac{n}{d}$ from O. If angle OCP = 2θ , then $\sin \theta = \frac{n}{2d} \frac{1}{\lambda}$, or $n\lambda = 2d \sin \theta$. The Bragg law then is geometrically satisfied for any point in

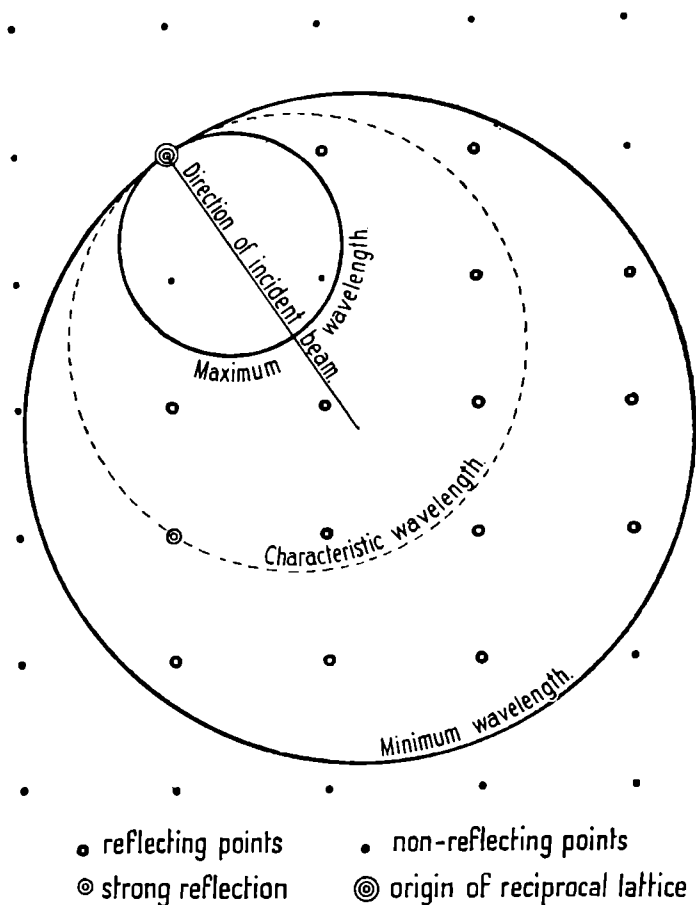


FIG. 64. Laue method.
 (Lonsdale, *Proc. Phys. Soc.*, 54, 314, 1942.)

reciprocal space which lies on, or can be made to pass through, the surface of the *sphere of reflection*. Points in reciprocal space can be made to intersect this surface in a variety of ways. In the *Laue method* (fig. 64) the different wave-lengths in the incident beam correspond to an infinite series of spheres, all touching each other at O, and with their centres along a common direction. The sphere of maximum radius corresponds to the minimum wave-length given by the target. The sphere of minimum radius

corresponds to the longest wave-length effective in reflection. All reciprocal lattice points between the maximum and minimum spheres reflect simultaneously. If CO lies on some symmetry element in the reciprocal lattice (along a 4-fold axis, for instance), then the spheres will be symmetrically arranged relative to the

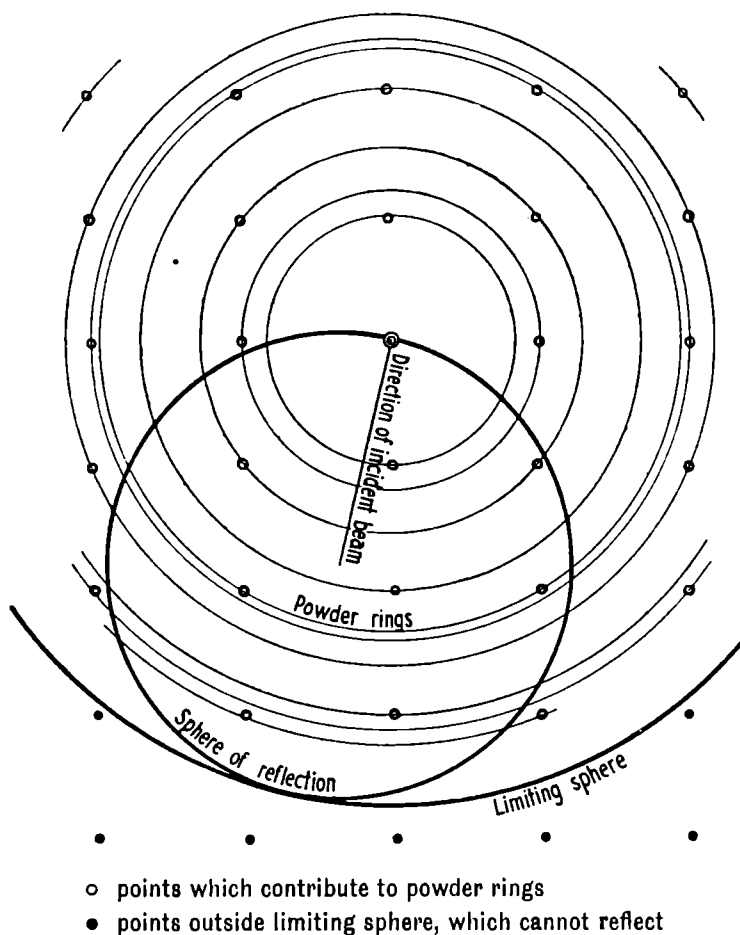


FIG. 65. Powder method.

(Lonsdale, *Proc. Phys. Soc.*, 54, 314, 1942.)

reciprocal lattice points, and the pattern observed will be a symmetrical one. In the *powder method* there will be a reciprocal lattice corresponding to each differently orientated crystallite (fig. 65). We may therefore consider the reciprocal lattice as being rotated in all directions about the origin, so that every point of the reciprocal lattice forms a sphere about the origin. Each of these spheres, if its radius is less than $2/\lambda$, will intersect the sphere

of reflection in a circle or ring. Reflections from all the points of the reciprocal lattice for which $2d$ is greater than λ will give the familiar concentric powder rings. In the *rotation method* the single crystal usually rotates either about a zone axis or, occasionally, about the normal to a set of crystal planes, and the

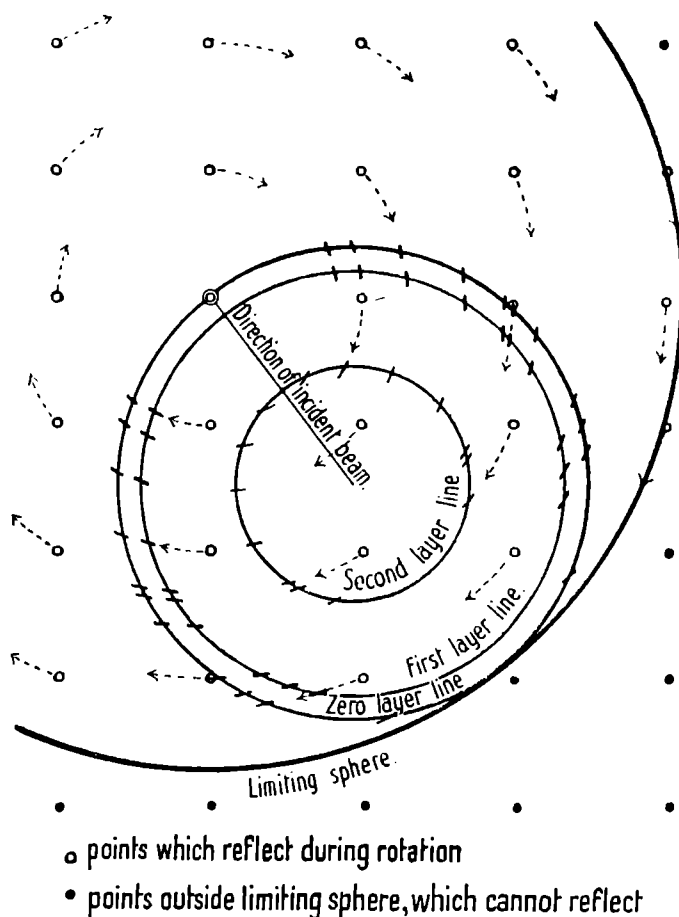


FIG. 66. Rotation method.

(Lonsdale, *Proc. Phys. Soc.*, 54, 314, 1942.)

X-ray beam is usually incident in a direction perpendicular to the axis of rotation. We can either regard the reciprocal lattice as rotating about a tangent to the sphere of reflection or, more simply, the sphere of reflection can be regarded as rotating in the stationary reciprocal lattice. In either case reciprocal lattice points will intersect the spherical surface one after another during the rotation, and the layer lines (fig. 66) will be formed by succes-

sive reciprocal lattice nets. In the *oscillation method* (fig. 67) only a few reciprocal lattice points can intersect the surface of the sphere of reflection as it oscillates to and fro between its limiting positions. Even in the rotation method not all planes can reflect in any given rotation because the number of reciprocal lattice points that can

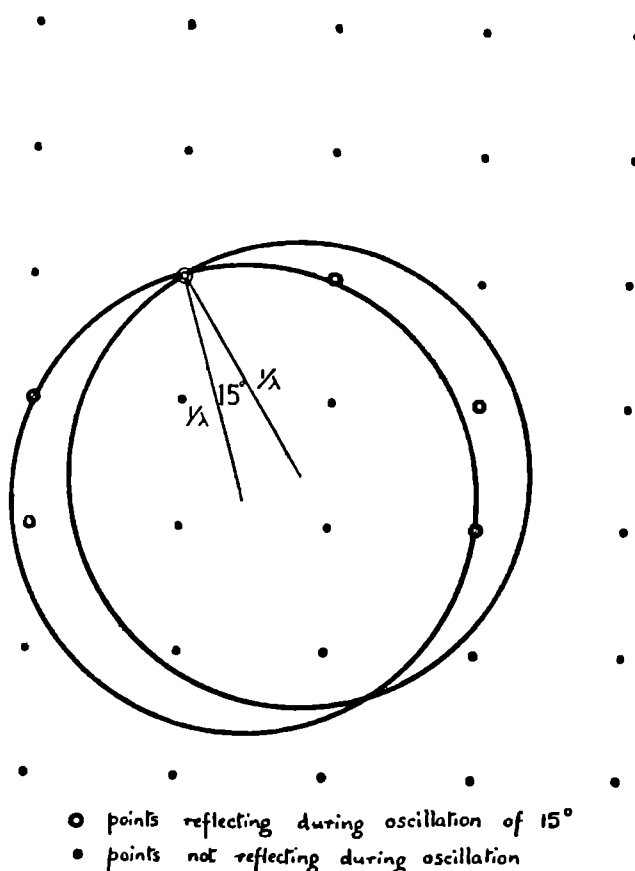


FIG. 67. Oscillation method.

(Lonsdale, *Proc. Phys. Soc.*, 54, 314, 1942.

intersect the surface of the sphere of reflection is restricted to those lying within the *tore* swept out by a circle rotating about a tangent. The planes that can reflect in all possible rotations are limited to those lying within the *limiting sphere* whose radius is $2/\lambda$. For all points outside this limiting sphere, $\sin \theta = \lambda/2d$ would be greater than 1, which is clearly impossible. Apart from the planes that *reflect*, however, the reflections that are *recorded* on a film, whether a plane film, a cylindrical film, or a screened moving film, will depend upon the geometry of the experimental

set-up (fig. 68). It has already been mentioned that the networks of the reciprocal lattice which are perpendicular to the rotation axis give the *layer lines*. Rows of points in reciprocal space which are parallel to the rotation axis give reflections which lie on closed curves, the shapes of which are clearly seen in Pls. III *d* and V *d*; these are usually known as *row lines*. The indices of all such points in a row must satisfy some zone law. For instance:

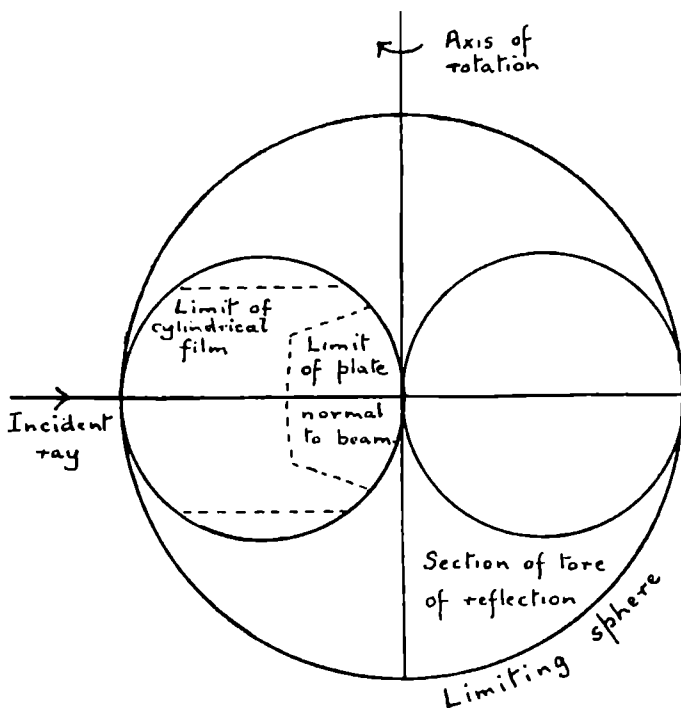


FIG. 68. Limiting sphere and limit of recorded reflections on spherical, cylindrical and plane films, for one rotation position (after Bernal).

if the crystal is rotating about the $[001]$ axis, then the points $120, 121, 122, 123 \dots$ will give reflections along a row line. These all belong to the zone $[2\bar{1}0]$, which is perpendicular to $[001]$.

From the spacings of the layer and row lines on the photograph we can get back to the spacings of the nets and rows of points in the reciprocal lattice either by the use of tables or by means of charts constructed by J. D. Bernal and described by him in the *Proceedings of the Royal Society* (1926), A. 113, 117 (fig. 69). Other charts can be used to work out the indices of reflections on cylindrical films, on oscillation or on Weissenberg photographs. Sets of photographs with three main crystal axes taken as rotation axes will cover practically the whole of the limiting

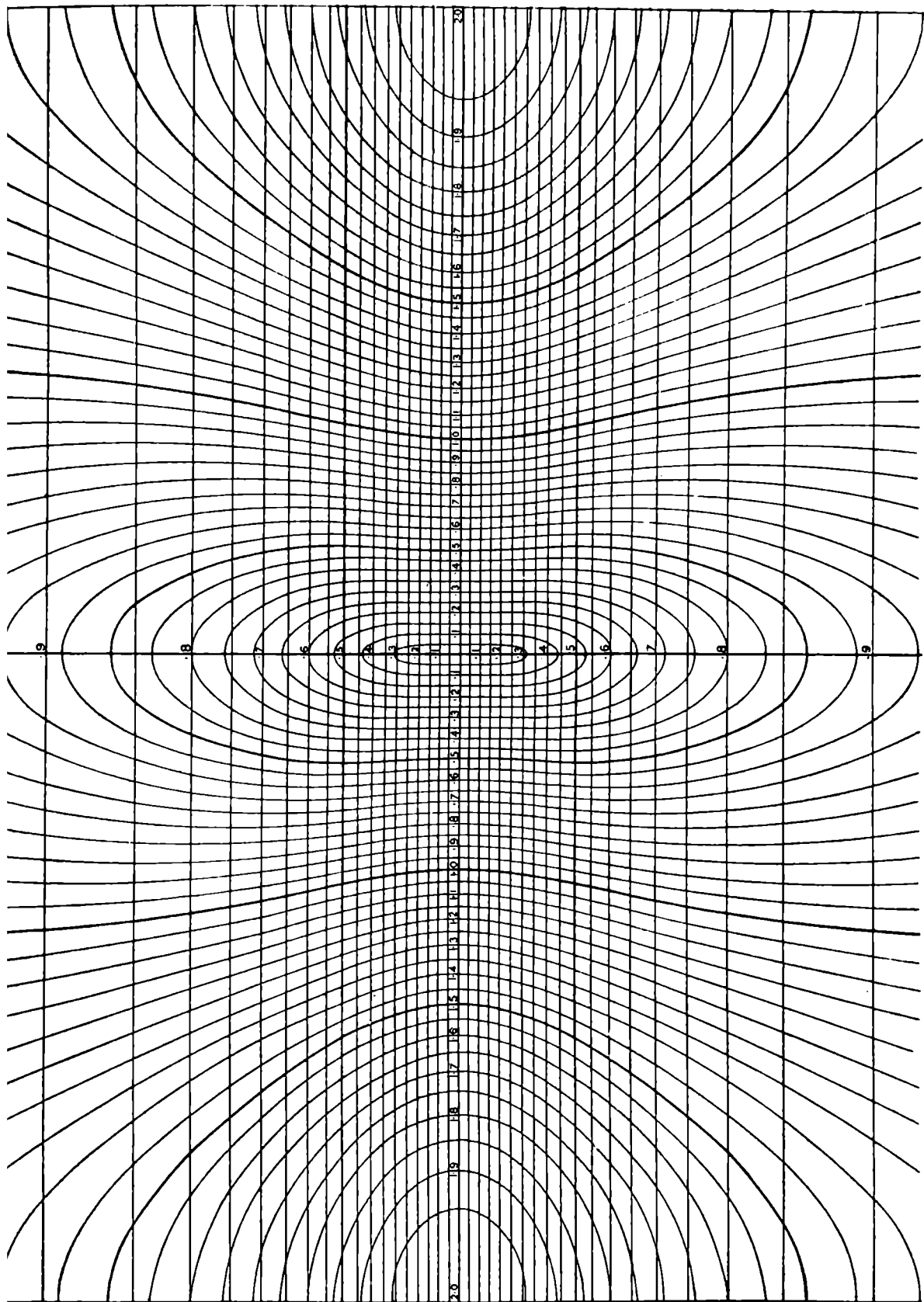


FIG. 69. Bernal chart for rotation method with cylindrical film, radius 3 cm.
(Bernal, *Proc. Roy. Soc., A.* 113, 117, 1926.)

sphere for a given wave-length, but by using another shorter wave-length it is often possible to extend the measurements considerably, since a shorter wave-length means a larger limiting sphere. Bernal, Crowfoot, Perutz, Riley and others have used oscillation photographs for the investigation of crystalline proteins, which have very large unit cells, with most useful results. The large size of the unit cell means that the reciprocal lattice points are very close together and even a small oscillation will give photographs on which several circular slices of the reciprocal lattice as it cuts the sphere of reflection can be clearly seen (Pl. VI *d*). Such photographs give the reciprocal lattice dimensions almost without any distortion (Pl. XII *d*); in fact, the shorter the wave-length relative to the size of the unit cell, the less is the distortion of the reciprocal lattice as seen on the photograph, but the less also, unfortunately, is the resolution. Some kinds of apparatus have been devised, notably by de Jong and Bouman, and by Buerger, which record the reciprocal lattice without distortion, even for small unit cells. But the complexity (and therefore cost) of such ingenious apparatus increases with the ease of interpretation.

DETERMINATION OF SPACE-GROUP

Once the photographic methods have given a series of reflections whose indices have been found by reciprocal lattice charts or by calculation, then the systematic absence of spectra can be



FIG. 70. Effect of doubling the number of lines in a grating is to eliminate odd order spectra.

detected, and it is such 'absent spectra' that provide the data for the deduction of space-group, by locating glide planes and screw axes. In the case of a line grating giving a set of optical spectra (fig. 70), an interleaving of the rulings by an exactly similar set will cancel all the odd order spectra. The effect of a

glide plane parallel, say, to (001) with translation $\vec{b}/2$, is to provide just such an interleaving, along the \vec{b} direction, of all planes in the $[001]$ zone which do not already pass through the point o ,

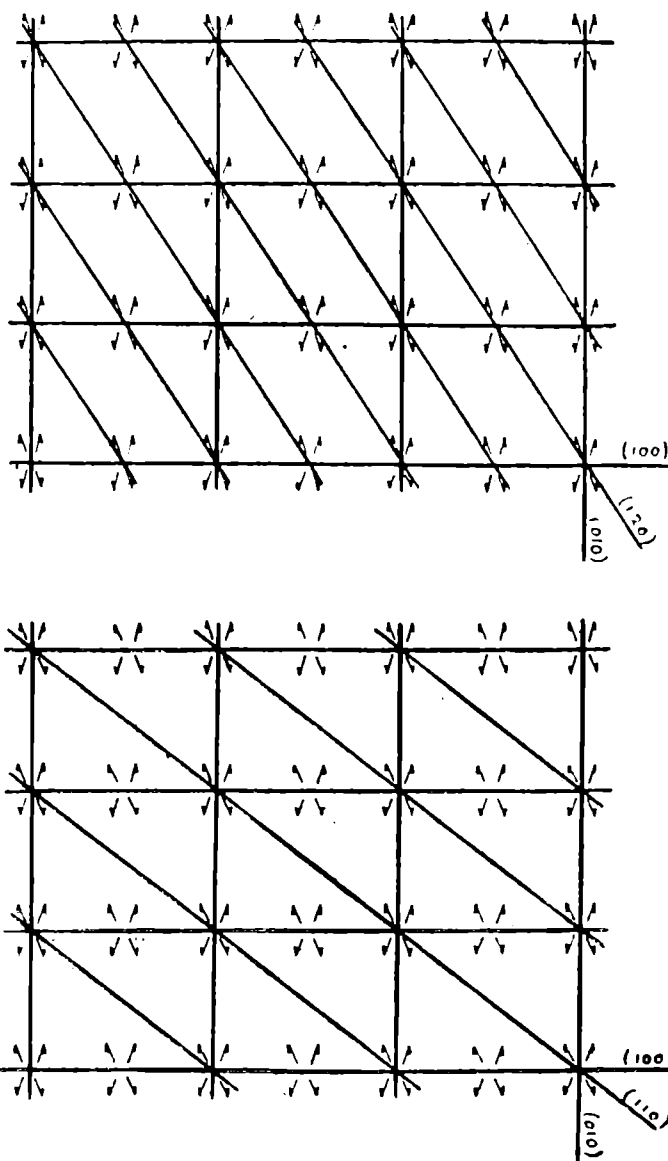


FIG. 71. A glide plane parallel to (001) , the plane of the paper, with glide of $\vec{b}/2$, causes the disappearance of odd order spectra from planes (hko) for which k is odd, but not from those for which k is even.

$b/2, 0$; in other words, all hko reflections will be absent if k is odd (h and k can here have any values, they need not be prime to each other) (fig. 71). If the glide plane is (010) and the transla-

tion $\frac{\vec{a} + \vec{c}}{2}$, then all hol reflections will be absent if $(h + l)$ is odd.

Screw axes cause the disappearance of sets of spectra from just the planes to which they are perpendicular. A 2_1 axis leaves only even orders of reflection; so does 4_2 or 6_3 ; a 3_1 or 3_2 axis perpendicular to (001) leaves $003, 006, 009 \dots$; so does 6_2 or 6_4 ; 4_1 and 4_3 eliminate all but $004, 008, 0012 \dots$; 6_1 and 6_5 leave only $006, 0012 \dots$. Tables are available from which the space-group can be found when a complete list of the missing spectra is made, although in a few cases the space-group cannot be determined uniquely because two or more space-groups may have the same 'absent spectra.' But in general a knowledge of the indices of all reflections which occur will give the framework on to which the atoms must fit (*International Tables for the Determination of Crystal Structure*, Part I).

ATOMIC OR MOLECULAR SYMMETRY

The next step is to determine the number of atoms or molecules in the unit cell and to decide what symmetry they must have. If the number is small the problem of structure determination may be simplified considerably by this procedure; at the worst it limits the number of variable parameters that have to be determined.

If the unit cell has volume V and density ρ , the mass of scattering material in the unit cell is $V\rho$. This must be equal to nM/N , where n is the number of molecules $A_x B_y C_z \dots$, M is the molecular weight in grams, N is Avogadro's number. All these quantities are known except n , which can therefore be found. V is a function of $a, b, c, \alpha, \beta, \gamma$. For a triclinic unit cell

$$V = abc \begin{vmatrix} 1 & \cos \gamma & \cos \beta \\ \cos \gamma & 1 & \cos \alpha \\ \cos \beta & \cos \alpha & 1 \end{vmatrix}^{\frac{1}{2}}$$

$$= abc \sqrt{1 - \cos^2 \alpha - \cos^2 \beta - \cos^2 \gamma + 2 \cos \alpha \cos \beta \cos \gamma}.$$

Actually we do not need to determine all these quantities, although we *can* if we wish get a, b, c from layer-line distances on rotation photographs and α, β, γ either from optical or Bragg spectrometer measurements, or from Laue or Weissenberg photographs. But the volume of the cell is simply its section multiplied by its height, and these can be found from a single rotation photograph

about a cell edge. The crystal density can be determined by flotation in a liquid which is a mixture of one a little lighter and another a little heavier than the crystals immersed in it. The density of the liquid in which the heaviest crystals, freed from air-bubbles, neither rise nor sink, is found by a specific-gravity bottle or other method. For very small crystals centrifuging may be necessary to hasten the settling-down process. Obviously one must choose liquids in which the crystals do not dissolve; or if that is impossible, saturated solutions can be used.

The unit cell must, of course, contain an exact number of molecules, and if, therefore, $n (= NV\rho/M)$ is not exactly integral, the difference must be due to inaccuracy in one or more of the measured quantities. If the size of the unit cell has been measured very accurately, and the density also, this gives an accurate method of determining the molecular weight, which is sometimes useful. Incidentally, ordinary rotation or Weissenberg photographs do *not* give accurate measurements of unit cell dimensions. Distances between the centres of spots on a quarter-plate cannot be measured more accurately than 1 in 500 at best. Using special methods that will be described later, unit cell dimensions can be obtained with an accuracy of 1 in 50,000, or even better.

The number of ways in which n molecules can be fitted into the unit cell is sometimes limited by the symmetry. Suppose that the space-group is Pmm (two planes of symmetry intersecting in a 2-fold rotation axis); and suppose that there is in it *one* 'molecule' AB, consisting of two atoms A and B. Either they can both lie

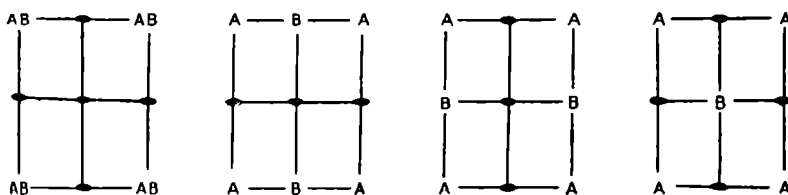


FIG. 72. Possible arrangement of one A and one B atom in Pmm .

along a single 2-fold axis at a distance apart which has to be determined (one variable parameter). Or A can lie on one 2-fold axis and B on another 2-fold axis, which can be done in three different ways, and again there will be one variable parameter to determine (fig. 72).

If A and B were both on the same axis, and if their distance apart were not $c/2$, then the structure could properly be regarded

as a molecular one, the molecular symmetry being a dyad axis. But if A and B are on different axes, then there is nothing to relate one particular B atom to one particular A atom; each B atom is equidistant from two or four or perhaps—if it is in the centre of the cell—from eight A atoms. It is then said to be 2-fold, 4-fold or 8-fold coordinated with A; and A atoms are similarly coordinated with the B atoms that are coordinated with them. In structures such as NaCl (three-dimensional chess-

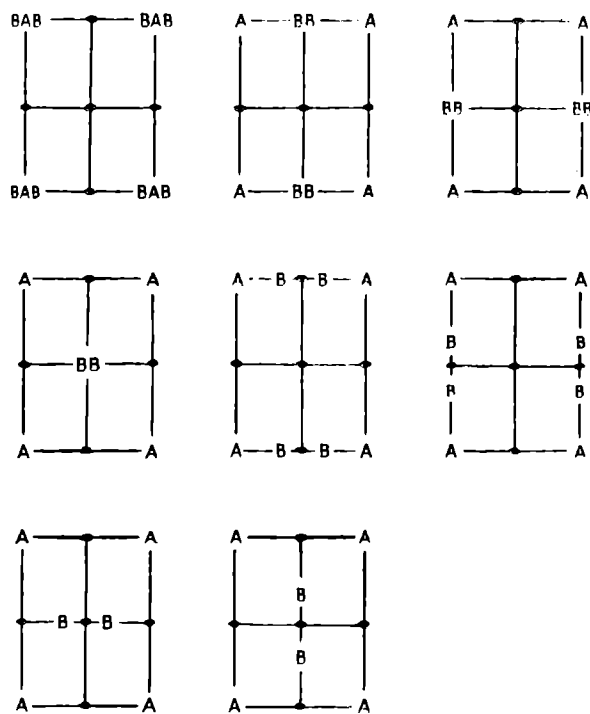


FIG. 73. Eight possible arrangements of one A atom and two B atoms in *Pmm*.

board arrangements) each atom is 6-fold coordinated; in CsCl each has 8-fold coordination.

If there are *one* A and *two* B atoms in the *Pmm* unit cell, then the number of possible arrangements and the number of variable parameters is even greater. All three atoms could lie along a single axis; in which case AB_2 might be a real molecule. Or the A atom might lie on one axis and the two B atoms on any of the other three; or the B atoms could both lie on one of the four planes of symmetry with two variable parameters involved in their positions (fig. 73). These would be non-molecular structures in which A and B would be differently coordinated. So

that even finding the arrangement of $A + zB$ in one of the simplest space-groups involves the systematic investigation of many possibilities.

Nature's love of variety is shown in figs. 74 and 75 by the

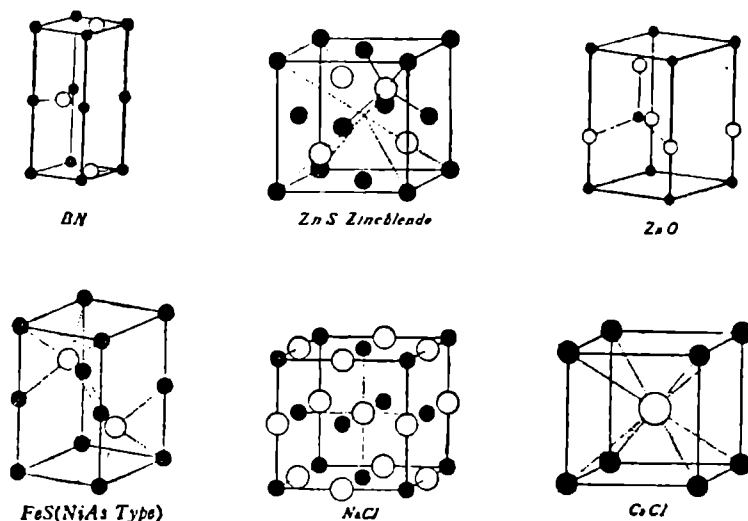


FIG. 74. Structure types of compounds AB .

(Goldschmidt, *Trans. Far. Soc.*, 254, 1929.)

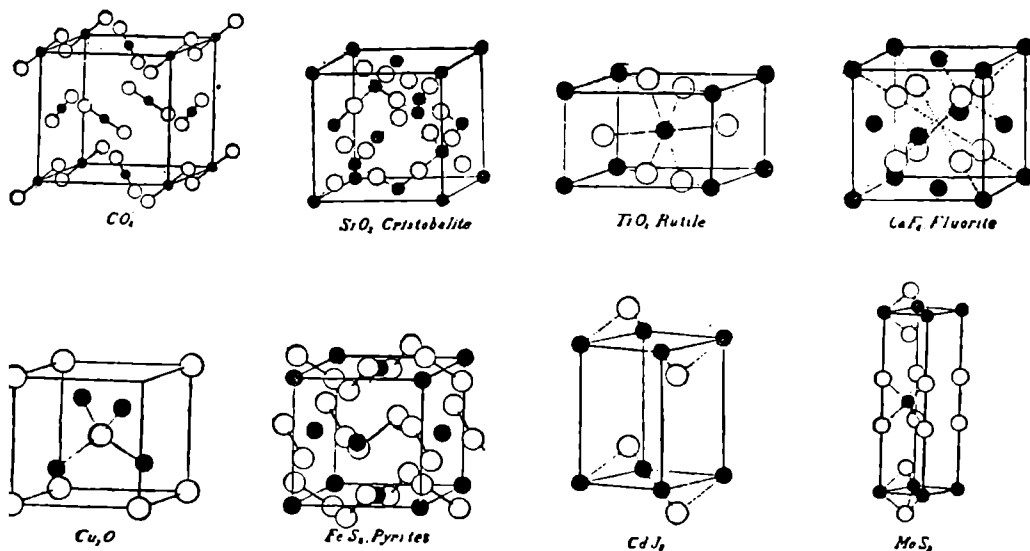


FIG. 75. Structure types of compounds AB_2 .

(Goldschmidt, *Trans. Far. Soc.*, 255, 1929.)

many ways in which AB and AB_2 compounds do in fact crystallise, of which these are only a few. All those that have been found are systematically described in the volumes of the *Strukturbericht*,

published originally in Leipzig and now being continued by a Committee of the International Union of Crystallography.

The elements themselves, of course, crystallise in quite a surprising variety of ways, some of them in more than one way. Carbon, for instance, crystallises as diamond or as graphite, with very different, almost contrasting, properties in the two cases; in fact there are at least two different crystalline forms of graphite also. Some metals, such as iron, crystallise in different ways at different temperatures; and so do many compounds. In dealing with fairly complicated organic molecules a knowledge of the number of molecules in a unit cell of given symmetry can provide important stereochemical information even without a detailed structure analysis. For example, in the case of dibenzyl there are two benzene rings joined by two CH_2 groups. The single bond between the CH_2 groups implies that it would be quite possible for the plane of one ring to be rotated with respect to that of the other. But the space-group of dibenzyl is $P2_1/a$ (a 2-fold screw axis perpendicular to a glide plane of translation $\vec{a}/2$) and the number of dibenzyl molecules in the unit cell is only two. Four asymmetric units would be required to build up the $P2_1/a$ symmetry (fig. 76), and the two molecules must each, therefore, have

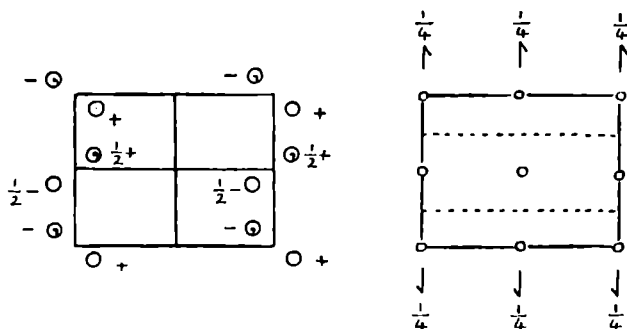


FIG. 76. $P2_1/a$ space-group, showing four asymmetric units, and symmetry.

(Mode of presentation used in *International Tables for the Determination of Crystal Structure*.)

2-fold symmetry. A molecule such as dibenzyl cannot have a screw axis or a glide plane; it could only have a centre of symmetry. For the dibenzyl molecule to have a centre of symmetry the two benzene rings must be parallel to each other; a stereochemical fact which could therefore be ascertained without knowing more than the number of molecules in the unit cell.

Similarly the fact that the succinic acid molecule has centrosymmetry shows that in the solid state the configuration is of the 'trans-' type.

Although single monomeric molecules can only have pure elements of symmetry, and not screw axes or glide planes, the same is not true of high polymers. In the case of high polymers such as rubber or textile fibres, or synthetic long-chain molecules such as polyethylene — $\text{CH}_2 - \text{CH}_2 - \text{CH}_2 - \text{CH}_2 - \dots$, the unit cell is only a part of a molecule and the molecule as a whole might have a screw axis.

Since X-rays cannot decide whether or not a centre of symmetry is present in the structure, and since this information is essential in order to determine not only space-group but molecular symmetry, it is necessary to test for the centre by finding out whether or not the crystals are piezo- or pyro-electric. Non-centrosymmetrical crystals, when compressed or extended, heated or cooled, develop electric charges, becoming $+^{\text{ve}}$ at one end and $-^{\text{ve}}$ at the other. Small crystals suddenly cooled in liquid air, if free to move, will repel each other; if the crystal is big enough to be placed between the plates of a little condenser the charges developed on cooling may be measured with a sensitive electrometer. But it must be remembered that small effects may be missed and that only positive results are really significant. More will be said about piezo-electricity in a later chapter, in relation to changes of crystal structure with temperature.

MEASUREMENT OF INTENSITY OF REFLECTION

But the real work of finding out just where the atoms are depends upon measurement of intensities. Much the best method of measuring intensities of reflection is by means of the ionisation or Geiger-counter spectrometer. By moving the crystal slowly through the reflecting position with angular velocity ω , and leaving the ionisation chamber slit wide open in the position (at angle 2θ) in which it collects the reflected beam, or by moving the Geiger tube at twice the rate of the crystal, a very accurate measurement of the integrated reflection can be made. This can be put on to an absolute scale by comparing it with the intensity I_0 of the primary beam, measured after a known reduction of intensity by absorption in a calculated thickness of Ni. This gives the absolute integrated reflection $E\omega/I_0$,

where E is the total energy received by the chamber during the reflection. It would be much too tedious, however, to do this for more than a relatively few planes unless an automatic recorder were used, and this introduces considerable difficulties of calibration. Sometimes 500 or 1000 reflections can be obtained on a few photographs. These can be photometered (special integrating photometers have been designed for obtaining quickly the whole intensity of a spot), and they can be put on to an absolute scale by comparison with a secondary standard. Two-crystal spectrometers have been designed by means of which the reflections from a crystal being investigated can be recorded, for comparison purposes, side by side with those of a standard crystal. A survey of photometric methods was made in the *Journal of Scientific Instruments* for July 1941 and November 1943. But the most recent photometric method, which seems to be just as accurate as any other measurements on photographs, is to make eye estimations with a series of comparison reflections recorded in various times to give an intensity scale (time and intensity being interchangeable for X-rays). Intensities of widely differing values can be brought within the range of visual (or other photometric) comparison by the use of a film pack; several films are placed one behind the other and processed together with each other and with an intensity scale; the reduction factor from each to the next is then determined for a number of reflections, either photometrically or by eye estimation. If there are n films, and the intensity (measured in terms of the intensity scale) is reduced by a factor R on passing through each film, then the apparent intensity of a spot on the n th film will be R^{n-1} of that on the first film. Let us suppose that the eye can accurately assess an intensity ratio of 100 : 1, and that for higher intensities the film begins to show reversal, but that in fact a ratio of 800 : 1 exists. It is necessary to arrange that $800 \cdot R^{n-1} = 100$. The value of R for double-coated blue base X-ray film is about 0.5, and therefore the condition will be satisfied by $n = 4$, if such films are used.

Suppose now that we have the intensities of all the observable reflections. How are they to be interpreted? What are the factors that will affect the intensity? They are rather a formidable array: The intensity of the incident beam, the wave-length of the X-rays used, the size, perfection and absorbing power of the crystal, the angle at which selective reflection takes place, the time during

GEOMETRICAL STRUCTURE DETERMINATION 103

which the crystal reflects, the number of planes which contribute to the particular reflection considered, the degree of polarisation of the incident and reflected beams, the geometry of the experimental arrangements, the scattering power of a single electron, the total number of extra-nuclear electrons present, the amplitude of thermal vibration of the atoms and the mutual arrangement of electrons (electron density distribution) in the structure.

But first of all we need only consider how just one single electron scatters X-rays; then we shall consider how the electrons in one atom add up their effects, or interfere with each other; after that we can consider how the diffraction by whole atoms adds up or interferes, according to their mutual arrangement, and finally all the other effects can be taken into account.

CHAPTER V

DETERMINATION OF ATOMIC AND ELECTRONIC DISTRIBUTION

THE SCATTERING OF X-RAYS BY ATOMS

WHEN an unpolarised X-ray beam is incident on an electron which is either free or relatively weakly bound it forces the electron to vibrate with a frequency ν_0 , which is the same as that of the incident radiation. The vibrating electron then emits secondary (scattered) radiation, still of frequency ν_0 , but of amplitude A_e different from the amplitude A_0 of the incident wave. This radiation will be polarised (fig. 77). The forced electronic

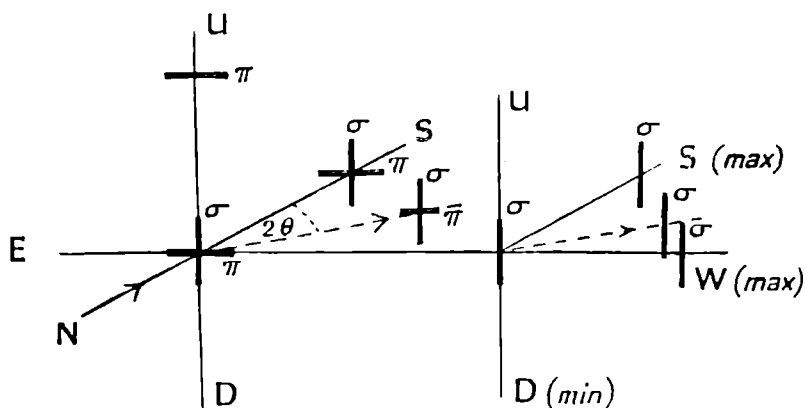


FIG. 77. Forced electronic vibration, and polarisation of scattered radiation.

vibrations must be perpendicular to the direction of the incident X-ray beam, which is travelling, shall we say, along the $N \rightarrow S$ direction. Let the electronic vibration be resolved into a π component along the EW direction and a σ component perpendicular to the NSEW plane. The radiation scattered in the NSEW plane due to the π component will be dependent on the angle of scattering 2θ (being zero along EW and a maximum along NS); that due to the σ component will be independent of angle. In fact, the radiation scattered in UDEW, the plane perpendicular to NS, will be completely plane polarised. The intensity of the scattered radiation is proportional to the square of the amplitude,

or if A_e^σ and A_e^π are the amplitudes of the σ and π components then $I_e = K[(A_e^\sigma)^2 + (A_e^\pi)^2]$. But for a free electron charge $-e$, mass m , the amplitude of the wave scattered at an angle 2θ and received at a distance R away is

$$A_e^\sigma = \frac{1}{\sqrt{2}} A_0 \frac{e^2}{mc^2} \frac{1}{R};$$

$$A_e^\pi = \frac{1}{\sqrt{2}} A_0 \frac{e^2}{mc^2} \cdot \frac{\cos 2\theta}{R} \quad (c = \text{velocity of light}).$$

Hence

$$I_e = I_0 \left(\frac{e^2}{mc^2} \right)^2 \frac{1 + \cos^2 2\theta}{2R^2},$$

where $I_0 = KA_0^2$ is the intensity of the incident beam. $\frac{1 + \cos^2 2\theta}{2}$

is known as the *polarisation factor*. If the incident beam is already polarised (as in the case of a beam monochromatised by crystal reflection), then the polarisation factor will be more complicated.

Since the intensity of the secondary radiation scattered from *any* particle is inversely proportional to the square of its mass, it will be readily understood that the contributions of the atomic nuclei to the scattered radiation are negligible. Even the lightest nucleus, the proton H^+ , is 1846 times as heavy as an electron.

The scattered waves from different parts of the atom will interfere with, or reinforce, each other. The intensity of the wave scattered in any particular direction by the whole atom must depend on the distribution of the electrons in the atom. The amplitude of the wave scattered by a bound electron is $A_e \cdot f_n$ where A_e is the amplitude of the wave scattered by a free electron and $f_n = \int_0^\infty U(r) dr \cdot \frac{\sin x}{x}$. In this formula $x = \frac{4\pi r \sin \theta}{\lambda}$ and $U(r) dr$

is the probability of finding the electron between the distances r and $r+dr$ from the nucleus. The amplitude of the wave scattered by all the Z electrons in the atom is obtained by summing $A_e \cdot f_n$ from $n=1$ to $n=Z$. The intensity I_λ is thus $I_e \left(\sum_1^Z f_n \right)^2$, and it can be estimated by making assumptions about the distribution of electron density in the atom. The *atomic scattering factor* $f \left(= \sum_1^Z f_n \right)$

is simply proportional to the atomic number Z for $\theta=0$, but becomes smaller as $\frac{\sin \theta}{\lambda}$ increases. The rate of fall is more rapid the more attenuated is the electron cloud. This factor f is a constantly recurring feature of X-ray work; it occurs in X-ray scattering by gases and liquids, in Bragg reflection by crystal planes, in the expression for the diffuse scattering due to thermal

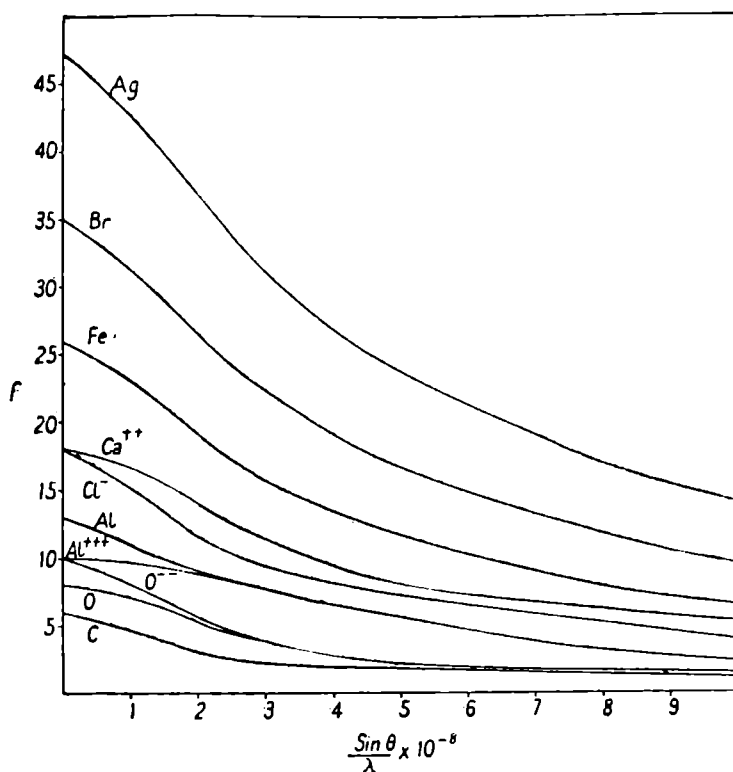


FIG. 78. Atomic scattering curves for some atoms and ions.

(Bunn, *Chemical Crystallography*: Clar. Press.)

and other disturbances of crystal regularity. It can be measured using any of these methods and then, by comparison with calculation, it can be used to test various theories of atomic structure. In principle, the simplest way of measuring f is to determine the scattering curve (intensity v. $\frac{\sin \theta}{\lambda}$) for gases; and this has been done for Ar, Ne, He, H_2 , O_2 , etc. The measured curve (fig. 78), however, includes also the Compton (incoherent) scattering mentioned in Chapter II, which must be subtracted in order to

obtain the true f curve. One result of the experimental determination of f has been to confirm the inadequacy of the old Bohr orbital model of the atom. Much better agreement is obtained by applying wave-mechanical theory to the calculation of the electron density distribution in atoms. For light atoms a method devised by Hartree gives the most consistent results, but for heavy atoms, such as Hg, the Thomas-Fermi method is better. Calculated atomic scattering factors have been tabulated and are given in the *International Tables for the Determination of Crystal Structure*, Part II, and in many textbooks. It should be remembered, however, that the figures given only hold for values of the wavelength λ not near to a critical absorption edge. When an atom has been profoundly disturbed by the removal of an inner electron and is trying to readjust itself it cannot be expected to scatter 'normally.' The modification required when λ approaches λ_K is discussed by Compton and Allison in *X-rays in Theory and Experiment*.

Now, while the scattering from a single atom must depend on the arrangement of the electrons in it, the scattering from a collection of atoms will equally depend on their mutual arrangement. For a random arrangement of atoms, such as a simple gas, the scattering curve is, as we have assumed above, similar to that of a single atom. But if we are dealing with a gas composed of free molecules each of which contains heavy atoms in fixed positions relative to each other, or with a liquid or glass, in which the atoms are not regularly arranged, but in which there are certain distances of closest or favoured approach, then there will be reinforcement or interference of scattered waves from neighbouring atoms. Fig. 10 shows a comparison of the experimental scattering curve for CCl_4 with that calculated on the assumption of a tetrahedral arrangement of Cl atoms 2.99 A.U. apart. It is found that as the Cl atoms are successively replaced by H, the remaining Cl atoms mutually repel each other and their distance apart increases.

Even monatomic liquids, such as liquid argon or mercury, give one or more interference rings, which must indicate *some* regularity of arrangement. The atoms naturally cannot interpenetrate, but neither, on the other hand, are they completely close-packed. The observed scattering curves give a measure of the probability of finding any two atoms at a particular distance apart (Pl. VI e). The scattering curves for polyatomic liquids

are more complex. That of liquid CCl_4 , shown in fig. 79, is very different from the scattering curve of gaseous CCl_4 . The first maximum is now given by the most favoured closest molecule to molecule distance, and it is only at large angles that the molecules in the liquid scatter as if they were isolated. Comparison with theoretical calculation also shows that the CCl_4 molecules are definitely *not* able to rotate freely in the liquid state. When the molecules have a pronounced asymmetry of shape this is even more certainly the case, and so it is for polar molecules such as

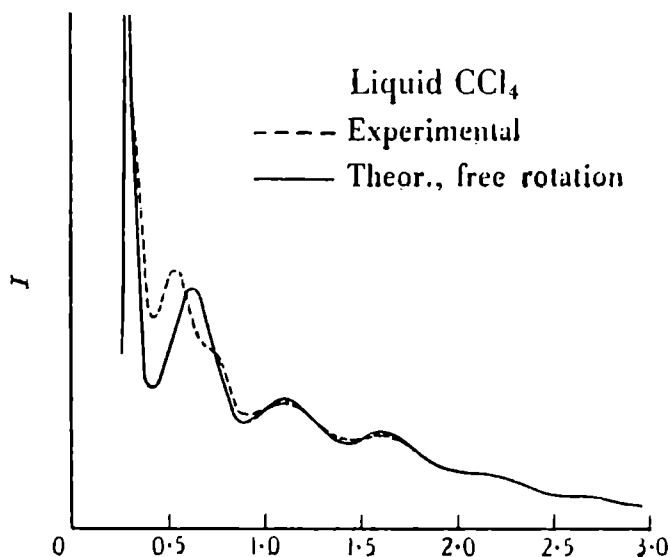


FIG. 79. Molecular scattering for liquid CCl_4 .

(Pirene, *The Diffraction of X-rays and Electrons by Free Molecules*: C.U.P.)

H_2O . Nevertheless any regular groupings of molecules in liquids are of comparatively short duration.

But when atoms or molecules are permanently arranged in a regular, periodic way, the reinforcement or interference of the scattered X-rays that takes place depends entirely on the arrangement of ions, atoms or molecules in the unit cell.

GEOMETRICAL STRUCTURE FACTOR

In Chapter III we considered the bare framework of the structure, including symmetry, unit cell, space-group. Now we have to consider the contents of the unit cell, the *crystal base*, in order to be able to determine the amplitude of the wave scattered in any given direction by the united contributions from all the

atoms in the unit cell. The *structure amplitude* $|F(hkl)|$ for any given hkl reflection is this amplitude divided by the amplitude of the wave scattered by a single electron under corresponding conditions. Defined in this way $|F(hkl)|$ includes the atomic scattering factor f also, but we shall ignore that for the time being and determine only the geometrical structure factor S , the value that $|F(hkl)| = \sum f \cdot S$ would have if f were unity, if there were scattering points each equivalent to one electron, instead of extended atoms, in the unit cell. In fig. 80, *a* shows the wave scattered by such a point, in the Bragg direction. Other atoms in the crystal, arranged at repeat distances, that is, at the other

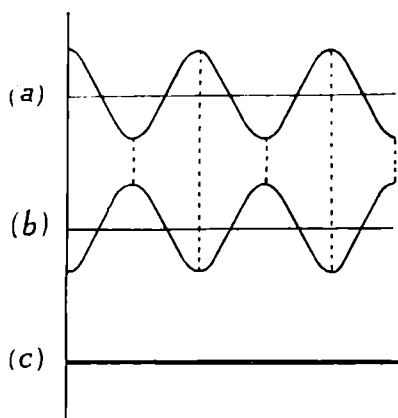


FIG. 80. Interference of waves which are opposite in phase
 $\cos x + \cos(x - \pi) = 0$.

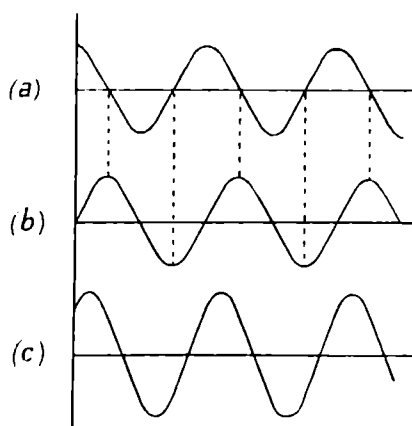


FIG. 81. Addition of waves differing in phase by $\pi/2$.
 $\cos x + \cos\left(x - \frac{\pi}{2}\right) = \sqrt{2} \cos\left(x - \frac{\pi}{4}\right)$.

corners of the same or another unit cell, give waves identical with this, which simply reinforce it. If there are scattering points in the unit cell, *not* at the corners, they will give scattered waves not in phase with those at the origin, that is, they do not have their maximum amplitudes in the same place at the same time. We have to add the scattered waves in order to find the resultant wave due to all the scattering points in the unit cell. *b* shows the wave due to a scattering point half-way along a repeat distance. Waves *a* and *b*, when added, cancel each other; the result is complete interference (*c*, fig. 80).

A scattering point one-quarter of the way along the repeat distance will not interfere in the first order, but will produce (*c*, fig. 81) a wave of larger amplitude, different in phase from that of either of the two constituent waves.

The same thing may be expressed in a different way. The scattering by the point A at the corner can be represented by unit vector \vec{A} (fig. 82). That of a point B whose position relative to the first is such as to interleave the planes passing through A at

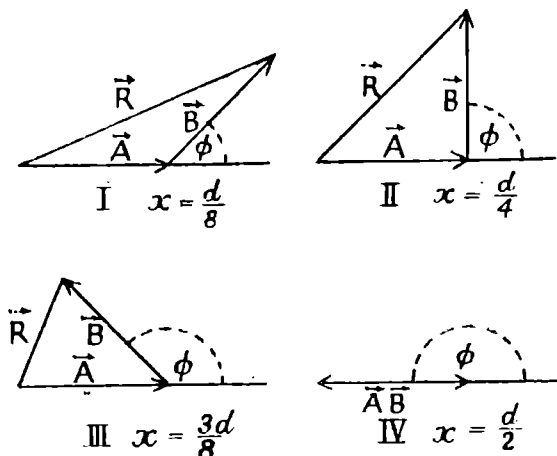


FIG. 82. Vector addition of similar amplitudes.
 Ratio of intensities of spectra will be
 $\text{I} : \text{II} : \text{III} : \text{IV} = 2 \cos 22\frac{1}{2}^\circ : \sqrt{2}0 : 2 \cos 67\frac{1}{2}^\circ : 0$
 in the case illustrated.

a distance x/d relative to the spacing d , is represented by unit vector \vec{B} at an angle $\phi = 2\pi x/d$ from \vec{A} . Their resultant is \vec{R} , whose length and direction give the amplitude and phase of the resultant wave due to scattering from the A and B points. But now it will be seen that f cannot be neglected if there are different

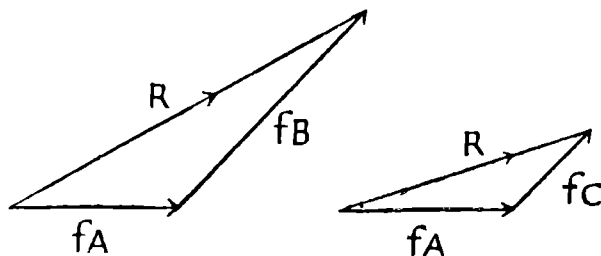


FIG. 83. Vector addition of scattering, introducing atom factors.

kinds of atoms in the unit cell, for in fact the lengths of \vec{A} and \vec{B} are proportional to the values of f_A and f_B corresponding to the Bragg angle θ of the reflection hkl being considered, for the particular wave-length used, and both amplitude and phase of the resultant \vec{R} will depend on these values (fig. 83).

The *structure factor* $F(hkl)$ (fig. 84) is the result of vectorially adding up the scattering due to all the atoms in the cell, each

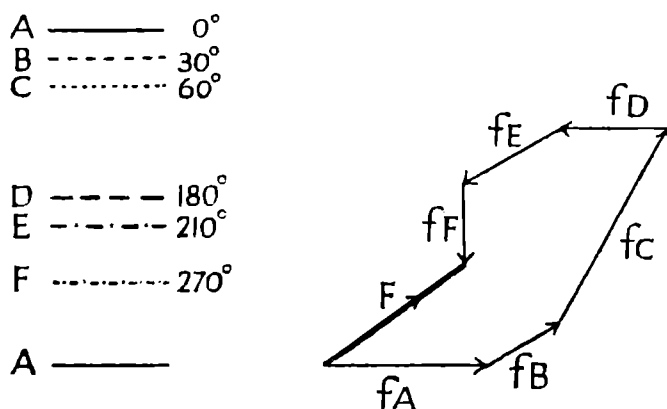


FIG. 84. Vector determination of structure factor; first order amplitude F .

being given its value of f appropriate to the particular spectrum hkl . If x_j, y_j, z_j are the values of $\frac{x}{a}, \frac{y}{b}, \frac{z}{c}$ for the atom j , then

$$|F(hkl)| \cos \alpha = \sum_j^n f_j^{hkl} \cos 2\pi(hx_j + ky_j + lz_j) = A,$$

$$|F(hkl)| \sin \alpha = \sum_j^n f_j^{hkl} \sin 2\pi(hx_j + ky_j + lz_j) = B,$$

where n is the number of atoms in the unit cell, $|F(hkl)|$ is the amplitude and α the phase of the resultant wave.

$$|F(hkl)| = \sqrt{A^2 + B^2} ; \tan \alpha = B/A.$$

Now, a fundamental fact about X-ray measurements is this: we can measure the intensity of reflection, which is proportional to the (amplitude)²; and therefore by making appropriate corrections we can obtain the amplitude $|F(hkl)|$. But we cannot *measure* the phase α , except in very special cases.

If we could measure both amplitude and phase of resultant waves scattered in any direction, then the determination of crystal structure would be a very simple affair, for any such wave gives a measure of the periodic distribution of scattering matter in that particular direction. We could represent the waves optically and superimpose them or draw them by means of harmonically

spaced lines (fig. 85) or, in the case of more complex structures, we should in fact add the waves by means of calculation. Machines have also been devised for adding up large numbers of such terms.

But this direct method can seldom be used. Even if the structure is a centro-symmetrical one, so that for every atom at

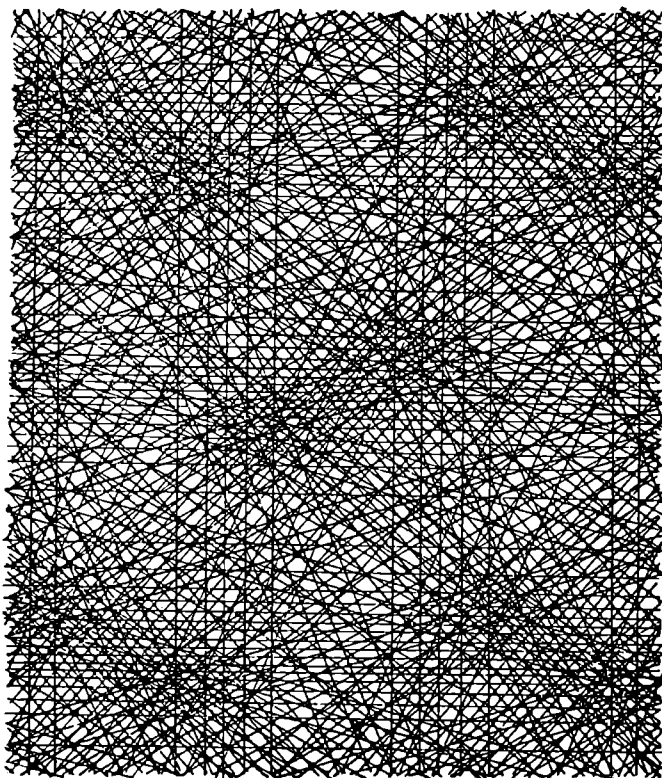


FIG. 85. Diffracting unit reconstructed by superposition of harmonically spaced lines. The 'molecules' are seen most clearly if the page is held level with the eye (Robertson).

$x y z$ there is another at $-x - y - z$, and therefore $B = 0$, it is still impossible, in the general case, to know whether a is 0 or π , whether $F(hkl)$ is $+^{\text{ve}}$ or $-^{\text{ve}}$. The method that must be used to determine a structure is one that seems very imprecise and indirect: we must make the best guess we can at the atomic arrangement, calculate what scattering effects such a structure would give, compare the calculations with the observed intensities and positions of the spots or lines on the X-ray photographs, and judge the correctness of the guess by the measure of agreement obtained.

This raises a most important question: when we have good agreement by this 'trial and error' method, will the solution be a unique one? The answer is *no* and *yes*. Theoretically it will not be unique; there are many possible periodic arrangements of scattering matter that will give an observed set of data. In practice, however, it *will* be unique if it shows discrete atoms arranged in such a way as to give what looks like a sensible structure from a chemical and physical point of view. Really we need not worry about this, because in formulating a trial structure we shall obviously start with discrete atoms of reasonable shapes and put them in reasonable positions—not interpenetrating, for example. The only difficulties that are likely to arise in this respect will occur in the case of structures where there are both heavy and light atoms. It would be difficult to locate H atoms with real certainty, even if they were not ionised.

Now let us consider a very simple case. Leaving the atomic scattering factor f out of account, a simple periodic arrangement of atoms, or sheets of atoms, would give a series of X-ray spectral orders of constant intensity. If after applying all necessary corrections we find that we are left with a set of spectra from one plane, which have a constant structure factor, then we can be sure that we are dealing with the 'layer plane' of a structure such as graphite (fig. 130, page 175).

If the planes of atoms are interleaved with other sheets of scattering material (as, for example, in C_8K , fig. 131), then the intensities will be changed and the structure factors of the different spectra will vary. If the interleaving is of *equal* scattering power and exactly half-way (fig. 86), then the 1st, 3rd and all odd-order spectra will disappear; this, we found, happens for certain sets of spectra when there is a 2-fold screw axis or a glide plane present in the structure. If the interleaving occurs at one-quarter of the repeat distance, then the fourth order is strong, the second disappears and the first and third are intermediate in value. That happens in the diamond structure (fig. 127), where there is a 3:1 periodicity of arrangement of the (111) planes. In ZnS, which has a structure similar to diamond, the interleaving atoms are not quite equal in scattering power and the second order of reflection from the (111) planes is weakened but not absent.

We have already seen that the general structure factor expression is simplified if the structure has a centre of symmetry, so that for every atom at $x\ y\ z$ there is another at $-x\ -y\ -z$, in which case

all *sine* terms cancel each other. In general, the fact that there are symmetrical relationships between atoms in the unit cell enable us to simplify the structure factor expression considerably in most cases. If, for example, there are 8 atoms *anywhere* in the unit cell, then those 8 atoms could have 24 different parameters: 3 coordinates each. But if the 8 atoms are reflections of each other in mutually perpendicular symmetry planes, then the number of unknown parameters is only 3 instead of 24. When we know what symmetry the crystal possesses, centres, axes, screw axes,

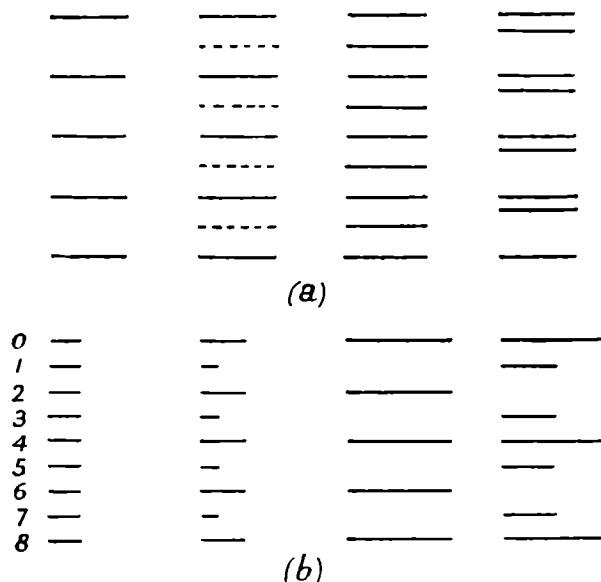


FIG. 86. (a) Interleaving of layer planes and
(b) resultant effect on intensity of spectra.

planes, glide planes, then the coordinates of equivalent points in the unit cell can be written down, since the different kinds of symmetry involve definite relationships between the coordinates. For example:

Centre of symmetry at (000)	$x y z$	\bar{x}	\bar{y}	\bar{z}
„ „ „ $(\frac{1}{4}\frac{1}{4}0)$	$x y z$	$\frac{1}{2} - x$	$\frac{1}{2} - y$	\bar{z}
2-fold axis at $(\frac{1}{4}0z)$ parallel [001]	$x y z$	$\frac{1}{2} - x$	\bar{y}	z
Screw „ „ „ „	$x y z$	$\frac{1}{2} - x$	\bar{y}	$\frac{1}{2} + z$
Plane of symmetry at $(\frac{1}{4}yz)$ parallel (100)	$x y z$	$\frac{1}{2} - x$	y	z
Glide plane, as above, translation $\frac{\vec{b} + \vec{c}}{2}$	$x y z$	$\frac{1}{2} - x$	$\frac{1}{2} + y$	$\frac{1}{2} + z$

For the space-group *Pmmm* the general coordinates of equivalent points are $\pm |xyz \ x\bar{y}\bar{z} \ \bar{x}y\bar{z} \ \bar{x}\bar{y}z|$. The corresponding structure factor (with $\cos a = \pm 1$) is

$$\begin{aligned} |F(hkl)| &= 2\sum f [\cos 2\pi(hx + ky + lz) + \cos 2\pi(hx - ky - lz) \\ &\quad + \cos 2\pi(-hx + ky - lz) + \cos 2\pi(-hx - ky + lz)] \\ &= 8\sum f \cos 2\pi hx \cos 2\pi ky \cos 2\pi lz. \end{aligned}$$

The coordinates of equivalent points for all the space-groups are given in the *International Tables for the Determination of Crystal Structure*, Part I, and special coordinates are also given, for the cases where the atom actually lies at or on a symmetry element (itself having the symmetry concerned). The general structure factor formulae are also given, expressed in the form most convenient for computation, that is, expressed as a product, as far as possible, rather than as a sum. It is sometimes possible to make the structure factor formulae simpler still by separation of planes in different zones, planes for which one index is odd, and so on. But even when the labour involved has been shortened by using all possible devices in the form of mathematical tables, calculating and other special machines, the process of computing structure factors for comparison with observed structure factors is a lengthy and tedious business, which can seldom be avoided.

At this stage let us stop and get clear our aim. We know the space-group and the numbers of different kinds of atoms in the unit cell. We know, from tables or from previous experimental results, the atomic scattering factor for each atom, the way in which its scattering power will fall off as the Bragg angle increases. We know *how* to calculate the structure factor, the sum of the scattered waves from all atoms in the unit cell. But in order to perform the calculation we must know the coordinates of the atoms, or of sufficient atoms for us to be able to obtain all the rest by symmetry operations. Now, there are two tasks before us: (1) to obtain those atomic coordinates by intelligent deduction or inspired guesswork; (2) to correct the observed intensities for all other influences in order to obtain 'observed structure factors' with which to compare the calculated ones. Let us consider the second stage first, because it may be possible to *use* the observed structure factors, when we have them, to give us hints as to the whereabouts of the atoms.

INTENSITY FORMULAE. DEDUCTION OF OBSERVED STRUCTURE FACTORS

The factors which influence the observed intensities have already been mentioned at the end of Chapter IV. They are clearly very complicated, but they can be divided into three sections: (1) factors which depend on the size and texture of the crystal used, and on the experimental method adopted; (2) factors dependent on the Bragg angle; (3) factors dependent on the actual structure of the crystal. A list of intensity formulae is given in the *International Tables for the Determination of Crystal Structure*, Part II, and elsewhere, but only two of these will be considered. They give the whole intensity—the *integrated intensity*, as it is called—of the reflection, under the stated conditions of the experiment, relative to the intensity of the primary beam. The first formula applies to a powder photograph recorded on a cylindrical film of radius R .

$$\frac{I_l}{I_0} = \frac{l}{8\pi R} \left(\frac{Ne}{mc^2} F(hkl) \right)^2 \lambda^3 p V \frac{1 + \cos^2 2\theta}{\sin^2 2\theta} \cdot \cos \theta \cdot A,$$

where

I_l = diffracted energy in a length of arc l ,

I_0 = energy of primary beam per second per unit area,

N = number of unit cells per unit volume (that is, the reciprocal of the volume of the unit cell),

e, m = electronic charge and mass in $e \cdot m$ units,

c = velocity of light,

$F(hkl)$ = structure factor, including atomic scattering factor modified by thermal vibration,

λ = wave-length of X-rays,

p = the number of (hkl) planes giving interference rings that coincide (the multiplicity factor, values of which are listed in the *International Tables*),

V = volume of powder irradiated,

A = absorption factor (depending, in general, on the wave-length and intensity distribution in the incident beam, the nature, size and texture of the crystal, and the Bragg angle).

The terms involving θ need further explanation. $(1 + \cos^2 2\theta)$ is the *polarisation factor* previously mentioned (page 105), which

must be modified still further if the incident beam is monochromatised by crystal reflection.

Since the crystals are finite and since X-ray reflection is not absolutely sharp at the Bragg angle, but occurs over a small range of angle, it follows that each reciprocal lattice point has a finite *size* and takes a finite *time* to pass through the surface of the sphere of reflection. The *Lorentz factor* (in this case $\frac{1}{\sin 2\theta}$) is a measure of this time, which varies, in general, not merely with Bragg angle but with other geometrical conditions of reflection.

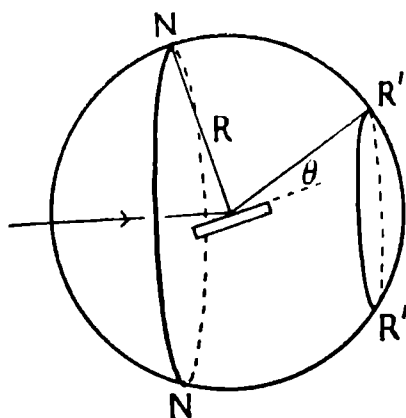


FIG. 87. Origin of factor $\frac{\cos \theta}{\sin 2\theta}$ in powder photographs.

The factor $\frac{\cos \theta}{\sin 2\theta}$ arises in two ways (fig. 87). First of all, if the distribution of crystallite orientation is uniform then the circumference of the circle NN will be a measure of the *number of crystallites in the proper reflecting position* θ . But this is $2\pi R \sin (90 - \theta)$ or $2\pi R \cos \theta$. The reflected rays will be recorded on the circle R'R', circumference $2\pi R \sin 2\theta$, and in this case the smaller the circle the greater the *blackening on the photographic film*. Hence the appropriate factors are $2\pi R \cos \theta$ and $\frac{1}{2\pi R \sin 2\theta}$, or $\frac{\cos \theta}{\sin 2\theta}$, taking both together.

The exact form of the temperature correction (here included in $F(hkl)$) and of the absorption factor A will be considered later.

The expression for the integrated intensity which applies in the

case of a small single crystal, volume V , rotating with uniform angular velocity ω about an axis normal to the incident beam, is

$$\frac{E\omega}{I_0} = \frac{\tau}{4\pi} \left(\frac{Ne}{mc^2} F(hkl) \right)^2 \lambda^3 p' V \frac{1 + \cos^2 2\theta}{\sin 2\theta} \frac{\cos \theta}{\sqrt{(\cos^2 \phi - \sin^2 \theta)}} \cdot A,$$

where

E = total energy in reflected beam while crystal is rotating for time τ ,

p' = the number of (hkl) planes giving reflections that coincide (not the same as p in powder photographs).

ϕ = angle between the reflecting plane and the axis of rotation.

This formula becomes inexact in the special case where ϕ and θ are nearly equal. It also applies only to a mosaic crystal, made up

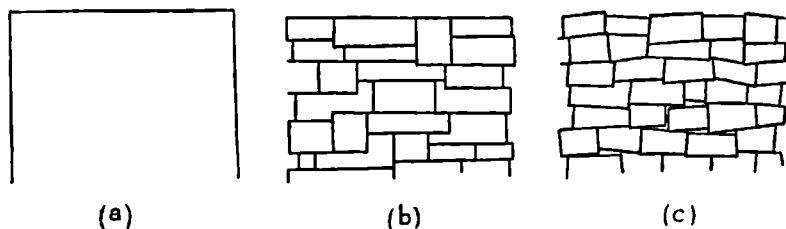


FIG. 88. (a) Perfect crystal; (b) mosaic of parallel crystallites; (c) mosaic of disorientated crystallites.

of small crystallites which are slightly disorientated with respect to each other, or which are at least discontinuous. Experience has shown that that is the usual state of crystals (fig. 88). The formula for a mathematically perfect crystal is quite different. If the crystal is too good for the mosaic formula to apply, then corrections for partial perfection may be introduced into the absorption factor A ; or, in the case of organic crystals, the crystal may be dipped into liquid air before X-ray examination, thus ensuring that it is broken up into a mosaic; or the intensities of the large-spacing reflections, which are particularly affected by crystal perfection, may be found from powder photographs (using a really fine-grained powder) and only the intensities of the small-spacing planes taken from the rotation photographs.

In any case it is possible either to measure or to eliminate all factors other than the structure factor $F(hkl)$ which is required for as many planes as possible. R , l , τ can be measured, N is

known from the unit cell dimensions, V can be obtained by weighing the crystal on a very sensitive microbalance and using the known density, or by actual measurement under the microscope if the crystal is of regular shape; λ is known, p' and the terms involving θ are obtained from tables, A is calculated from the linear absorption coefficient μ and the crystal shape. When, finally, a list of 'observed structure factors' is obtained, this can be inspected to see whether it gives any hints as to where the atoms must be.

USE OF OBSERVED STRUCTURE FACTORS IN STRUCTURE DETERMINATION

If, for example, any are outstandingly large, then most of the atoms must lie on or near to the corresponding planes. That is particularly useful if the intensity measurements are made on an *absolute* scale (either by direct comparison with I_0 or by using as secondary standard another crystal whose absolute intensities are known), because then we can compare the observed structure factor with the structure factor which would correspond to all the atoms in the unit cell scattering in phase with each other. There are quite a number of *layer structures* in which one set of planes contains all the atoms. Such structures usually possess one outstanding cleavage. Even then, however, the arrangement of atoms *in* the plane has still to be determined. It is most useful to find a very large structure factor for one or more small-spacing (large θ) planes, because that locates the atoms very precisely.

As an example, let us take the case of hexamethylbenzene, a triclinic crystal that was the first example of a benzene derivative to be worked out in full. The observed intensities showed little sign of regularity, but when they had been corrected to give structure factors (thus eliminating, to a large extent, the disturbing influence of the triclinic asymmetry) various important factors emerged. First of all, it was clearly a layer structure: one of the principal planes, (001), gave an outstandingly large structure factor value, and the various orders of reflection from that plane fell off in accordance with what would be expected from a reasonable atomic scattering factor curve. Then it was found that the structure factors clearly indicated some approach to hexagonal symmetry of the atoms *in* the (001) plane, although there was no hexagonal

symmetry of the structure as a whole. Finally it was observed that three small-spacing planes, (340) , $(4\bar{7}0)$ and $(\bar{7}30)$, the traces of which on the (001) plane were nearly at 120° to each other, also had exceptionally large structure factors. It seemed that the most likely positions of the atoms would be at the intersections of these planes (fig. 89). There were 72 such intersections in each unit cell. The formula of hexamethylbenzene is $C_6(CH_3)_6$ and there was only one molecule in the unit cell, so that there were 12 carbon atoms to place on the 72 intersections (the hydrogen atoms could be neglected in view of their small scattering power).

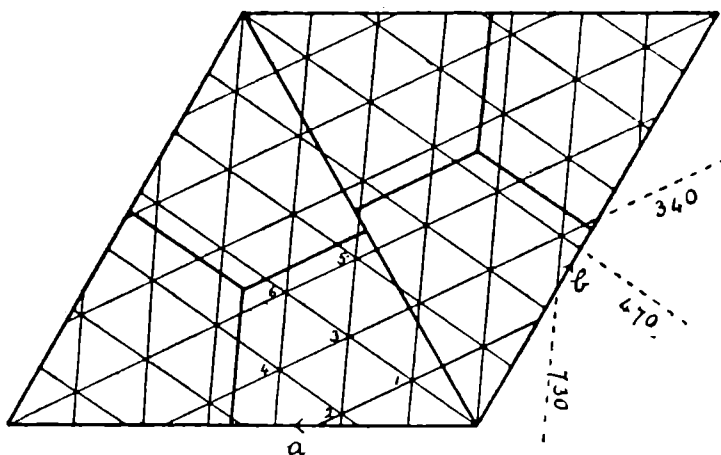


FIG. 89. Hexamethylbenzene; pseudo-hexagonal symmetry, and intersections of small-spacing planes having large values of $F(hkl)$.

But the pseudo-hexagonal symmetry brought the problem on to a more reasonable scale; it meant that there were 2 carbon atoms to place on 2 of 12 intersections. A few structure factors were calculated for each possibility and it was found that only by placing the carbon atoms on intersections 1 and 3 could agreement be obtained with the observed structure factors. This result (fig. 90) was very satisfactory, for the molecule emerged with its pseudo-hexagonal symmetry, and the carbon-carbon distance in the plane benzene ring turned out to be similar to the carbon-carbon distance in graphite. The atomic coordinates were then checked and adjusted by working out all the structure factors and comparing them with observed values. The agreement, shown in fig. 91, was good by the standards of those days; and a Fourier synthesis, afterwards carried out with great care by Brockway

ATOMIC AND ELECTRONIC DISTRIBUTION

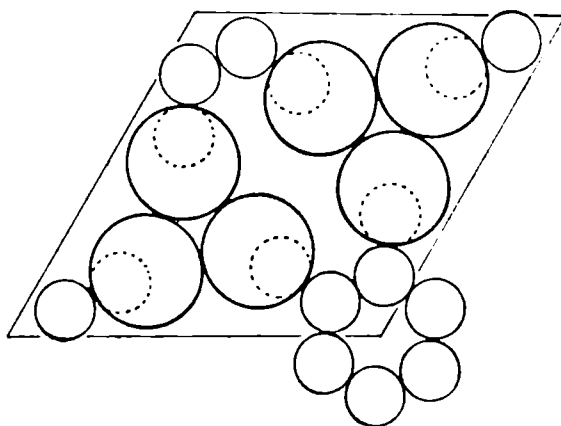


FIG. 90. Hexamethylbenzene; result of placing carbon atoms on intersections 1 and 3 in each unit cell. One complete benzene ring is shown. The heavy lines indicate distances of nearest approach of molecules, and may be taken as indicating the sphere of influence of the (CH_3) group.

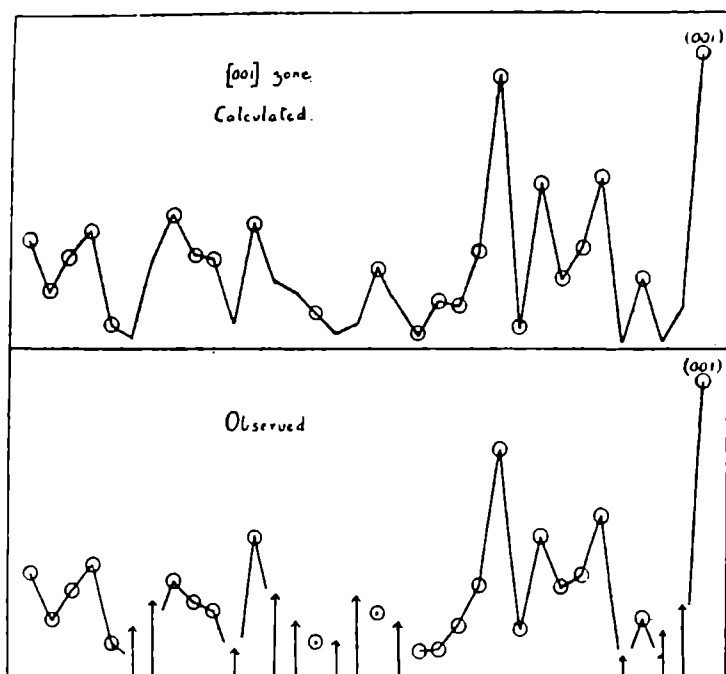


FIG. 91. Structure factor agreement for $(h0l)$ planes in $\text{C}_8(\text{CH}_3)_8$, indicating that the structure must be nearly correct.

and Robertson, confirmed the structure with only small corrections in atomic positions (fig. 92).

OTHER GUIDES TO STRUCTURE DETERMINATION

Not all 'trial and error' structures are so clearly indicated by the observed structure factors, however, and we are often glad to have other means of finding the coordinates. Sometimes we can find a direction in the crystal in which there is only one

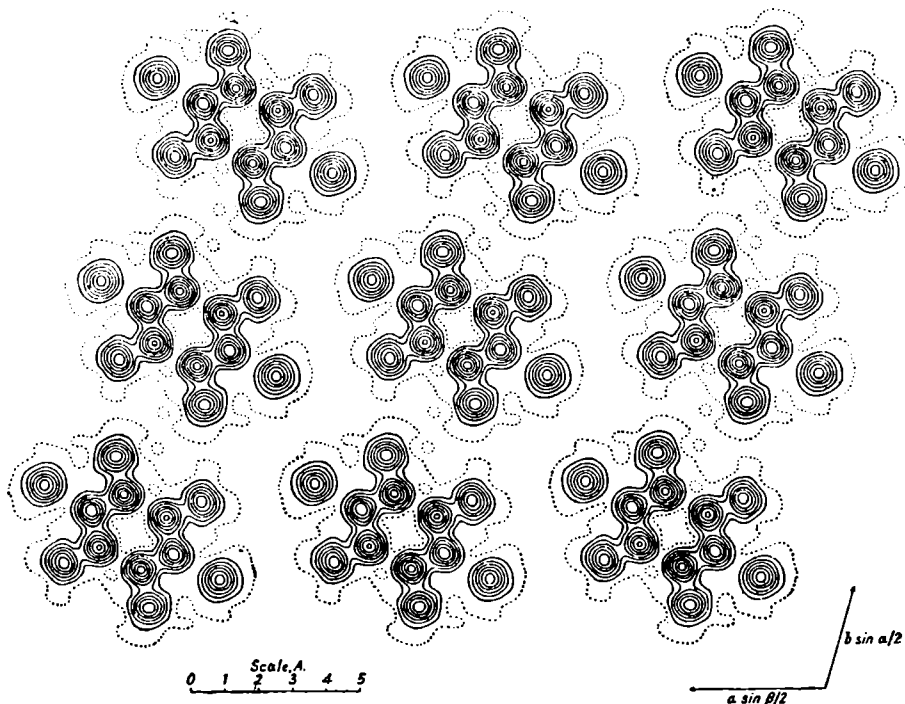


FIG. 92. Later Fourier synthesis of $C_6(CH_3)_6$ by Brockway and Robertson. The molecules are seen projected on a plane normal to the c axis.

(Brockway & Robertson, *Journ. Chem. Soc.*, 1324, 1939.)

parameter to be adjusted, as for example in rutile (fig. 75, page 99) or in the other crystalline form of TiO_2 , anatase (fig. 93). In rutile the atomic coordinates are: Ti $(000)(\frac{1}{2}\frac{1}{2}\frac{1}{2})$; O $(uu0)(\bar{u}\bar{u}0)(\frac{1}{2}-u\frac{1}{2}+u\frac{1}{2})(\frac{1}{2}+u\frac{1}{2}-u\frac{1}{2})$. In anatase they are Ti $(000)(\frac{1}{2}\frac{1}{2}\frac{1}{2})(\frac{1}{2}0\frac{1}{4})(0\frac{1}{2}\frac{3}{4})$; O $(00\pm u)(\frac{1}{2}\frac{1}{2}\pm u)(\frac{1}{2}0\frac{1}{4}\pm u)(0\frac{1}{2}\frac{3}{4}\pm u)$. In either case it is quite a simple matter to plot the structure factors $|F(hkl)|$ for a few simple planes graphically, using a range of values of the parameter u , and then to pick out the particular point where the relative values agree with experiment. In structures as simple

as these, comparison with the visual estimate of intensity of a few powder lines would probably be enough to fix the parameter with some certainty.

When there are several parameters to adjust in a unit cell of relatively high symmetry it may sometimes help to use 'figure fields' (fig. 94, page 124) or contour graphs which indicate how the structure factors change with change of coordinates.

We may find guidance from other structures previously worked out, which have shown the kind of groupings that usually occur. Certain preliminary assumptions as to atomic and ionic sizes are justified by experience (fig. 95, page 125) although the distances between atoms will depend on their state of binding or coordination number. Tables of ionic and atomic diameters in various states of coordination and for various percentages of ionic character are published, and the relation of ionic size to structure type is gradually becoming clearer. A particularly careful study has been made of the silicate minerals, in all of which the Si atom lies between four tetrahedrally arranged oxygen atoms, although the fact that different tetrahedral groupings can share one or more oxygen atoms has led to a large variety of structures. It would be quite legitimate, in determining the unknown structure of a different silicate, to assume, as a fundamental, the tetrahedral grouping of oxygen atoms about the silicons.

Pauling has pointed out that even quite complex ionic structures obey certain fairly simple rules, which were deduced partly from known structures and partly from the equations for the crystal energy. They are not rigorous in their application, but they are certainly useful in helping to suggest trial structures. They are based on the observation that each cation ($+^{\text{ve}}$ ion) is surrounded by a number of anions ($-^{\text{ve}}$ ions, of which the most typical are

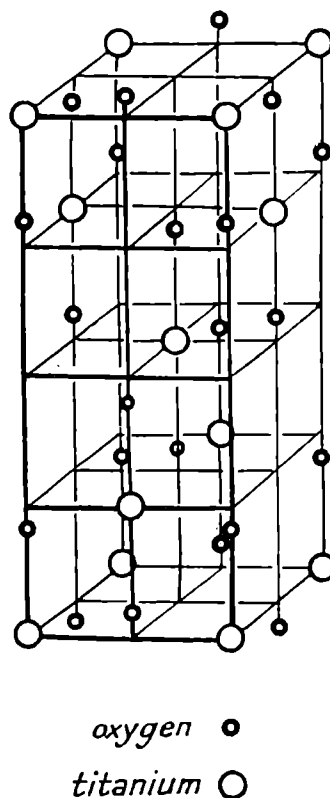


FIG. 93. Structure of anatase TiO_2 . Sizes of atoms are not significant.

oxygen and fluorine) forming a *coordination polyhedron*, which may be a tetrahedron, octahedron, etc. These rules, which are explained fully in Pauling's book, *The Nature of the Chemical Bond*, are as follows:

1. A coordinated polyhedron of anions is formed about each cation, the cation-anion distance being determined by the *radius sum*, and the coordination number by the *radius ratio*, of the cation and anion.

2. In a stable ionic structure the valency of each anion, with

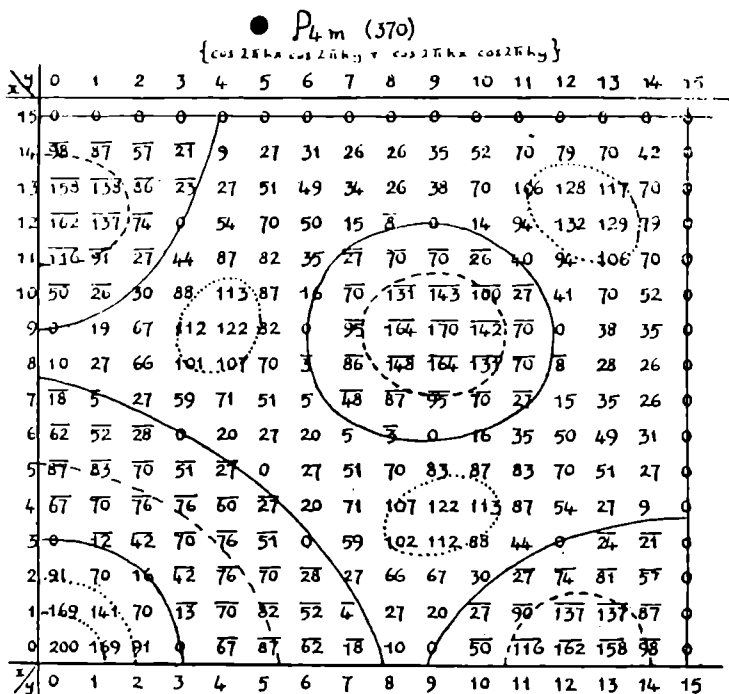


FIG. 94. The Bragg-Lipson figure field for the expression shown, for variation of x and y in sixtieths of the unit cell sides. The pattern repeats by reflections at $x=y=\frac{1}{2}a$.

changed sign, is exactly or nearly equal to the sum of the strengths of the electrostatic bonds to it from the adjacent cations; the strength of the electrostatic bond being defined as the charge (in electrons) of the cation divided by its coordination number. This means that there is everywhere *local neutralisation of charge*.

3. The presence of shared edges and especially of shared faces of the coordination polyhedra in a coordinated structure decreases its stability (since it decreases the cation-cation distance); this effect is large for cations with large valency and small coordination number.

4. In a crystal containing different cations those with large valency and small coordination number tend not to share polyhedron elements with each other. (This follows as a corollary

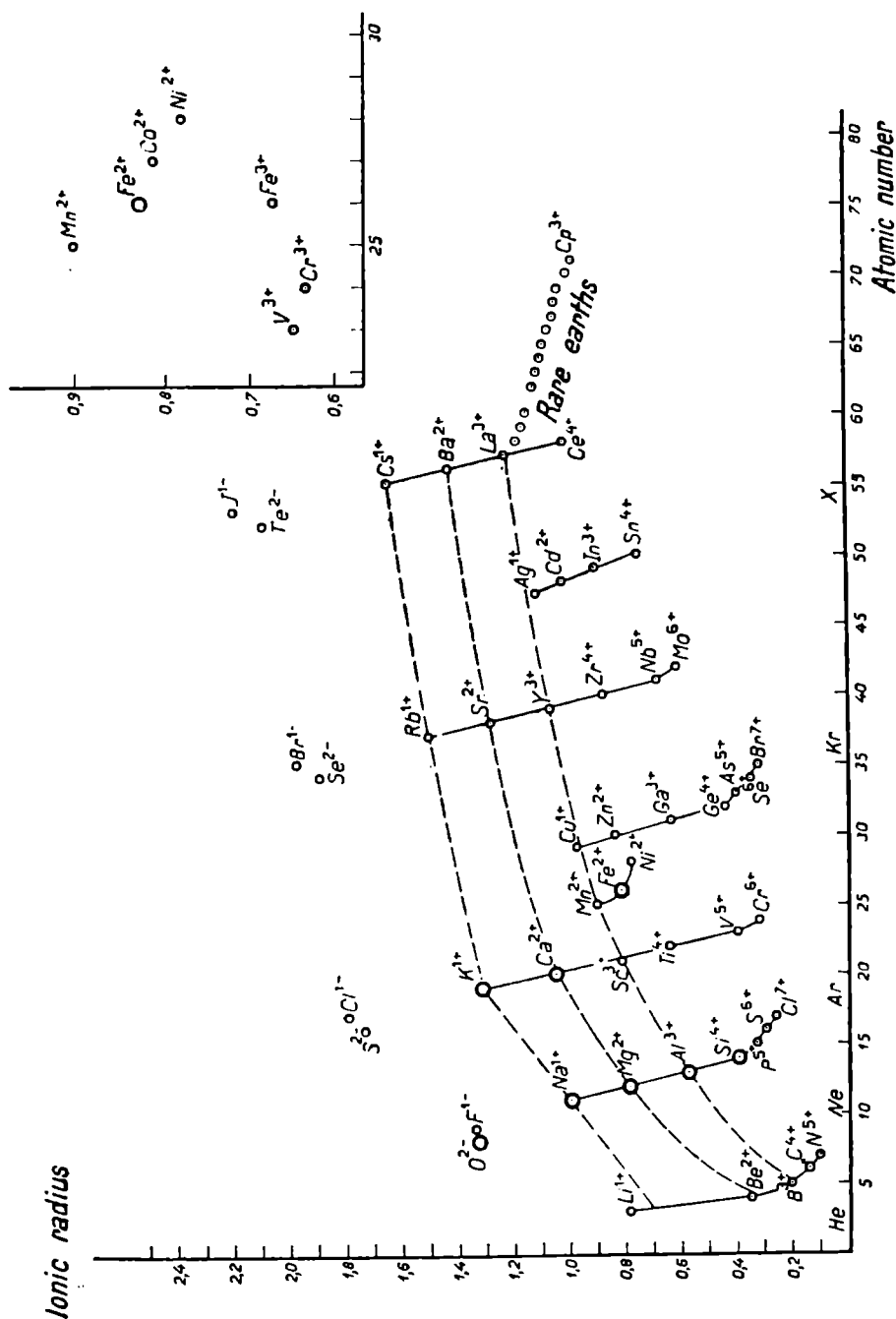


FIG. 95. Ionic radius plotted against atomic number.

(Bijvoet, Kolkmeijer & MacGillavry, *Röntgenanalyse von Krystallen*: Springer.)

of rule 3.) They tend, in fact, to be as far apart as possible in the structure.

In carbon compounds, also, the interatomic distances corresponding to single, double, triple or aromatic bonds are known within certain limits (fig. 96). It is also known that molecules in

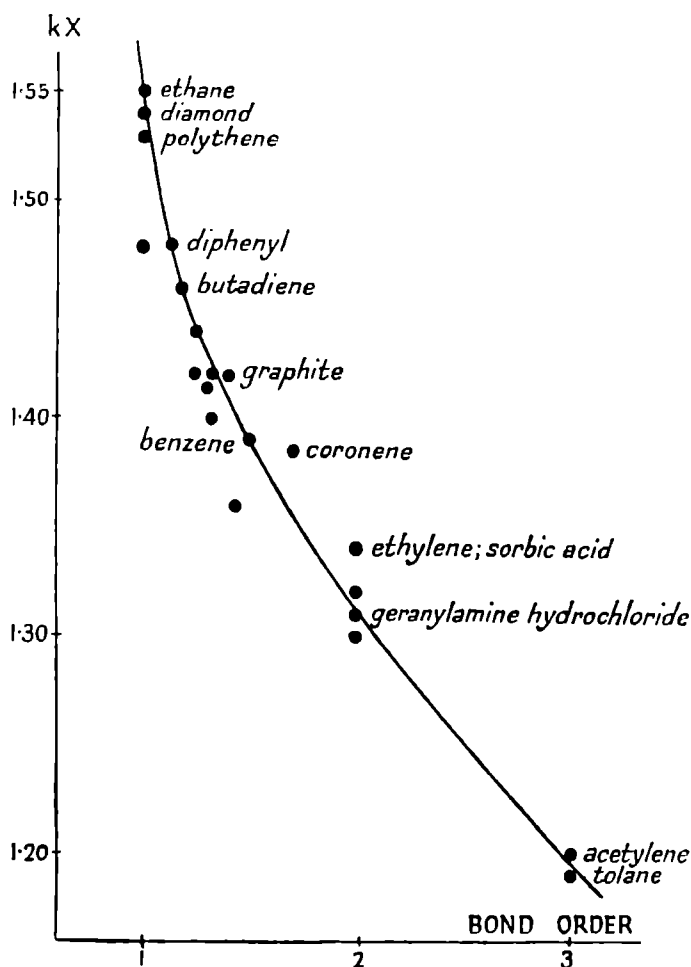


FIG. 96. Carbon to carbon distances v. bond order for various compounds, some of which are named.

organic compounds held together by residual van der Waals forces are usually about 3.5 to 4 A.U. apart. That proved to be the case in $C_6(CH_3)_6$. But further accurate structure analyses have shown that in molecular compounds or in molecules linked by hydrogen bonds (see p. 182) the distances will be smaller, as in oxalic acid dihydrate (fig. 97) or in resorcinol (fig. 136, page 183). All these are most useful facts to take into account.

The size and shape of the unit cell can give guidance, especially in the case of a series of isomorphous compounds, or those of similar structure. W. H. Bragg showed in the early 1920's that the length of the molecules of naphthalene and anthracene *must* lie along the c axis of the unit cell, in order to account for the increase of length of the c axis of anthracene relative to that of naphthalene, in otherwise similar cells. He showed that the

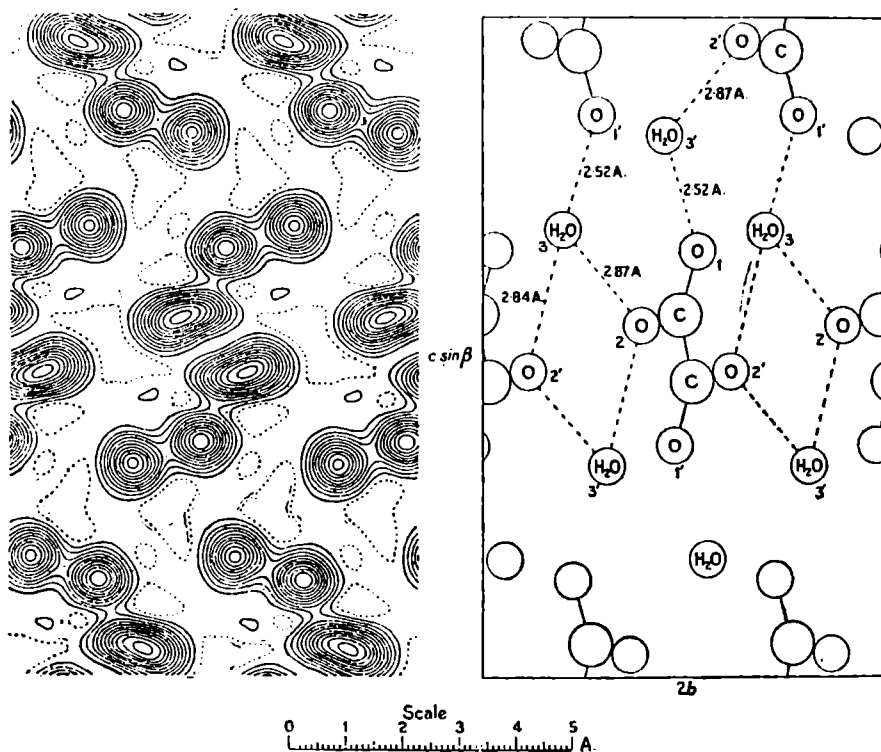


FIG. 97. Fourier projection of oxalic acid dihydrate, showing hydrogen bonds.

(Robertson & Woodward, *Journ. Chem. Soc.*, 1819, 1936.)

molecule, in each case, had a centre of symmetry and that the molecule, in the centre of the (001) face was a reflection of those at the corners. But this was not enough information to enable him to make an accurate guess at the molecular shape and orientation. Later, Bhagavantam showed from optical and magnetic measurements what the correct molecular orientation must be, while Robertson independently arrived at the same orientation from a consideration of the observed structure factors.

Measurements of diamagnetic anisotropy and of refractive indices can give most useful information about molecular orienta-

tion, particularly in the case of aromatic compounds. The molecules of benzene derivatives have a particularly *large* diamagnetic susceptibility and a *small* refractive index in a direction normal to the plane of the benzene ring, and if there is any tendency to parallelism of such molecules in the structure it will show up as an increase in crystal susceptibility or decrease in refractive index in a particular direction. In triphenylbenzene, for example, the diamagnetic susceptibilities and gram molecular refractivities for vibrations along the principal crystallographic directions are:

$$\chi_a = -141, \quad \chi_b = -155, \quad \chi_c = -309 (\times 10^{-6} \text{ c.g.s.e.m.u.}),$$

$$R_a = 115.5, \quad R_b = 115.0, \quad R_c = 77.6,$$

where

$$R = \frac{n^2 - 1}{n^2 + 2} \cdot \frac{M}{\rho} \quad (n \text{ refractive indices, } M \text{ molecular weight, } \rho \text{ density}),$$

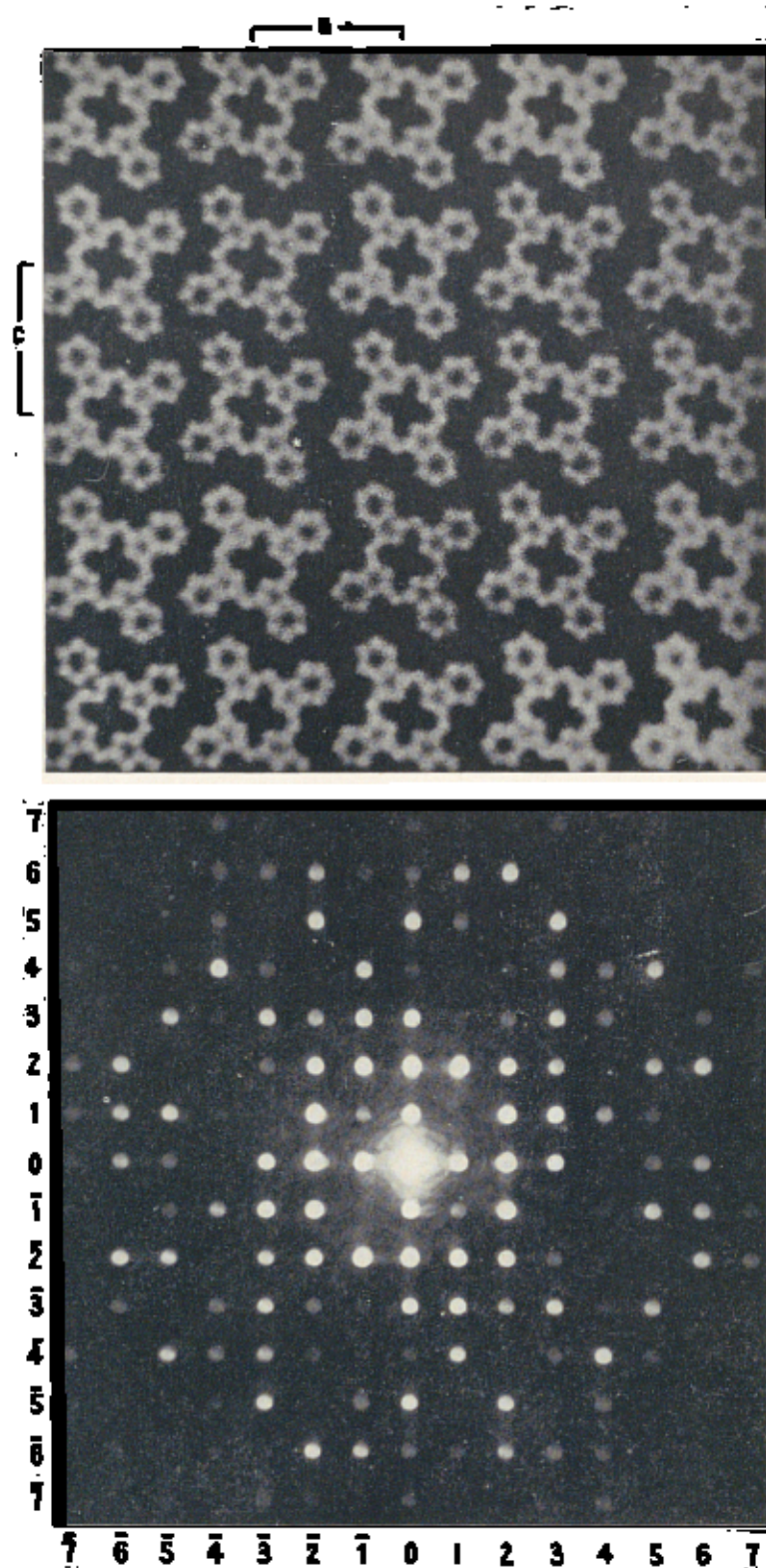
showing quite clearly that the molecular planes must be more nearly parallel to (001) than to (100) or (010). Aliphatic molecules of the chain type, on the other hand, have a *large* diamagnetic susceptibility and a *large* refractive index along the length of the chain. Such molecules, arranged parallel or nearly parallel to each other, form an optically positive crystal, whereas layer type crystals such as hexamethylbenzene or triphenylbenzene are optically negative.

Checks on a proposed structure can be made either by calculation or by optical methods. In the 'fly's-eye' device the atoms in the unit cell are indicated by points of light and then photographed through a multiple-pinhole camera on to a plate (fig. 98 and Plate VII). The plate, representing the projected structure, is then used as a diffraction grating, and the resultant spectra should agree in intensity with the distribution of scattering power in the appropriate network of the reciprocal lattice. This method was used in working out the structure of penicillin salts to eliminate some of the *wrong* structures first, and it proves very valuable in cases where the labour of repeated calculations would be almost intolerable.

ELECTRON DENSITY DISTRIBUTION BY FOURIER SYNTHESIS

Suppose now that we are satisfied with the trial structure: what is the next step? In order to find the structure factor for any plane we have to combine the waves scattered by all the

VII



Above : Pattern representing the b projection of the phthalocyanine structure.

Below : Optical diffraction pattern given by it.

(Bunn, *Chemical Crystallography* : Clar. Press.)

electrons in the unit cell, in the proper direction for reflection by that plane, making allowance for phase differences between the waves. In order to find the electron density distribution in the structure, we again have to combine a series of waves. The appropriate equation in the most general case (no symmetry centre) is

$$\rho(xyz) = \sum_{-\infty}^{+\infty} \sum_{-\infty}^{+\infty} \sum_{-\infty}^{+\infty} \frac{|F(hkl)|}{V} \cos [2\pi(hx + ky + lz) - \alpha(hkl)],$$

where $\rho(xyz)$ is the electron density at the point (xyz) , these coordinates being expressed as fractions of the unit cell axes; V is

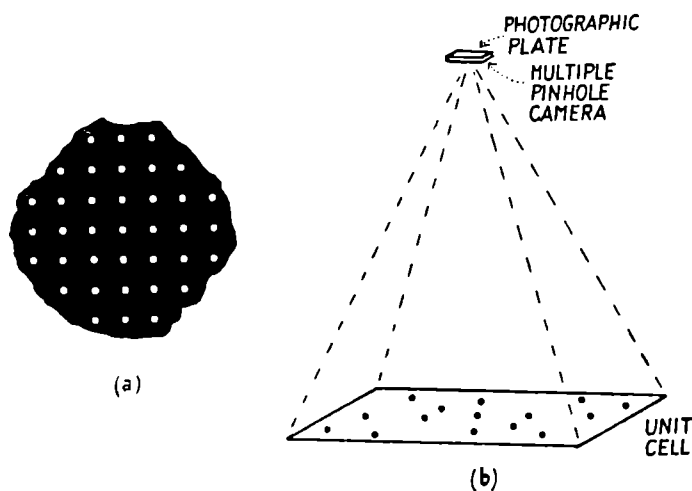


FIG. 98. (a) Part of multiple pinhole camera; (b) arrangement for making repeating patterns by the multiple pinhole camera. Atoms in the unit cell are represented by points of light.

(Bunn, *Chemical Crystallography*: Clar. Press.)

the volume of the unit cell. As we mentioned before, it is the fact that this formula contains the phase, $\alpha(hkl)$, as well as the amplitude $|F(hkl)|$ of the structure factor, that generally prevents its direct application. But since our trial structure gives us the atomic coordinates, we are now in a position to calculate the phase from the formula $\tan \alpha = B/A$ (p. 111), for every observed structure factor. These calculated phases may not be exactly right in every case; that depends on how near our trial structure is to the truth; but they will give us a good start, and if necessary they can be improved by carrying out successive Fourier syntheses and gradually refining the atomic coordinates from which the phases are calculated.

If the trial structure has a centre of symmetry, the sine terms of the structure factor cancel out and the phase of the structure wave is either 0 or π , so that each term in the Fourier series is simply positive or negative :

$$\rho(xyz) = \sum_{-\infty}^{+\infty} \sum_{-\infty}^{+\infty} \sum_{-\infty}^{+\infty} \pm \frac{|F(hkl)|}{V} \cos 2\pi(hx + ky + lz).$$

The first term of this series, $F(000)$, is the total number of electrons in the unit cell, the maximum scattering power for zero angle of diffraction.

The labour of evaluating the electron density $\rho(xyz)$ at sufficiently close intervals over the *whole* of the unit cell, however, would be unnecessary except in very special cases. The usual procedure is to carry out two-dimensional analyses, using for each just the structure amplitudes of planes in a principal zone, say $F(hko)$, and thus obtaining the electron densities in the structure projected on to a plane perpendicular to the zone axis. The formula then becomes

$$\rho(xy) = \sum_{-\infty}^{+\infty} \sum_{-\infty}^{+\infty} \pm \frac{|F(hko)|}{A} \cos 2\pi(hx + ky).$$

The sides of the projection may be divided into thirtieths, sixtieths or one-hundred-and-twentieths, according to its size; in the first case the values of x and y would be 0, $\frac{1}{30}$, $\frac{2}{30}$, $\frac{3}{30}$. . ., or of $2\pi x$ would be 0° , 12° , 24° , 36° . . . The symmetry of the projection will always reduce the area that actually needs to be covered by the calculations, and the complete structure can be reconstructed from one or more projections of this kind, as long as the atoms are sufficiently well resolved.

The above expression, however, is not in a convenient form for computation and is better given as

$$\rho(xy) = \sum [\sum k \cos h\theta_1] \cos k\theta_2 - \sum [\sum k \sin h\theta_1] \sin k\theta_2,$$

where

$$k = \pm \frac{|F(hko)|}{A}, \quad \theta_1 = 2\pi x, \quad \theta_2 = 2\pi y.$$

By summing the expressions in brackets *first*, this gives

$$\rho(xy) = \sum P \cos k\theta_2 - \sum Q \sin k\theta_2$$

as the expression for the final summation. Even these computations involve quite a lot of tiresome work, and many methods and

machines have been and are now being devised to lighten the processes of calculation.

When the structure has no centre of symmetry the two-dimensional expression is

$$\rho(xy) = \sum \sum k \cos (h\theta_1 + k\theta_2 - a),$$

which can be put into the form

$$\begin{aligned} \rho(xy) = \sum [\sum (k' \cos h\theta_1 + k'' \sin h\theta_1)] \cos k\theta_2 \\ - \sum [\sum (k' \sin h\theta_1 - k'' \cos h\theta_1)] \sin k\theta_2, \end{aligned}$$

where $k' = k \cos a$ and $k'' = k \sin a$, and this reduces, as before, to an expression of the form

$$\rho(xy) = \sum P \cos k\theta_2 - \sum Q \sin k\theta_2.$$

Now, these two-dimensional syntheses, which mean adding up the waves diffracted from all sets of planes in one zone, are some-

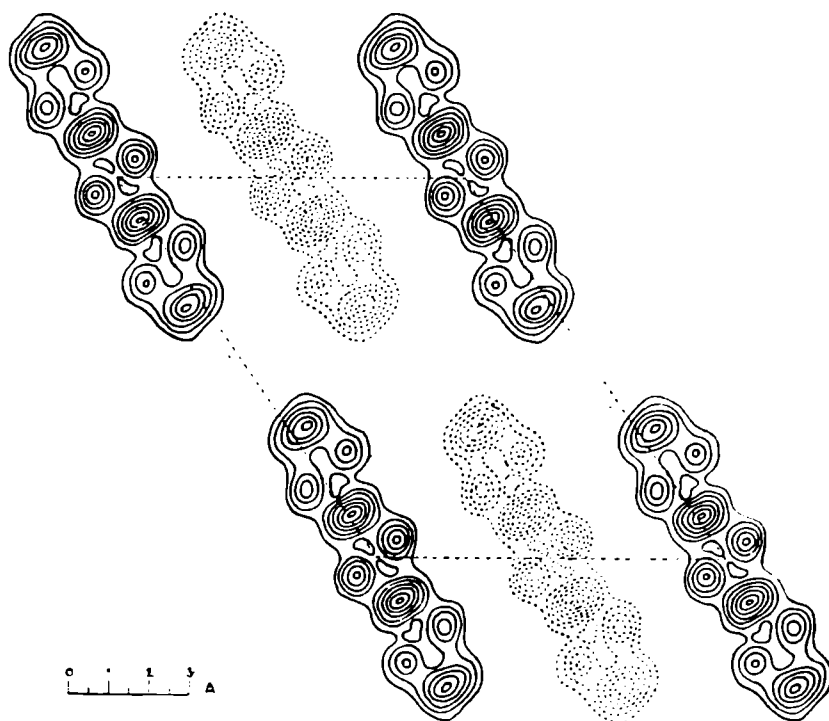


FIG. 99. Fourier projection of anthracene along $[010]$, showing resolved molecules and nearly resolved atoms.

(Robertson, *Proc. Roy. Soc., A*, 140, 79, 1933.)

times very satisfactory in giving a clear picture of the atoms projected along the zone axis (fig. 99) but quite often they do not, either because the molecules are unfavourably placed

(fig. 100), or because molecules overlap in that projection (fig. 101) and the atoms cannot be really satisfactorily resolved. If the coordinates $x_1 y_1$ of an atom can be found from one projection,

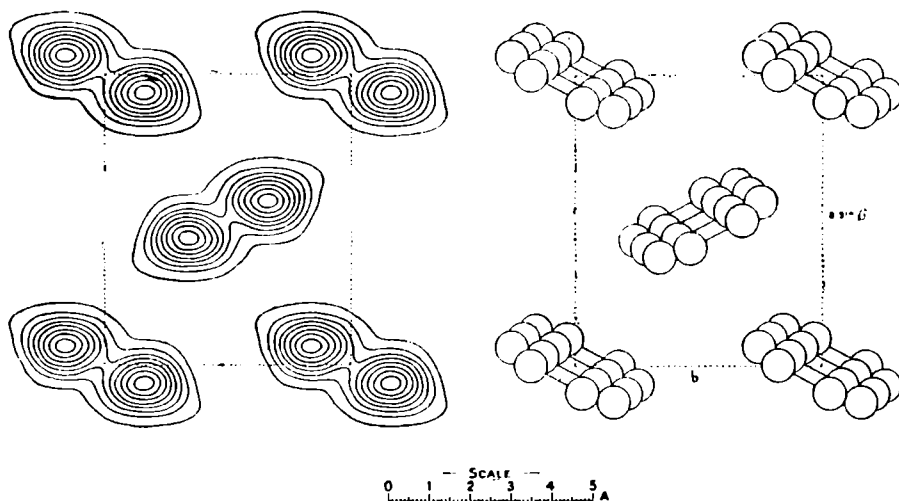


FIG. 100. Fourier projection of anthracene along $[001]$, showing resolved molecules but unresolved atoms.
(Robertson, *Proc. Roy. Soc., A.* 140, 79, 1933.)

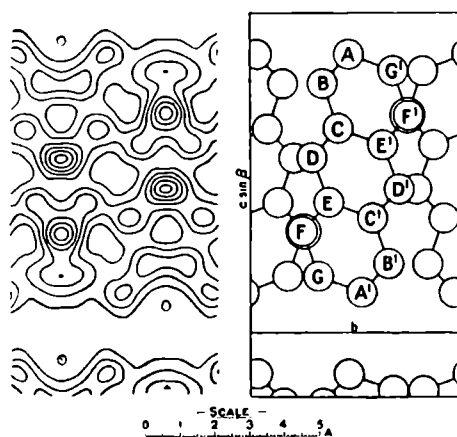


FIG. 101. Fourier projection of anthracene along $[100]$, molecules unresolved.
(Robertson, *Proc. Roy. Soc., A.* 140, 79, 1933.)

however, or if they are known from the trial structure, then the z coordinate can be found by evaluating

$$\rho(x_1 y_1 z) = \sum_{-\infty}^{+\infty} \sum_{-\infty}^{+\infty} \sum_{-\infty}^{+\infty} \frac{|F(hkl)|}{V} \cos [2\pi(hx_1 + ky_1 + lz) - a(hkl)]$$

and finding where a maximum occurs. This is a *line synthesis*. Or, if only one coordinate is known accurately, a *section synthesis* can be carried out. The overlapping of molecules can be avoided by summing only between limited values of one coordinate.

A serious limitation on the accuracy of Fourier syntheses arises from two facts. The first is that the series ought to, but never can, include structure factors for *all* points in reciprocal space. We cannot usually measure even all those within the limiting sphere. By taking a shorter wave-length we can increase the radius of the limiting sphere (that is, we can obtain values of $F(hkl)$ for planes of smaller spacing) and therefore increase the number of terms in the series, but this, unfortunately, also increases the amount of work involved in the summations. If the series, however, is terminated while the values of $|F(hkl)|$ are still large, then the lack of convergency involves us in false detail, regions of negative density and so on. The second fact is that since the atoms are not stationary, but are continuously vibrating, the electron density picture is a smudged one. There are indications that if we could only eliminate thermal vibration and yet have a convergent Fourier series, it would be possible to locate electron concentrations between atoms, which would throw much valuable light on valency, molecular or metallic binding forces. This is only practicable for light atoms. Usually the lowering of temperature, which decreases thermal vibration, means a large increase of intensity of reflection especially for high-order planes, thereby increasing the non-convergency of the series. In fact, one device used for increasing convergency is the introduction of an *artificial temperature factor*. This does eliminate defraction effects due to non-convergency, but introduces further smudging of the true electron density pattern.

DIRECT METHODS OF STRUCTURE ANALYSIS

Now, although it is true that, in general, direct methods of structure analysis are not possible, yet in special cases they can be applied. Sometimes the structure contains one or two *heavy atoms in special positions* that so much overshadow all the other atoms in the unit cell that they control the signs of the structure factors. One such heavy atom in the unit cell will make all or nearly all the structure factors positive. A preliminary Fourier synthesis with all positive terms will indicate the positions of all

atoms, and then, if calculation with the resulting coordinates changes the signs of any terms, a second or third synthesis is usually sufficient to give the complete structure. This method was used in the case of Pt phthalocyanine (fig. 102), where it was

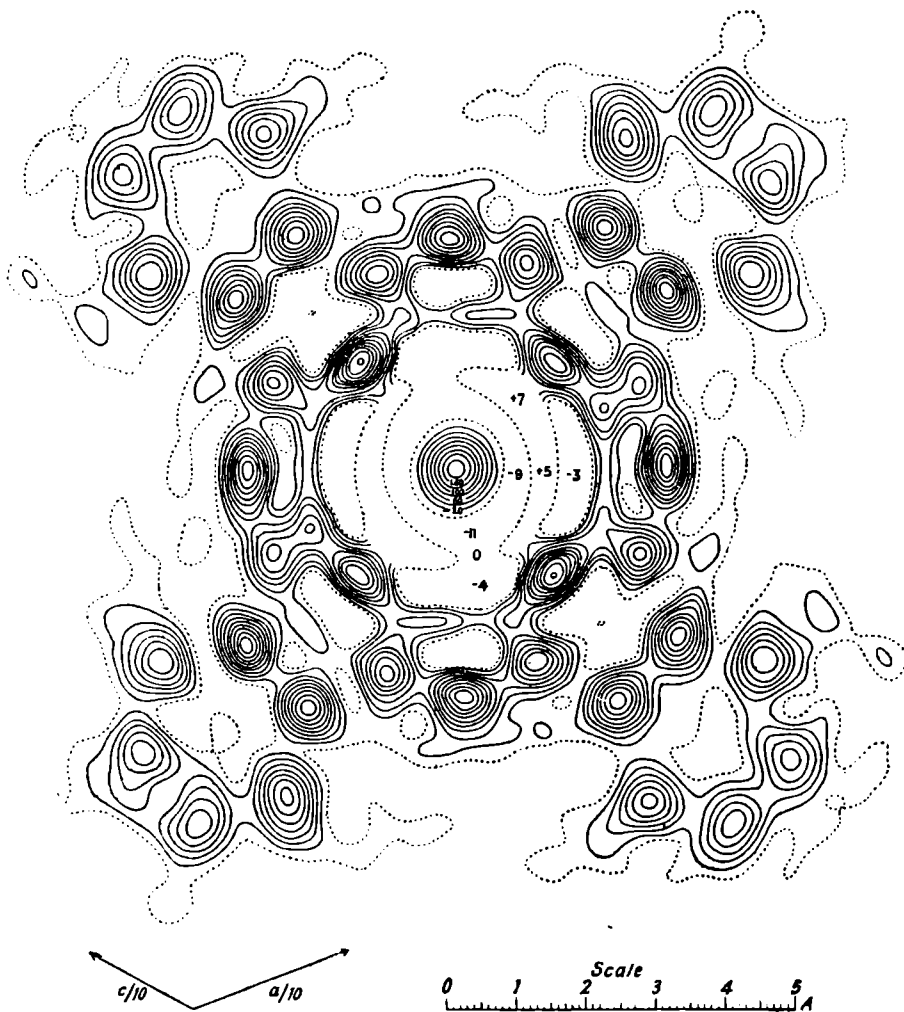


FIG. 102. Fourier projection of Pt phthalocyanine
(at 26.5° to actual molecular plane).

(Robertson & Woodward, *Journ. Chem. Soc.*, 38, 1940.)

clear that although there were two molecules in the unit cell, the Pt atoms had to lie at centres of symmetry and predominantly determined the signs of the Fourier terms.

Alternatively, it may be possible to examine two, or more members of a chemical series which crystallise similarly (that is,

are *structurally isomorphous*) but in *one* of which there is a heavy atom. The contribution of the heavy atom to the waves scattered in different directions must always be of the same sign. The signs of corresponding structure factors in the two isomorphous structures must be such that their difference is the contribution of the heavy atom. In the case of Ni phthalocyanine and metal-free phthalocyanine, in which the unit cell contained two molecules,

$$F_{\text{NiPh}}(hkl) - F_{\text{H}_2\text{Ph}}(hkl) = 2F_{\text{Ni}} \quad (\text{fig. 103, page 136}).$$

A comparison of the K and Rb penicillin salts was also employed in the determination of their structures. The method is not, of course, applicable unless the structures are isomorphous. Pt phthalocyanine and Ni phthalocyanine could not be compared in this way, nor could Na and Rb penicillin, since their structures are not strictly similar; although in the case of the penicillin salts there were relationships between the *packing* of the molecules in the Na salt on the one hand and in the K and Rb salts on the other which did help in the final elucidation of these most difficult structures.

Sometimes it is useful to employ what is called a *Patterson synthesis*, and to plot the values of $P(xyz)$ where

$$P(xyz) = \sum_{-\infty}^{+\infty} \sum_{-\infty}^{+\infty} \sum_{-\infty}^{+\infty} \frac{|F(hkl)|^2}{V^2} \cos 2\pi(hx + ky + lz).$$

This function, which is independent of the phase of the structure factor, gives a weighted average distribution of electron density about any point in the crystal. A maximum value (peak in the contour map) of $P(xyz)$ at a particular point $x_1 y_1 z_1$ defines a vector joining the origin of the Patterson function to $x_1 y_1 z_1$, and this vector corresponds to a vector in the real crystal, the interatomic distance between two atoms. It is not always possible, however, to decide directly to *which* pair of atoms in the unit cell this vector refers, although it is easier if absolute intensities are measured, so that the heights of the Patterson peaks have absolute significance, in terms of the pairs of atoms to which they correspond. The Patterson method is most useful when the unit cell contains a few heavy atoms not in special positions, giving really outstanding Patterson peaks. The Patterson pattern then gives the direction and magnitude of the

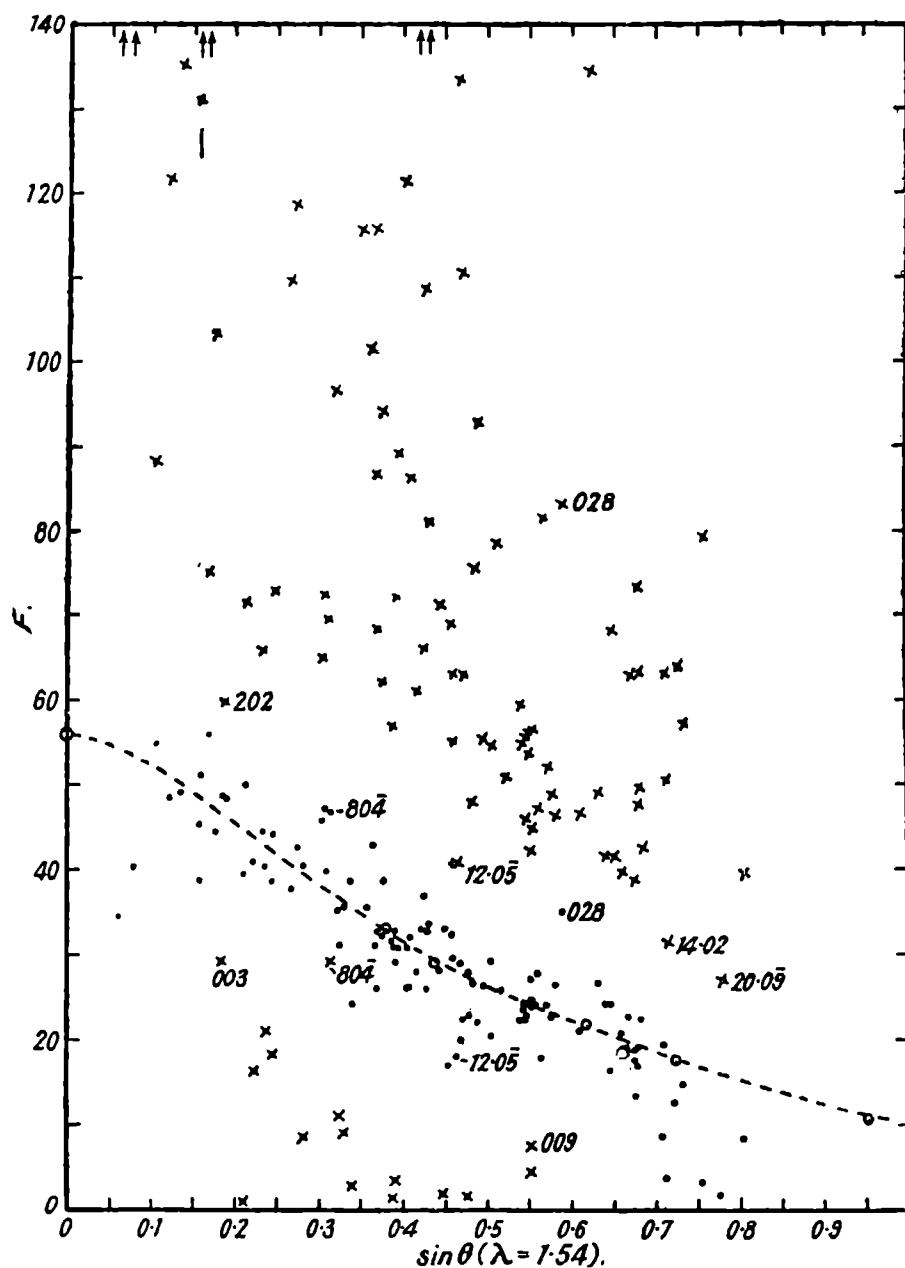


FIG. 103. Determination of phase constants. Crosses and dots represent values of $[F_{\text{Ni phthalocyanine}} \pm F_{\text{H}_2\text{Ph}}]_{hkl}$. The dots, which congregate about the atomic scattering curve for Ni, are accepted.

(Robertson, *Journ. Chem. Soc.*, 1199, 1936.)

vectors joining these heavy atoms (fig. 104). The placing of such heavy atoms in a structure usually decides the signs of sufficient

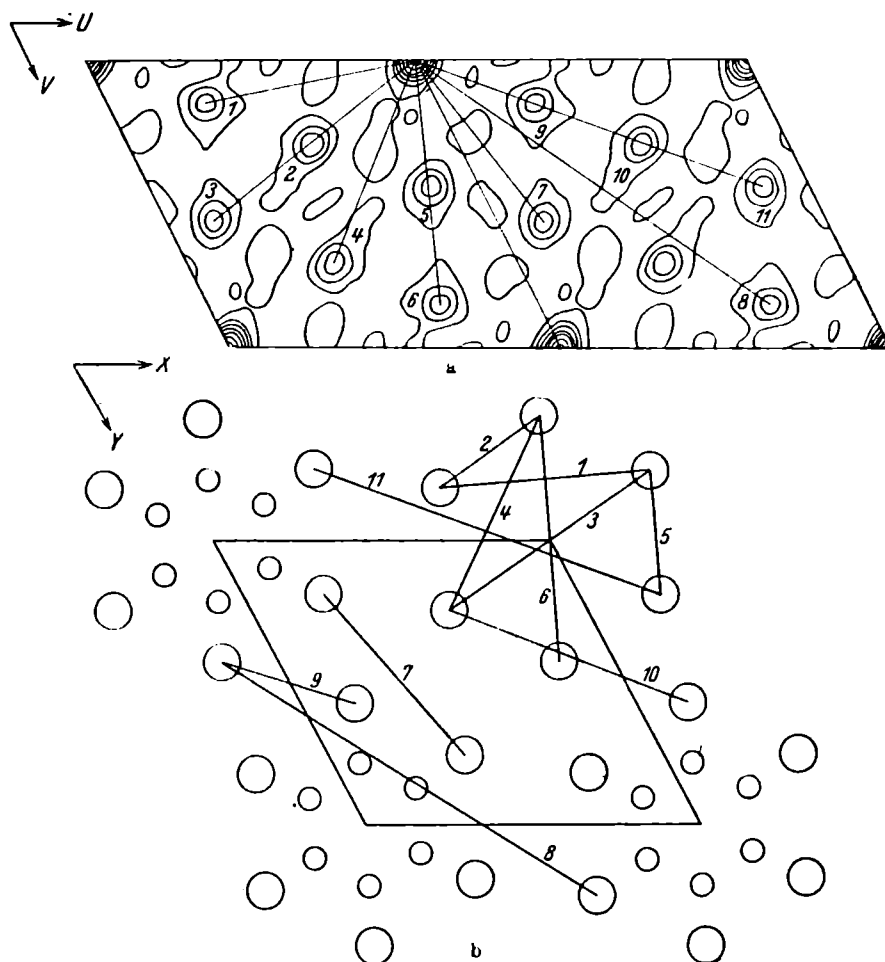


FIG. 104. (a) Result of 2-dimensional Patterson analysis of C_6Cl_6 , showing various important vectors.

(b) These vectors interpreted as inter-atomic distances in the actual projected structure.

(Bijvoet, Kolkmeijer & MacGillavry, *Röntgenanalyse von Krystallen*: Springer.)

structure factor terms to enable a preliminary Fourier synthesis to be carried out.

A good account of this whole subject appeared in the Physical Society's *Reports on Progress* (1938), 4, 332.

CHAPTER VI

EXTRA-STRUCTURAL STUDIES

IN this chapter we shall discuss some of the factors that make the measurement and interpretation of intensity of X-ray reflection more difficult, but which are of great intrinsic interest. These include crystal texture, small crystallite size, and imperfections of structure, together with the ubiquitous thermal vibration of atoms.

REFLECTION FROM A PERFECT CRYSTAL

In the last chapter we discussed only the intensity formulae for reflection from *mosaic* crystals, single crystals made up of little blocks or crystallites, or crystals in which the planes are bent or warped, or in which the spacing is not quite regular. Such formulae contain N^2 , $|F(hkl)|^2$ and a polarisation factor $(1 + \cos^2 2\theta)$. In the formula for the intensity of reflection from a perfect crystal,

$$\rho = \frac{E\omega}{I} = \frac{8}{3\pi} \cdot \frac{Ne^2\lambda^2}{mc^2} \cdot \frac{1 + |\cos 2\theta|}{2 \sin 2\theta} \cdot F(hkl),$$

the number of atoms N in the unit cell and the structure factor $F(hkl)$ occur in the first power only, and the polarisation factor is $1 + |\cos 2\theta|$, the cosine term being always positive. This means that the intensity of reflection is proportional to the amplitude of the resultant wave, and not to the square of the amplitude. A comparison of the intensity calculated from the perfect crystal formula and from the mosaic crystal formula shows that the latter is very much the bigger of the two. For example, ρ for the 111 reflection from a perfect diamond, using $\text{CuK}\alpha$ radiation, is $4 \cdot 10^{-5}$, whereas for a mosaic diamond it is $2 \cdot 10^{-3}$, fifty times the other. This result does seem surprising, but it is easily verified experimentally. If the intensity of reflection from a fresh cleavage surface of calcite is measured, and the surface is then broken up by grinding, the intensity of reflection is greatly increased. In the same way, an increase of intensity may be obtained either by finely powdering a crystal or by spraying it

with or dipping it into liquid air, so that it is broken down into smaller crystallites.

Only a very few crystals give the intensity corresponding to a perfect structure: clear, water-white isotropic diamonds, freshly cleaved calcite and some specimens, or parts of specimens, of rock-salt have been found to do so. Neither, however, are crystals necessarily completely mosaic. Most crystals give absolute intensity values somewhere between the two extremes, but more nearly of the mosaic type. The differences are most marked for strongly reflecting planes of large spacing, and the actual intensity values observed for a partly mosaic crystal depend both upon crystallite size and upon the degree of disorientation, for a so-called 'single crystal' may consist of a few large perfect crystallites, parallel to each other within less than a second of arc and more than 0.1 mm. linear dimensions, or of many very minute crystallites one degree or more out of alignment.

REFLECTIONS FROM REAL CRYSTALS

There could be three ways of dealing with real crystals. The first, rarely possible, would be to anneal so slowly that *perfect* crystals were obtained. The second would be to treat them roughly, so as to make them as nearly a perfect *mosaic* as possible. This is often done; whether by using a ground surface for measurement of intensity by ionisation methods, or by using a small crystal and giving it a preliminary dip into liquid air, or by powdering the crystal so finely that all particles are less than 10^{-4} cm. linear dimensions, the intensities of the low-order reflections being obtained from the powder lines. The third method, employed by early crystallographers rather extensively, is to use the crystal *as it is*, but to make corrections in the *mosaic* crystal formula to allow for the degree of *perfection* which actually exists. This is certainly difficult and it is only adopted when the second method is impracticable. It would not, for instance, be possible to alter the texture of a diamond by dipping it into liquid air. Its thermal conductivity is far too big, and its heat capacity and coefficient of thermal expansion too small. Besides, the specimen might be too precious to treat roughly.

The correction for perfection introduces two factors known as primary and secondary extinction.

Primary extinction. When an X-ray beam is diffracted by a mathematically perfect crystal consisting of m planes, the angle at which Bragg reinforcement of scattering takes place is $\theta \pm \epsilon$, where ϵ is of the order of a few seconds of arc. Partial reinforcement takes place as long as the path difference between rays reflected from the first and the m th planes is less than λ , absorption being neglected. The phase difference, for successive planes, between rays reflected at angle $(\theta + \epsilon)$ and those reflected at θ is $2d \sin(\theta + \epsilon) - 2d \sin \theta = 2d\epsilon \cos \theta$. For m planes it would be $2d \cdot m \cdot \epsilon \cos \theta$. Complete interference occurs when $2d \cdot m \cdot \epsilon \cos \theta = \lambda$ or $\epsilon = \lambda / (2d \cdot m \cdot \cos \theta)$. Since λ and d are of the same order of magnitude, ϵ will be of the order of $1/m$; for a crystal of about 10^{-3} cm. linear dimensions, m will be, say, 50,000, and the width of the X-ray reflection will be very small.

Not only is ϵ small, but if the single perfect crystal is relatively large only the skin of the crystal, the few layers on which the incident beam impinges first, are able to take part in reflection. The reason is that within a perfect crystal not only will there be a lot of multiple reflection, but the multiply reflected and transmitted beams will mutually interfere. A change of phase of $\pi/2$ occurs on reflection which is not important in the ordinary way, but which is significant when it means that a twice-reflected beam is opposite in phase to the incident (primary) beam, and partially interferes with it. Both reflected and transmitted beams, in fact, are frittered away, as it were, by interference; so that after passing through some 10^4 crystal planes there is no primary beam left in the right direction for Bragg reflection, and the reflected beam is reduced not only by interference, but by the fact that the rest of the crystal, under the skin, cannot reflect a primary beam that does not reach it.

The effect of this primary extinction, therefore, is an enormous apparent increase in absorption, over a very restricted range of angle. The fact that the angle is so restricted means that the actual loss of intensity from the primary beam during, say, a complete crystal rotation will be very small, and the intensity of reflection will also be small.

Waller has shown that the primary extinction in a partly mosaic crystal can be allowed for, in the case of reflection from the surface of a crystal plate, by inclusion in the mosaic intensity formula of a factor $\frac{\tanh mq}{mq}$, where m is the number of perfect

planes occurring in regular succession, and q = fraction of incident amplitude reflected from a single plane. Neglecting

polarisation, $q = \frac{Ne^2}{mc^2} \cdot 2d^2F(hkl)$. This is *independent of the wave-*

length λ , and for the first five orders of reflection from the cleavage plane of NaCl the correction factor has the values, for various perfect crystallite thicknesses, $D = md$, and for any radiation

D	$n =$	2	4	6	8	10
10^{-3} cm.		0.14	0.46	0.81	0.90	0.99
10^{-4} „		0.85	0.98	1.00	1.00	1.00
10^{-5} „		1.00	1.00	1.00	1.00	1.00

It is therefore negligible for small crystallites and high orders.

It should be particularly remembered that annealing will increase the perfection of a crystal and may therefore reduce its reflecting power. This is especially to be expected when variations of reflecting power due to thermal vibration are being measured at various temperatures. The changes observed with rising temperature are not always reproducible when the temperature is lowered.

Secondary Extinction. In imperfect single crystals, reflection is no longer limited to a skin, but takes place throughout the whole crystal. The angular range of reflection is also greater, being governed by the amount of disorientation of the constituent crystallites. Nevertheless the primary beam in the Bragg direction θ becomes progressively weaker on passing through the crystal, because it is being constantly reflected away. The total amount of reflection is therefore less than it would be if each crystallite were bathed in a primary beam of the original strength (fig. 105, p. 142). The effect is that of an increase of ordinary absorption over the range of angle in which reflection occurs. W. H. Bragg measured this increase in 1914 by an ionisation method. So did Rutherford and Andrade in the same year by means of a photographic method using a divergent beam of γ -rays (fig. 106, p. 142). The same thing can be shown by means of a widely divergent beam of Cu (or Ag) radiation using diamonds and other not strongly absorbing crystals. If a diamond plate, 1 or 2 mm. thick, is placed directly in contact with the source of divergent X-rays and the transmission picture observed on a photographic film at a few cm. distance, a very beautiful design of white (absorption)

lines on a grey background can be obtained in a few seconds' exposure (Pl. VIII). The difference between a crystal showing

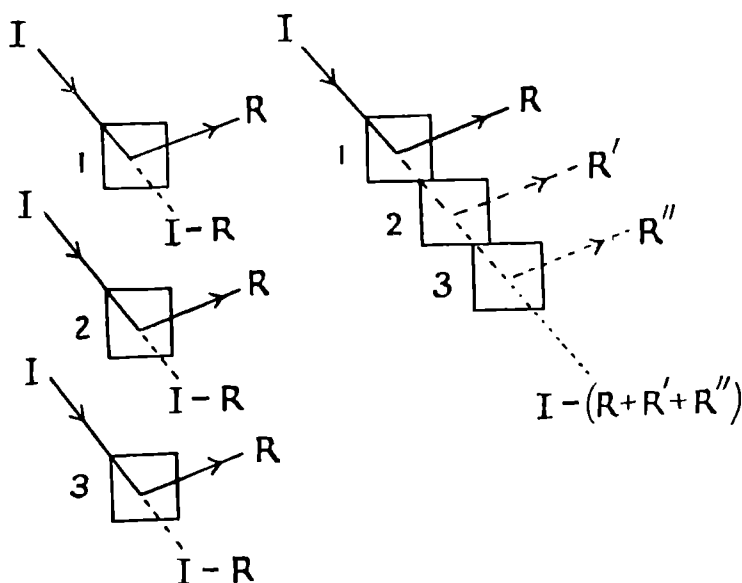


FIG. 105. Secondary extinction; intensity $(R + R' + R'')$ is less than $3R$.

primary extinction and one showing secondary extinction only is quite striking by this method. In the case of reflection from a perfect crystal the actual amount of radiation removed from the

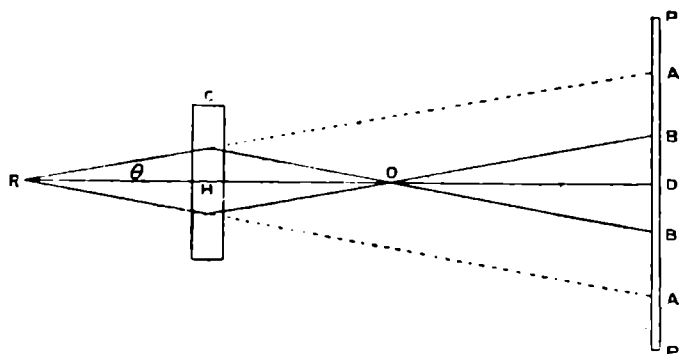


FIG. 106. Rutherford and Andrade's experiment. R , source of γ -rays; C , crystal; P , photographic plate; BB traces of reflected beams; AA white lines marking directions from which X-rays have been removed by reflection.

primary beam is so small that no absorption lines are visible. Some such crystals, however, may be broken up into a mosaic by dipping them into liquid air, and a divergent beam photo-

graph will then show a good absorption (secondary extinction) pattern (Pl. VIII *b* and *c*).

Bragg, James and Bosanquet showed that secondary extinction could be allowed for, in the case of NaCl, by using an expression $(\mu + gQ)$ for the absorption coefficient, instead of just μ , in the intensity expression $I = I_0 e^{-\mu t}$, where Q is the intensity of reflection and g is a constant. In that case one would expect secondary extinction to be of importance only for strongly reflecting planes, having a large value of Q . This is true as long as the crystallites in the mosaic are sufficiently disorientated for there to be no appreciable multiple reflection from parallel blocks. If there is multiple reflection, then the expression that should be

used is $\mu' = \mu + g_1 Q - g_2 Q^2 \dots = \mu + g_1 \left(1 - \frac{g_2 Q}{g_1}\right) Q = \mu + g' Q$,

where g' increases as Q decreases. The secondary extinction is then less obviously outstanding for the strongly reflecting planes. The two cases are well illustrated by the divergent beam photographs of different diamonds shown in Pl. VIII *d* and *e*. In VIII *d* the absorption lines corresponding to the 111 and, to a lesser extent, the 220 reflections are outstanding. In VIII *e* those corresponding to the higher order reflections 113, 004, 331 and 224 ($\text{CuK}\beta$) are of greater relative importance. The first is evidently a diamond in which the crystallites are disorientated, the second is one in which they are parallel though of course discontinuous. Each is a mosaic. So also is the diamond giving Pl. VIII *f*, where the crystal distortion is more obvious.

The problem of crystal texture is a difficult one, but it will have to be studied much more in the future than it has been in the past, because many of the properties of the ordinary solids used or met with every day are *structure-sensitive*; they depend upon texture. Strength, hardness, breaking-load, malleability vary enormously with the arrangement of the crystallites in the solid, especially, of course, in the case of metals and alloys. Constituents of living fibrous matter, such as cotton, hemp, silk, or muscle, wool, hair, are built up of long chain-like molecules which can grow and bend but which stand considerable longitudinal stress, and again, the arrangement of these is very important.

Crystallite size is also very important, especially in the case of fibres and catalysts, because the smaller the crystallite the greater is the relative amount of surface. When crystallite size becomes very small, smaller than, say, 100 A.U. in any direction, the X-ray

reflections become broadened, whether the crystallites are arranged to form a single mosaic crystal, a fibre or a powder (Pls. IX *a*; XII *a*, *b*, *c*).

Considering again the scattering power in reciprocal space, described in Chapter IV, it will be remembered that the reciprocal lattice points *are* only points for a space-lattice of infinite dimensions. As the crystallite size diminishes in any direction the size of the reciprocal lattice regions of scattering increases in that direction. For small spherical particles the scattering regions will be large and spherical; for small disc-shaped particles the scattering regions will be rod-shaped, and in every case the

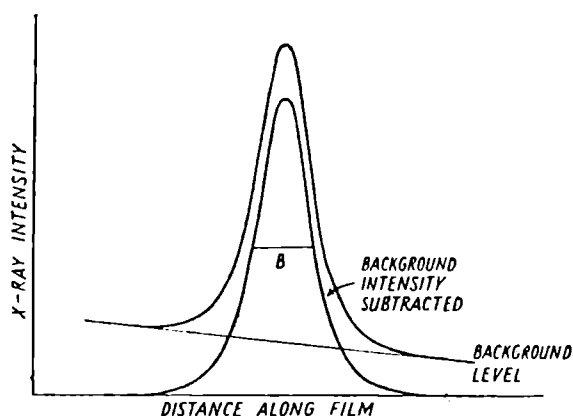
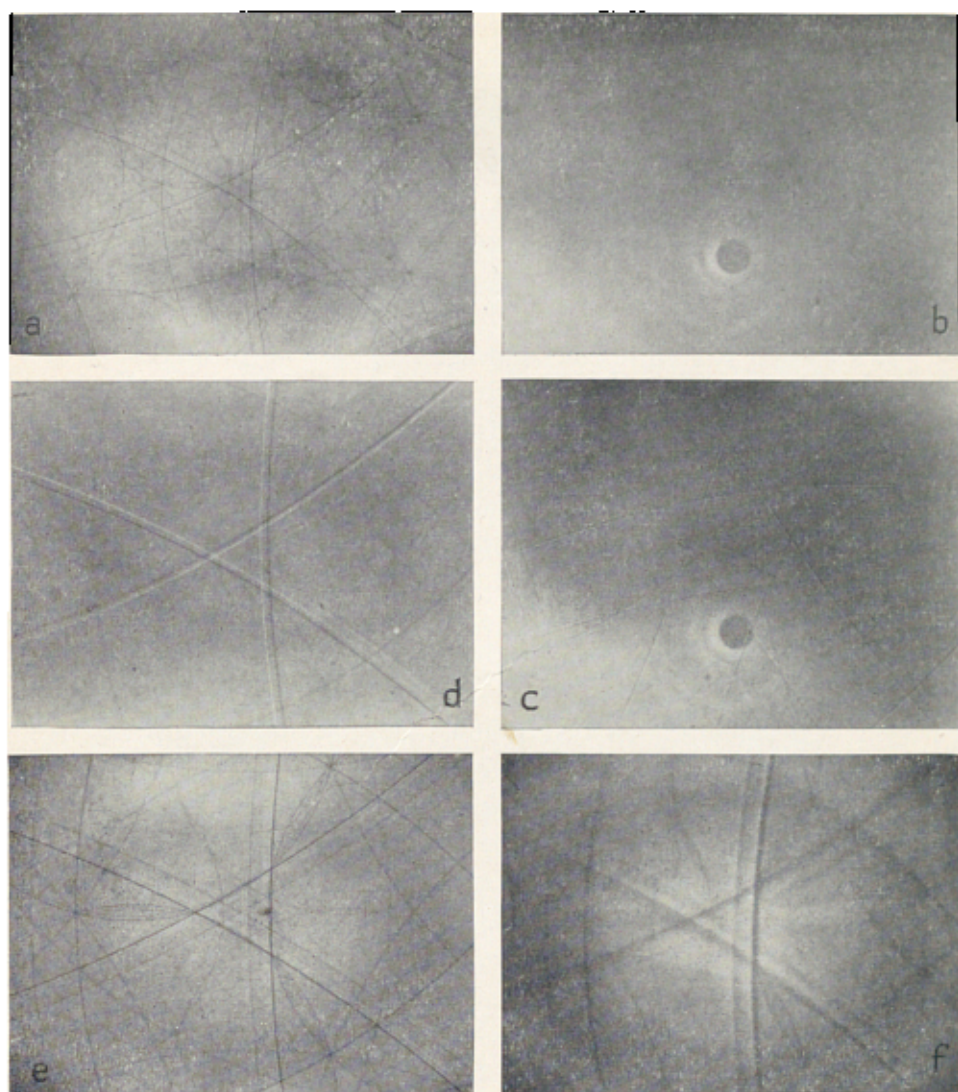


FIG. 107. Method of measuring line width *B* (width at half-maximum after subtraction of background).

(Bunn, *Chemical Crystallography*: Clar. Press.)

scattering regions will be reciprocal in shape to the shape of the particle. Fibre photographs often show a spreading of individual reflections, because the needle-like crystallites in fibres correspond to disc-shaped reflecting regions in reciprocal space. Powders composed of very small particles give powder photographs with broadened lines (Pl. IX *a*), and from the *relative* widths of different lines on the photograph the shapes and sizes of the particles may be deduced. The line width, *B*, is measured, after subtraction of the background, at the point where the photometered intensity has fallen to one-half its maximum value (fig. 107). For spherical particles of uniform diameter *t* and cubic symmetry the value of *B* varies with Bragg angle θ , and that part of the broadening which is due to small particle size is given by $\beta = \sqrt{B^2 - b^2}$, where *b* is the line width for particles larger than



(a) Divergent beam photograph of diamond, CuK radiation, film parallel to octahedral planes of crystal.

(b) Divergent beam pattern of hexamine before dipping crystal into liquid air (lines almost invisible).

(c) Divergent beam pattern of hexamine after liquid air treatment, when crystal has regained room temperature (lines beginning to show up).

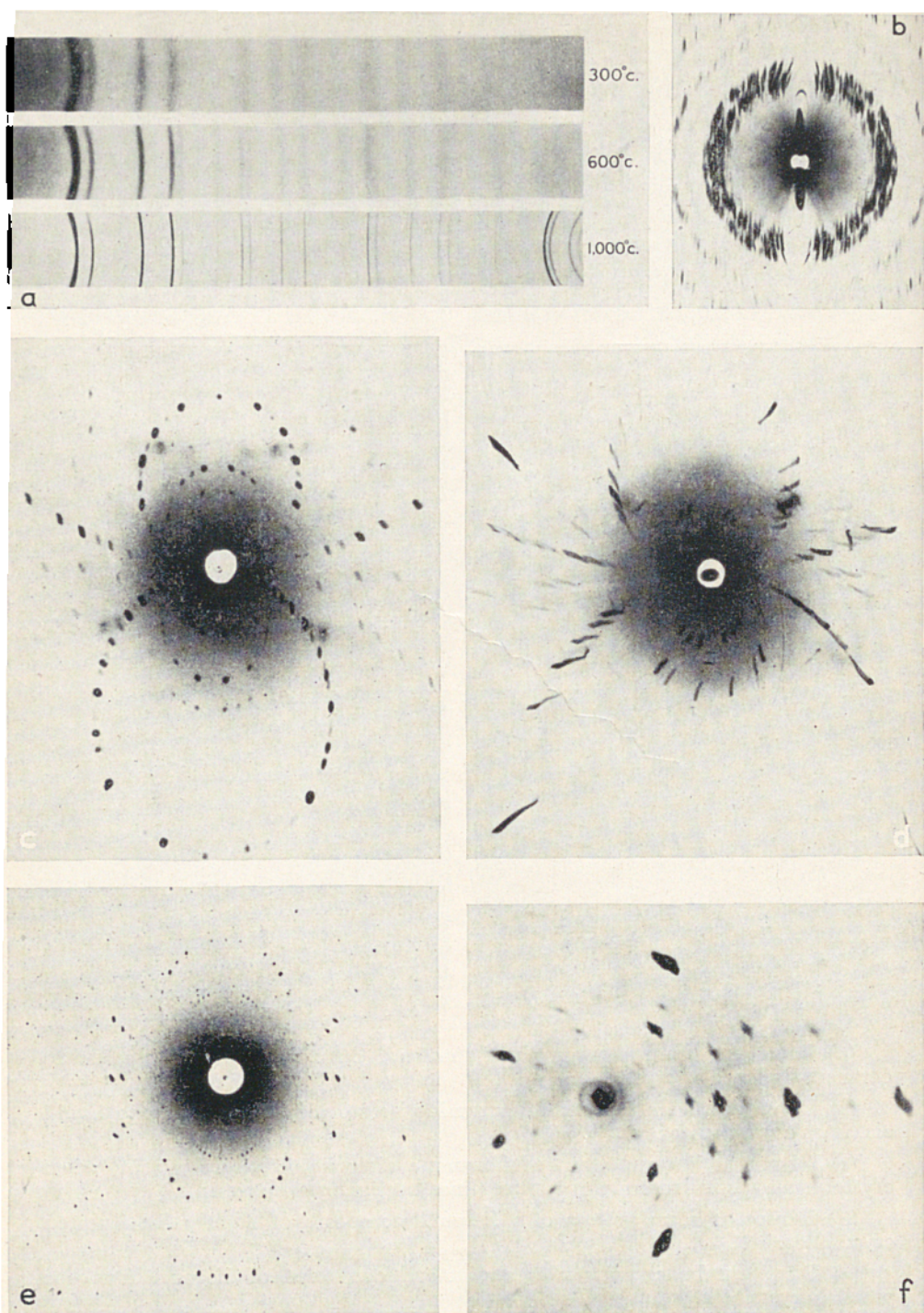
(d) Divergent beam pattern of a diamond composed of slightly disorientated crystallites.

(e) Divergent beam pattern of a diamond composed of discontinuous but parallel crystallites.

(f) Divergent beam pattern of a diamond composed of large disorientated blocks, each consisting of parallel crystallites.

All the above are positive prints: the negatives show white lines on a grey background.

IX



(a) X-ray powder photographs (10 cm. camera, CuK α radiation) of thoria gel heated at successively increasing temperatures; broadened lines indicate small particle size (Rooksby).

(b) Effect of large grain size on powder lines from ice.

(c) Laue photograph of spirally distorted crystal of urea oxalate; X-rays perpendicular to spiral axis, which is along the length of the crystal.

(d) Same crystal turned through 90° in horizontal plane; X-rays now along length of crystal.

(e) Laue photograph of spirally distorted needle of potassium penicillin II.

(f) Laue photograph of spirally distorted natural diamond.

10^{-4} cm. linear dimensions, and $\beta = \frac{C\lambda}{t} \cdot \sec \theta$ radians. C is approximately unity. A good method of obtaining B and b under similar conditions is to mix a suitable powder containing particles greater than 10^{-4} cm. diameter with the fine powder being investigated and to interpolate to find b for the lines required.

It is interesting to find that although, by different methods of preparation, yellow and red forms of Cu_2O can be obtained, these only differ in particle size, the yellow form being composed of colloidal particles, the red of particles large enough to give lines of normal width. Other useful particle-size measurements have been made on carbon-black, various colloidal suspensions, pigments, rubber and cellulose. As the particle size decreases to molecular or atomic dimensions the rings on a powder photograph will broaden until they correspond to those typical of an amorphous solid or a liquid. X-ray photographs of, say, ice (Pl. I *d*) taken below, at and above the melting-point show a liquid ring superimposed on a pattern of sharp spots; there is, in fact, a definite structural break between the solid and the liquid states, which is as sharp as one would expect from the abrupt change in properties that takes place. But in the case of graphite degenerating into carbon-black there is no sharp break, and the diffraction lines given by the colloid correspond to the main interference lines of the crystal.

Low-angle scattering, the X-ray scattering that occurs at very small angles with the primary beam, which was observed by Barkla and by Crowther in 1911, provides another method of measuring small particle size and shape. If a beam of light traverses a medium containing small opaque particles, these give rise to a halo of diffracted light surrounding the incident beam: the halo round the moon produced by small droplets of fog is a well-known example. The smaller the particles the larger the halo, the method being most suitable for particles of size 20-500 A.U. diameter. The scattering depends only on the size and shape of the particles and is *independent of their internal structure*; they may be crystalline or amorphous. The angle ϵ at which the intensity of diffraction becomes zero is given by $\epsilon = \lambda/d$, where d is the average diameter of the particles. The intensity of low-angle scattering depends on the difference between the electron density of the particles and that of the medium in which

they are embedded. The method is best used with monochromatic radiation (fig. 108).

This method has been used, notably by A. Guinier in Paris, to study the difference between solid plexiglass and a colloidal solution of plexiglass; coal samples before and after activation, a process which enormously increases the free surface by decreasing particle size; carbon black; catalytic nickel; the beginnings of age-hardening in Al—Cu alloys, when small plate-like Cu-rich crystallites are beginning to separate out from the matrix; and age-hardening effects in Al—Zn alloys.

Another interesting low-angle scattering study was that of a glassy silica, which is usually assumed to be made up of tiny cristobalite crystals of colloidal dimensions. Warren and Biscoe

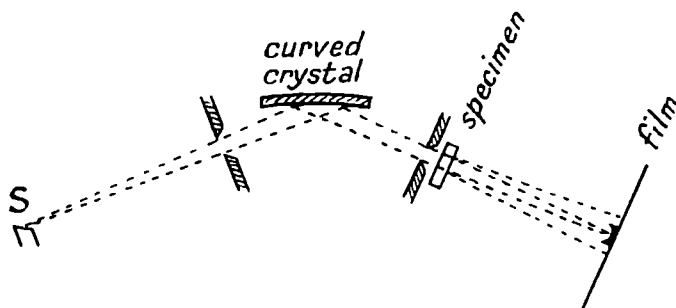


FIG. 108. Low-angle scattering by small particles, using focussed monochromatic X-rays (after Guinier).

have shown by ordinary X-ray diffraction methods that there is some evidence for this: the main diffraction peak does correspond to the main cristobalite reflection (fig. 109), although the fact that the line breadth gives a 'particle size' of less than 8 A.U., while the unit cell of cristobalite is 7 A.U. each way, means that the 'crystallites' can only be about one unit cell each; which is rather stretching the definition of a crystallite! However, the next question of interest is, how do these little particles, 8 A.U. across, join together? Is the glassy silica like a pail full of pebbles or a pail full of water? An investigation of the low-angle scattering should indicate whether the structure is essentially continuous or essentially discontinuous on a scale larger than that of atomic distances, for a *continuous* medium would give no low-angle scattering. Actually it is found that vitreous silica gives the pattern characteristic of a continuous structure, silica gel that of a discontinuous one. This must mean that the glass consists of little

regular units about 8 A.U. in size fairly widely dispersed in irregular but continuous intervening material. No doubt these very small and comparatively infrequent crystallites act as seeds when devitrification sets in, favouring cristobalite as the devitrification product.

The method has considerable promise in the study of colloidal

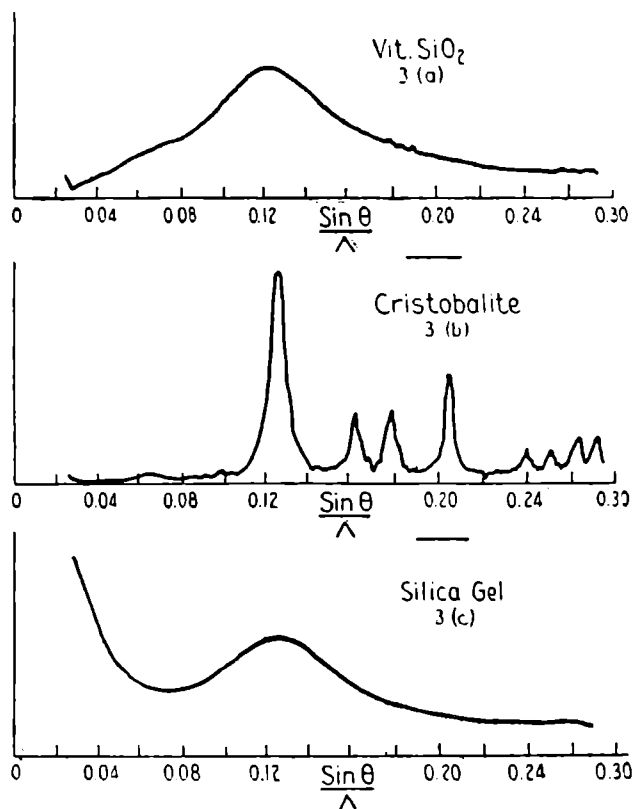


FIG. 109. Microphotometer records of X-ray diffraction patterns: (a) vitreous silica, (b) cristobalite, and (c) dried commercial silica gel.

(Warren & Biscoe, *Structure of Silica Glass by X-ray Diffraction Studies*, Jour. Amer. Ceramic Soc., 21, 402, 1938.)

solutions and of large molecules having molecular weights of the order of 10,000 to 100,000. It should be noted that *line-broadening* in powder photographs, which gives *crystallite* size, gives a *lower* size limit, whereas *low-angle scattering*, which is dependent on over-all *particle* size, gives an *upper* size limit, and the two may be very different if the particle is composed of smaller crystallites.

Grain size. When the crystallites of which a powder or a composite solid are made up are *larger* than about 10^{-3} cm.

diameter, the powder lines are no longer uniform in intensity but become spotty (Pl. IX *b*) even though the specimen is allowed to rotate. It is, in fact, possible to draw graphs relating grain size to dimensions of the diffraction images. This question of grain size is of great importance commercially, for so many physical properties depend upon it: tensile strength, Brinell hardness of metals, magnetic permeability and hysteresis loss in steels, corrosion and so on. *Strain*, however, is another important factor on which X-rays can throw considerable light, but which, at the same time, may give misleading results if its presence is not recognised.

It is not easy in practice to distinguish between broadening of powder lines due to small particle size and to a variation in lattice parameter from point to point in each crystal grain. It should be possible to distinguish them because of the different way in which the broadening will vary with the reflecting plane. For small particle size $\beta \cos \theta$ should be constant, for lattice-parameter variation $\beta \cot \theta$ should be constant; but if the particles are not spherical or the distortion is not isotropic, then trouble may arise. Controversy over the nature of cold work in metals was based on this very question.

It is possible to have warping or twisting of the crystallites in comparatively large mosaic crystals, either through strain during growth or through cold-working, and this is most easily studied by means of Laue photographs (Pl. III *e*). If the crystallite orientations deviate from a mean position in a small but random way the Laue photograph shows what is known as *asterism*, a radial extension of all spots, the ratio of major to minor axis of each spot (ideally elliptical) being $1/\theta$ (fig. 110). If the crystallites are *spiralled* slightly about a single axis, as not infrequently happens either during growth or through mechanical cold-working, all the spots on a Laue photograph taken with the X-rays normal to the axis will be rotated through a small angle, from which the pitch of the spiral can be measured. As Pl. IX *c* and *d* show, the appearance of the Laue photograph can be greatly influenced by the position of the crystal relative to the beam. In Pl. IX *e* and *f* this kind of spiralling effect is seen in crystals as different as a needle of K penicillin II and a large fragment of diamond.

Back-reflection Laue and powder photographs are particularly useful, because they avoid the absorption difficulty and enable a massive specimen to be conveniently examined simply by placing

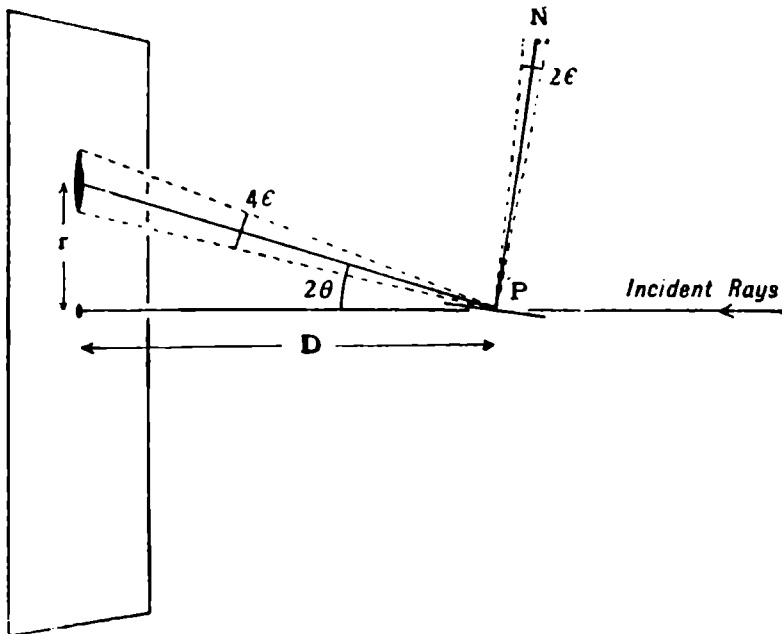


FIG. 110. Asterism, due to random deviation of normal to crystal plane from its mean position. Length of reflection, in plane of incidence $= 4D\epsilon$. Width of reflection normal to plane of incidence is $r \cdot 2\epsilon = 2\theta D \cdot 2\epsilon = 4\theta \cdot D\epsilon$ approximately. Ratio width to length of reflection $= \theta$ radians.

(W. L. Bragg, *The Crystalline State*, Vol. I: Bell.)

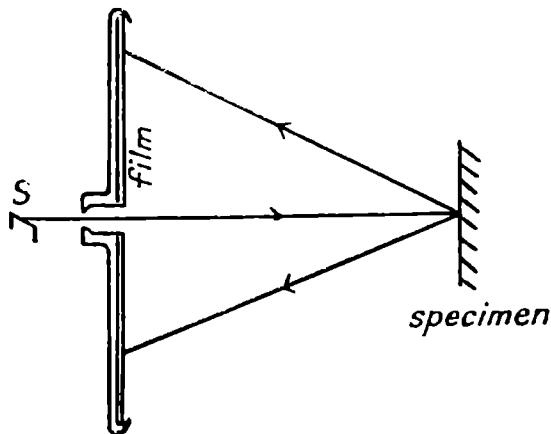


FIG. 111. Back reflection photography of massive specimen.

it in front of the X-ray beam (fig. 111). Such photographs now form part of the routine examination of steels, light alloys and metal machinery in general (Pl. I c and V a).

FACTORS THAT DISTURB THE REGULARITY OF CRYSTAL STRUCTURE

So far we have discussed problems of crystal texture. The so-called structure-sensitive properties of solids are really texture-sensitive. But there are also problems relative to irregularities of atomic arrangement, and of these none, perhaps, are more important than the *thermal vibrations* of the atoms. They are important first of all because they are universal, and secondly because they may give information about the forces that bind atoms or molecules together.

From the very earliest days of crystal analysis it was known that the atoms in crystals could not be stationary; they must be vibrating about their mean lattice positions and the vibrations must become more violent as the temperature rises. The effect on the X-ray reflections is the same as that on an optical spectrum when the lines of a grating are broadened, that is, their intensities are reduced. Debye and Waller showed that the X-ray intensity of reflection at temperature T is given by $I_T = I_0 e^{-2M}$, where I_0 is the intensity corresponding to a regular, stationary arrangement. M can be expressed as $8\pi^2 \frac{\sin^2 \theta}{\lambda^2} \cdot \overline{u_x^2}$, where $\overline{u_x^2}$ is the mean square displacement of the atoms, in any arbitrary direction x , from their mean positions; or as $8\pi^2 \frac{\sin^2 \theta}{\lambda^2} \left(\beta T + \frac{\gamma}{T} + \frac{\alpha}{T_3} \right)$, where α, β, γ depend on the mass of the atoms, the zero-point energy of the crystal and on its elastic constants. Early experiments showed that crystals do possess zero-point energy. Not that the atoms are moving at absolute zero, but that there is a certain probability that the atoms will not be exactly at their proper lattice positions, even at absolute zero. The elastic constants, or ratio of stress to strain for different kinds of stress, are known for a few crystals, but not for many. They can be calculated from the observed values of the compressibility, Young's Modulus, shear modulus and so on. In general terms it can be seen that if the elastic constants are large, then a large force is required to produce a small distortion. This shows that the forces between the atoms are strong, and consequently the thermal vibrations will be small. That is the case in diamond and in hard metals such as tungsten. If the elastic constants are small, as they are in soft metals like Na and Pb, then a small force will produce large distortion; the interatomic forces must be weak and the thermal vibrations may be very large.

It was indeed found from the early measurements that M varied considerably from one crystal to another, and that some atoms were more tightly bound to their mean positions than others, even in the same crystal. By experimentally determining I_T at different temperatures for different planes in the NaCl crystal, Waller, James and Firth found the values of M for planes containing both Na and Cl ions and for planes containing Na and Cl ions alternately (fig. 112); and by comparing them were able to show that the mean amplitude of vibration of the Na ions was greater than that of the Cl ions. Indeed it is a rule that metallic atoms are usually more loosely bound than the halogen, oxygen or other atoms with which they combine. The scale of the vibrations is shown in the following table:

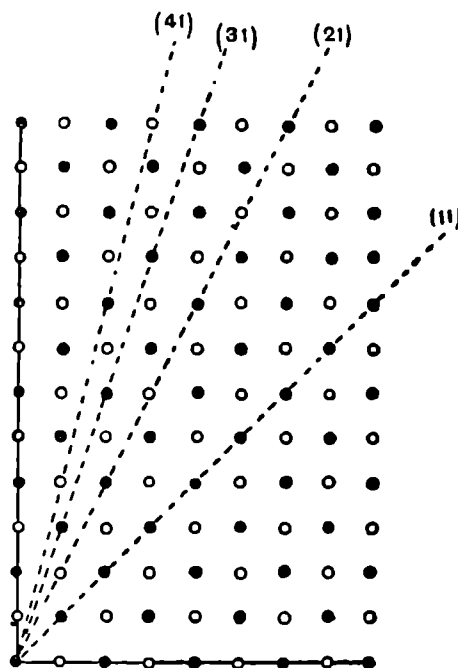


FIG. 112. Planes containing atoms of both kinds, e.g. (41) and (21); and planes containing each kind of atom alternately, e.g. (31) and (11) in the chess-board pattern.

(W. H. & W. L. Bragg, *X-rays and Crystal Structure*: Bell.)

TABLE III
Root mean square amplitude of vibration in NaCl

Temp.	86° K	290° K	500° K
Na . . .	0.152	0.242	0.315 A.U.
Cl . . .	0.133	0.218	0.283 „

Distance Na→Cl 2.820 A.U.

The *maximum* amplitudes of vibration may, however, be much greater than these values.

Now, although the intensity of Bragg reflection is decreased by these atomic vibrations, the total amount of scattering must remain

the same. What then becomes of the 'lost' intensity? Debye suggested that it was smeared over the background of the photograph, so to speak, independently of the crystal orientation; but this was wrong. What actually happens is that, in reciprocal space, the reduction of scattering power *at* the reciprocal lattice points is compensated for by a spreading of the reflecting power *around* the reciprocal lattice points, rather like the spreading that corresponds to a decrease of particle size, but with some fundamental differences. We can think of it in this way. The thermal vibrations, which are of a frequency of about 10^{13} per second, are slow compared with the frequency of X-rays, which is of the order of 10^{18} per second. As far as the X-rays are concerned, the atoms seem to be stationary, but displaced from their mean positions. The displacements of the atoms, however apparently random they may be, can be regarded as made up of $3N$ superimposed stationary waves, where N is the number of atoms in the crystal. Suppose we consider just one wave and find out how it influences the X-ray reflection from different planes. Let us, as an analogy, consider the reflection of the sun's rays from rippling water (Pl. III *f*). If the wave is travelling towards the observer the reflection will be seen as a streak, elongated in the direction of propagation of the wave. Similarly, in reciprocal space, the existence of a wave in the crystal, a wave which to the X-rays is a stationary wave, causes a spreading of reflecting power along the direction of propagation of the wave. Actually one single wave gives a pair of reflecting points, one on each side of the reciprocal lattice points. Long waves of low frequency give scattering points near to the reciprocal lattice points; short waves of high frequency give points farther from the reciprocal lattice points. The Bragg reflections themselves may be said to correspond to waves of infinite length. But the *intensity* of these scattering points outside the reciprocal lattice points depends on the amplitude and polarisation of the corresponding waves, and will be different for different reciprocal lattice points, each of which corresponds to a different set of planes in the crystal.

Let us take some simple examples. Fig. 113 shows the effect of *longitudinal* waves whose direction of propagation is along $[100]$. The displacement of the atoms is along $[100]$, that is, normal to the (100) and in, say, the (010) planes. Atoms may be moved about *in* a plane without affecting the intensity of reflection from that plane, but displacements normal to a plane

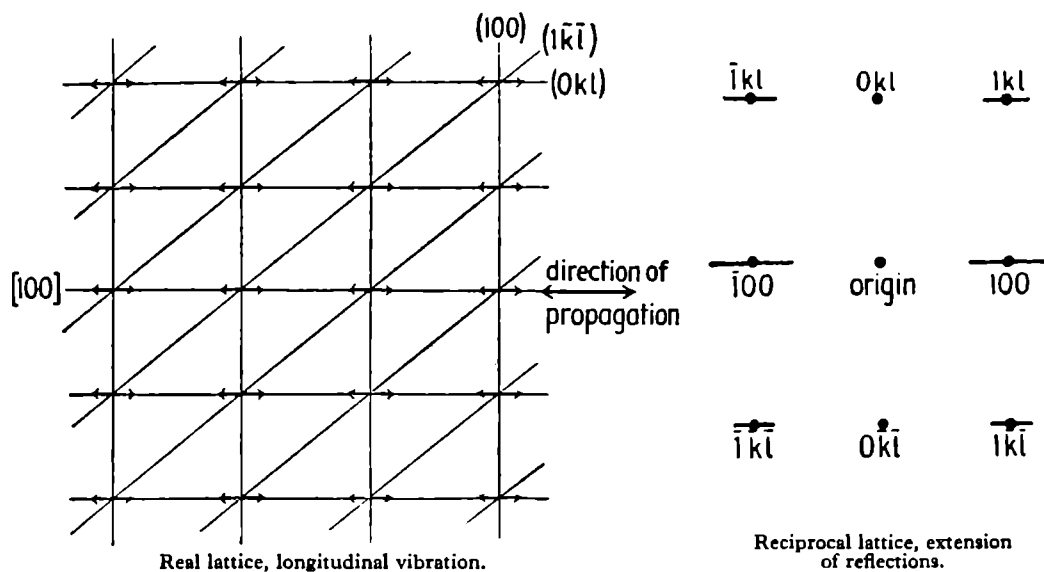


FIG. 113. Spreading of reflecting power in reciprocal space due to longitudinal vibrations.

(Lonsdale, *Proc. Phys. Soc.*, 54, 314, 1942.)

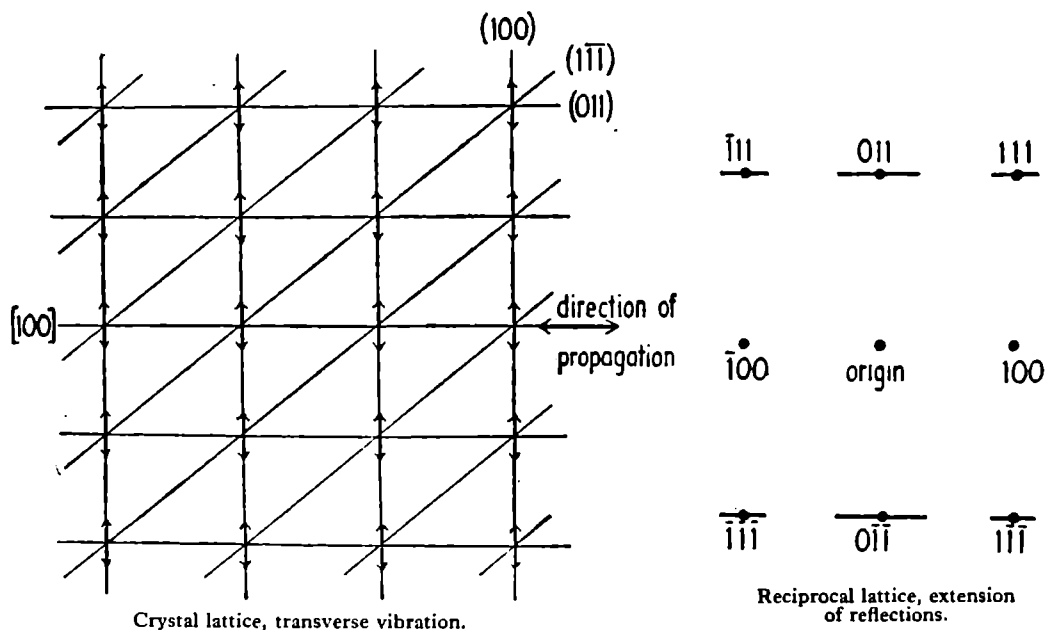


FIG. 114. Spreading of reflecting power in reciprocal space due to transverse vibrations.

(Lonsdale, *Proc. Phys. Soc.*, 54, 314, 1942.)

have a maximum disturbing effect upon the intensity. The intensity of scattering along the $[100]$ direction will be a maximum

for the $h00$ reciprocal lattice points and zero for the oko reciprocal lattice points. Fig. 114 shows the effect of *transverse* waves whose direction of propagation is along $[100]$, the displacements being normal to (011) planes and in (100) planes. Intensity of scattering along the $[100]$ direction for such waves will be a maximum for the okk and zero for the $h00$ reciprocal lattice points.

This gives a way of distinguishing between the effects due to thermal vibration and those due to small particle size. The shapes of the scattering regions in reciprocal space corresponding to small particle size are the *same* for all reciprocal lattice points, whereas for thermal vibrations the shapes *differ* for different reciprocal lattice points. The effect of $3N$ thermal waves in the crystal, of many different polarisations and amplitudes, is a sort of cloud of scattering power around each reciprocal lattice point, but the cloud has, in general, a different shape for each point. What effect will this have in terms of an X-ray photograph? The effect is that instead of reflection occurring only when a reciprocal lattice point comes actually on the sphere of reflection, reflection will occur when the sphere of reflection comes near enough to a point to intersect the cloud around it. It will be a rather weak, diffuse reflection compared with the proper Bragg reflection, but still it will be there. From the shape and intensity of the diffuse reflection in various crystal orientations we may deduce the shape of the cloud about the reciprocal lattice point.

The best way of observing the diffuse reflections is to use a stationary crystal and parallel monochromatic radiation. If the crystal is allowed to rotate, or is powdered, the diffuse reflection only forms a shoulder about the Bragg reflection and is only observable for strongly vibrating planes, such as layer planes. A second-best way is to take a Laue photograph with radiation containing a strong characteristic component. This gives the usual Laue pattern, due to general radiation, superimposed on a diffuse pattern from those planes that are *near* to reflecting positions for the crystal orientation and characteristic radiation chosen. Pls. X and XI show some of the photographs obtained in these two ways. The diffuse spots on the Laue photograph of α -resorcinol (Pl. X *a*) taken at room temperatures are clearly arranged along layer lines, and comparison with an oscillation photograph (Pl. X *b*) taken within $\pm 7.5^\circ$ of the same crystal position shows that they do in fact correspond closely to Bragg reflections occurring within that region. Photographs of this kind permit a rough

comparison of intensities to be made, and show that the Bragg reflection is more than 1000 times as intense as the corresponding diffuse reflection. The fact that the diffuse reflection is due to thermal vibration can, and always should, be checked by means of photographs taken at different temperatures. Photographs can be taken at low temperatures by the simple device of enclosing the crystal in a protecting tube made of cellulose acetate and allowing a fine stream of liquid air to fall steadily over it. The liquid air will itself give a diffraction ring (Pls. VI *e*, X *c*, *d*), but that can be by-passed by observing the Laue pattern at, say, a mean diffraction angle of 90° (X-ray film parallel to X-ray beam), outside the region of liquid air diffraction (Pl. X *e*, *f*).

At low temperatures the diffuse pattern is weakened or absent and the Bragg reflections are more intense and more numerous. In some cases (Pl. XI *a* and *b*) the shapes of the scattering regions are so very anisotropic that bridges stretch from one reciprocal lattice point to another or there may even be sheets of scattering power through reciprocal lattice nets. This is well illustrated by the photographs of ice near to the melting-point and of benzil single crystals. This must mean that along certain directions in the crystal there are waves of very short wave-length but of relatively large amplitude. Such directions can be very sharply defined (as in the monochromatic photographs of benzil), so much so that it seems almost certain that they must correspond in some way to chains of atoms in the crystal. Some light can be thrown on this by considering what effects would be expected from chain structures or layer lattices. Measurements have shown that although long-chain molecules, such as paraffins or fatty acids, have considerable flexibility and are compressible in directions parallel to their length, they are almost incompressible in directions perpendicular to their length. This is just as well, in fact, since otherwise the corn in the field, the stalks of flowers and the branches of trees, which are all built up of fibrous molecules extended more or less parallel to their lengths, instead of merely swaying to and fro, would expand and contract in a most disconcerting way. Since the atoms can only move perpendicular and not parallel to the length of the chain, longitudinal waves in the direction of the chain length are forbidden and (as shown in fig. 113) the diffuse scattering regions for all sets of planes normal, or nearly normal, to the chain lengths will be *discs* of very small thickness in a direction parallel to the chain length. The corre-

sponding diffuse reflections will be thin streaks (fig. 115), as in the photographs of sorbic acid (fig. 116; Pl. XI *c*). This method has proved useful in deciding, for crystals of unknown structure,

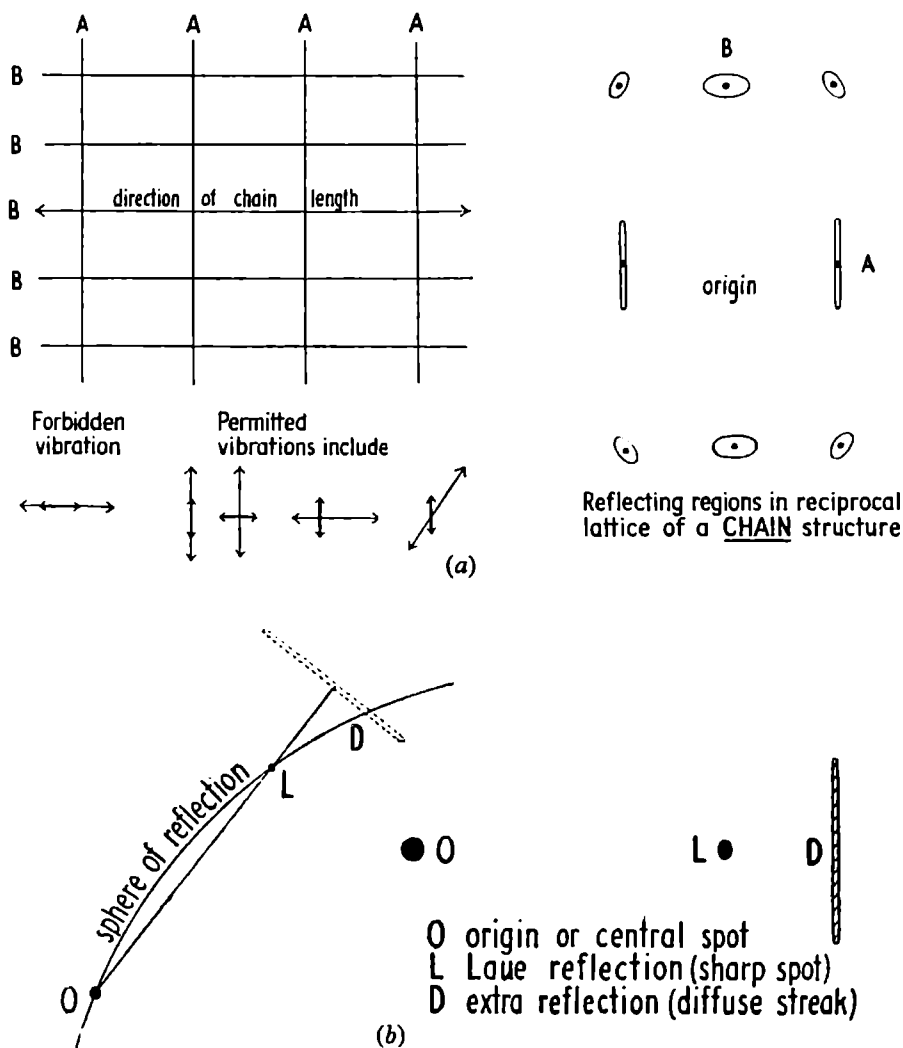


FIG. 115. (a) Spreading of reflecting power in reciprocal space for a chain structure.

(b) Appearance of diffuse reflection corresponding to disc-like region in reciprocal space.

(Lonsdale, *Proc. Phys. Soc.*, 54, 314, 1942.)

along which directions the lengths of chain molecules actually lie.

The diffuse reflections characteristic of layer structures are very different (Pl. XI *d*). Here the atomic displacements take place most easily in a direction normal to the layer plane. These dis-

placements may correspond to longitudinal waves whose direction of propagation is normal to the layer, or to transverse waves whose direction of propagation is parallel to the layer, or to waves in other directions. This results in an intense ellipsoidal cloud of scattering power surrounding the reciprocal lattice points which correspond to the layer planes. This cloud is very much extended and the actual diffuse scattering persists over a wide range of mis-setting of the crystal. In Pl. XI *d*, for instance, the large diffuse spot which corresponds to the vibrations of the layer planes is clearly visible even as far as $\pm 15^\circ$ or more from the correct setting for Bragg reflection. Jahn has given a formula for a cubic crystal of any Bravais lattice which relates the intensity *I* of diffuse scattering power in any direction about any reciprocal lattice point to the values of the elastic constants. [A cubic crystal has three elastic constants, c_{11} , c_{12} and c_{44} , which measure the ratio of the applied stress to the resultant strain for various directions of measurement.]

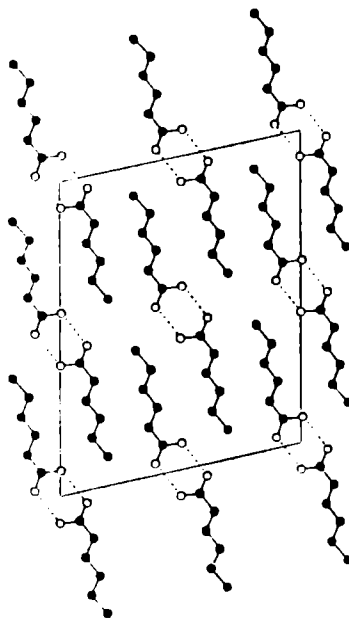


FIG. 116. Sorbic acid structure; projection on (010) plane.

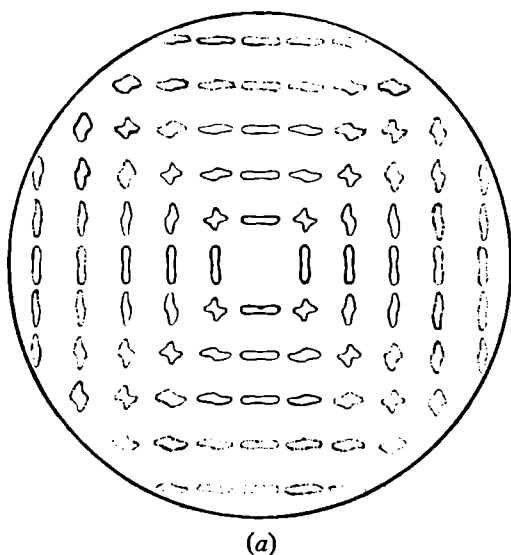
(Lonsdale, Robertson & Woodward, *Proc. Roy. Soc., A*, 178, 43, 1941.)

$$\begin{aligned}
 I \propto \frac{R^2}{r^2} \{ & c_{44}^2 + \sum L^2 [c_{44}(c_{11} - c_{44})(m^2 + n^2) + (c_{11} + c_{12})(c_{11} - c_{12} - 2c_{44})m^2 n^2] \\
 & - 2 \sum M N m n (c_{12} + c_{44}) [c_{44} + (c_{11} - c_{12} - 2c_{44})l^2] \} \\
 & + \{ c_{11} c_{44}^2 + c_{44}(c_{11} + c_{12})(c_{11} - c_{12} - 2c_{44}) \sum l^2 m^2 + (c_{11} + 2c_{12} + c_{44}) \\
 & (c_{11} - c_{12} - 2c_{44}) l^2 m^2 n^2 \}.
 \end{aligned}$$

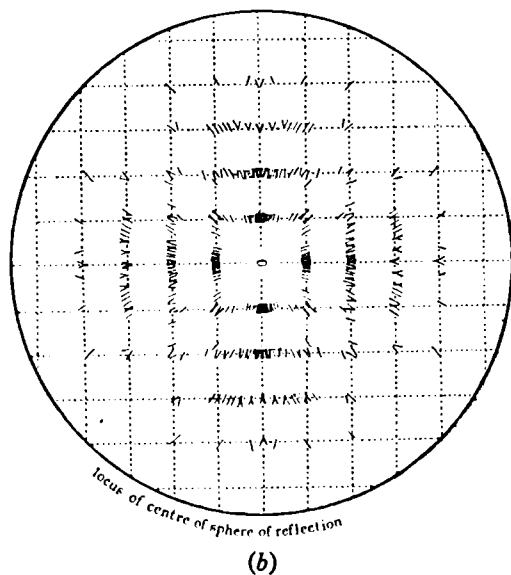
I is the intensity of diffuse scattering at a distance *r* in the direction [*l*, *m*, *n*] from a reciprocal lattice point *P*, distant *R* from the origin of reciprocal space, the direction cosines of *R* being [*L*, *M*, *N*].

If the elastic constants are known, then from the Jahn formula it is possible to plot surfaces of isodiffusion (equal scattering power) around the various reciprocal lattice points, and these

can be compared with experiment in two ways. The first is illustrated in fig. 117, which shows the isodiffusion surfaces



(a)



(b)

FIG. 117. (a) Isodiffusion surfaces for KCl, AgK radiation, $[001]$ zone calculated from Jahn's formula.

(b) Same observed; from a series of Laue photographs.

(Lonsdale, *Proc. Phys. Soc.*, 54, 314 1942.)

in KCl as calculated from the formula, using the data $c_{11} = 3.88$, $c_{12} = 0.64$, $c_{44} = 0.65 (\times 10^{11} \text{ dynes/cm}^2)$ at 290° K and as deduced from a series of Laue photographs of KCl taken with radiation containing an intense AgK α component (see Pl. XI e). The second method, more useful when the isodiffusion surfaces are very anisotropic, is to consider particular crystal orientations for individual reciprocal lattice points. Fig. 118 shows the shape of the surfaces and the section of the scattering cloud by the sphere of reflection when the crystal orientation is 4° from the 002 Bragg reflecting position, for single crystals of metallic sodium, the $[1\bar{1}0]$ axis being vertical. Comparison with Pl. XI f shows a close agreement with experiment, and this is equally true for other orientations and other reciprocal lattice points. It is an interesting consequence of the theory, well verified by experiment, that although sodium has

a body-centred cubic, and lead a face-centred cubic structure, their diffuse scattering regions for different reciprocal lattice

points are somewhat similar both in shape and extent, because of the similarity of the values of the elastic constants. Tungsten, on the other hand, with a body-centred cubic structure, has

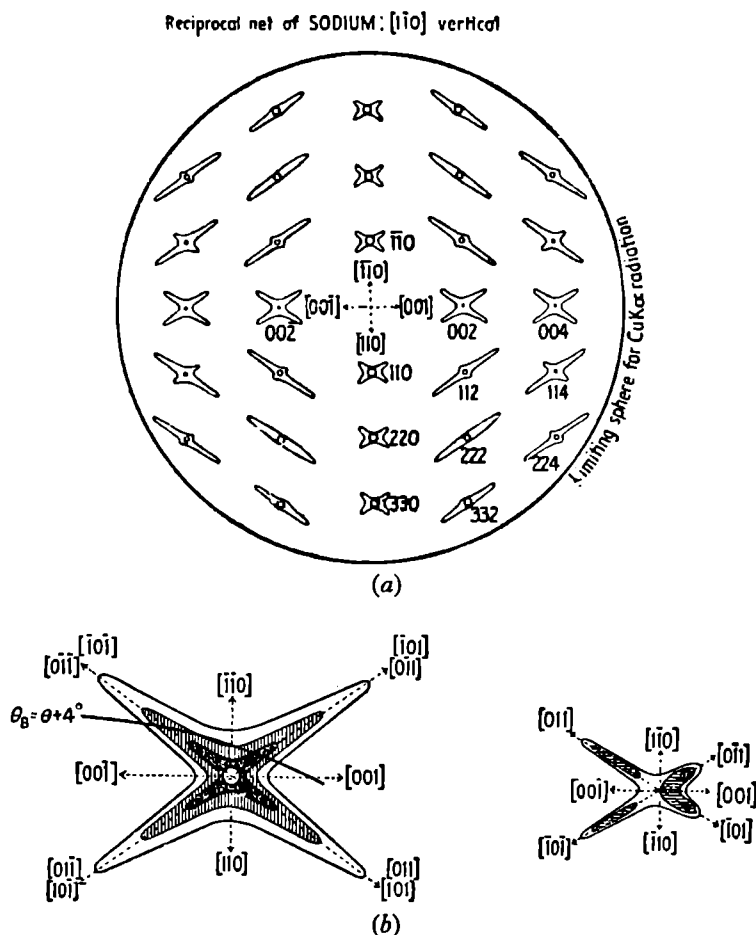


FIG. 118. (a) Isodiffusion surfaces for metallic sodium; CuK radiation; [110] vertical; calculated from Jahn's formula. (b) Section of 002 scattering cloud by sphere of reflection and resulting 'diffuse reflection.' Compare with plate XI f.

(Lonsdale, *Proc. Phys. Soc.*, 54, 314, 1942.)

elastic constants quite different from those of sodium and its diffuse scattering regions are very much smaller and of quite different shapes.

Theory indicates that the intensity of thermal diffuse scattering increases according to a law $I \propto T \cdot e^{-T/T_h}$, where

$$T_h = \frac{mka^2\Theta^2}{3h^2(h_1^2 + k_1^2 + l_1^2)}. \quad [m = \text{atomic mass in gm., } a \text{ the lattice}$$

constant; k , h the Boltzmann and Planck constants; Θ the characteristic temperature; and $h_1 k_1 l_1$ the Miller indices of the nearest Bragg reflection.]

As long as T is less than T_h , I increases, but above that temperature it will decrease. For most substances T_h is higher than the melting-point even for the maximum observable values of $(h_1^2 + k_1^2 + l_1^2)$. For lead, however, for which $T_h(h_1^2 + k_1^2 + l_1^2) = 6880$,

it should be possible to observe a decrease of diffuse intensity for high order planes $[(h_1^2 + k_1^2 + l_1^2) > 24]$ even before the melting-point at 327°C. is reached.

Sometimes extra, non-Bragg, reflections are observed on Laue photographs, which do not vary with temperature. These may arise from any disturbance or irregularity of the three-dimensional periodicity of the crystal, such disturbance being either static or dynamic. Some of the kinds of irregularity that can occur in real crystals are illustrated in fig. 119 for a simple one-dimensional lattice. Crystals are always finite, of course, but it is only

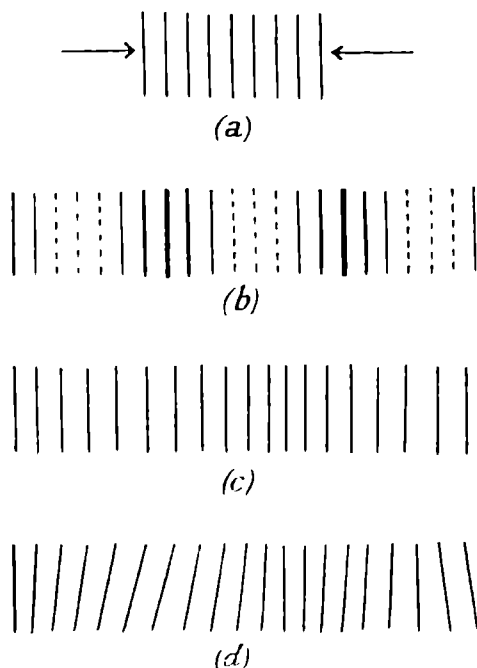
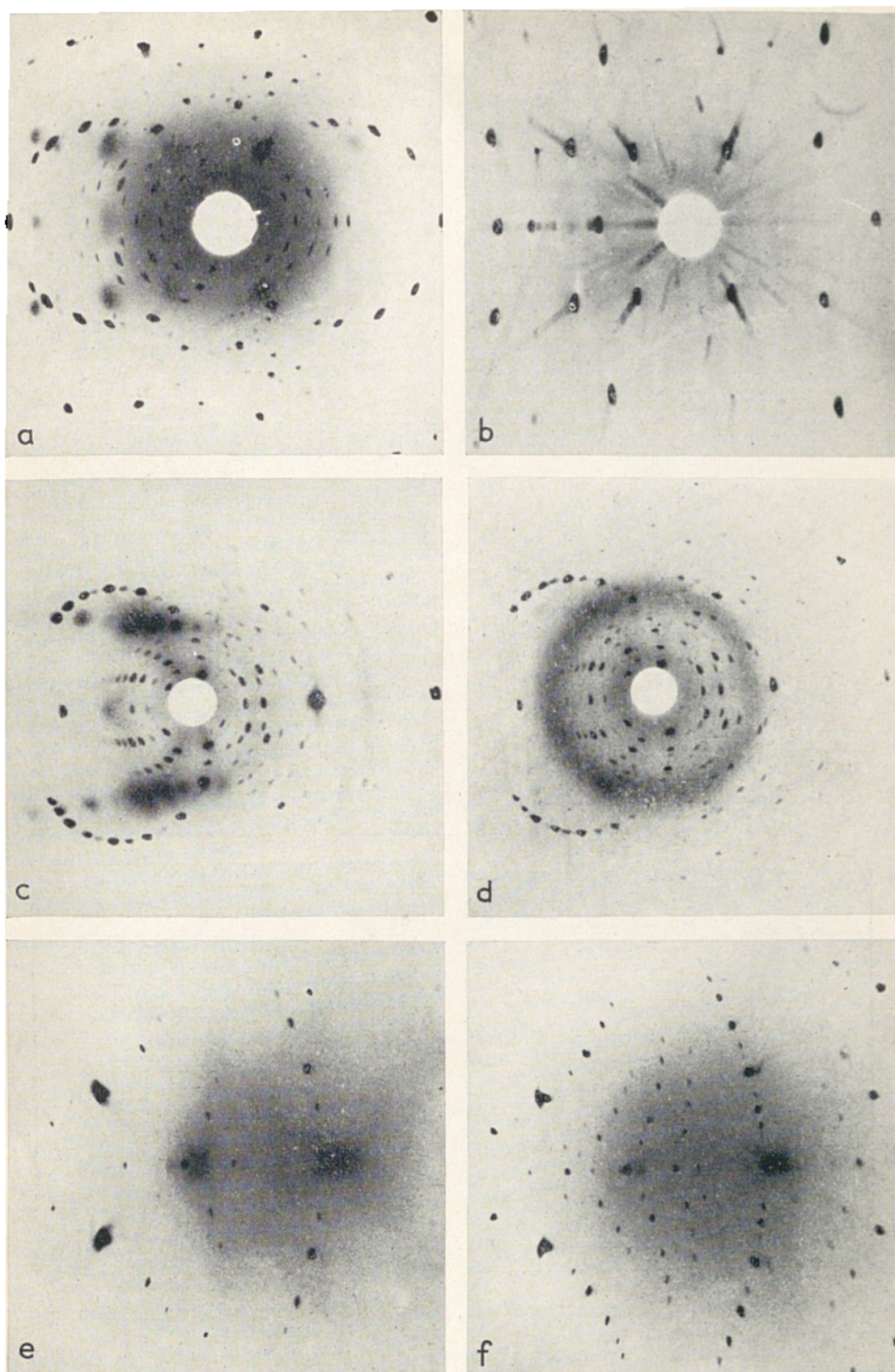


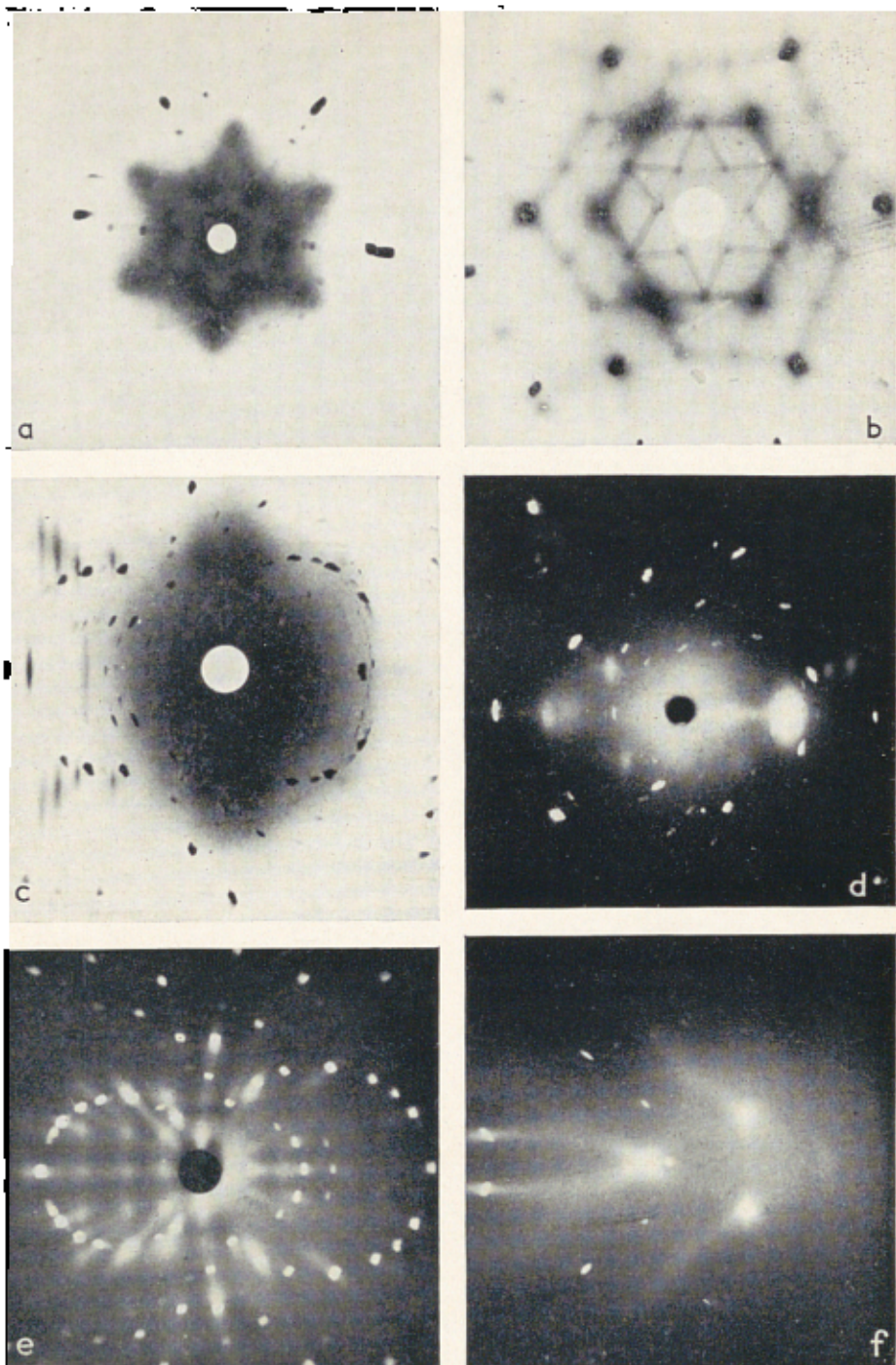
FIG. 119. Irregularities in a one-dimensional atom grating.

- (a) Finite number of lines.
- (b) Varying scattering power.
- (c) Varying spacing.
- (d) Varying tilt.

when the crystallites become of colloidal size (much too small for single crystal photography) that observable spreading of scattering power occurs. Sinusoidal periodicity of spacing, giving side-bands on powder photographs and side-spots on oscillation photographs, has been found for ternary alloys of approximate composition Cu_4FeNi_3 at a certain stage of their heat treatment. The alloy, which quenched from temperatures above 800°C. is face-centred cubic with lattice constant 3.5830 A.U. , finally reaches an equilibrium state of two face-centred cubic phases, one rich in $\text{Fe} + \text{Ni}$ with lattice constant 3.5692 A.U. , the other rich in Cu , with lattice



- (a) Laue and diffuse spots from α -resorcinol ; note the arrangement of the diffuse reflections along the layer lines.
 (b) Corresponding oscillation photograph of α -resorcinol.
 (c) Laue and diffuse pattern of sorbic acid at room temperature.
 (d) Same at liquid air temperature, showing liquid air ring.
 (e) Laue and diffuse pattern of lead single crystal at room temperatures ; film parallel to X-ray beam.
 (f) Same at liquid air temperatures ; no liquid air ring visible in this position.



(a) Laue and diffuse patterns of ice, X-rays along hexagonal axis; note the strong diffuse streaks; -5°C .

(b) Monochromatic stationary photograph of benzil, X-rays along principal axis; the streaks are here very well defined.

(c) Laue photograph of sorbic acid, in crystal orientation which shows well-marked diffuse streaks due to the vibrations of planes normal, or nearly normal, to the chain length.

(d) Laue photograph of hexamethylbenzene, showing one very strong, large diffuse reflection (and another large but very weak reflection on the other side of the central spot) both due to the vibrations of the layer planes (positive print).

(e) Laue photograph of KCl, using AgK radiation; crystal cube face 20° from X-ray beam direction, showing square pattern of diffuse reflections (positive).

(f) Laue photograph of sodium single crystal, film parallel to X-ray beam showing diffuse reflections of peculiar shapes (positive print).

constant 3.5956 A.U. During the process of separation of these phases, considerable disturbance of the regularity of the atomic arrangement must take place, and the same is true of the process of age-hardening in alloys. Variations of spacing, variations of the tilt of planes, and breaking up into small crystallite regions must also accompany distortion caused by cold-working of any kind. Irregularity of the atomic arrangement in random and defect structures, referred to more fully in the next chapter, must cause local distortions and local variations in the weighting of planes and will cause displacement of the atoms from their regular positions. This effect has been detected, beyond the usual thermal displacements, in crystals of mixed alkali halides.

THERMAL VIBRATION, CRYSTAL STABILITY AND THERMAL TRANSFORMATIONS

When the energy of thermal vibration exceeds that due to the forces tending to produce a regular crystalline arrangement, a solid will *melt*. Thermal *expansion* of a crystal also results from increasing thermal vibration, usually anisotropic in character. An investigation of the thermal expansion of the phthalocyanines, plate-like organic molecules which stack themselves together in the crystal in a zigzag way (fig. 120, page 162), has shown that the expansion is not only anisotropic, but may even be negative in certain crystal directions, simply because the vibrating molecules can pack themselves more comfortably if they *turn* slightly, instead of merely taking up more room in all directions. Graphite also expands considerably in a direction normal to the layers of carbon atoms (fig. 130), but contracts slightly parallel to the layers, up to a temperature of 400° C., and in this case it seems to be a simple Poisson contraction that is involved, similar to the sideways contraction of a stretched wire. The stable state of a solid at any temperature is one in which the interatomic and intermolecular forces balance locally, all vibration being taken into account, and in which the free energy is a minimum; or, in other words, in which the work required to separate the atoms is a maximum. With increasing temperature these conditions will change, but before a crystal actually melts it may undergo one or more transitions to other crystalline modifications. Such transitions will always be accompanied by changes in physical properties, often

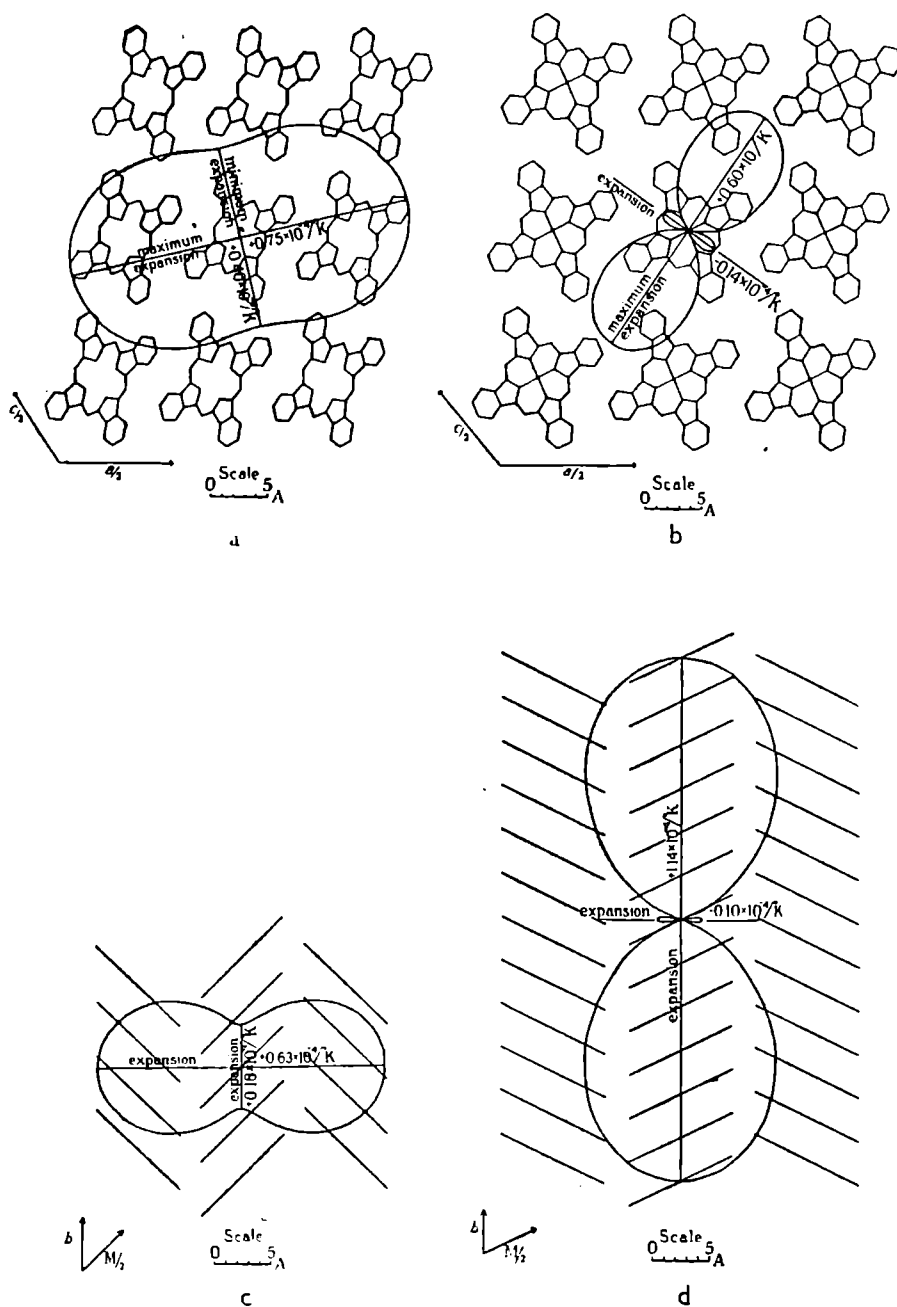


FIG. 120. (a) Metal-free phthalocyanine; thermal expansion in $[010]$ zone.
 (b) Pt phthalocyanine; same.
 (c) Metal-free phthalocyanine; thermal expansion in plane containing the $[010]$ axis and the width of the molecules, showing effect on slope and separation of molecules.
 (d) Pt phthalocyanine; same.

(Ubbelohde & Woodward, *Proc. Roy. Soc., A* 181, 415, 1943.)

quite large ones. The $\alpha \rightarrow \beta$ transformation in quartz (fig. 121) involves very small changes in atomic positions, which can take place without the rupture of any atomic bonds and which is therefore rapid and reversible, and yet the elasticity of quartz undergoes large changes at the $\alpha \rightarrow \beta$ transition point. The change from quartz to tridymite, another form of SiO_2 , is a slow and irreversible one, as it involves an exchange of oxygen atoms between silicon atoms and does involve the breaking of atomic bonds. Recent investigations of Rochelle salt, sodium potassium tartrate, have shown that changes in the structure which are extremely insignificant from a crystallographic point of view are never-

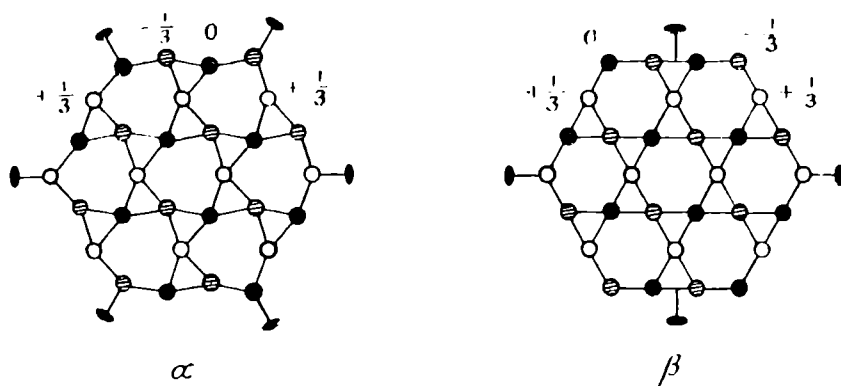


FIG. 121. Diagrammatic representation of the $\alpha \rightarrow \beta$ transformation of quartz.

theless associated with changes of dielectric constant and piezo-electric modulus so large (fig. 122, page 164) that these and similar crystals are sometimes called ferro-electrics, although seignette-electrics is a better name. In the case of Rochelle salt the change takes place only within the range of temperature -20° to $+25^\circ$ C., and the enhancement of dielectric constant and piezo-electric modulus takes place along one crystalline axis only. The crystal, originally orthorhombic, changes to monoclinic symmetry, but the change of angle involved is only $2'$.

There are other types of transition which correspond, in a sense, to a partial break-down of crystal forces, so that although the substance is still crystalline yet some atoms or groups of atoms are rotating. Such a rotation was suspected, in the case of some long-chain molecules of primary alkyl ammonium halides, to account for the high apparent molecular symmetry, a symmetry higher than that which could possibly belong to a stationary zigzag chain of carbon atoms. But many other examples have been found. At low temperatures, for example, NaCN has a

structure in which the CN groups are stabilised along a particular crystallographic direction. But at room temperatures NaCN has the same crystal structure as NaCl. The CN group therefore must either be rotating or must assume sufficient different orientations to give statistical cubic symmetry. In some cases which at first seemed to imply molecular rotation, it has been

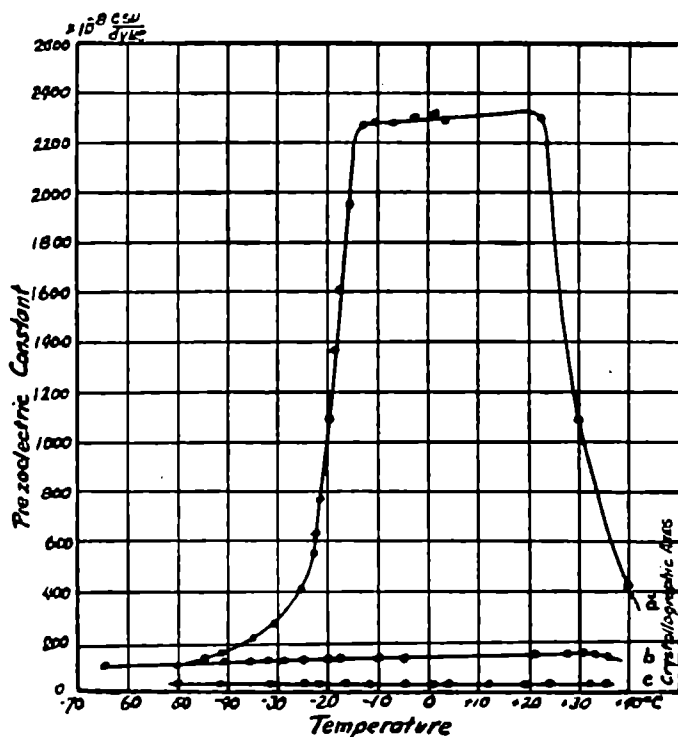


FIG. 122. Change of piezo-electric constant in Rochelle salt within the range of temperature -20° to $+25^{\circ}$ C. (Curie region).

proved that there is no *room* for rotation to take place, and that the symmetry is due to a statistical summation of certain definite molecular configurations or orientated vibrations. Pirsch has shown that for crystals in which the molecules are rotating, the heat of fusion is unusually small and the melting-point high. In other words, since the crystalline forces have already partly broken down, the energy required to remove *all* regularity of structure is small. The entropy change at a thermal transformation is of the same order of magnitude as that on melting, and is accompanied by sudden changes in, for example, specific heat. All these changes will be understood more fully when we know more about the actual thermal vibrations in crystals.

CHAPTER VII

THE IMPORTANCE OF THE STUDY OF CRYSTALS

THIS chapter aims at describing something of the achievements of X-ray crystallography in different departments of science. The field is much too wide to do more than pick and choose. Many applications of the new method have been indicated in previous chapters: the determination of X-ray wave-lengths and of fundamental constants such as Planck's constant, Avogadro's number and hence the electronic charge; the structure of the atom and the mechanism of radiation. Physics owes a good deal to the X-ray crystallographer. So do mineralogy and metallurgy. Chemistry, I think, owes most of all. The field of biology is only just on the verge of exploration, though results of the greatest importance have already been obtained.

INTERATOMIC AND INTERMOLECULAR FORCES

You will remember that from the *positions* and the presence or absence of spots or lines on the photographs it is possible, by calculation and the use of tables, to determine the geometrical framework, the symmetry and underlying lattice of the structure. That, of course, is of interest to the crystallographer even if we determine nothing more. But a study of the *intensities* of reflection will, after much labour, give also the distribution of scattering material, that is, the electron density distribution in the unit-cell, which is repeated in three dimensions in space. This information is invaluable to the chemist because it enables him to extend his study of the constitution of matter to the solid state. The composition of solid substances could previously only be discovered by dissolving, melting or vaporising them and then experimenting with them. But this destroyed their solid character and might well change the nature of the interatomic bonds altogether. We know that in crystals various forces are operative. There are the universal van der Waals forces, weak forces of attraction between atoms and molecules of whatever kind; the forces that make even an inert gas liquefy and solidify at low enough temperatures; and there are the intrinsic repulsion forces which become increasingly

important at small distances and which balance the forces of cohesion. Then there are electrostatic forces, such as those existing, for example, in NaCl, between the positively charged Na^+ ion, and the negatively charged Cl^- ions surrounding it, or between the permanent dipoles of acid and H_2O groupings, or between ions and permanent dipoles, or between charged groups and dipoles induced by them. There are homopolar forces, covalent linkages due to the sharing of electrons by pairs of atoms, or to molecular orbitals embracing a number of atoms; and there are metallic forces, where metal atoms have contributed electrons to a pool of so-called free electrons and are then held as charged atomic cores in the quantised electronic atmosphere. The stable state of a crystalline solid is one in which these forces balance locally, in spite of the thermal vibrations of the atoms and molecules, and in which the crystal as a whole is electrically neutral. X-ray crystal analysis, by providing measurements of the distances between atoms and of the electron density distribution in and between molecules, has shown that there is no justification for regarding some of these bonds as chemical and some as physical in character, they are all of equal importance in regard to the constitution of the solid substance.

THE IMPORTANCE TO CHEMISTRY OF ATOMIC RADII

W. L. Bragg's study of the intensities of reflection from the alkali halides showed that in them the atoms were ionised. Chemists had, of course, known from electrolysis that this was the case in solution, but they could not know whether or not there were ions in the solid state. Early X-ray investigators not only showed that the atoms were ionised, but that no ionic *molecule* existed at all in these compounds. Each Na^+ ion was surrounded by six Cl^- ions and each Cl^- by six Na^+ and there was no indication whatever of any pairing off. There is *coordination*, but no molecule, in most inorganic compounds. The Na atom, in becoming ionised, has, so to speak, shed a skin, and is then able to gather around it a number of neighbours of opposite sign, which will be attracted by the Na^+ and repelled by each other. The degree of coordination is not controlled by valency. NaCl and MgO have the same coordination of cations by anions and vice versa, but where in the NaCl structure the coordination number is 6, in CsCl it is 8, whereas in BeO it is 4. Pioneer work by W. L. Bragg,

Wasastjerna, V. M. Goldschmidt and Pauling showed that the arrangement of ions in a crystal is largely determined by the respective sizes of the cation and anion, by the *radius ratio*, due consideration having been given to the forces of attraction or of repulsion which exist when charged bodies come into proximity. Not merely the arrangement, but the very *existence* of certain compounds may depend on this factor. For example, sodium metaphosphate (NaPO_3) and sodium orthophosphate (Na_3PO_4) can both exist, because the P^{5+} ion is large enough for either three or four O^{2-} ions to be grouped around it. But the smaller N^{5+} ion will accommodate only three O^{2-} ions, and therefore, although NaNO_3 exists, Na_3NO_4 does not.

RANDOM STRUCTURES AND MIXED CRYSTALS

The fact that it is geometry rather than valency that decides stereochemistry and may even influence the very existence of compounds is nowhere so strikingly illustrated as in *random structures* such as that of Li_2TiO_3 . This compound has a rock-salt-like structure. The unit cell contains *four* O^{2-} ions and *four* cations, in the average proportions of two Li^+ to one Ti^{3+} ions, quite randomly distributed. The real formula must, of course, be written $\text{Li}_{2n}\text{Ti}_n\text{O}_{3n}$, but apart from maintaining over-all electrical neutrality the valencies appear to be of very minor structural importance. Size is the important thing. NaBiS_2 and KBiS_2 form crystals similar to rock-salt, but NaCrS_2 and KFeS_2 do not, because atoms of very different sizes cannot replace each other at random (see Table IV).

TABLE IV

Li^+	Ti^{3+}	Na^+	Bi^{3+}	K^+	Cr^{3+}	Fe^{3+}
0.78	0.64	0.98	1.15	1.33	0.64	0.67

In some structures Cl and H_2O , which occupy approximately the same space, can also replace each other at random.

Provided that two substances have interatomic bonds of the same kind, it is largely a question of geometry as to whether they can form a solid solution (*mixed crystals*) or not. NaCl and KCl

can; or KCl and KBr; so can Li_2TiO_3 and MgO. These are all *isomorphous* compounds (similar structurally), but this is not essential. MgCl_2 can dissolve in LiCl, although every Mg^{2+} ion that enters the LiCl lattice displaces two Li^+ ions and leaves one vacant cation position.

An even more important example of a random structure is a disordered alloy. If AuCu_3 is quenched from a high temperature there is a random distribution of atoms on a face-centred cubic lattice. On slow cooling or annealing, the Au atoms segregate to the corners of the cubes and the three Cu atoms occupy the centres of the faces (fig. 123). A really disordered structure can

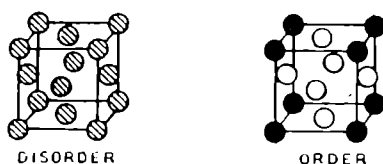


FIG. 123. Disordered and ordered AuCu_3 structure.

be regarded as an ordered lattice plus a gas, and besides its ordinary X-ray pattern it should give the background scattering typical of a gas, with considerable low-angle scattering. In fact, disordered alloys do *not* give such low-angle scattering, but there is a marked scattering corresponding to what may be called short-range order, the tendency of an atom of one kind to surround itself by those of another kind; and there is also strong evidence, as one might expect, that the disordered lattice is not regular, but is locally distorted in much the same way as mixed crystals of alkali halides (although in the latter case, as a rule, the disorder is only partial and is confined to either cations or anions).

DEFECT STRUCTURES IN RELATION TO CONDUCTIVITY

The occurrence of conductivity in purely ionic compounds has been explained by supposing that there are, in the structure, a certain number of vacant places due perhaps to too violent thermal vibration having detached an ion from its proper place and either left it in an interstitial position or removed it altogether via the intercrystalline cracks in the mosaic structure. The number of such accidental holes is small, however, even near to the melting-point. The number of holes is very much increased, with a

corresponding increase in ionic conductivity, in those crystalline structures known as *defect structures*, where there are not enough atoms to fill all the equivalent positions in the lattice, and high symmetry is only attained by a statistical occupation of a number of equivalent crystallographic positions by a smaller number of atoms. This occurs, for instance, in the solid solution of MgCl_2 in LiCl , referred to above. It also happens in the high temperature form of Ag_2HgI_4 . The low temperature tetragonal form (fig. 124) becomes cubic at about 50°C ., turning from yellow to red. The four I atoms occupy a face-centred lattice; so do the metal atoms, but in this case there are only three atoms ($2\text{Ag} + \text{Hg}$) to fill four equivalent positions. One in every four cation positions

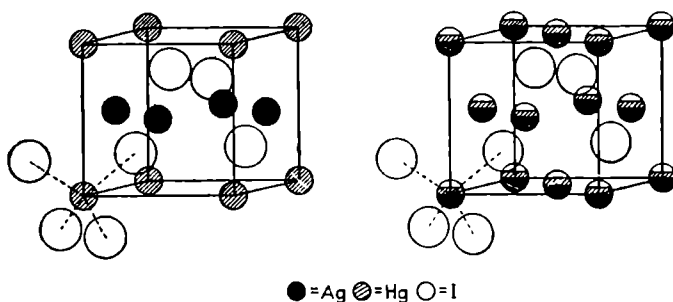


FIG. 124. Ag_2HgI_4 ; ordered β and disordered, defect α structures.

(Clark, *Applied X-rays*: McGraw-Hill.)

is vacant, but the arrangement of vacant places is random. The high temperature form of AgI is an even more extraordinary example. γAgI has a diamond-like structure; βAgI a wurtzite-like structure; these are both quite normal; but αAgI , stable between 145.6°C . and the melting-point, 552°C ., is body-centred cubic, with two molecules in the unit cell. The two I atoms occupy the centre and corners of the unit cell (8 corners = 1 atom, because each one is divided among 8 unit cells). There are no two equivalent positions left for the Ag atoms, and these, in fact, form a statistical arrangement which is so fluid that it can almost be called an interstitial liquid in the more rigid lattice of large iodines. The following table shows what an enormous change of ionic conductivity this involves. The drop of conductivity on melting shows, moreover, that the silver atoms (Pauling states that the $\text{Ag} - \text{I}$ bonds have only 11 per cent. ionic character) move *more easily* in the crystalline

framework of iodines than they can when the lattice breaks down by melting.

TABLE V

Temp. .	142·4	145·6	146·5	150	300	547	552	554	650° C.
Elect. cond. .	0·00033	↔	1·31	1·33	1·97	2·64	melts	2·36	2·47

These are cases of compounds of definite composition behaving in an unusual way. But there are other, more gruesome skeletons hidden in the cupboard of the classical chemist. Why, in spite of the *law of definite proportions*, does FeS always show, on analysis, a deficit of Fe, being stable over a range of 50 to 55·5 atomic per cent. of S? Why is FeO also always deficient in Fe, although electrically neutral? Actually the point is that in these structures there are always some vacant cation places and some ferric ions to maintain electrical neutrality. It has been suggested that it is the existence of these vacant places that enables easy oxidation to take place. Fe atoms tend to jump from one vacant place to another, and thus to migrate from the interior to the surface of the lattice, where there is a layer of O atoms with which to combine. In the process the structure changes from an Fe-deficient FeO, through Fe_3O_4 , to Fe_2O_3 . The structural chemistry of groups such as oxides, sulphides, halides and hydrates really could not be studied at all by the classical methods of chemistry.

The development of X-ray analysis to give electron density contour maps has led to the realisation that many compounds are not completely ionic, nor are they wholly covalent. They have to be described as having a *percentage ionic character*. This has already been mentioned in Chapter V in reference to the structures of the silicates, where the Si—O bond has 50 per cent. ionic character. The different silicate types provide admirable examples of the fact that structure is decided by atomic or ionic radii, plus numerical ratio of cation to anion, plus anion electronegativity. As the ratio of silicon to oxygen increases from 1:4 in SiO_4 (as in topaz, $(\text{AlF})_2 \cdot \text{SiO}_4$) to 1:2 in SiO_2 (quartz, cristobalite, tridymite), so the structure type changes from closed groups, through chains, bands and sheets, to three-dimensional net-works of Si—O groupings. Figs. 125 and 126 show some of

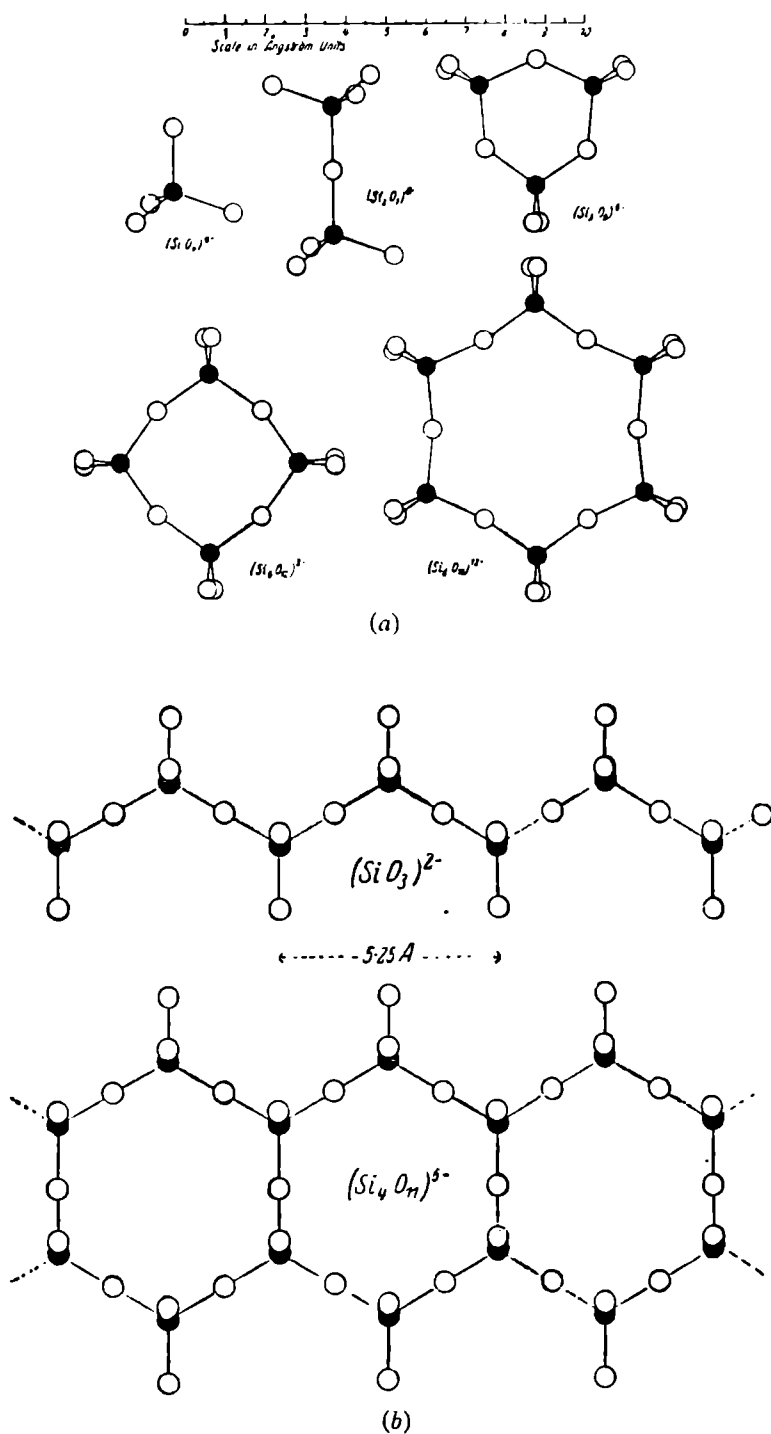


FIG. 125. Types of silicon-oxygen grouping in the silicates.
 (a) Closed groups; (b) Chains and bands.

(W. L. Bragg, *Zeit. f. Krist.*, 74, 237, 1930.)

these groupings. It is no wonder that W. L. Bragg's work on the silicates has been described as having 'transformed a chemical riddle into a system of simple and elegant architecture.'

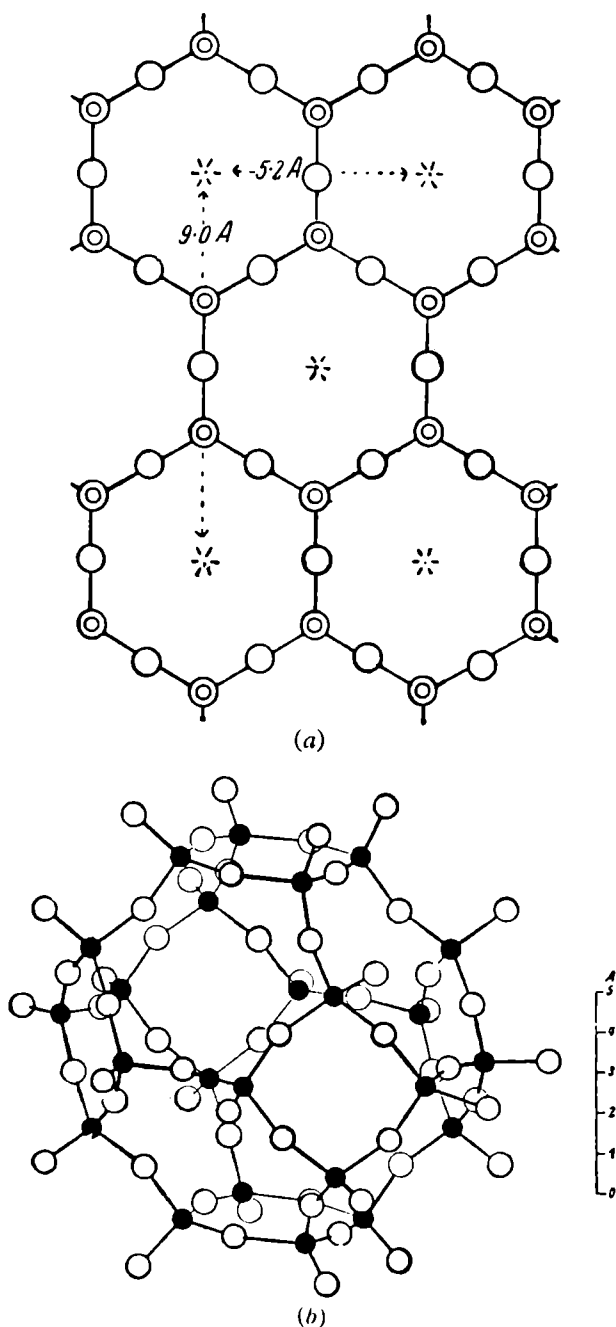


FIG. 126. Types of silicon-oxygen grouping in the silicates. (a) Sheet (mica); (b) Three-dimensional net (ultramarine).

(W. L. Bragg, *Zeit. f. Krist.*, 74, 237, 1930.)

Covalent compounds can also form structures in which there are finite molecules linked together by van der Waals or other weak forces, or in which there are groupings of atoms infinite in one, two or three directions. Diamond is an example of a three-dimensional homopolar grouping (Fig. 127). The whole

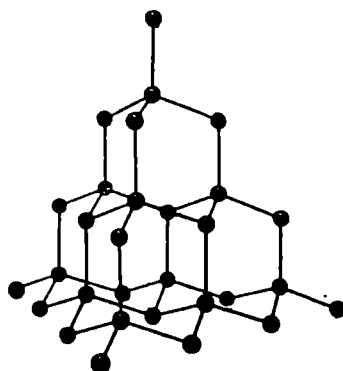


FIG. 127. Diamond structure; a trigonal axis of cube is vertical.

crystal is really one molecule and any breakdown of the structure involves the rupture of strong interatomic bonds. Rhombic sulphur, or hexamethylene tetramine, on the other hand, forms structures with finite molecules (fig. 128, p. 174) in which the first bonds to break would be the weak intermolecular bonds. It is considerations such as these that explain the abrupt change in melting-point in the fluorides as the valency of the cation increases from three to four (Table VI).

TABLE VI

	NaF	MgF ₂	AlF ₃	SiF ₄	PF ₅	SF ₆
M.P.	980°	1400°	1040°	-77°	83°	-55° C.

This is sometimes used as a classical example of an abrupt change from ionic to covalent atomic binding. In fact, there is no such change; the percentage ionic character of the Si-F bond differs very little from that of Al-F. But the atomic grouping in AlF₃ is infinite in three dimensions while that in SiF₄ consists of finite groups. Melting in the first three compounds means the breaking of interatomic bonds; in the last

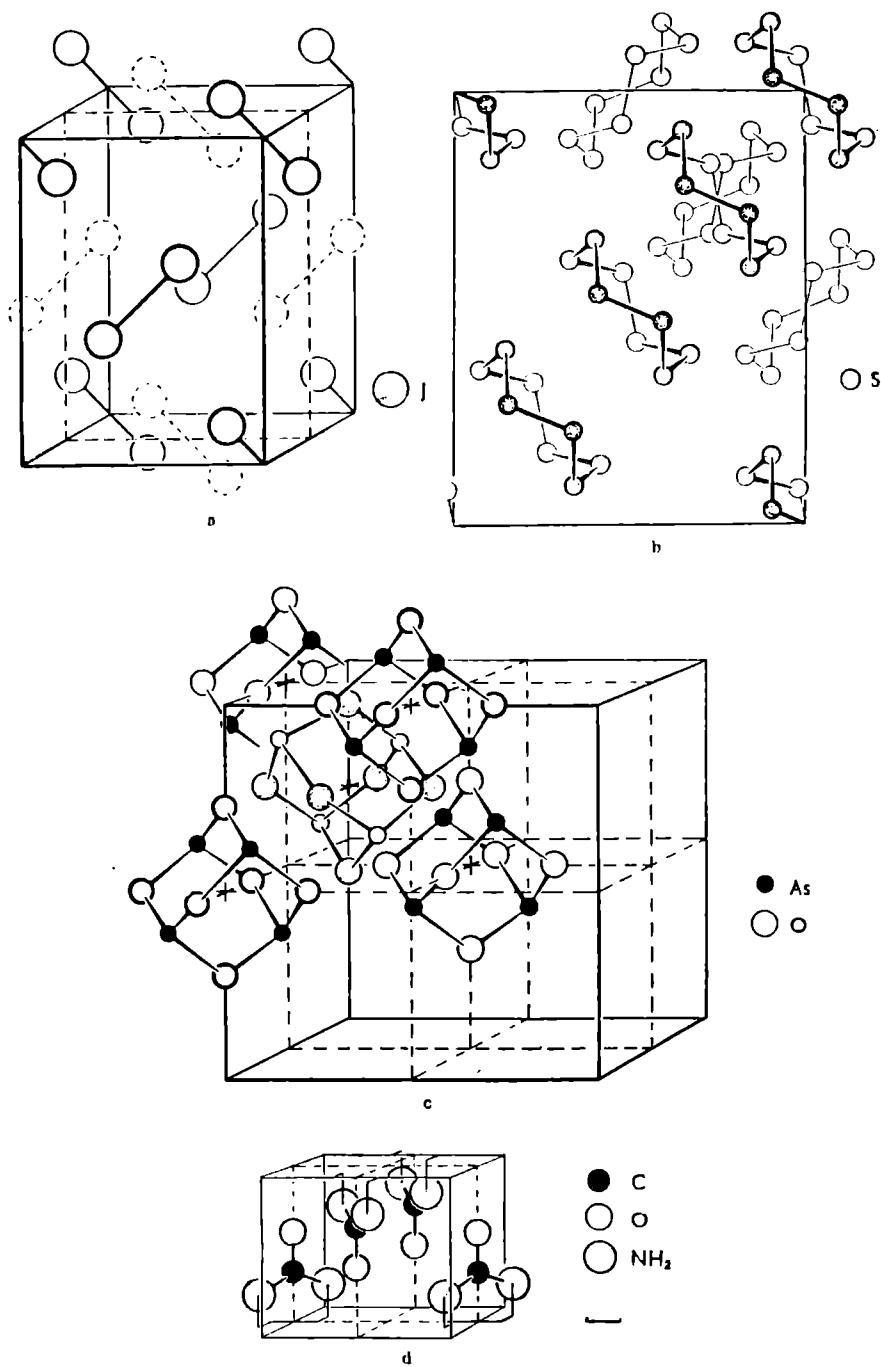


FIG. 128. Structures with finite molecules
 a, I_2 ; b, S_8 ; c, As_4O_6 ; d, $CO(NH_2)_2$.

(Bijvoët, Kolkmeijer & MacGillavry, *Röntgenanalyse von Kristallen*: Springer.)

three it means only the breaking of intermolecular bonds. This is diagrammatically shown in fig. 129.

A typical example of a structure composed of layer molecules,

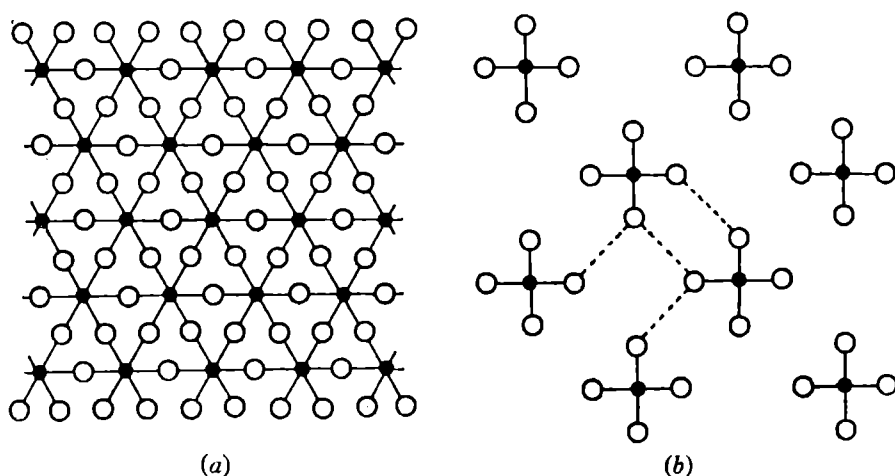


FIG. 129. Diagrammatic representation of an infinite AX_3 structure (2 : 6 coordination) and a structure of finite BX_4 molecules (1 : 4). In (a) all bonds are alike. In (b) there are B-X bonds and much weaker X-X bonds. The latter will break first on melting, even if A-X and B-X are equally strong.

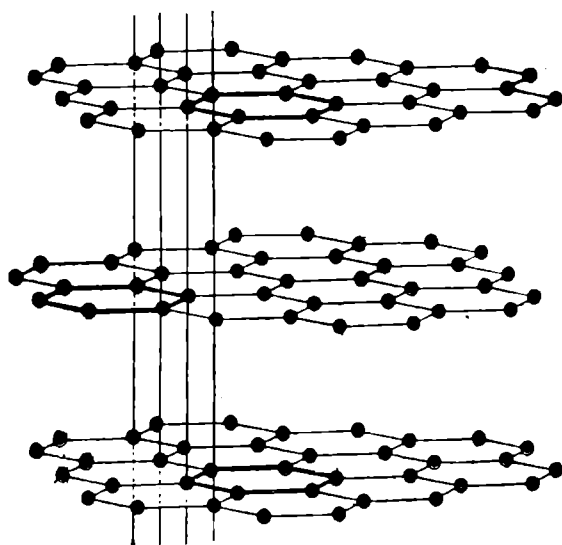


FIG. 130. Graphite I structure; alternative networks are duplicate, so that the *repeat* distance is twice the *layer* distance.

infinite in two directions, is graphite (fig. 130), the other crystalline form of carbon. In diamond the carbon valency bonds are tetrahedrally arranged and are about 1.544 A.U. in length. In graphite

the bonds *in* the layer molecules are trigonally arranged and are only 1.421 A.U. in length, and there is a weak force of the van der Waals type between the planes, which are 3.42 A.U. apart. The structure of graphite illustrates the importance of regarding the van der Waals force as a kind of chemical bond, because it is the existence of this kind of bond that permits the formation of the compounds C_8K , $C_{16}K$ (fig. 131) and others of a similar kind, where the metal atoms fit between the graphite layers,

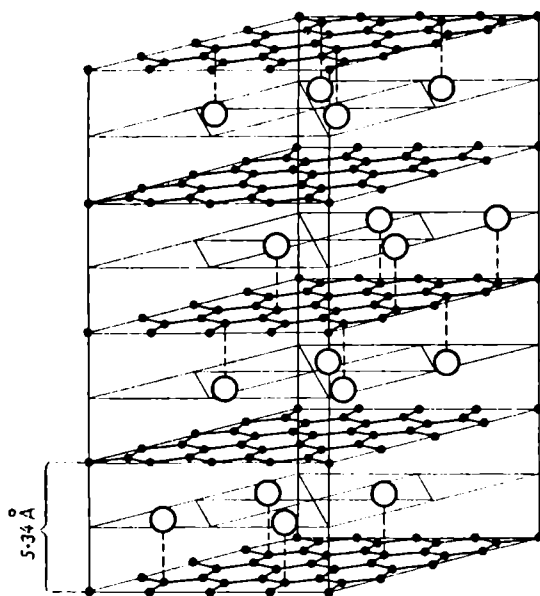
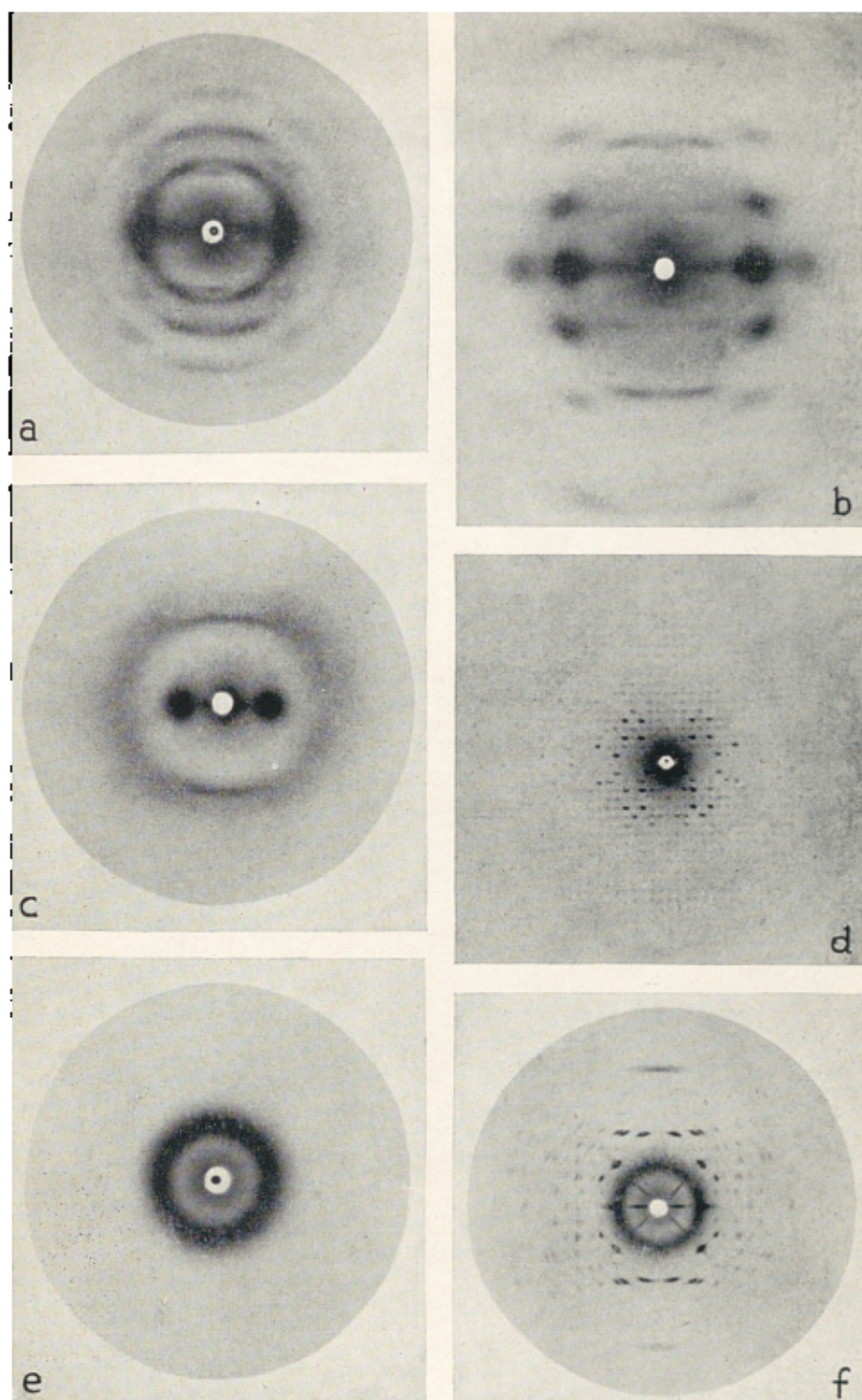


FIG. 131. Structure of C_8K , showing K atoms between graphite layers, which are forced apart to distance 5.34 A.U.

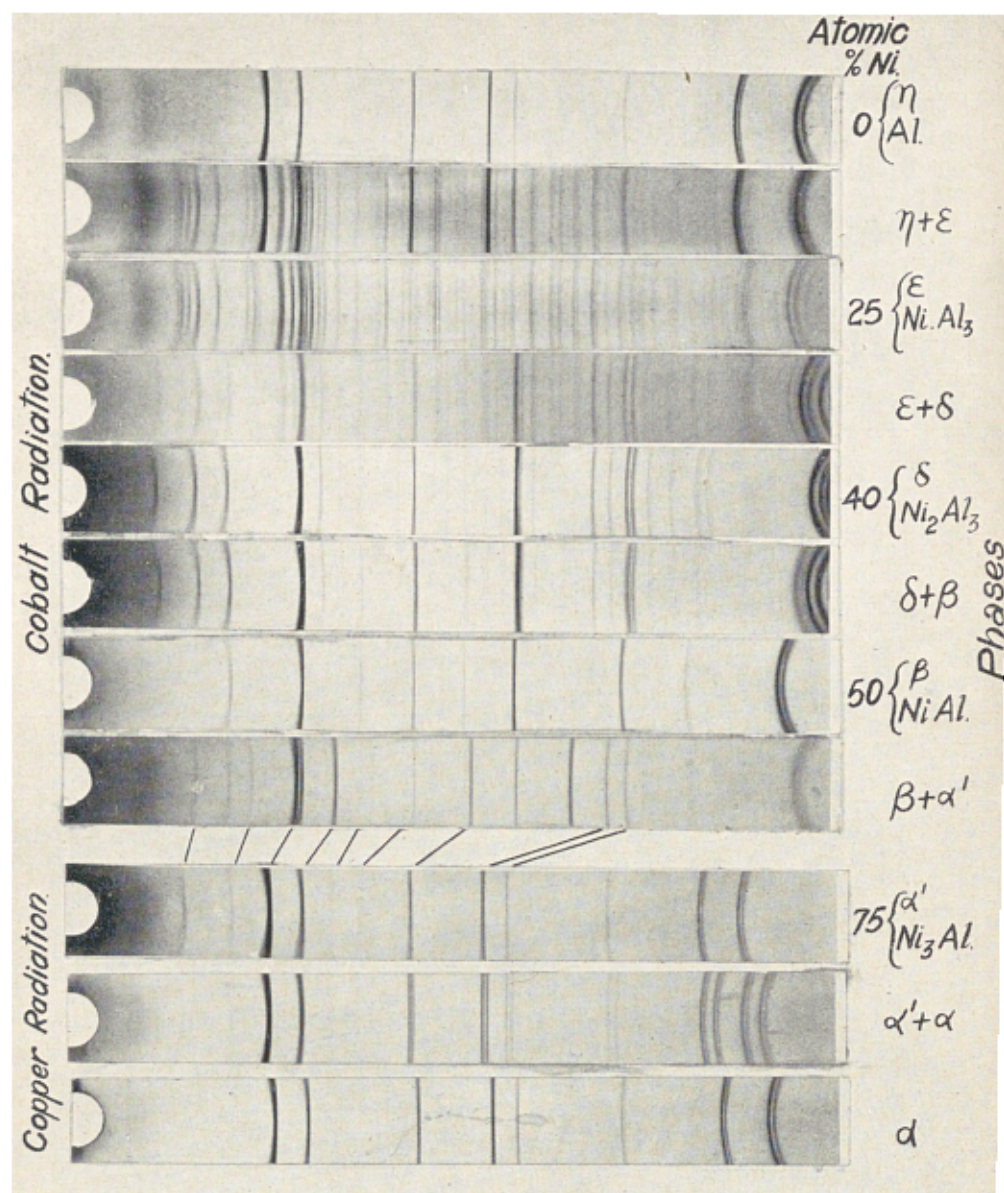
(Bijvoet, Kolkmeijer & MacGillavry, *Röntgenanalyse von Krystallen*: Springer.)

forcing them apart. The intruding groups can also be O, F, S, the sulphate group and so on. Charcoal, which is really graphitic in character, although without sufficient periodicity to be called properly crystalline, adsorbs gases and vapours to such a remarkable degree that it can catalyse reactions by bringing reacting gases together. At liquid air temperatures this property of gas adsorption, especially by coconut charcoal, is greatly increased. X-ray investigation explains both these effects quite simply. Charcoal gives a very much broadened powder ring, showing that it is composed of crystallites of a colloidal size. These crystallites have more surface, relative to their volume, than a large single crystal of graphite, and therefore provide more opportunity



- (a) Fibre photograph of ramie (artificial silk) (Asbury).
 (b) Fibre photograph of the fibroin of natural silk (Asbury).
 (c) Fibre photograph of unstretched wool (α keratin) (Asbury).
 (d) Oscillation photograph of β -lactoglobulin (Riley).
 (e) Fibre photograph showing amorphous condition of unstretched polyisobutylene (Asbury).
 (f) Fibre photograph showing crystalline condition of fully stretched polyisobutylene (Asbury).

XIII



Powder photographs of series of Ni-Al alloys.
(Bradley, Bragg & Sykes, *Journal of the Iron and Steel Industry*.)

for gas atoms to enter between the layers. At room temperatures, however, the layers are thermally vibrating rather vigorously and the entry of gas molecules is not so easy as at liquid air

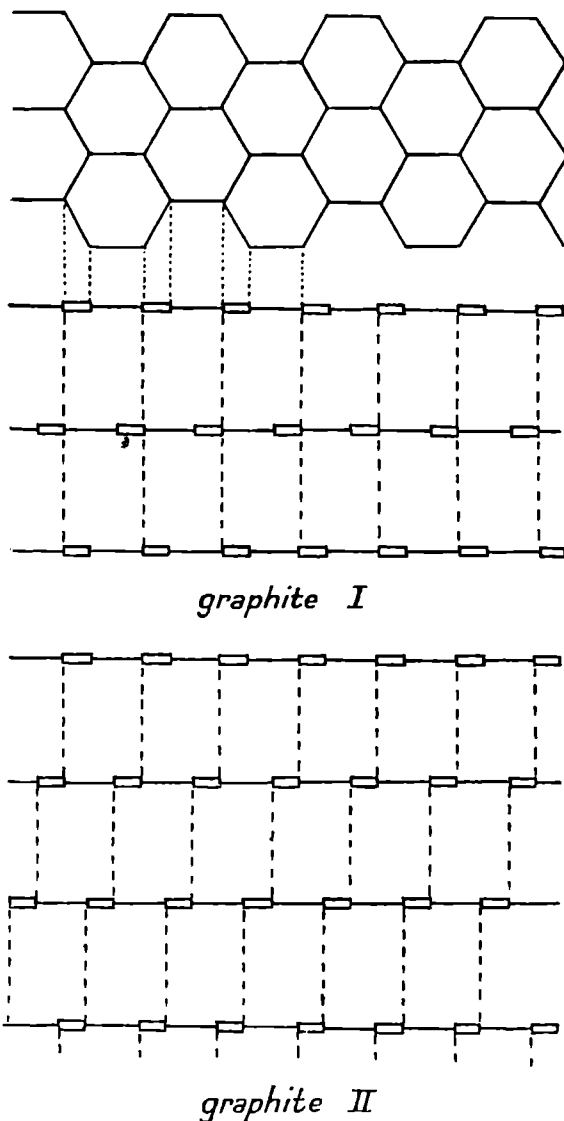


FIG. 132. The layers of graphite II are similar in structure to those of graphite I, but the arrangement of successive layers is different, repeating only after *three* layers.

temperatures, where they are practically quiescent. This adsorptive power of activated charcoal is extremely important, because it means that double-walled metal containers can be used, instead of silvered glass, to preserve liquid air, helium, hydrogen,

etc. Metal always contains a certain amount of gas, which is given off in a low vacuum, but charcoal can be used to remove this occluded gas and to maintain a good vacuum between the walls of the double vessel.

The graphite layer molecules can be arranged together in different ways. Fig. 130 showed only one of these ways; fig. 132, p. 177, shows another, which seems to occur to the extent of about 14 per cent. in most samples of graphite, natural or artificial. But even these

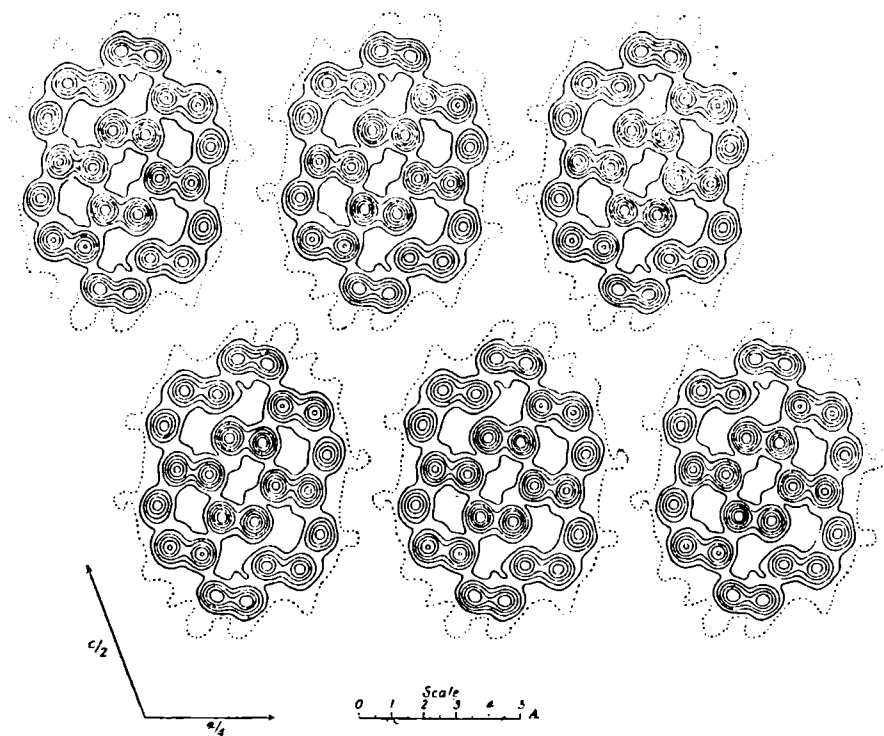




FIG. 133. Fourier projection of molecules of coronene.




(Robertson & White, *Journ. Chem. Soc.*, 607, 1945.)

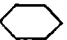

two account only for some 94 per cent. together, and 6 per cent. of each graphite sample consists of some other structure or structures composed of the same layer molecules put together differently.

In Chapter V the analysis of the structure of $C_6(CH_3)_6$ was described. In this, as in many other benzene derivatives which have been investigated by X-ray crystallographic methods, the carbon-to-carbon bonds are similar to those in graphite, or a little shorter. In coronene, for example (fig. 133), the bonds vary in length from 1.43 to 1.385 (± 0.01) A.U., and the whole molecule is plane, like a little sheet of graphite.

X-RAY EVIDENCE FOR RESONANCE OR MESOMERISM

Such aromatic derivatives provide ample evidence for the phenomenon known as resonance, or mesomerism, where the chemical formula of a compound can be written down in a variety of ways, but the actual structure can be regarded as partaking of all these *canonical structures*. Its actual energy will, in fact, be less than that of any of them, and it will therefore be more stable than any one would be alone. The *bond order* in a resonance molecule where the bonds are all alike is given, to a close approximation, by the number of valency electrons taking part divided by the number of actual bonds. In graphite this will be $4/3$, in benzene derivatives having a single nucleus it will be $3/2$, one valency electron of each carbon atom forming a single covalent bond with the substituents. Another way of expressing this is to say that the graphite bonds are $\frac{2}{3}$ single + $\frac{1}{3}$ double ($\frac{2}{3} \cdot 1 + \frac{1}{3} \cdot 2 = \frac{4}{3}$), whereas those in benzene, C_6H_6 , are $\frac{1}{2}$ single + $\frac{1}{2}$ double ($\frac{1}{2} \cdot 1 + \frac{1}{2} \cdot 2 = \frac{3}{2}$), being formed by resonance between the two possible Kekulé structures  and .

Actually, however, the three Dewar structures, , , , also contribute to a small extent. Now, the length of the bond depends on the bond order (fig. 96, p. 126), and X-rays can be used to give measurements of bond lengths, accurate to about 1 or 2 per cent., by means of careful Fourier analyses based on large numbers of intensity measurements. Valency angles can be determined with about the same degree of accuracy. Fig. 134, p. 180, illustrates the kind of measurements that have been made on geranylamine hydrochloride; and fig. 135, p. 181, shows the electron density contours for bonds of various orders, as measured by J. M. Robertson on sorbic acid, $H_3C - C = C - C = C - COOH$, and

tolane,  - C \equiv C - .

Resonance can occur not merely between possible covalent structures, but also between covalent and ionic configurations. This is illustrated by the alternative structures possible for the carbonate group $[CO_3]^{2-}$ which X-rays has shown, in calcite for example, to possess plane trigonal symmetry; or for the water

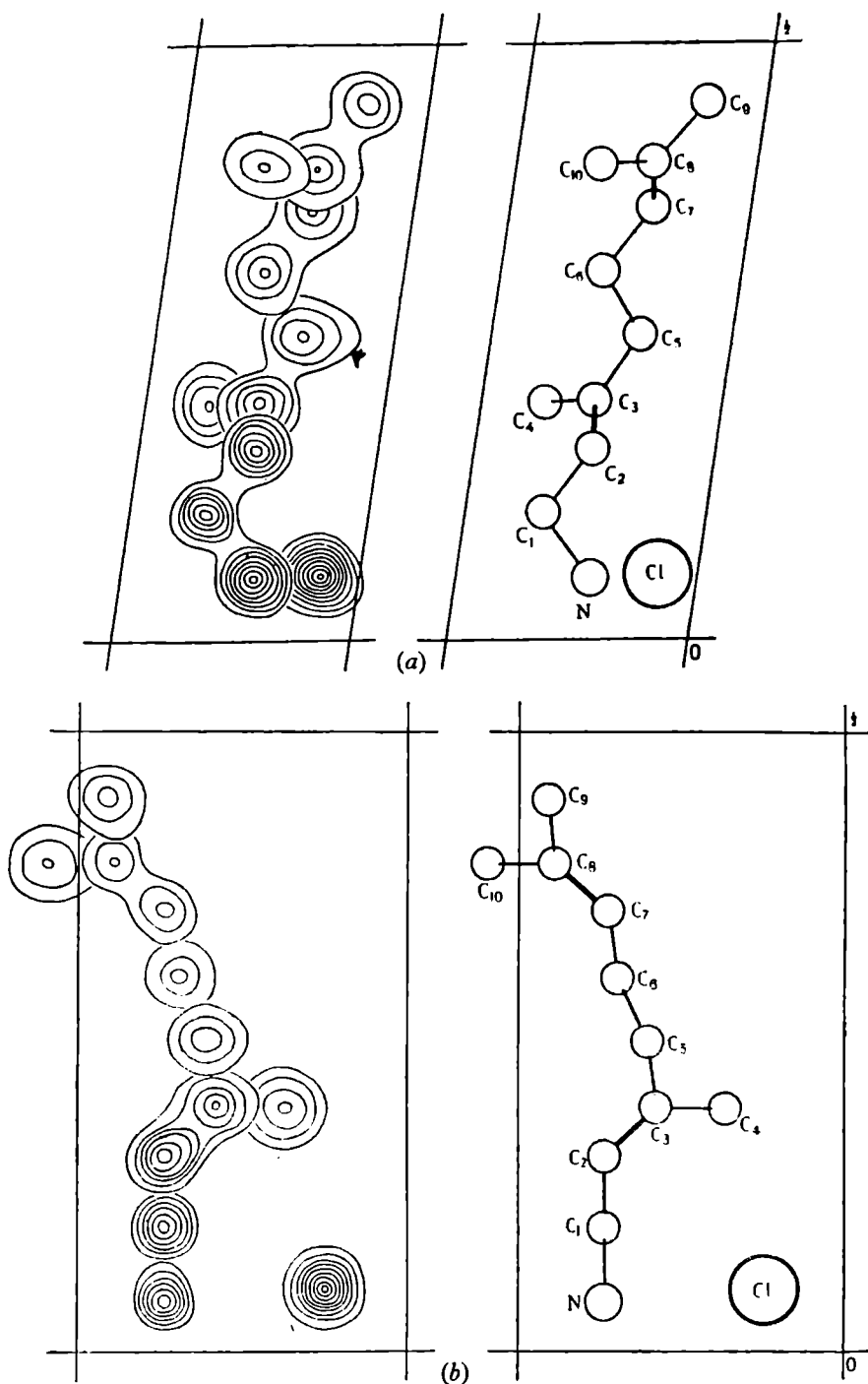
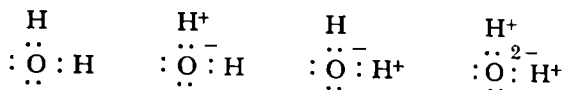


FIG 134. Projection of geranylamine hydrochloride molecule on (a) (010), (b) (001).

N-Cl	1.49 kX	C ₃ -C ₄	1.44 kX	± 0.04 kX
C ₁ -C ₂	1.54	C ₄ -C ₅	1.51	
C ₂ -C ₃	1.31	C ₅ -C ₆	1.31	$\pm 4^\circ$
C ₃ -C ₄	1.53	C ₆ -C ₇	1.53	
C ₄ -C ₅	1.51	C ₇ -C ₈	1.54	
N ₁ -C ₁ -C ₂	109°	C ₂ -C ₃ -C ₄	115°	
C ₁ -C ₂ -C ₃	126°	C ₃ -C ₄ -C ₅	112°	
C ₂ -C ₃ -C ₄	124°	C ₄ -C ₅ -C ₆	129°	
C ₃ -C ₄ -C ₅	121°	C ₅ -C ₆ -C ₇	124°	
C ₄ -C ₅ -C ₆	115°	C ₆ -C ₇ -C ₈	121°	
		C ₇ -C ₈ -C ₉	115°	

(Jeffrey, *Proc. Roy. Soc., A.* 183, 388, 1945.)

molecule, which can be described as resonating between the four possible structures



the first of which is completely covalent and the last completely ionic.

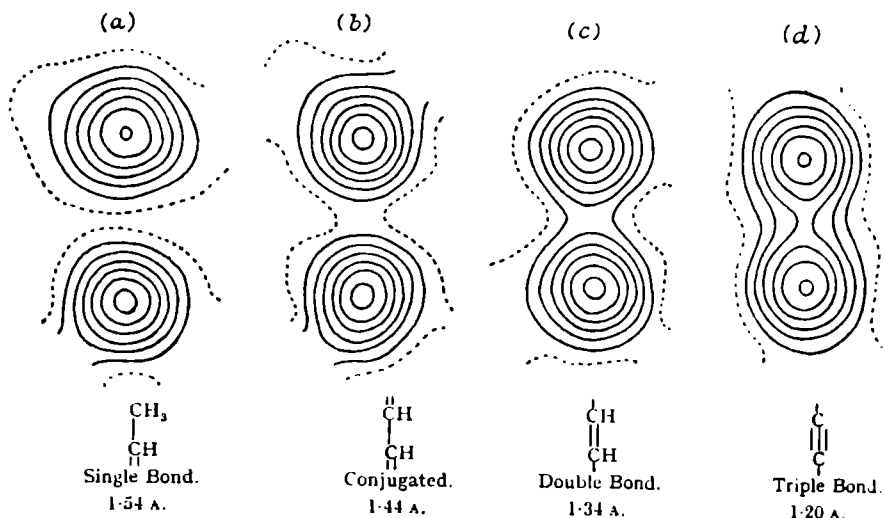
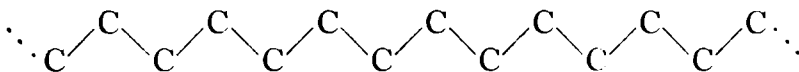


FIG. 135. Electron density contours for bonds of different orders between carbon atoms.

(Robertson, *Journ. Chem Soc.*, 249, 1945.)

ELECTRON CLOUD DISTORTION IN MOLECULE FORMATION

In purely aliphatic compounds, such as the paraffins and fatty acids, the carbon-carbon bond lengths are similar to those in diamond, and the valency angles are approximately tetrahedral. An examination of the very long aliphatic chains that occur in polythene:



chains more than 1000 atoms long, has shown the existence of two effects: firstly, that the atoms are vibrating normal but not parallel to the length of the chain; secondly, that the electron clouds are actually extended in a direction normal to the chain. The first conclusion agrees well with the results of X-ray investigation of thermal scattering in long-chain or fibre structures. These long chains are flexible but not compressible.

HYDROGEN BONDS

X-ray methods have provided numerous examples of structures in which molecules, instead of being linked together by van der Waals forces, are joined by shorter and somewhat stronger *hydrogen* bonds. When a hydrogen atom links *two* other atoms together it has only *one* electron available for a covalent bond and therefore the bond is largely ionic in character. It is formed only between the more electronegative atoms such as O and O, or N and O, or N and F. Although stronger than the van der Waals force, it is still relatively weak and can easily be altered or ruptured. Hydrogen bonds form inter- and intra-molecular bridges in proteins; in fact, many problems of the structure and changes in structure of proteins and other biologically important substances involve the existence, formation, rupture or polarisation of such bonds. Hydrogen bonds occur in organic and inorganic acids, in alkalis, neutral hydroxides and hydrates; notably, of course, in both liquid and solid water. In compounds such as resorcinol, $C_6H_4(OH)_2$, such bonds link all the molecules together into a three-dimensional network (fig. 136). The effect of replacing H by D (deuterium) in such compounds has been studied by means of X-rays, and so have the coefficients of expansion. The anomalous dielectric properties of certain crystals, for example Rochelle salt (fig. 122), between certain temperature limits, are thought to be due to particular structural conditions which allow an easy transfer of the H atom from one oxygen atom to another; and it is certain that it is the H bond that accounts for the abnormally high dielectric constant of ice and of water, and for their high melting- and boiling-points compared with, say, H_2S or H_2Se .

ADDITIVE MOLECULAR COMPOUNDS

Both water of crystallisation (see fig. 97, p. 127), and adsorbed water can be studied by X-ray methods. The layer spacing of clay structures can be increased from 10 A.U. to 20 A.U. by adsorption of H_2O layers held in position by residual forces. Many proteins also contain considerable amounts of water. These are special cases of structures which consist of molecules of different kinds which fit together conveniently and therefore crystallise together, the forces between the molecules being van der Waals forces, hydrogen bonds, weak forces of an electrostatic kind due to

polarisation and so on. For instance, methyl iodide and rhombic sulphur crystallise together in the proportion $\text{CH}_3\text{I} \cdot 3\text{S}_8$. Picryl iodide ($2 \cdot 4 \cdot 6$ trinitroiodobenzene), which is normally tetragonal,

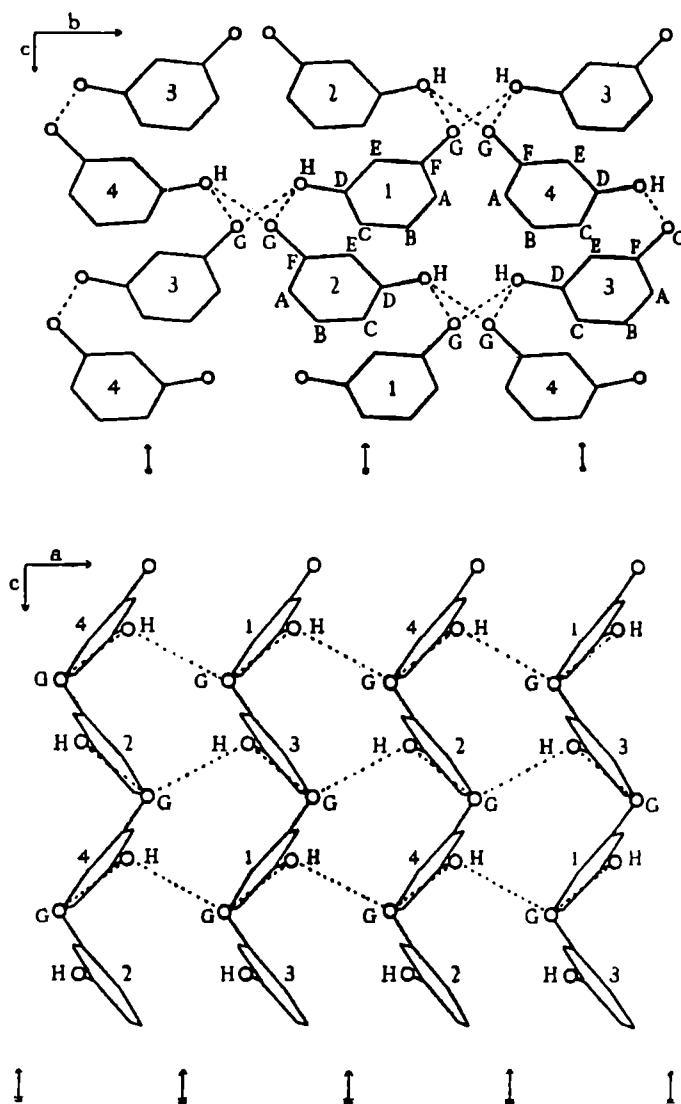


FIG. 136. Structure of β -resorcinol, showing hydrogen bonds.

(Robertson & Ubbelohde, *Proc. Roy. Soc., A*, 167, 122, 1938.)

and hexamethylbenzene, which is normally triclinic, crystallise together in a pseudo-hexagonal (and partly disordered) orthorhombic layer lattice. Studies of insect cuticles made by Fraenkel and Rudall have shown that these apparently consist of alternating monolayers of protein and polysaccharide.

STUDIES OF FIBROUS STRUCTURES

Polysaccharides, polymerised cellulose chains, such as occur in cotton, hemp and artificial silk, give good and very characteristic X-ray photographs (Pl. XII *a*). A *fibre photograph*, taken with the X-ray beam perpendicular to the length of the stationary fibre, is just like a rotation photograph of a single crystal taken with the X-rays perpendicular to a principal axis. This is because the fibre itself consists of small crystallites, or micelles, having one axis in common (or nearly in common) but otherwise of random orientation. The spots on fibre photographs are not usually very sharp, partly because the orientation even with respect to the fibre axis is not perfect, partly because the chains undergo considerable thermal vibration laterally, and partly because the micelles, or chain-bundles, are of small lateral dimensions.

The protein fibres (fibroin) of real silk also give good X-ray photographs (Pl. XII *b*), the repeat distance along the fibre length, 7 A.U., corresponding to a single unit of a fully-extended polypeptide chain. That is presumably why silk is not particularly elastic. Any stretching of silk must correspond, not to the unfolding of a chain, but to a slipping of chain-bundles which is not reversible. Wool, hair, horn, spine are all proteins of the keratin group. The X-ray photographs they give are not nearly so good as those of silk (Pl. XII *c*), but they are very characteristic, and they change in a characteristic way when the wool or hair is stretched, the change being consistent with an unfolding of an originally folded chain. Astbury has pointed out the close similarity between the X-ray patterns given by wool, horn and hair on the one hand and of the myosin of muscle on the other. This proves very strikingly that in spite of their very different chemical constitution there is something intrinsically similar about them, and that something is their *structural architecture*.

GLOBULAR PROTEINS
AND OTHER BIOLOGICALLY IMPORTANT STRUCTURES

In the same way studies of insulin and of haemoglobin have shown that there are definite similarities between the *intra-molecular structures* of these very different proteins. Unlike the fibrous proteins such as silk, wool and muscle, haemoglobin, insulin and some of the viruses are visibly crystalline and give

amorphous solid; stretched, they give typical crystal patterns, showing that the long chains have been pulled out sufficiently straight to possess marked periodicity (Pl. XII *e, f*). On the basis of X-ray data it is believed that rubber is the *cis*-form and gutta-percha the *trans*-form of polymerised isoprene; that the *trans*-form is hindered from folding up and is therefore not elastic.

Two of the most difficult, and certainly the most striking, of X-ray determinations of crystal structure have been those of cholesteryl iodide, by Carlisle and Crowfoot, and of the potassium, rubidium and sodium penicillin salts, by Crowfoot and Rogers-Low, and by Bunn and Turner-Jones respectively. In each case X-ray and chemical investigations were mutually dependent on each other for information, but the final details of the spatial arrangement of the atoms were given by a three-dimensional Fourier synthesis.

METAL AND ALLOY STRUCTURES

The peculiar and characteristic properties of metallic structures are toughness, ductility, high optical reflecting power and thermal and electrical conductivity. The simple view generally accepted is that a metal, or an alloy, consists of positive ions embedded in a cloud or atmosphere of electrons and held together by the attractive forces between the ions and electrons. Such structures are tough, yet ductile, because the ions, though firmly held together, can easily rearrange themselves; while the free electrons give the high conductivity.

Most of the metallic elements crystallise either in the face-centred or the body-centred cubic, or in the close-packed hexagonal classes. Several have more than one modification. The interatomic distances in crystals of the metallic elements are often a good deal larger, sometimes twice as large as the ionic diameters of the same elements in the univalent condition, so that it is clear that even though the metal atoms have lost electrons and have become ionised, yet the ions are being held apart by the electronic atmosphere. In crystals such as those of Cu, Ag and Au, where the ionic and the atomic radii are more nearly equal, the electron clouds may overlap and the crystals are comparatively incompressible.

The ferromagnetism of Fe, Co and Ni is not a characteristic

property of the crystal structure as such; it depends on the critical size of an incompletely filled electron shell relative to the distance between adjacent atoms. Manganese is not itself ferromagnetic, because although it has an incompletely filled electron shell its atoms are too close together; but it gives a ferromagnetic nitride, because the small N atoms push the Mn atoms apart until they are at the right distance apart for ferromagnetism. Similar considerations explain the ferromagnetic properties of certain alloys.

Some alloys are chemical compounds of definite composition, while others are solid solutions of varying complexity. Continuous series of alloys, or individual specimens, can be studied by means of X-ray powder photography. Pl. XIII shows a series of photographs of the binary alloy system NiAl, beginning with pure Ni at the bottom and going to pure Al at the top. Far more photographs than this would be needed to study the system thoroughly over a wide range of temperature, but these are typical. It is of great importance in this kind of work that lattice parameters should be determined with the utmost precision, especially near to the boundaries of the different phases, where the structure changes its type. By differentiation of the Bragg

relation $d = \frac{\lambda}{2 \sin \theta}$, with respect to θ , we obtain the way in

which the angle of diffraction varies with variation in spacing:

$$dd = -\frac{\lambda \cos \theta}{2 \sin^2 \theta} \cdot d\theta, \text{ or } \frac{dd}{d} = -\cot \theta \cdot d\theta. \text{ A small relative change}$$

in spacing therefore produces the biggest angle variation when $\cot \theta$ is small, that is, when θ approaches 90° . Accurate lattice measurements can only be made from reflections at Bragg angles near to 90° , for which 2θ approaches 180° . It is necessary in precision work of this kind to choose and, if necessary, to change the incident X-radiation as the spacings change, so that back reflections are obtained. It is also necessary to make corrections which will be referred to later.

Let us consider Pl. XIII in some detail. Pure Ni (bottom) has a face-centred cubic structure. The doubling of the reflection lines on the right-hand side of the pattern is due to the effect of the separate α_1 and α_2 components of the CuK radiation used. The effect of adding up to 25 per cent. Al is to cause a doubling of *all* the lines, none of which are quite coincident in position with

those of the original. What this means is that there are now *two* face-centred cubic structures each of slightly different lattice spacings from each other and from the original Ni structure. One (α) is a solid solution of a little Al in Ni, a disordered structure of the face-centred cubic type but with spacings a little larger than those of pure Ni; the other (α') is an ordered Ni_3Al structure, with Al at the corners of each unit cell, Ni at the centres of the faces. When the composition 75 per cent. Ni–25 per cent. Al is reached, this second phase alone remains. But now there is no high-order line with θ sufficiently near to 90° for precision measurements to be made, and it becomes necessary to change the radiation to that of Co. As the percentage of Al increases a new (β) phase appears, which corresponds to an ordered body-centred cubic NiAl structure. The powder photographs show the existence of the β and α' phases side by side as far as 50 per cent. Ni–50 per cent Al, where only the β phase is left. The next single (δ) phase, corresponding to 40 per cent. Ni, 60 per cent. Al (Ni_2Al_3), is rather more complex; it is a distorted body-centred cubic structure. The ϵ phase, NiAl_3 , is a complex orthorhombic structure; the larger number of lines shows the increasing complexity and lower symmetry. The pure 100 per cent. Al structure (which begins to appear when the 75 per cent. Al stage is passed) is again a face-centred cubic structure but with a lattice spacing larger than that of pure Ni. (In comparing the powder photographs it must be remembered that a change from Cu to Co radiation has been made, which approximately balances the change of spacing.)

By means of photographs of this kind *phase diagrams* can be constructed (fig. 138) which are often more detailed and accurate than the phase diagrams obtained by the ordinary methods of metallography. Rules have been formulated, as the result of large numbers of experimental investigations, which enable us to know what structures to expect from particular combinations of metals. For example, if the atomic diameters of two metals differ by more than 15 per cent., then the two are unlikely to form a solid solution; if one metal is relatively very electronegative compared with another, then there is a tendency to form a stable intermediate stage instead of a solid solution. Hume-Rothery found that particular X-ray patterns are associated with particular *ratios of free electrons to atoms*, irrespective of the actual formula of the intermetallic compound giving the pattern. This is shown in Table VII.

TABLE VII

Phase	β	γ	ϵ
$\frac{\text{Electrons}}{\text{Atoms}}$	$\frac{3}{2}$	$\frac{21}{13}$	$\frac{7}{4}$
Intermetallic compounds	CuZn AgCd CoZn ₃ Cu ₃ Al FeAl Cu ₅ Sn	Cu ₅ Zn ₈ Fe ₅ Zn ₂₁ Cu ₉ Al ₄ Cu ₃₁ Sn ₈	CuZn ₃ Ag ₅ Al ₃ Cu ₃ Sn

[It is supposed that the metals contribute the following numbers of electrons to the alloy : Co (o), Fe (o), Cu (1), Ag (1), Zn (2), Al (3), Sn (4).]

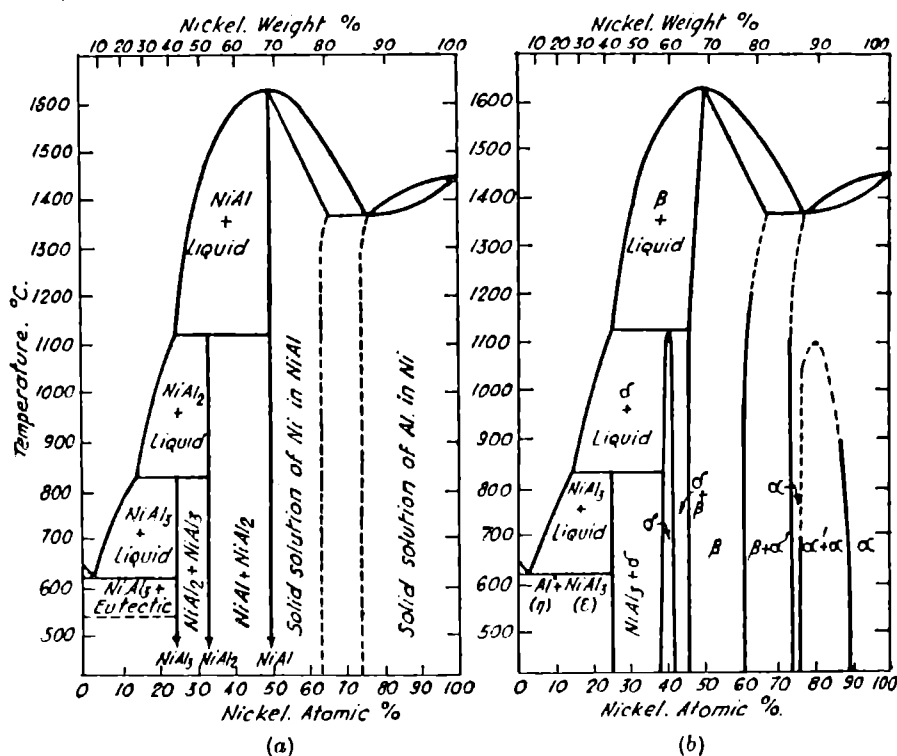


FIG. 138. Phase diagram for Ni-Al system.

(a) from ordinary metallurgical methods.

(b) from X-ray data.

(Bradley & Taylor, *Proc. Roy. Soc., A.* 159, 56, 1937.)

In particular we may notice the rather complex γ cubic structure found for brass of composition Cu₅Zn₈ and similar alloys in which there is a ratio of 21 free electrons to 13 atoms. This was one of the earliest alloy structures to be analysed, and it has since been found that the structural framework can accommodate different

atomic arrangements. In fact, there may be a statistical distribution of atoms in some γ alloys.

Precision cameras suitable for making the accurate measurements required for this work, measurements accurate to 1 in 50,000 or better, have been designed and are now commercially available. If the camera is properly made it should be free from eccentricity errors due to mis-centring of the specimen, but absorption, which causes a shift of the apparent maximum of the reflection lines, has always to be considered. Other possible errors, due to film shrinkage, length of specimen, refractive index of X-rays, distribution of intensity in the incident beam, can usually be eliminated or corrected for. An excellent paper by Taylor and Sinclair in the *Proceedings of the Physical Society*, London, March 1945, gives an account of the procedure for obtaining correct lattice parameters under various experimental conditions.

ANALYTICAL CHEMISTRY

On p. 18 reference has been made to the identification of chemical elements by means of their characteristic X-ray spectra, and on p. 78 the 'finger-print method' of identification by means of X-ray diffraction patterns has been mentioned. *Both* these have been extremely useful, both to science and industry, in their different spheres. The X-ray spectroscopic methods (emission and absorption) are able to identify the actual elements whatever their state or condition of combination or aggregation, and are constantly applied in nuclear physics and chemistry today, for the identification of fission products, isotopes and so on. The X-ray crystallographic methods, which identify the actual compounds, can only be used when the unknown substance is one whose pattern is already on the reference file and is available for comparison. The number of such substances is now several thousand and is rapidly increasing. The finger-print method can be applied to mixtures, to solid solutions and even to mixtures of solid solutions, as well as to pure compounds, and can be used, of course, to indicate particle size as well as actual identity. It is widely used in industry, since it can often eliminate the necessity for difficult and lengthy chemical analysis. This and other applications of X-ray crystallography have been described by H. P. Rooksby in *Reports on Progress in Physics*, 1944-1945, published by the Physical Society, and provide convincing evidence of the growing realisation by industry of the value of this comparatively new science.

TEXTBOOKS FOR REFERENCE

- Astbury, W. T., *Fundamentals of Fibre Structure*; Oxford University Press, 1933.
- Barrett, C. S., *Structure of Metals*; McGraw-Hill Book Co., New York, 1943.
- Bijvoet, J. M., Kolkmeijer, N. H., and MacGillavry, C. H., *Röntgen-analyse von Krystallen*; Springer, Berlin, 1940.
- Booth, A. D., *Fourier Analysis*; Cambridge University Press, 1948.
- Born, M., *Die Gittertheorie des festen Zustandes*; Springer, Berlin, 1926.
- Bragg, W. H., *An Introduction to Crystal Analysis*; G. Bell & Sons, Ltd., London, 1928.
- Bragg, W. L., *The Crystalline State*, Vol. I., G. Bell & Sons, Ltd., London, 1933; *Atomic Structure of Minerals*, Cornell University Press, 1937.
- Brasseur, H., *Les Rayons X et leurs Applications*; Desoer, Liège, 1945.
- Buerger, M. J., *X-ray Crystallography*; Wiley, New York, 1942.
- Bunn, C. W., *Chemical Crystallography*; Clarendon Press, 1945.
- Burgers, W. G., *Rekristallisation verformter Zustand und Erholung*; Akad.-Verlags, Becker und Erler, Leipzig, 1941.
- Clark, C. D. H., *The Fine Structure of Matter*; Chapman & Hall, London, 1937.
- Clark, G. L., *Applied X-rays*; McGraw-Hill Book Co., New York, 1940.
- Compton, A. H., and Allison, S. K., *X-rays in Theory and Experiment*; Macmillan & Co., London, 1935.
- Desch, C. H., *The Chemistry of Solids*; Cornell University Press, 1934.
- Evans, R. C., *Crystal Chemistry*; Cambridge University Press, 1946.
- Ewald, P. P., *Die Erforschung des Aufbaues der Materie mit Röntgenstrahlen (Handbuch der Physik, Vol. 23 (2))*; Springer, Berlin, 1933.
- Guinier, A., *Radiocristallographie*; Dunod, Paris, 1945.
- Hartshorne and Stuart, *Crystals and the Polarizing Microscope*; Arnold, London, 1934.
- Hevesy, G. v., *Chemical Analysis by X-rays and its Applications*; McGraw-Hill Book Co., New York, 1932.
- Hilton, H., *Mathematical Crystallography*; Clarendon Press, 1903.
- Hume-Rothery, W., *The Metallic State*; Clarendon Press, 1931.
- International Tables for the Determination of Crystal Structure*, 2 vols.; Borntraeger, Berlin, 1935.
- James, R. W., *The Crystalline State*, Vol. II; G. Bell & Sons, Ltd., London, 1948.
- Niggli, P., *Grundlagen der Stereochemie*; Verlag Birkhäuser, Basel, 1945.
- Pauling, L., *The Nature of the Chemical Bond*; Cornell University Press, 1945.
- Phillips, F. C., *An Introduction to Crystallography*; Longmans, Green & Co., London, 1946.

- Pirene, M. H., *The Diffraction of X-rays and Electrons by Free Molecules*; Cambridge University Press, 1946.
- Randall, J. T., *The Diffraction of X-rays and Electrons by Amorphous Solids, Liquids and Gases*; Chapman & Hall, London, 1934.
- Schall, W. E., *X-rays. Their origin, dosage and practical application*; John Wright & Sons, Bristol, 1944.
- Spiegel-Adolf, M., and Henny, G. C., *X-ray Diffraction Studies in Biology and Medicine*; Grune and Stratton, New York, 1947.
- Sproull, W. T., *X-rays in Practice*; McGraw-Hill Book Co., New York, 1946.
- Stillwell, C. W., *Crystal Chemistry*; McGraw-Hill Book Co., New York, 1938.
- Strukturbericht*, 7 vols.; Akademische Verlagsgesellschaft, Leipzig, 1913-1939.
- Taylor, A., *An Introduction to X-ray Metallography*; Chapman & Hall, London, 1945.
- Tutton, A. E. H., *Crystallography and Practical Crystal Measurement*, 2 vols.; Macmillan & Co., London, 1922.
- Wells, A. F., *Structural Inorganic Chemistry*; Oxford University Press, 1945.
- Wooster, W. A., *Crystal Physics*; Cambridge University Press, 1938.
- Wrinch, D., *Fourier Transforms and Structure Factors*; American Society for X-ray and Electron Diffraction, 1946.
- Wyckoff, R. W. G., *The Structure of Crystals*; Chemical Catalog Co., New York, 1931; Supplement, Reinhold Publ. Corporation, New York, 1935.
- Zachariasen, W. H., *Theory of X-ray Diffraction by Crystals*; Wiley, New York, 1945.

INDEX OF SUBJECTS

(Numbers in heavy type indicate the more important references)

- Absent spectra, 79, 80, **94-96**, 108-110, 113, 114
- Absolute intensity, 34, **101**, 102, 116-119, 138, 139
- Absorption coefficients, 26, **29**, 119, 143
 - edges, 15, **28**, 30, 31, 60, 107
 - factor, 101, 116-119, **140-142**
 - selective, **30**, 31
- Age-hardening, **82**, 146, 161
- Air scattering, **24**
- Alkali halides, 10, 14, 161, **166-168**
- Alloys, 3, 7, 78, 82, 87, 143, 146, 149, 160, 161, **186-190**
- Ambiguity of structure, 113
- Amorphous solids, 6, **21**, 107, 145-147
- Amplitude, structure, **108-111**, 129-133
- Anisotropy, 7, 56, **127**, **128**, 155-161
- Argon, 34, 38, 106, 107
- Asbestos, 21, **81**
- Asterism, **148**, 149
- Atomic absorption coefficient, 29
 - coordinates, **111-115**, 120, 122, 129, 132, 134
 - numbers, 17, 18, 24, 105, 106, 125
 - radii or sizes, 4, 15, 123, **166**, **167**, 170, 188
 - structure, 4, **17-19**
 - symmetry, **96-101**, 115
- Atomic scattering factor, 18, 19, **105-107**, 109-116, 119
- Avogadro's number, by X-rays, **33**
- Axes of coordinates, **52-56**, 76
- Axial angles, **53**, 56, 76, 96, 97
 - lengths, **53**, 56, 68, 83, 96, 97
 - ratio, 68, **76**, 78
- Back reflection photography, 10, 24, **148**, **149**, 187
- Benzene derivatives, 119-122, 126, 131, 132, 134-137, 178, **179**, 183
- Bernal chart, **92**, **93**
- Blood tests, 36
- Bohr atom, 17, 19, 107
- Bond distances, 19, 20, 120, **126**, 176, 178, **179-181**
 - order, **126**, **179**, 181
- Bragg angle, **14**, 15, 80, 116, 117, 144, 187
 - law, 8, **14**, **15**, 24, 31, 32, 74-79, 85, 88, 91
 - ionisation spectrometer, **15**, **16**, 51, 96
- Bragg-Lipson figure fields, 123, **124**
- Bravais lattice, **72**, **73**, 74, 80, 83
- Calcite, 74, 138, 139
- Calibration for intensity measurements, **34**, **35**, 102
- Canonical structures, 179
- Carbon to carbon bonds, 20, 120, **126**, **175-181**
- Carbon, forms of, 6, **100**, 145, 146, **175**, 176
- Catalysts, 143, 146, 176
- Centro-symmetry, **60**, 76, 100, 101, 112-114, 127, **130**, 131, 134
- Characteristic X-rays, 4, 9, 10, 15, 17, 23, **25-27**, 37
- Chemical reactions, 6
- Cholesteryl iodide, 186
- Classes, 32
 - symmetry, **60-63**, 65, 69, 76
- Cleavage, 7, 13, 81, 119, 138
- Cohesion, 5, 166
- Colloids, 85, **145-147**, 160
- Compton effect, **26**, **27**, 106
- Contamination of target, 26, **43**
- Continuous X-ray spectrum, 14, 17, **23-26**, 37
- Coordination number, 98, 99, **123-125**, 166
 - polyhedron, 123, 124
- Corpuscular theory, 4, 8, 13, 17
- Covalent compounds, **173-178**
 - bonds, 166, 173, 182
- Critical absorption wave-lengths, 15, **28**, 107
 - glancing angle, **32**
- Crystal base, **108**
 - drawing, **63**
 - projection, **62-68**
 - systems, 56, **58-62**, 69, 76-78
 - texture, 24, 50, 87, 116, **138-143**
- Crystallite size, 50, 85, 87, 138, 139, **143**, 146, 147, 176, 184

- Crystallography, early, 6, 7, 16
 Cubic structures, 10, 14, 74, **78**
 Cuprous oxide, 10, 145
- Defect structures, 161, **168-170**
 Demountable X-ray tubes, 37, 39, 43, 49
 Density, crystal, 8, 15, 97
 Diamagnetic susceptibility, 7, **128**
 Diamond, 6, 8, 10, 51, 100, 113, 138, 139, 141, 143, 148, 150, **173, 175, 181**
 Dielectric constant, 163, **182**
 Diffraction by a row of points, **11, 81, 82**
 by a ruled grating, 32
 Diffuse scattering, 106, **152-161**
 Distortion, 24, 36, 76, 78, 143, **148, 150, 161, 168, 181**
 Divergent beam method, 80, **141-143**
- Elastic constants, 150, 155, **157, 159, 181**
 Electron density distribution, 74, 103, **112, 128-137, 165, 166, 170, 179**
 microscope, 2, 50
 tube, 36, **39-43, 45**
 Electronic charge, determination by X-rays, **33, 165**
 Electrostatic bonds, **124, 166, 182**
 Equivalent points, **114, 115, 169**
 Etch figures, 56, 57
 Excitation potential, **25, 28**
 Extinction, **140-143**
- Ferro-electrics, **163**
 Ferromagnetism, **186, 187**
 Fibre photograph, 81, 144, **184**
 Fibrous structures, 21, 143, 155, 181, **184**
 Figure fields, 123, **124**
 Filament tubes, 36, **39-43, 45**
 Filters, X-ray, **30, 31, 48**
 Finger-print method of identification, **78, 190**
 Fluorescence, 3, **33**
 yield, 29
 Fluorescent X-rays, 4, **26-29, 31**
 screens, 3, **33, 34, 35**
 Fly's-eye method, **128, 129**
 Focus of X-ray tubes, 35, **40-43**
 Forced electronic vibration, 27, 104
 Fourier synthesis, 120, 122, **128-137, 178-181, 186**
 Friedel's law, 60
- Gas tubes, **36-38**
 Gaseous state, 5, 18, 21
 Gases, scattering by, **19, 106, 107**
 Geiger-counter method, **34, 101**
 General radiation, 14, **23-26, 37, 75**
 Geometry of crystals, **50-80**
 Glass, **21, 22, 50**
 Glide plane, **68-72, 80, 94, 95, 100, 101, 114**
 Gnomonic projection, 62, **66, 67, 76**
 Goniometer, optical, **51, 75, 96**
 Grain size, **145-148**
 Graphite, 6, 100, 113, 145, 161, **175-178**
 Greinacher circuit, 47, 48
 Gutta-percha, 185, 186
- Habit, crystal, 50, 51, **85**
 Haemoglobin, 184
 Halation, **24, 145**
 Harmonics, wave-length, 29, **49**
 Heating effect of X-rays, 26
 cathode stream, **39-44**
 Heavy atom technique, **133-137**
 Hexamethylbenzene, **119-122, 126, 128, 178, 183**
 High voltage generation, **44-48**
 Homopolar bonds, 166, **173**
 Hot-cathode tube, 36, **39-43, 45**
 Hume-Rothery rules, **188, 189**
 Hydrogen bond, 126, 127, **182, 183**
- Ice, 26, 145, 155, **182**
 Identification, of elements by X-ray spectra, **18, 190**
 by finger-print method, **78, 190**
 Identity period, 11, 12, 15, **81-84**
 Incoherent scattering of X-rays, 26, 27, **106**
 Indices of crystal planes, axes, zones, **53-56, 77, 79, 80, 84**
 Intensifying screens, **33, 34**
 Intensity, calculated, 104, 112, **116-118, 138, 159**
 formulae, 49, **116-119, 138**
 measurement, 15, 26, **34, 35, 101, 102, 111, 119, 139, 179**
 observed, 37, 74, **102, 112, 115, 116, 138, 139**
 of diffuse scattering, **152-159**
 Interatomic distances, 123, 124, **126, 186**
 forces, 123, 133, 150, **165-167, 173**

- Interfacial angles, 6, 7, **51**, 52, 76, 77, 79
- Intermolecular forces, 173, 175
- Interplanar spacings, 14, 15, **53**, **54**, 77-79, 84, 85, 87, 176, 187
- Inversion axes, **56**, 60, 62, 63, 69
- Ion tubes, 36, 39-43
- Ionic character, 123, 169, **170**, 173, 182
 - conductivity, **168**, **169**
 - radius, 123, **125**, 166, **167**, 170
 - structures, **123**, **124**, **166**
- Ionisation, 4, 13, 26, 27, 34, 37, 38, 139
 - spectrometer, **15**, 34, 51, 96, 101, 141
- Isomorphous structures, 127, **135**, 168

- Jahn formula, **157-159**

- K absorption edge or limit, 15, **28**
 - radiation, 4, 16, **25**, 26, 27, 30
- Kinetic theory, 5

- L radiation, 4, 16, 25, 26
- Lattice theory, **52-62**, **68-74**
 - reciprocal, **84-94**, **152-159**
- Laue equations, 12, 15, 81-83
 - experiment, history of, 7-12
 - method, 7, 13, 24, **75**, **88**, 154-157
 - photographs, 10, 24, 56, 64, 66-68, 75, **76**, 82, 148, **154**, 155, 158, 160
- Law of definite proportions, 4, **170**
 - rational indices, 53
- Layer lines, 79, **81-84**, **90-93**, 154
 - structures, 113, **119**, 156, 157, **175-178**, 183
- Lead, 158, 160
 - stop, **24**, 25
- Limiting sphere, **90-92**, 94, 133
- Lindemann glass, 29, 38
- Line broadening, **143-148**
 - focus, 40
 - spectrum, 4, 17, **25**
 - synthesis, **133**
- Linear absorption coefficient, **26**, 29, 119
- Liquid crystals, **21**
- Liquids, nature and properties of, 5, 18, 20, 21
 - scattering by, **20**, 106, 107, 108, 145, 155, 185
- Lithium windows for X-ray tube, 29
- Long-chain molecules, 78, 85, 101, 143, **155**, **181**, **184-186**
- Lorentz factor, **117**
- Low-angle scattering, **145-147**, 168
- Low-temperature experiments, 139, **155**, 163, 177

- Magnetic anisotropy, 56, 127, **128**
- Mass absorption coefficient, **29**
- Melting-point, 21, 50, 145, 155, 160, **161**, 164, 168, 169, 173, 182
- Metallic bonds, 133, 166, **186**
- Metals, 7, 78, 143, 149, **186-190**
- Mica, 13, 15, 172
- Microscope, X-ray method compared with optical, 1
- Miller indices, 15, **53**, 55
- Mirror plane, **56**, 57, 62, 63, 68, 70-72, 97, 98, 114
- Mixed crystals, 161, **167**, 168
- Molecular compound, 126, **173-176**
 - weight determination, 15, 96, 97, 147
 - symmetry, **96-101**
- Monochromatisation of X-rays, 29, 42, **48**, **49**, 105, 117, 146
- Mosaic crystal, 24, 50, **118**, 138, 139, 142, 143, **148**
- Moving target tubes, 40, 41
- Multiple reflection, **140**, **143**
- Multiplicity factor, 77, 78, 79, **116**, 118
- Muscle, 143, 184

- Nature of X-rays, 3, 4, 12, 13, **17**, 23-35
- Newman interrupter, 44
- Nickel filters, **30-31**, 38
- Nickel-aluminium alloy system, 187-189
- Nomenclature in lattice theory, **56-63**, 65, 68-72
- Non-Bragg reflection, **152-160**

- Optical goniometer, **51**, 75, 76
 - measurements, 50, 51
 - spectra, 94, 150
- Order and disorder, 87, 161, **168**, 188
- Orientation, 10, 24, 68, **75**, 76, 117, 127, 128, 148, 152, 158, 184
- Orthogonal projection, 62, 63
- Oscillation method, 25, **79**, **91**, 94
- Oxygen, 21, 30, 106, **123**, 167, 170-172

- Packing of atoms or molecules, 97, 123, 135, 161, 164, 166-178
- Particle size, 78, 87, 144-148, 152, 154, 160, 184, 190
- Patterson synthesis, 135, 137
- Pauling's rules, 123-125
- Penicillin salts, 85, 128, 135, 148, 186
- Perfect crystals, 51, 118, 138, 139
- Phase diagrams, 188, 189
of scattered wave, 109-111, 129, 131, 132, 136, 140
- Photographic blackening, 3, 27, 28, 35, 117
emulsion, 30, 35
film pack, 35, 102
methods, 13, 17, 24, 30, 35, 91, 102
- Photographs, back reflection, 10, 24, 148, 187
fibre, 81, 144, 184
Laue, 9, 10, 24, 56, 64, 66-68, 75, 76, 82, 96, 148, 154-156, 158, 160
oscillation, 25, 79-80, 94, 154
powder, 25, 26, 76-78, 116, 118, 144, 145, 148, 187, 188
rotation, 25, 26, 55, 78-81, 84, 91, 92, 96, 97, 184
Weissenberg, 79, 84, 92, 96, 97
- Photometry, 35, 102
- Phthalocyanines, 134-136, 161, 162
- Piezo-electricity, 101, 163, 164
- Planck's constant, measurement of, 24, 165
- Polarisation of X-rays, 3, 49, 103, 104
factor, 105, 116, 138
- Polymorphism, 6, 100
- Polysaccharides, 183, 184
- Powder method, 76-78, 89, 90, 116, 123, 144, 145, 147, 148, 187
- Precision measurements, 32, 97, 187, 190
- Primary extinction, 139-142
- Primitive triplet, 53, 56
- Projection of crystals, gnomonic, 62, 66, 67, 76
orthogonal, 62, 63
spherical, 63, 64
stereographic, 62, 64-66, 68, 76
- Properties of solids, 5, 6, 21, 143
X-rays, 3, 4, 23-36
- Proteins, 94, 182-185
- Pseudo-symmetry, 59, 119, 120, 183
- Pyro-electricity, 101
- Quality of X-rays, 4, 36, 37, 39
- Quantum theory of radiation, 16, 17, 24, 28
- Quartz, 6, 49, 51, 56, 57, 163, 170
- Radius ratio, 124, 167
- Random structures, 161, 167-169
- Real crystals, 139-143, 160
- Reciprocal lattice, 84-94, 144, 152-159
- Reciprocity law, 35, 102
- Rectification of tube current, 36, 44-47
- Reflecting power, 84, 85, 140, 141, 152, 153, 156
- Reflection by planes of atoms, 13-15, 17
- Refractive index for X-rays, 31, 190
- Resolution by light, electron waves and X-rays, 2, 50
- Resolution in Fourier diagrams, 132, 133
- Resonance, 179-181
- Rochelle salt, 163, 164, 182
- Rock-salt, 8, 10, 74, 139, 143, 151, 166, 167
- Rotation of atoms or molecules, 20, 108, 163, 164
axes, 56-63, 69-72, 97, 98, 114
method, 25, 78, 81-84, 86, 90-93, 96
- Row lines, 79, 92, 93
- Rubber, 101, 145, 185, 186
- Ruled grating, diffraction by, 32
- Safety devices, 36, 47, 48
- Saturation current, 39
- Scattering angle, 26, 105
by air, 24
by electrons, 26, 103, 104-107, 129
by gases, 19, 106, 107
by liquids, 20, 106, 107, 108
power, 87, 130, 144, 152, 157, 160
of X-rays, 3, 9, 18, 20, 27, 81, 104-108
- Screw axes, 69-72, 80, 94, 96, 100, 101, 114
- Sealed-off tubes, 36, 39, 43, 44
- Secondary extinction, 139, 141-143
- Section synthesis, 133
- Self-screening, 31
- Short wave-length limit, 23, 24
- Silicate minerals, 123, 170-172
- Silk, 22, 143, 184
- Size of atoms or ions, 4, 15, 123-125, 166

INDEX OF SUBJECTS

197

- Slit systems, 32
- Sodium, 10, 158, 159
- Solid solutions, 161, 167, 169, 187-190
- Solids, state of knowledge in 1912, 5-7
- Space-group theory, 68-72, 78, 94-101
- Spectra, X-ray, 4, 15, 17, 18, 23-28, 86, 87, 94-96, 113
- Sphere of reflection, 87-92, 117, 154, 156, 158, 159
- Spherical projection, 63, 64
- Spiralled crystallites, 148
- Stereographic projection, 64, 66, 68, 76
- Strain in crystals, 56, 148
- Striations, 56, 57
- Structure amplitude, 108-111, 129-133
 - factor, 108-123, 127-133, 138
- Symmetry, 7, 24, 56, 63, 68-74, 84, 96-101, 113-115
- Temperature correction, 117, 133, 150, 151
- Textile materials, 7, 21, 101, 143, 184, 185
- Texture of crystals, 24, 50, 87, 116, 118, 138-150, 184
- Thermal conductivity, 7, 39, 139, 168-170, 186
 - diffuse scattering, 106, 152-161, 181
 - expansion, 139, 161, 162, 182
 - transformation, 161-164
 - vibrations, 10, 20, 87, 103, 116, 133, 138, 141, 150-164, 166, 168, 177, 184
- Total reflection of X-rays, 32
- Totally reflecting collimating system, 32
- Trial and error structures, 112, 113, 119-128
- Tungsten, 26, 39, 43, 44, 150, 159
- Two-crystal spectrometer, 102
- Unit cell, 52, 53, 58-60, 63, 72, 76, 78, 84, 85, 94, 96-98, 108-111, 123, 129
- Units of length, 2, 30
- Vacuum technique, 36-39, 178
- Valency, 124, 133, 166, 167
- Valency angles, 180, 181
- van der Waals forces, 126, 165, 173, 176, 182
- Volume of unit cell, 96, 97, 129
- Water, 181, 182
- Wave-length, 2, 4, 8, 12, 14, 23, 24, 28, 30
 - measurement, 4, 15, 24, 32, 165
- Weissenberg method, 79, 84, 92
- White radiation, 14, 17, 23-26, 37, 75
- Windows of X-ray tubes, 29, 30, 38, 43
- Wool, 143, 184
- X-ray crystallography as an industrial tool, 3, 24, 78, 149, 190
 - frequency, 27
 - spectroscopy, 15, 16, 18, 190
 - stop or trap, 24, 25
 - tubes, demountable, 37, 39, 43, 49
 - gas-type, 36-38
 - filament-type, 36, 39
 - sealed-off, 36, 39, 43, 44
- X-rays, absorption of, 3, 4, 13, 26-31, 80, 101, 140-143, 148, 190
 - generation of, 23, 36-48
 - nature of, 3, 4, 12, 13, 17, 23-35
 - photographic action of, 3, 35
 - properties of, 3, 4, 23-36
 - scattering of, 3, 9, 18, 20, 27, 81, 104-108, 155, 157-160
 - wave-length, measurement of, 4, 15, 24, 32, 165
- Young's Modulus, 150
- Zero-point energy, 150
- Zinc blende, 8, 10-12, 14, 113
- Zone, 51, 54, 64, 67, 76, 78, 85, 86, 92, 130, 131
 - axes, 51, 54, 55, 78, 83, 86, 87
 - law, 54, 92

INDEX OF NAMES

- Allison, 107, 191
 Andrade, 141, 142
 Astbury, 71, 184, 185, 191
 Avogadro, 8, 29

 Barkla, 4, 9, 27, 145
 Barlow, 7, 12, 14
 Barrett, 191
 Bernal, 92-94
 Bhagavantam, 127
 Bijvoet, 73, 125, 137, 174, 176, 191
 Biscoe, 147
 Bohr, 17, 19
 Booth, 191
 Born, 191
 Bosanquet, 143
 Bouman, 94
 Bradley, 189
 Bragg, W. H., 8, 13-17, 52, 57, 112, 127, 141, 151, 191
 Bragg, W. L., 8, 13-16, 52, 53, 57, 66, 72, 77, 124, 143, 149, 151, 166, 171, 172, 191
 Brasseur, 191
 Brockway, 120
 Buerger, 94, 191
 Bunn, 51, 55, 64, 78, 106, 129, 144, 186, 191
 Burgers, 191

 Carlisle, 186
 Cauchois, 18, 28
 Charles II, 4
 Clark, C. D. H., 191
 Clark, G. L., 169, 191
 Compton, 107, 191
 Crowfoot, 94, 186
 Crowther, 145

 Darwin, 13, 17
 Debye, 150
 Desch, 191

 Evans, 191
 Ewald, 8, 191

 Faraday, 1
 Firth, 151

 Friedel, 60
 Friedman, 34
 Friedrich, 8, 9, 10

 Goldschmidt, 99, 167
 Guinier, 29, 42, 43, 74, 146, 191

 Hartree, 107
 Hartshorne, 191
 Henny, 192
 Hevesy, 191
 Hilton, 191
 Hume-Rothery, 188, 191

 John, 157, 158, 159
 James, 143, 151, 191
 Jeffrey, 180
 de Jong, 94

 Knipping, 8, 9, 10
 Kolkmeijer, 73, 125, 137, 174, 176, 191

 von Laue, 8, 11, 12
 Lavoisier, 6
 Lipson, 124
 Lonsdale, 80, 86-91, 153, 156-159

 MacGillavry, 73, 125, 137, 174, 176, 191
 Millikan, 8, 33
 Moseley, 13, 17, 18
 Müller, 38

 Niggli, 191

 Patterson, 135
 Pauling, 123, 124, 167, 169, 191
 Pepys, 4
 Perrin, 8
 Perry, 5
 Perutz, 94
 Phillips, 65, 191
 Pirenne, 19, 20, 108, 192
 Planck, 16, 165
 Pope, 7, 12, 14

INDEX OF NAMES

199

- | | |
|-------------------------------------|------------------------------|
| Randall, 192 | Turner-Jones, 186 |
| Riley, 94 | Tutton, 57, 62, 63, 192 |
| Robertson, 112, 122, 127, 131, 132, | |
| 134, 136, 157, 179, 181, 183 | Ubbelohde, 162, 183 |
| Rogers-Low, 186 | |
| Röntgen, 3, 8, 33, 36 | Waller, 150, 151 |
| Rooksby, 190 | Warren, 147 |
| Rutherford, 17, 141, 142 | Wasastjerna, 167 |
| | Weissenberg, 79 |
| Schall, 37, 45-48, 192 | Wells, 175, 192 |
| Shearer, 38 | White, 178 |
| Sinclair, 190 | Woodward, 127, 134, 157, 162 |
| Sommerfeld, 8, 19 | Wooster, 38, 192 |
| Spiegel-Adolf, 192 | Wrinch, 192 |
| Sproull, 192 | Wyckoff, 67, 192 |
| Stillwell, 192 | |
| Stuart, 191 | Yardley, 71 |
| | |
| Taylor, 189, 190, 192 | Zachariasen, 21, 192 |
| Tolansky, 51 | |